The association between tissue non-specific alkaline phosphatase expression and differentiation of mesenchymal stromal cells

by

Cara-Lesley Bartlett

Dissertation presented in partial fulfilment for the degree of

Doctor of Philosophy (Internal Medicine)

at the University of Stellenbosch

Promoter: Professor William F. Ferris

Co-Promoter: Professor Nigel J. Crowther

March 2017

DECLARATION

By submitting this thesis electronically, I declare that the entirety of the work contained therein is my own, original work, that I am the sole author thereof (save to the extent explicitly otherwise stated), that reproduction and publication thereof by Stellenbosch University will not infringe any third party rights and that I have not previously in its entirety or in part submitted it for obtaining any qualification.

March 2017

ABSTRACT

Diseases resulting from the dysregulation of adipocyte and osteoblast differentiation include diabetes type II and osteoporosis. Both adipocytes and osteoblasts are derived from the same progenitor cell type, known as mesenchymal stromal cells (MSCs), which may also differentiate into cells of several mesenchymal lineages. A more detailed understanding of the mechanisms involved in the differentiation of MSCs would provide valuable insight into the underlying causes of, as well as facilitate the development of improved treatments for, diseases related to MSC differentiation dysregulation.

Tissue-nonspecific alkaline phosphatase (TNAP) is highly expressed in several tissues including bone tissue, where it has a well-established role in skeletal mineralisation. In recent years TNAP expression has been reported in adipocytes, and has been identified as identical to the stem cell marker, mesenchymal stem cell antigen-1 (MSCA-1). The above findings indicate that TNAP has diverse roles, and may be one of the factors involved in determining the differentiation pathway of MSCs.

Previous studies have found that inhibition of TNAP in the mouse preadipocyte cell line, 3T3-L1 resulted in a decrease in lipid accumulation during *in vitro* adipogenic differentiation, suggesting that TNAP is involved in adipogenesis. In the present study, rat-derived primary MSCs were isolated from bone marrow (bmMSCs) as well as subcutaneous (scADSCs) and peri-renal visceral adipose (pvADSCs) depots, and differentiated *in vitro* towards either an adipocytic or osteoblastic phenotype. The expression of TNAP was assessed in rat-derived MSCs undergoing both adipogenic and osteogenic differentiation.

TNAP expression levels were highest in bmMSCs, followed by scADSCs and pvADSCs, with higher alkaline phosphatase (ALP) activity observed during adipogenesis compared to osteogenesis in all three MSC types. The addition of the reported TNAP inhibitor, levamisole during osteogenesis prevented mineralisation in all MSC types, but had no significant effect on lipid accumulation during adipogenesis. Other reported inhibitors were also examined; Histidine was not successful in reducing lipid accumulation or mineralisation, while L-homoarginine was able to significantly reduce lipid accumulation in all MSC types. The inhibitor results were not conclusive due to possible off target effects within the cells. Attempts to inhibit adipogenic differentiation by knockdown of TNAP expression in

scADSCs using shRNA were not successful, as indicated by the presence of lipid droplets in cells where TNAP-specific shRNA was present.

This study also revealed that ALP activity was localised to the membrane of intracellular lipid droplets characteristic of adipocytes, and that the same TNAP mRNA transcript type which is preferentially expressed in bone tissue is also preferably expressed during adipogenic differentiation of bmMSCs and scADSCs, while expression in pvADSCs was below detectable levels.

TNAP isoforms differ from one another due to differences in posttranslational glycosylation pattern. Glycosylation differences were observed between bmMSCs differentiated from a naïve state towards an adipogenic, compared to an osteogenic, phenotype. Differences were also observed between scADSCs and bmMSCs when differentiated towards adipocytes. This may indicate that a distinct isoform of TNAP exists in adipocytes.

In conclusion, this study confirms earlier findings on the presence of TNAP in adipocytes. Differences in TNAP expression from MSCs isolated from different tissue depots were also discovered. This study provides a characterisation of the role of TNAP in adipogenic differentiation; however, the exact mechanisms remain to be elucidated.

Key words: Tissue-nonspecific alkaline phosphatase, mesenchymal stromal cell, bone-marrow, adipocyte, osteoblast, rat, levamisole, L-homoarginine, histidine, glycosylation.

AFRIKAANSE OPSOMMING

Die wanregulering van adiposiet en osteoblast differensiasie lei tot verskeie siektetoestande, insluitende tipe II diabetes en osteoporosis. Beide adiposiet en osteoblast seltipes is afstammelinge van dieselfde stamseltipe, naamlik mesenchiem stromale selle (MSSe). Meer breedvoerige kennis van die onderliggende faktore wat bydra tot hierdie wanregulering kan aanleiding gee tot verbeterde behandelingsmetodes vir siektes geassosieer met afwykende MSS differensiasie.

Daar is ‘n hoë uitdrukking van weefsel nie-spesifieke alkaliese fosfatase (WNAF) in verskeie weefseltipes, insluitende been, waar dit ‘n welbekende rol speel in skelet mineralisering het. Daar is onlangs bevind dat WNAF in adiposiete uitgedruk word en dat dit identies is tot die stamsel merker, mesenchiem stamsel antigeen-1. Hierdie bevindinge dui daarop dat WNAF verskeie diverse funksies het en dat die ensiem een van die bepalende faktore mag wees wat bydra tot differensiasie van stamselle.

Vorige navorsing het gewys dat inhibisie van WNAF in die muis pre-adiposiet sellyn, 3T3-L1, lei tot ‘n afname in lipied akkumulasie tydens *in vitro* adipogeniese differensiasie. Dit impliseer dat WNAF betrokke is by adipogenese. In die huidige studie was daar gebruik gemaak van rot-afgeleide primêre MSSe geïsoleer uit beenmurg (bmMSSe), asook selle verkry uit subkutaan (skAASSe) en peri-renale visserale (pvAASSe) vet depots. Hierdie selle was gedifferensieer, *in vitro*, in ‘n adiposiet of osteoblast fenotipe. Die uitdrukking van WNAF was bepaal in rot-afgeleide MSSe wat gestimuleer was om *of* adipogeniese of osteogeniese differensiasie te ondergaan.

Vlakke van WNAF uitdrukking was die hoogste in bmMSSe gevolg deur skAASSe en pvAASSe. Daar was meer alkaliese fosfatase aktiwiteit tydens adipogenese in al drie MSS tipes. Verder het die WNAF inhibitor, levamisool, mineralisering tydens osteogenese voorkom in al drie MSS tipes. Die inhibitor het egter geen beduidende effek gehad op lipied akkumulasie tydens adipogenese nie.

Die effek van twee ander moontlike WNAF inhibitore, histidien en L-homoarginien, was ook ondersoek. Histidien het nie lipied akkumulasie of mineralisering onderdruk nie.

Inteenstelling hiermee het L-homoarginien lipied akkumulasie beduidend in al drie MSS tipes verminder. Resultate verkry met inhibitore was nie beslissend nie. Dit mag wees as gevolg van moontlike buite-teiken effekte van die inhibitore in hierdie selle. Dus was daar gepoog om adiposiet differensiasie te inhibeer deur die afklop van WNAF uitdrukking in skAASSe. Dit was bewerkstellig deur gebruik te maak van klein haarnaald RNAs (khRNAs). Selle het egter steeds lipied druppels vertoon in die teenwoordigheid van WNAF spesifieke khRNAs.

Eksperimente in hierdie tesis het ook onthul dat WNAF aktiwiteit gelokaliseer is in die membraan van intrasellulêre lipied druppels. Verder is daar ook gedemonstreer dat dieselfde WNAF boodskapper RNA-transkripsie tipe wat met voorkeur in beenweefsel uitgedruk word, ook met voorkeur tydens adipogeniese differensiasie uitgedruk word in bmMMSe en skAASSe. Die uitdrukking van hierdie transkripsie tipe was nie in pvAASSe gevind nie.

Verskille in post-translasie glikosilasie gee aanleiding to verkillende isoforme van WNAF. Glikosilasie-verskille was gesien in MSSe differensiasie in ‘n adipogeniese fenotipe in vergelyking met differensiasie in ‘n osteogeniese fenotipe. So ook was daar verkille gemerk tussen skAASSe en bmMSSe wat gedifferensieer was in ‘n adiposiet fenotipe. Dit mag aandui dat ‘n eiesoortige WNAF isoform in adiposiete voorkom.

Bogenoemde saamgevat, die huidige studie bevestig vroeëre bevindinge dat WNAF teenwoordig is in adiposiete. Verskille is gewys in die uitdrukking van WNAF in MSSe geïsoleer uit versillende weefsel depots. Hierdie studie voorsien ‘n karakterisering van die rol wat WNAF speel in adipogeniese differensiasie, maar die presiese funksie van WNAF is egter nog ontwykend.

Sleutel woorde: weefsel nie-spesifieke alkaliese fosfatase, mesenchiem stromale selle, beenmurg, vetsel, rot, levamisool, L-homoarginien, histidien, glikosilasie.

ACKNOWLEDGEMENTS

I would like to express my sincere appreciation to the following people and organisations:

The MRC, Stellenbosch University FMHS and the Harry Crossley foundation for funding.

My supervisor Prof. William Ferris and my co-supervisor Prof. Nigel Crowther, for their expert guidance and supervision throughout the duration of this project.

The late Prof. Stephen Hough, for his valued advice and expertise.

Dr. Hanél Sadie-van Gijsen for her technical advice and training.

Dr. Mari Van De Vyver for assistance with data processing and statistics.

To my colleagues and dear friends, the “coffee club”: Dr. Ellen Andrag, Alex Jacobs and Martine van den Heever, for the years of friendship, advice, shared expertise, and the many fruitful scientific discussions over the years.

Dr. Ellen Andrag, for help with translation of the abstract into Afrikaans.

Finally, to my parents, Alan and Gail Bartlett, for their endless love, support and encouragement throughout my university career.

TABLE OF CONTENTS

LIST OF ABBREVIATIONS

A	
AD	Alzheimer's disease
ADP	Adenosine diphosphate
ADSC	Adipose-derived stromal cell
ALP	Alkaline phosphatase
AM	Adipogenic differentiation medium
AMP	Adenosine monophosphate
ARBP	Acidic ribosomal phosphoprotein
Arg	L-homoarginine
ATP	Adenosine triphosphate
ANOVA	Analysis of variance
B	
BCIP	5-Bromo-4-Chloro-3-Indolyl Phosphate
bHLH	basic helix loop helix
BMP	Bone morphogenetic protein
bmMSCs	Bone marrow-derived mesenchymal stromal cells
BSA	Bovine serum albumin
BSP	Bone sialoprotein
BrdU	5-bromo-2-deoxyuridine
C	
C	Celsius
Ctrl	Control
$CaPO_4$	Calcium phosphate
cAMP	Cyclic adenosine monophosphate
cGMP	Cyclic guanidine monophosphate
Cbfa1	Core-binding factor 1
CFU-F	Colony-forming unit- fibroblast
CI	Contact inhibition
Col I	Collagen I
CpG	Cysteine phosphate guanine
C/EBPs	(CCAAT)/enhancer binding proteins
cDNA	Copy DNA
COL1A2	Type I collagen
D	
d	Day
Dex	Dexamethasone
DMEM	Dulbecco's Modified Eagle's Medium
dNTP	deoxy nucleotide triphosphate
E	
EAP	Embryonic ALP
EC	Embryonic cancer
ECAP	*Escherichia coli* alkaline phosphatase

ECM	Extracellular matrix
EG	Embryonic germ
ES	Embryonic stem
EtBr	Ethidium bromide
EtOH	Ethanol

F

FACS	Fluorescence-activated cell sorting
FBS	Foetal bovine serum
Fig.	Figure

G

g	Gram
g	Gravity
GAD	Glutamate decarboxylase
GABA	γ-aminobutyric acid
GCAP	Germ-cell alkaline phosphatase
GIO	Glucocorticoid-induced osteoporosis
GCs	Glucocorticoids
G-CSF	Granulocyte colony stimulating factor
GOI	Gene of interest

H

HBSS	Hank's balanced salt solution
His	Histidine
hr	Hour
hrs	Hours

I

IAP	Intestinal alkaline phosphatase
IBMX	3-isobutyl-1-methylxanthine
IgG	Immunoglobulin
IL-1β	Interleukin-1β
iPS	Induced pluripotent stem

L

L	Litre
LBK ALP	Liver/bone/kidney alkaline phosphatase
LCFA	Long chain fatty acid
Lev	Levamisole
LPS	Lipopolysaccharide

M

M	Molar
min	Minute
miRNA	Micro RNA
mM	Millimolar
mRNA	Messenger RNA
MSC	Mesenchymal stromal cell
MSCA-1	Mesenchymal stem cell antigen-1

Msx	Homologue of the *Drosophila* muscle segment box
MV	Matrix vesicle

N

n.a.	Not applicable
nM	Nanomolar
nm	Nanometer
NPP1	Nucleotide pyrophosphatase phosphodiesterase 1

O

OC	Osteocalcin
OD	Optical density
OM	Osteogenic differentiation medium
OPN	Osteopontin

P

P	Passage
PBS	Phosphate buffered saline
PCG	Primordial germ cell
PC-1	Plasma cell glycoprotein-1
PCho	Phosphocholine
PEA	Phosphoethanolamine
Pi	Inorganic phosphate
PLAP	Placental alkaline phosphatase
*p*NP	*para*-Nitrophenol
*p*NPP	*para*-Nitrophenyl phosphate
PPARγ	Peroxisome proliferator-activated receptor γ
PHOSPHO1	Phosphatase orphan 1
PLP	Pyridoxal-5'-phosphate
PMNs	Polymorphonuclear cells
polyP	Inorganic polyphosphates
PrP^{C}	Prion protein
PPi	Inorganic pyrophosphate
pvADSC	Peri-renal visceral adipose derived stromal cell

R

RCCS	Rotary cell culture system
redox	Reduction/oxidation
RG	Reference gene
RISC	RNA-induced silencing complex
RNA	Ribonucleic acid
RNAi	RNA interference
ROS	reactive oxygen species
rpm	Revolution per minute
RT	Room temperature
RT-qPCR	Real time quantitative polymerase chain reaction

Runx2	Runt-related transcription factor 2
S	
sec /s	Second/s
Sca-1	Stem cell antigen-1
scADSC	Subcutaneous adipose-derived stromal cell
SE	Standard error
SGM	Standard growth medium
shRNA	Short hairpin ribonucleic acid
siRNA	Short interfering ribonucleic acid
SVF	Stromal vascular fraction
T	
TNAP	Tissue-nonspecific alkaline phosphatase
TN-α	Tumour necrosis factor-α
TGF-β	Transforming growth factor-β
TZDs	Thiazolidinediones
U	
U	Units
UDP	Uridine diphosphate
U/mg	Units per milligram
U/ml	Units per millilitre
UTR	3` untranslated region
V	
V	Volts
v/v	Volume per volume
W	
w/v	Weight per volume
WGL	Wheat germ lectin

LIST OF FIGURES

LIST OF TABLES

CHAPTER 1

Alkaline phosphatase (ALP) and the osteogenic and adipogenic differentiation of mesenchymal stromal cells (MSCs).

1.1 Introduction

Glucocorticoid-induced osteoporosis (GIO) is the most common form of secondary osteoporosis. It is characterized by rapid initial increase in bone resorption, resulting from a transient increase in osteoclast activity, followed by a marked impairment in bone formation due to a chronic decrease in the numbers of osteoblasts, the cells responsible for bone mineralisation. GIO may therefore be viewed as primarily an osteoblast problem, with low numbers caused by decreased proliferation, increased apoptosis and elevated transdifferentiation of osteoblasts into an adipocytic phenotype. This increased switching of progenitor cells from an osteoblastic to an adipocytic phenotype produces "fatty bones", which is indicative of the disease (Weinstein, 2001; Compston, 2010). A better understanding of the factors involved in the differentiation of precursor cells towards either an adipocytic or osteoblastic phenotype would provide a foundation for the development of better treatment of diseases resulting from adipocyte and osteoblast dysregulation, such as osteoporosis and type II diabetes.

The enzyme tissue-nonspecific alkaline phosphatase (TNAP) is expressed in bone, liver, kidney and neural tissue, as well as in adipose and other tissues, and also has a role in stem cell differentiation. The presence of TNAP in mesenchymal stromal cells (MSCs), which are the progenitor cells of osteoblasts and adipocytes, as well as in differentiated MSCs, indicates that TNAP may be playing an important role in MSC biology and differentiation (Sobiesiak *et al.*, 2010; Kollmer *et al.*, 2013).

In humans, four alkaline phosphatase (ALP) isozymes of have been discovered, and are defined based on their gene sequence and tissue location (Harris, 1990). The basic types of ALP have been identified as three tissue-specific ALPs, including placental (PLAP), germ-cell (GCAP) and intestinal (IAP) ALP, as well as one tissue-nonspecific ALP (TNAP) which is highly expressed in bone, liver and kidney and also at low levels in a variety of other tissues (Fishman, 1990; Harris, 1990; Millán *et al.*, 2006).

Due to its established function in bone mineralisation and high expression levels in osteoblasts, TNAP has been used as a classical marker for osteogenesis. Osteogenesis is the process where mesenchymal stromal cells (MSCs), the progenitor cells of several mesenchyme-derived tissue including bone, fat, muscle and cartilage, differentiate into

osteoblasts, the cells which form bone (Rebelatto *et al.*, 2008). Recently, findings which seem to cast doubt on the role of TNAP as an exclusive marker of osteogenesis include the discovery that TNAP is expressed during, and may be involved in, the control of adipogenesis, which is the process whereby MSCs differentiate into adipocytes (Ali *et al.*, 2005; Kollmer *et al.*, 2013).

A study found that both TNAP mRNA and protein expression levels were inhibited after treatment of primary cultured rat bone marrow MSCs with the glucocorticoid (GC), dexamethasone (Dex) and levels of the adipogenic markers PPARγ and aP2 were up-regulated in a dose-dependent fashion, resulting in the cells differentiating into adipocytes (Lin *et al.*, 2010). A study using the murine preadipocyte cell line 3T3-L1 found that upon addition of either of the TNAP-specific inhibitors, histidine or levamisole, after initiation of adipogenesis using adipogenic differentiation medium containing Dex, insulin and 3-isobutyl-1-methylxanthine (IBMX), a decrease in both alkaline phosphatase (ALP) activity and lipid accumulation was observed. Levamisole is known to be an uncompetitive inhibitor of TNAP, while the mechanism of inhibition by histidine is also thought to be uncompetitive (Cyboron *et al.*, 1982; Ali *et al.*, 2006). The tissue-specific ALP inhibitor Phe-Gly-Gly did not alter ALP or lipid accumulation in the same experiment, as it is known that Phe-Gly-Gly is a tissue-specific ALP isozyme inhibitor (Ali *et al.*, 2005). A further study using 3T3-L1 cells and primary cultured human preadipocytes showed ALP activity and lipid accumulation were blocked by histidine after the initiation of adipogenesis in these cells. Furthermore, only IBMX was found to be crucial for adipogenesis as removal of this from the growth medium prevented lipid accumulation and blocked ALP activity, indicating a role for cAMP/cGMP (Ali *et al.*, 2006).

These findings present strong evidence for the involvement of TNAP in lipid accumulation, as inhibition of ALP activity was found to directly affect adipogenesis (Ali *et al.*, 2006). It is also believed that TNAP in 3T3-L1 and human preadipocytes is localised to the membrane surrounding the lipid droplets as ALP activity has been identified in this area, suggesting strongly that TNAP is involved in control of lipid accumulation within these cells (Ali *et al.*, 2005; Ali *et al.*, 2006). This is in contrast with the location of TNAP in osteoblastic cells, which is on the cell surface as well as on the surface of matrix vesicles secreted by the osteoblastic cells (Orimo, 2010).

As outlined previously, it has been demonstrated that TNAP is present in a wide variety of tissues, and may be an essential enzyme for an array of different functions apart from its established role in bone mineralisation. Importantly for this study, is the observation that TNAP is involved in adipogenesis from murine preadipocyte cell line, 3T3-L1 cells (Ali *et al.*, 2005; Ali *et al.*, 2006). The following project aimed to elucidate the function of TNAP during adipogenesis, using a rat-derived MSC model, using both naïve and differentiating primary-cultured MSCs as opposed to immortalised cell lines, such as MBA15.4 and 3T3-L1 cells. These cell lines, by nature, have a corrupted cell cycle and this may not only affect proliferation but also other cell fates such as differentiation. For this reason, results obtained using immortalised cell lines may be less significant than those from primary cells (Marko *et al.*, 1995; Czekanska *et al.*, 2014). The present study contrasted the expression of TNAP during differentiation of MSCs derived from rat bone marrow and adipose tissue, towards an adipocyte phenotype with the differentiation of the same cells towards an osteoblast phenotype. The main aim of this study was to further elucidate the function of this enzyme in cells derived from bone marrow and adipose tissue.

This following literature review discusses the biochemistry and roles of alkaline phosphatases as well as biology and differentiation of mesenchymal stromal cells (MSCs), with specific focus on the role of tissue-nonspecific alkaline phosphatase within the context of osteoblastogenesis and adipogenesis of MSCs.

1.2 Literature Review

1.2.1 Alkaline phosphatase background

Although it has been studied for over 80 years, much still remains to be discovered about alkaline phosphatase (ALP). Discovered in 1923 by Robert Robison, ALP was first hypothesized to function in bone mineralization; a hypothesis that was only proven to be correct more than 60 years later, in 1988 (Whyte, 2010). The name, “alkaline” phosphatase for this enzyme is a misnomer, resulting from *in vitro* studies of its pH optimum using artificial substrates, as alkaline phosphatase is known to function at physiological pH (pH 6.4 - 7.6) (Sprokholt *et al.*, 1982; Whyte, 2010). ALP is found ubiquitously in a vast array of organisms, from bacteria to plants and animal species.

1.2.2 Biochemistry of ALPs

Alkaline phosphatases are found widely in many species, ranging from bacteria to higher eukaryotes, including man (Millán *et al.*, 2006). ALPs function to catalyse the hydrolysis of phosphomonoesters, which results in the release of inorganic phosphate molecules (Hoylaerts *et al.*, 2006), and also have transphorylation activity when in the presence of high concentrations of phosphate acceptor molecules (Millán, 2006). Bacterial alkaline phosphatases are found in the bacterial cytosol, where they additionally function as part of a pathway to oxidise phosphite to phosphate (Yang and Metcalf, 2004). Substrates for ALPs include nucleic acids, which are dephosphorylated at the 5' phosphate group. This has been exploited in molecular biology, where shrimp ALP is added to reactions in order to dephosphorylate the 5' ends of the DNA after endonuclease digestion, which prevents self-ligation of DNA (Nilsen *et al.*, 2001; Twyman., 2006). Shrimp ALP is used here due to its thermolability, and may be irreversibly inactivated at 65° C, a temperature which does not harm the other reaction components (Nilsen *et al.*, 2001). ALPs belong to the enzyme superfamily: nucleoside pyrophosphatase/phosphodiesterases (Gijsbers *et al.*, 2001; Millán *et al.*, 2006) and have homology with many different enzymes.

1.2.3 Alkaline phosphatase structure and function

The largest differences are found between ALPs of bacteria and that of mammals. These differences include the K_m value, specific activity, glycosylation state, inhibitor susceptibility and heat stability (Millán *et al.*, 2006). Mammalian ALPs have a higher pH optimum (pH 8-10) than their bacterial counterparts; however, TNAP functions *in vivo* at physiological pH, suggesting that the usage of the term "alkaline" is not entirely correct (Millán *et al.*, 2006; Halling Linder *et al.*, 2009; Whyte, 2010). The K_m and specific activity is higher for mammalian ALPs compared to bacterial ALPs, while the heat stability is lower (Millán, 2006). Additionally, mammalian ALPs are inhibited uncompetitively by L-amino acids and peptides (Millán, 2006).

ALP enzymes have structural features which are highly conserved across all species, such as the catalytic site, as well as many major differences. The catalytic site of ALPs contains a catalytic serine, as well as three metal binding sites, namely M1 (also called Zn1) containing a Zn^{2+} ion, M2 (or Zn2) also containing a Zn^{2+} ion and M3, which contains a Mg^{2+} ion (Millán, 2006). The *Escherichia coli* ALP is coded for by the *phoA* gene and is known as *E.*

coli ALP (ECAP) or PhoA, and was for many years the only available model for investigating the structural features of ALPs (Kozlenkov *et al.*, 2002; Hoylaerts *et al.*, 2006). ECAP exists as a soluble homodimer, as is located in the bacterial periplasm. ALPs exist nearly exclusively as homodimers in nature, with few exceptions, such as the silkworm (*Bombyx mori*) ALPs. Silkworm ALP isozymes exist as either a soluble or membrane bound form, encoded by two distinct genes, and are mainly present in a monomeric form (Eguchi, 1995).

The elucidation of the structure of human placental ALP (PLAP) has allowed for the structure of other mammalian ALPs to be modelled (Kozlenkov *et al.*, 2002; Hoylaerts *et al.*, 2006). All mammalian ALPs have a homodimeric structure with a catalytic site present on each monomer. The two Zn^{2+} ions at sites M1 and M2 provide stability to the tertiary structure, while the Mg^{2+} ion at M3 acts as a cofactor for catalytic activity (Millán *et al.*, 2006). From the PLAP model, it was found that the central core consisting of a β-sheet and several α-helices was highly similar to that of ECAP (Kozlenkov *et al.*, 2002). ECAP contains four cysteine residues, giving rise to two disulfide bonds (Sone *et al.*, 1997), however all mammalian ALPs contain five cysteine residues, nonhomologous to the ECAP cysteines, of which four are involved in disulfide bonds. The fifth mammalian ALP cysteine residue appears to have a nonessential function, as mutations at this position have an insignificant effect on enzyme activity (Kozlenkov *et al.*, 2002). Certain amino acid residues which are important for metal ion binding in the active site in PLAP, are conserved between mammalian ALPs, namely Asp-42, His-153, Ser-155, Glu-311, Asp-316, His-320, Asp-357, His-358, His-360, and His-432. Of these, His-153 is not conserved in PhoA, nor is His-317, both of which are located near the Mg^{2+} site on PLAP (Kozlenkov *et al.*, 2002; Millán, 2006). Figure 1.2.3.1 presents a structural model of TNAP which illustrates the main features of this enzyme in its naturally occurring homodimeric structure (Millan and Whyte, 2016).

The mammalian ALPs are stabilized in their homodimeric structure by a “crown” or top loop domain, unique to mammalian ALPs and so named because of its position on the molecule, as well as by residues on the amino terminal sequence, which help to bind the monomers together (Le Du *et al.*, 2001; Hoylaerts *et al.*, 2006). The crown domain consists of a 60-residue segment from each monomer containing two small β-sheets consisting of three parallel strands, and enclosed by six large flexible loops containing a short α-helix (Le Du *et al.*, 2001). The crown domain is the least conserved feature amongst mammalian ALPs.

Variations in isozyme-specific properties of mammalian ALPs have been attributed to the crown domain, particularly to the residue at position 429 within the crown domain, including differences in heat-stability, uncompetitive inhibition and allosteric behaviour (Millán, 2006). Mammalian ALPs are noncooperative allosteric enzymes, meaning that the binding of substrate in the active site of one monomer will not affect the active site of the second monomer, when all the required metal ions are present on both subunits (Hoylaerts *et al.*, 1997; Le Du *et al.*, 2001). The crown domain may facilitate interactions between mammalian ALPs and proteins in the extracellular matrix, and has been found to be involved in the collagen-binding ability of TNAP (Bossi *et al.*, 1993; Hoylaerts *et al.*, 2006; Millán *et al.*, 2006).

The amino terminal sequence of mammalian ALPs contains an α-helix, which is not present in ECAP, and may be involved in stabilising the dimerization of the monomers, as the α-helix sequence of one monomer interacts with and embraces the second monomer (Hoylaerts *et al.*, 2006; Millán, 2006). The amino terminus is also required for catalytic activity of mammalian ALPs, as an example, it has been found previously that deletion of 5 residues of this sequence reduced the alkaline phosphatase activity of TNAP, whereas deletion of 9 residues totally eliminated catalysis (Hoylaerts *et al.*, 2006). Despite the above similarities, several differences exist between alkaline phosphatases from different species, as well as between the various isozymes and isoforms within a species (Millán, 2006; Millán *et al.*, 2006).

In mammalian ALPs, a highly conserved tyrosine residue at position 367 is vital for catalytic ability. The Tyr-367 residue of one monomer protrudes into the active site of the second monomer in the vicinity of the M1 (Zn1) ion, where the hydrophobic phenyl ring of Tyr-367 contributes to the formation of the hydrophobic pocket within PLAP. Tyr-367 functions to stabilise the inhibitors of ALP, as removal of Tyr-367 destabilised the inhibitor binding at the active site of the enzyme (Kozlenkov *et al.*, 2002).

A fourth metal binding site, designated as M4, has been identified in mammalian ALPs, but not in ECAP, and contains a noncatalytic Ca^{2+} ion. The M4 site is found in the peripheral domain, and in PLAP consists of residues 250-297, a sequence which contains two α-helices. It is thought that the Ca^{2+} ion at the M4 site is necessary to stabilise the conformation of the α-helices in the peripheral domain (Llinas *et al.*, 2005).

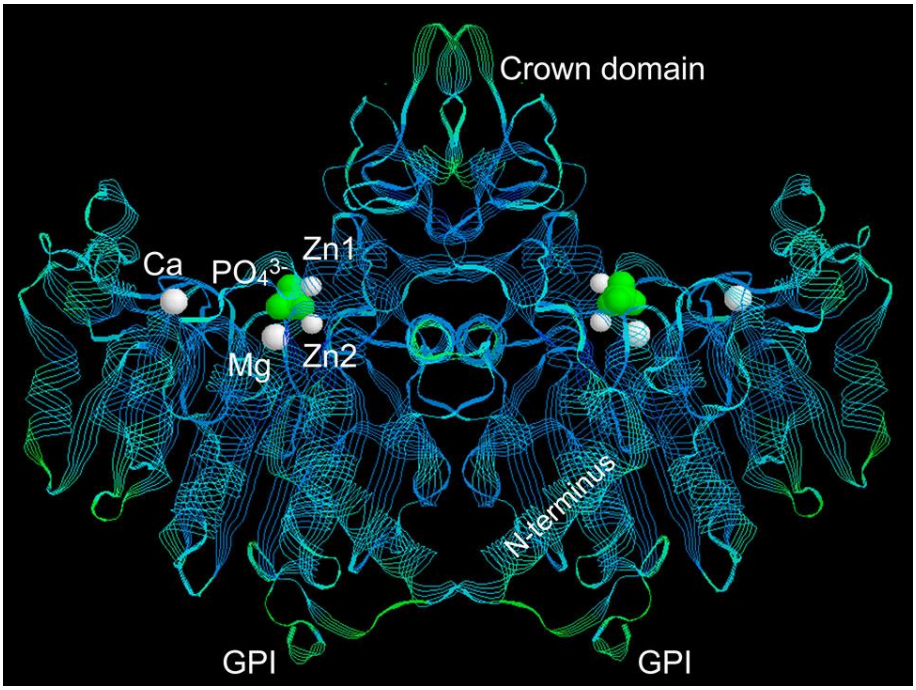

Figure 1.2.3.1: Representation of the homodimeric structure of human tissue-nonspecific alkaline phosphatase (TNAP). A phosphate ($PO4^{3-}$) ion is shown in green at the active site of each monomer, surrounded by the three active site metal ions: two Zn^{2+} (Zn1 and Zn2) and one Mg^{+} (Mg) ions, shown in white. The position of the structural Ca^{2+} ion binding site is also shown in white. The positions of the crown domain and N-terminus are illustrated, as well as the position of the glycosylphosphatidylinositol (GPI) anchors at the carboxyl terminus for each monomer. Image taken from (Millan and Whyte, 2016).

In vitro studies have shown that ALPs are able to hydrolyse a broad range of substrates, however only a small number have been confirmed as natural substrates of ALP; these include inorganic pyrophosphate (PP_i), as well as phosphoethanolamine and pyridoxal-5′-phosphate (Whyte *et al.*, 1995). PP_i is an inhibitor of mineralisation, which is hydrolysed by TNAP to form inorganic phosphate (P_i), a necessary component for mineralisation of bone tissue (Orimo, 2010). Pyridoxal-5'-phosphate (PLP) was discovered to be a substrate of the TNAP present in leukocytes and the human osteosarcoma cell line SAOS-2. The TNAP in SAOS-2 cells is additionally able to hydrolyse phosphoethanolamine (PEA) (Wilson *et al.*, 1983; Fedde *et al.*, 1988). Human PLAP and intestinal ALP (IAP) were found to hydrolyse all tested phosphatidates, while TNAP was not able to hydrolyse phosphatidates with long fatty acyl chains or another natural substrate for ALPs, inorganic polyphosphate (polyP) (Lorenz and Schroder, 2001). In contrast to mammalian ALPs, ECAP is not able to hydrolyse phosphatidate (Sumikawa *et al.*, 1990). TNAP is additionally able to hydrolyse nucleotides, such as ATP, ADP and AMP (Say *et al.*, 1991), and has also been reported to have phosphodiesterase activity (Rezende *et al.*, 1994).

Mammalian ALPs are ectoenzymes, and are anchored to the exterior of the cell membrane via a glycosylphosphatidyl inositol (GPI) anchor, which is attached post-translationally at the carboxyl terminus (Harris, 1990). GPI anchors are glycolipids found widely in eukaryotes, which function to anchor, as the name suggests, a large variety of proteins to cell membranes. GPI anchors only traverse the outer leaflet of the phospholipid bilayer, allowing the tethered protein to move readily across the surface of the membrane to different locations on the cell or vesicle. GPI-anchored proteins are often associated with lipid rafts, which are groupings of lipidated proteins, cholesterol and glycosphingolipids on the cell surface forming small areas on the cell where the close proximity of its constituents promotes and enhances specific processes such as cell signalling (Paulick and Bertozzi, 2008).

1.2.4 Mammalian ALP isozymes

In humans, four distinct isozymes of ALP are present, encoded at four separate gene loci: three tissue-specific isozymes, namely placental ALP (PLAP), germ cell ALP (GCAP) and intestinal ALP (IAP) and a single tissue-nonspecific ALP isozyme (TNAP). The tissue-specific isozymes are found clustered on chromosome 2, and share a sequence homology of 90 – 98%. TNAP is found on chromosome 1 and has approximately 50% homology to the tissue-specific ALPs (Hoylaerts *et al.*, 2006). The *E. coli* ALP (ECAP), at 471 amino acids long, is only 25% homologous to human TNAP, and 29% homologous to human PLAP. A low degree of homology is, as expected, observed between human and *E. coli* ALPs, and differences in the primary amino acid sequence can be clearly visualised using a multiple sequence alignment of the amino acid sequences of human TNAP, PLAP as well as ECAP (Fig. 1.2.4.1) (Weiss *et al.*, 1986).

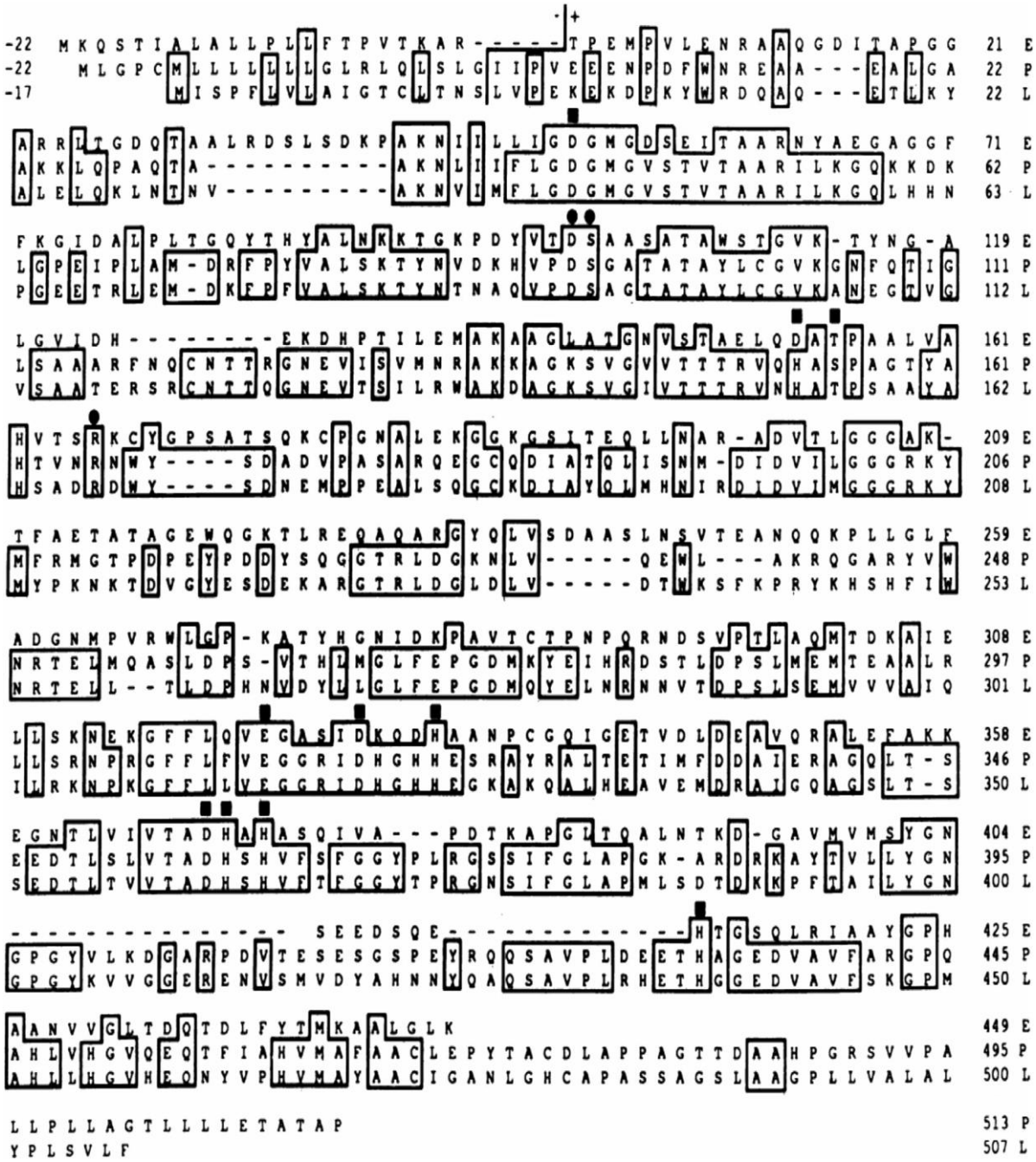

Figure 1.2.4.1: Comparison of the amino acid sequences of E.coli (E), human placental (P), and human L/B/K (L) ALP precursor proteins. Gaps that have been introduced into the sequences to maximise pairing of homolougous amino acids are indicated by -. Amino acid +1 corresponds to the first residue in each of the mature proteins. Amino acids that are identical in all three proteins or in the two human proteins are boxed. Amino acids that comprise the active site region in the *E. coli* ALP, including the metal ligand sites (■) and the residues that interact with substrate phosphate (●), are indicated. Amino acids are shown in single letter code. Taken from (Weiss *et al.*, 1986).

It is currently presumed that an ancestral form of mammalian tissue nonspecific ALP appeared first, and at some point in time a gene duplication event occurred, resulting in the development of one gene into TNAP and the other into an ancestral IAP. It is believed that a

further duplication event of the IAP gene occurred, giving rise to GCAP, followed by another duplication from which PLAP arose (Fishman, 1990). The IAP is assumed to have been the original tissue-specific ALP form, as IAP is present in all mammalian species, while PLAP is only present in humans and apes (Doellgast and Benirschke, 1979; Fishman, 1990). The presumed relationship between the various human ALP isozymes is illustrated in figure 1.2.4.2.

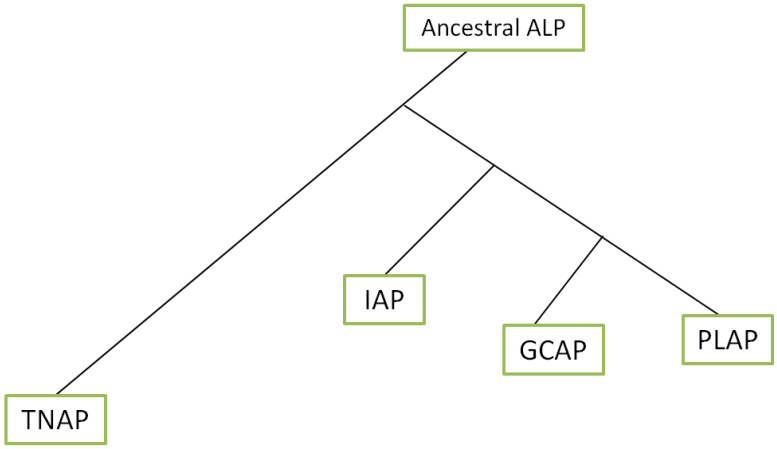

Figure 1.2.4.2: Phylogenetic representation of the presumed relationship between mammalian alkaline phosphatase isozymes. Adapted from Fishman, 1990.

It is worth noting that some ALP isozymes may be absent in some species and present in others. Similar to humans, mice possess four ALP isozymes, however PLAP and GCAP are absent in mice, and instead an intestinal-like ALP (IAP-like) and embryonic ALP (EAP) are present in addition to IAP and TNAP (Hahnel *et al.*, 1990). Moreover, species-specific differences may exist in the tissue distribution pattern of the same ALP isozyme. For example, while rat and human serum contain the bone isoform of TNAP, the predominant ALP present in human serum is the liver isoform of TNAP, while the liver isoform of TNAP is absent in rat serum, and instead the intestinal ALP is the most predominant ALP (Dziedziejko *et al.*, 2005).

1.2.4.1 Tissue-specific ALP isozymes

Human PLAP, as the name suggests, is synthesized in placental tissue, but may also be found in normal serum in trace amounts (Vergote *et al.*, 1992). PLAP has 30% sequence identity with ECAP (Le Du *et al.*, 2001), and 87% sequence identity with IAP (Henthorn *et al.*, 1988). PLAP is heat-stable, and like other mammalian ALPs, is post-translationally modified and contains two *N*-glycosylation sites. Phosphatidates as well as inorganic polyphosphates

(polyP) have been confirmed as natural substrates for PLAP (Millán, 2006), with the enzyme being uncompetitively inhibited by L-amino acids including, L-Phe, and L-Trp and L-Leu (Le Du *et al.*, 2001).

PLAP is expressed most highly during the second and third trimesters, at which time it is also one of the major circulating ALP isozymes, but disappears rapidly from serum after birth (Valenzuela *et al.*, 1987). A role for PLAP in the transferral of maternal IgG to the foetus has been suggested, as well as in cell division in both normal and cancerous cells (Stefaner *et al.*, 1997; She *et al.*, 2000; Le Du *et al.*, 2001). PLAP has been identified as a tumour marker, as it is ectopically expressed in cancer cells, where it is known as the Regan isozyme, named after a patient by the name of Mr. Regan, who had a PLAP-like isozyme of ALP in his cancer cells and serum. This led to the hypothesis that cancer cell progression may result from the deregulation of embryonic genes, or specifically by derepression of the genome in cancer cells, allowing enhanced expression of enzymes in cells or tissues where they are not normally expressed (Fishman *et al.*, 1968; Fishman *et al.*, 1968). PLAP may also be involved in the modulation of foetal growth, as the addition of highly purified PLAP to cultures of NIH 3T3 mouse embryo fibroblasts, as well as human foetal fibroblasts, was able to promote DNA synthesis and cell proliferation, in synergism with Zn^{+}, Ca^{2+} and insulin. She *et al.* suggested that the mitogenic effect of PLAP may be due to the ability of PLAP to activate a variety of growth regulatory enzymes, including c-Raf-1, p42/p44 mitogen-activated protein kinases, p70 S6 kinase, Akt/PKB kinase and phosphatidylinositol 3P-kinase. The mechanism by which PLAP is able to stimulate DNA synthesis and cell proliferation is unknown, and the addition of either TNAP or IAP was not able to stimulate DNA synthesis in the same way as PLAP, indicating that the mechanism may be unrelated to the phosphatase activity of the enzyme (She *et al.*, 2000).

Germ cell ALP (GCAP), also known as placental-like ALP, and is found at low levels in germ cells, as well as in embryonal tissue, testis, thymus, cervix, lung and in trace amounts in placental tissue (Povinelli and Knoll, 1991; Tsai *et al.*, 2000; Sharma *et al.*, 2014). GCAP is heat-stable and has a 98% sequence homology to PLAP. Similarly to PLAP, GCAP, which is also called the Nagao isozyme, (Chang *et al.*, 1980; Goldstein *et al.*, 1982) and may have enhanced expression in cancer cells, such as germ-cell tumours of the testis, and particularly seminomas (Wahren *et al.*, 1979). The Nagao isozyme, was named after the patient in which it was initially discovered, where it was found to have similar properties of heat stability,

immunological properties, electrophoretic mobility and urea sensitivity, but was more susceptible to inhibition by L-Leucine, and also displayed differences in enzyme kinetics compared to PLAP (Nakayama *et al.*, 1970; Millan and Manes, 1988).

IAP is highly expressed in intestinal tissue, both during foetal development and adulthood. Most species have only one IAP isoform, however two IAP isoforms have been identified in rat, and four IAP isoforms in cow (Ghosh *et al.*, 2013; Estaki *et al.*, 2014). IAP is expressed by all gut enterocytes in the duodenum in high levels, and in decreased concentrations in the jejunum, ileum and colon. IAP is secreted from gut enterocytes in luminal vesicles, from both the apical and basolateral surfaces, where it enters the intestinal lumen, as well as the circulation (Estaki *et al.*, 2014).

The cell walls of Gram-positive bacteria contain lipopolysaccharide (LPS), the presence of which in the blood as a consequence of bacterial infection, results in an inflammatory response by the host. IAP is able to dephosphorylate the lipid A moiety on the LPS molecule, which detoxifies the LPS, preventing inflammation and sepsis (Estaki *et al.*, 2014). Nucleotides are known to inhibit the growth of gut bacteria. IAP promotes the growth of aerobic and anaerobic gut bacteria by dephosphorylating ATP as well as other nucleotide triphosphates, found in the lumen (Malo *et al.*, 2014). IAP has anti-inflammatory properties, as the addition of IAP is able to inhibit the release of the inflammatory cytokine IL-8 by cells induced by the presence of pro-inflammatory ligands, such as uridine diphosphate (UDP), LPS, flagellin, Pam3Cys and TNF-α (Moss *et al.*, 2013). Several other functions for IAP have been identified, including modulation of long chain fatty acid (LCFA) absorption in the gut, detoxification of bacterial LPS, which reduces inflammation, as well as the regulation of bicarbonate secretion and gut pH (Lalles, 2010; Estaki *et al.*, 2014; Lalles, 2014).

1.2.4.2 Tissue-nonspecific ALP (TNAP)

TNAP is found at low levels in a large variety of tissues, but predominantly in hepatic, renal and skeletal tissue, for which reason it is often referred to as liver/kidney/bone ALP (LBK ALP) (Sharma *et al.*, 2014). TNAP, like the tissue-specific ALPs, exists either as a homodimer in circulation or a tetramer, where each unit is bound to the outer surface of the cell membrane by a GPI anchor. A high degree of heat stability is present in TNAP compared to tissue-specific ALPs, as a result of the conformation of the crown domain of the enzyme

(Bossi *et al.*, 1993). TNAP occurs in several isoforms, as a result of a large variety of post-translational modifications in the form of glycosylations. The various TNAP isoforms have an identical primary amino acid sequence, are often tissue-specific in expression pattern and vary in the characteristics, such as thermo-stability and sensitivity to various inhibitors (Nosjean *et al.*, 1997; Martins *et al.*, 2001)

1.2.4.2.1 Posttranslational modifications of TNAP

There are differences in glycosylation patterns between the TNAP expressed in bone and liver. O-linked glycosylations are found in bone and kidney TNAP isoforms, but are absent in the liver isoform. Differences concerning the presence or absence of O-glycosylations, as well as the number of O-glycosylations present, are thought to be the main factors contributing to the observed differences between TNAP isoforms, such as heat stability and inhibitor sensitivity (Nosjean *et al.*, 1997). Removal of the O-glycosylations had different effects on the activities of liver and kidney TNAP (Martins *et al.*, 2001). Differences in the activity levels of liver and kidney TNAP isoforms have also been found in the presence of certain drugs such as levamisole, indicating that the activity of these isoforms are not modulated in the same way, which is probably due to differences in glycosylation (Martins *et al.*, 2001). N-linked glycosylation is required for catalytic activity of all three TNAP isoforms, but is not essential for the other tissue-specific ALP (TSAP) isozymes (Martins *et al.*, 2001; Whyte, 2010). By examining the predicted translation of TNAP cDNA, five possible sites for N-linked glycosylation have been proposed in the protein sequence. It is not yet known how many of the possible N-linked glycosylation sites are actually glycosylated, but research has suggested that there is a difference in N-linked glycosylation between the two TNAP isoforms due to differences observed in their immunoreactivity (Nosjean *et al.*, 1997; Whyte, 2010). Heat stability differences between bone and liver TNAP isoforms have also been observed, with heat stability being lowered in both isoforms when the glycosylations are removed (Martins *et al.*, 2001).

The bone TNAP isoform is also found in circulation in the serum in soluble homodimeric form, due to cleavage of the GPI anchor by two endogenous phospholipases: GPI-specific phospholipase C and GPI-specific phospholipase D. Evidence exists that this soluble alkaline phosphatase is physiologically inactive, as infants suffering from hypophosphatasia: a condition resulting in impaired bone mineralisation arising from mutations in the TNAP

gene, who received either purified placental ALP or serum from patients with Paget's bone disease, as these patients have elevated levels of soluble ALP in the serum, showed no sign of clinical improvement (Millán *et al.*, 2006; Whyte, 2010). This however does not prove that that solubilised ALP is completely physiologically inactive.

1.2.4.2.2 Tissue distribution and known functional roles of TNAP isoforms

1.2.4.2.2.1 TNAP in skeletal tissue

The well-established primary function of TNAP in bone tissue is the hydrolysis of inorganic pyrophosphate (PPi) to organic pyrophosphate (Pi). PPi is an inhibitor of mineralisation, while Pi is an essential component needed for mineralisation of collagen-rich osteoid to calcified bone. TNAP has the ability to bind collagen types I, II and X via the crown domain, and therefore the formation of a complex between TNAP and collagen may contribute the function of TNAP within its role in the mineralisation of osteoid to calcified bone (Vittur *et al.*, 1984; Bossi *et al.*, 1993).

1.2.4.2.2.2 TNAP in liver and kidney tissue

In the liver, TNAP is expressed on the apical surface of hepatocytes and cholangiocytes. The constituents of bile, produced in the liver, are highly controlled by the intrahepatic biliary epithelium through the secretion and/or re-adsorption of various components prior to its release into the duodenum. TNAP present on the surface of the intrahepatic biliary epithelial cells plays a role in this regulation by actively down-regulating secretion of bile components (Alvaro *et al.*, 2000). In kidney, research suggests that TNAP may be involved in vascular calcification characteristic of renal failure. This may be due to increased activity of TNAP during conditions of renal impairment, resulting in an increase in hydrolysis of the mineralisation inhibitor PPi, which allows for calcification to occur (Lomashvili *et al.*, 2008).

1.2.4.2.2.3 TNAP in neural tissue

Significant levels of TNAP expression have been discovered in neural tissue, including endothelial cells of the brain (Fonta *et al.*, 2004; Negyessy *et al.*, 2010). The function of TNAP in the brain has not yet been firmly established, however there is evidence that it plays an important role due to the phenomena of epileptic seizures and neurological dysfunction

associated with either hypo- or hyperphosphatasia (Negyessy *et al.*, 2010). Studies in primate species have pointed to the possible role for TNAP in the blood/brain barrier and in neurotransmission (Fonta *et al.*, 2004). Data from various primates, including humans, as well as rat neuronal and endothelial cells show expression of the bone-specific isoform of TNAP, while in mice the liver isoform of TNAP is additionally expressed in neuronal cells (Brun-Heath *et al.*, 2011). TNAP has since been found in endothelial cells and at synaptic contacts within the brain, and the role in γ-aminobutyric acid (GABA) metabolism has been discovered. Pyridoxal-5′-phosphate (PLP) is an essential cofactor for the enzyme glutamate decarboxylase (GAD), the function of which is the synthesis of the inhibitory neurotransmitter, GABA. TNAP hydrolyses PLP to form pyridoxal (PL), and in mice where TNAP was knocked out, the deficiency in TNAP led to an increased level of PLP in the serum, while a decreased level of PLP was observed in neural tissue. The lack of PLP in neural tissue was proposed to lead to the impaired functioning of GAD and a subsequent reduction of GABA. Reduced levels of GABA are responsible for the seizures present in the mutant TNAP phenotype, and could be rescued by treatment of the animals with PL (Waymire *et al.*, 1995; Kellett *et al.*, 2011). In human adults, TNAP is expressed in the synaptic cleft of the nodes of Ranvier. Studies in mice have shown that in TNAP null mice, neurological symptoms including impaired myelination, synaptic dysfunction along with epilepsy are present, consistent with the symptoms which occur in severe hypophosphatasia in humans (Hanics *et al.*, 2012).

Evidence has been found that plasma TNAP is increased in patients with Alzheimer's disease (AD), where lower cognitive function in patients is associated with higher levels of plasma TNAP (Kellett *et al.*, 2011). The role of neuronal TNAP in AD is related to its ability to dephosphorylate hyperphosphorylated tau protein. AD is a neurodegenerative disease which is characterised by the presence of plaques of amyloid-β peptide and extracellular neurofibrillary tangles, consisting of the microtubule associated protein, tau. In AD, hyperphosphorylated tau protein disassociates from microtubules and forms aggregates inside neurons, causing degeneration and death of the neuron (Gomez-Ramos *et al.*, 2006; Diaz-Hernandez *et al.*, 2010). TNAP dephosphorylates the hyperphosphorylated tau protein, which may be aggregated or soluble, which then binds to muscarinic receptors M1 and M3 on adjacent neuron, inducing an increase in intracellular calcium levels (Diaz-Hernandez *et al.*, 2010).The disruption in calcium homeostasis which results is toxic to the neuron, resulting in neuronal death and further release of tau protein. Results using the neuroblastoma cell line,

SH-SY5Y, showed that TNAP expression increased when muscarinic receptors were activated by dephosphorylated tau, which has been proposed to be induced by the increase calcium concentration (Diaz-Hernandez *et al.*, 2010). A further function for neuronal TNAP has been postulated, wherein TNAP protagonistically affects the interaction of cellular prion protein (PrP^C) with the cell adhesion molecule, laminin, by altering the phosphorylation state of laminin, as laminin is thought to be a substrate of TNAP. The interaction of PrP^C with laminin is thought to be dependent on the phosphorylation state of laminin. PrP^C is a membrane-bound protein thought to be involved in cell signalling, as well as having a function as a membrane receptor. The regulation of laminin-PrP^C binding by TNAP may therefore also contribute to neuronal homeostasis (Ermonval *et al.*, 2009).

1.2.4.2.2.4 TNAP as a stem cell marker

The expression and regulation of alkaline phosphatases appears to be dependent on the cellular microenvironment, as well as the differentiation status of cells and tissues, both *in vivo* and *in vitro*. This makes ALP expression a good differentiation marker for certain cell types (Stefkova *et al.*, 2015). A high level of ALP activity has long been a marker for pluripotent stem cells, both in humans and mice, including embryonal cancer (EC), embryonic germ (EG), embryonic stem (ES) and induced pluripotent stem (iPS) cells (Stefkova *et al.*, 2015). The ALP isozymes expressed in stem cells include germ cell ALP (GCAP) in humans and embryonic ALP (EAP) in mice, as well as TNAP, while the remaining TSAPs are associated with more differentiated cells and tissues. TNAP is the main ALP of interest in the stem cell field, as in humans, TNAP is more widely and abundantly expressed than GCAP (Stefkova *et al.*, 2015).

In mice, EAP is mainly expressed in preimplantation embryos, however, from embryonic day 7 to 14, EAP decreases rapidly, and TNAP becomes the predominantly expressed ALP in primordial germ cells (PGCs) as they migrate towards the developing gonad (Hahnel *et al.*, 1990). In humans, GCAP rather than TNAP remains in migrating PGCs (Stoop *et al.*, 2005). TNAP expression is also high in mouse ES, EC, EG and PG cells (Ginsburg *et al.*, 1990; Narisawa *et al.*, 1997; Stefkova *et al.*, 2015). Stefkova *et al.* suggest that the shift in expression between ALP isozymes during development may be due to the changing environment of the cells during development, where different isozymes of ALP are better

suited to changing environmental conditions of the cells as development proceeds (Stefkova *et al.*, 2015).

Although ALP expression is high in ES cells, it has not been proven to be a universal stem cell marker for other stem cells, including adult stem cells. TNAP expression has been observed in some neural cells from populations which are rich in neural stem cells and progenitors, where TNAP expression was more associated with the behaviour, such as proliferation and migration, rather than phenotypic differences of the cells (Langer *et al.*, 2007). It was discovered by Sobiesiak *et al*. that TNAP is identical to mesenchymal stem cell antigen-1 (MSCA-1) (Sobiesiak *et al.*, 2010) which has long been used to aide identification of MSC populations, along with other markers (Battula *et al.*, 2009; Alexander *et al.*, 2010; Sobiesiak *et al.*, 2010). The presence of TNAP in naïve unexpanded human bone marrow-derived MSCs (bmMSCs) was variable, meaning that some cells expressed TNAP and some cells did not. Naïve bmMSCs expressing TNAP had less multipotential capacity and greater expression of osteogenic-related genes, while naïve bmMSCs that did not express TNAP could be differentiated into either osteogenic, adipogenic and chondrogenic lineages (Kim *et al.*, 2012). In 2013, Kollmer *et al*. detected TNAP expression in human MSCs derived from bone marrow while these cells were undergoing adipogenesis, in addition to the presence of the bone-specific markers osteopontin and osteocalcin (Kollmer *et al.*, 2013). In the same study, the adipogenic markers, adiponectin and leptin were identified in the human MSCs when induced towards an osteoblast phenotype. These results further illustrate the known plasticity observed between the adipogenic and osteogenic lineages (Kollmer *et al.*, 2013).

Interestingly, a high level of TNAP expression characterises pluripotency in pluripotent stem cell phenotypes, however a high level of TNAP expression in adult stem cell populations corresponds to differentiation and a reduction in stemness (Stefkova *et al.*, 2015).

1.2.4.2.2.5 TNAP in adipogenic differentiation

TNAP is well established as a marker for osteogenesis, however it has been found that it may also play a role in adipogenesis (Ali *et al.*, 2005). Steroid hormones, and particularly the steroid hormones known as glucocorticoids (GCs), have been found to stimulate adipocyte differentiation as well as regulate fat metabolism (Grégoire *et al.*, 1991). GCs have anti-inflammatory and immunosuppressive properties and have been used successfully for the

treatment of asthma, inflammatory bowel disease as well as arthritis and spinal cord injuries, however long term use of GCs can result in loss of bone density (Lin *et al.*, 2010). Studies have shown that both ALP mRNA and protein expression levels were inhibited after treatment of primary cultured rat bmMSCs with the GC, dexamethasone (Dex) and levels of the adipogenic markers PPARγ and aP2 were up-regulated in a dose-dependent fashion, resulting in the cells differentiating into adipocytes, implying that TNAP is not involved in adipogenic differentiation of these cells (Lin *et al.*, 2010). In contrast, a study using the murine preadipocyte cell line 3T3-L1 found that upon addition of either of the ALP inhibitors, histidine or levamisole, after initiation of adipogenesis using adipogenic medium containing Dex, insulin and 3-isobutyl-1-methylxanthine (IBMX), a decrease in both ALP activity and lipid accumulation was observed (Ali *et al.*, 2006). Levamisole is known to be an uncompetitive inhibitor of TNAP, while the mechanism of inhibition by histidine is uncertain (Cyboron *et al.*, 1982; Ali *et al.*, 2006). The ALP inhibitor Phe-Gly-Gly did not alter ALP or lipid accumulation in the same experiment, as it is known that Phe-Gly-Gly is a tissue-specific ALP isozyme inhibitor (Ali *et al.*, 2005), confirming a possible role played by TNAP in lipid accumulation. A further study using 3T3-L1 cells and primary cultured human preadipocytes showed ALP activity and lipid accumulation was blocked by histidine after the initiation of adipogenesis in these cells (Ali *et al.*, 2006). Furthermore, only IBMX was found to be crucial for adipogenesis as removal of this from the growth medium prevented lipid accumulation and blocked ALP activity (Ali *et al.*, 2006). These findings present strong evidence for the involvement of TNAP in lipid accumulation, as ALP activity was found to be directly affected when adipogenesis was inhibited (Ali *et al.*, 2006). It is also believed that TNAP in 3T3-L1 and human preadipocytes is localised to the membrane surrounding the lipid droplets as ALP activity has been identified in this area and co-localises with perilipins. As these are a family of proteins that bind to the surface of lipid droplets, where perilipin 1 is known to play a role in mediating lipolysis as well as modifying the structure of the lipid droplet (Wang and Sztalryd, 2011), this co-localization suggests strongly that TNAP may be involved in control of lipid accumulation within these cells (Ali *et al.*, 2005; Ali *et al.*, 2006).

1.2.5 Genetics of TNAP

In humans, the TNAP gene (designated *ALPL*) is present as a single copy in the haploid genome, located on the distal arm of chromosome one, at bands p34-p36.1 and stretches over a region of approximately 50 kb (Smith *et al.*, 1988; Weiss *et al.*, 1988). The *ALPL* homolog

in mice is designated as *Akp2* (Studer *et al.*, 1991), and in rats as *Alp1* (Toh *et al.*, 1989b). The TNAP gene from humans, rats and mice has been shown to consist of 13 exons, where the first two exons are noncoding, designated as exons 1a and 1b, followed by 11 coding exons interspersed between large introns (Toh *et al.*, 1989b; Matsuura *et al.*, 1990; Studer *et al.*, 1991). The first two exons (1a and 1b) are separated from one another by introns and also have separate promoter regions, which allows for either exon 1a or 1b to be incorporated into the mRNA in a mutually exclusive fashion. The second exon (exon II) is separated from exons 1a and 1b by a large introns, and contains a 5′-untranslated region as well as the translation start site ATG, while the final coding exon (exon XI) contains the translation stop site and a 3′-untranslated region (Weiss *et al.*, 1988). The structure of the *ALPL* gene is illustrated in figure 1.5.1. The arrangement of the *ALPL* gene allows for the production of two different mRNA molecules, which encode the same primary amino acid sequence, but have different 5′-untranslated regions (Studer *et al.*, 1991; Millán, 2006).

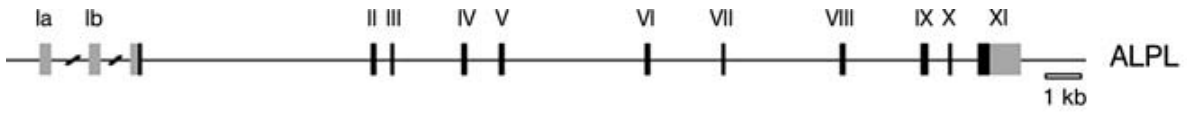

Figure 1.2.5.1: Representation of the genomic structure of the human ALPL gene. Exons are shown in black while the 5′- and 3′-untranslated regions are shown in grey. Taken from (Millán, 2006).

It has been found that in humans and rats, the upstream promoter (1a) is primarily used in osteoblasts, giving rise bone-type mRNA, while the downstream promoter (1b) is used mainly in kidney and liver tissues, where the mRNA transcript produced is referred to as liver-type mRNA (Zernik *et al.*, 1991; Sato *et al.*, 1994). The promoter activity of exon (1b) is five times weaker than that of the 1a promoter in neutrophilic granulocytes (Sato *et al.*, 1994). The TNAP present in human neutrophils cultured *in vitro*, is found on the plasma membrane and on the inner surface of secretory vesicles, however the expression of TNAP in the neutrophils of other species is variable, for example, TNAP is also found in the granulocytes of cows, horses and rabbits, but is absent from the granulocytes of cats, dogs and mice (Jain, 1968; Hulme-Moir and Clark, 2011). While the function of TNAP in neutrophils is unclear at present, it serves as a marker for different leukocyte populations and for tracking the location of secretory vesicles within the cell (Hulme-Moir and Clark, 2011). Bone-type mRNA is exclusively expressed in the neuronal and endothelial cells of brain tissue from humans, marmosets and rats, while mouse neurons additionally express liver-type

mRNA (Brun-Heath *et al.*, 2011). The alternative designation of 1B (B for bone) and 1L (L for liver) for exon 1a and 1b indicate the tissue where each TNAP isoform is preferentially expressed (Sato *et al.*, 1994; Millán *et al.*, 2006; Orimo, 2010). In mice, the 1a promoter is used preferentially for all TNAP-expressing tissue types except heart tissue, where the liver-type mRNA is expressed at high levels (Studer *et al.*, 1991). The upstream promoter (1a) contains several regulatory elements which may influence the expression of TNAP, these include a TATA box, four Sp1 binding sites and a retinoic acid response element (Sato *et al.*, 1994).

Several factors are known to increase TNAP expression in human cells, these include retinoic acid, cyclic AMP (cAMP) (Gianni *et al.*, 1993), the transcription factor Sp3, which is part of the same family of transcription factors as Sp1, and binds to a consensus GC box on the 1a promoter region (Yusa *et al.*, 2000), progestin, which induced TNAP expression in the human breast cancer cell line T47D (Di Lorenzo *et al.*, 1991), as well as granulocyte colony-stimulating factor (G-CSF), which was suggested to play a role in the regulation of TNAP expression in polymorphonuclear cells (PMNs) (Rambaldi *et al.*, 1990). It has been reported that TNAP expression was induced in a human osteoblast-like cell line, SaOS-2, using β-glycerophosphate and NaH_2PO_4, which may be due to an indirect signalling mechanism whereby the phosphate released from the hydrolysis of β-glycerophosphate induces a signal to increase TNAP expression, as neither of these compounds were found to directly increase TNAP at the transcriptional level (Orimo and Shimada, 2008). It has been reported that *ALPL* gene expression is regulated by DNA methylation of a CpG island on the proximal end of the *ALPL* gene. DNA methylation may occur where a cytosine precedes a guanine along the DNA sequence. It was reported in this study that the amount of TNAP activity in primary human osteoblasts, and the osteoblastic and mammary cell lines, MG-63 and MCF-1 respectively, was inversely correlated to the amount of DNA methylation present at the CpG island, i.e. the greater the methylation, the lower the amount of TNAP transcription (Delgado-Calle *et al.*, 2011).

1.2.6 Genetic mutations of TNAP – hypophosphatasia

Over 200 missense mutations in *ALPL*, the human gene for TNAP, have been reported to date and result in an inborn disorder known as hypophosphatasia (Orimo, 2010; Whyte, 2010). Hypophosphatasia is characterised by impaired mineralisation of bone throughout the body

with symptoms similar to rickets and osteomalacia (softening of bone) (Millán *et al.*, 2006; Orimo, 2010). The degree of severity of hypophosphatasia varies widely depending on which mutation is present in the ALPL gene, and can range from stillbirth or death in early infancy to merely teeth problems in adulthood. Hypophosphatasia has been found to affect only hard tissues, while liver and other tissues expressing TNAP in significant quantities are seemingly unaffected (Whyte, 2010). Bone TNAP is found to be naturally present in circulation. However, evidence suggests that these proteins are not physiologically active when found soluble in the serum, as administration of serum containing soluble TNAP does not ameliorate the effects of hypophosphatasia to a satisfactory level (Orimo, 2010; Whyte, 2010). No effective treatment for hypophosphatasia is available at present, although positive results have been obtained using allogenic mesenchymal stem cells for treatment of infantile hypophosphatasia (Tadokoro *et al.*, 2009). Along with the development of TNAP-knockout mice (Orimo, 2010), studies of hypophosphatasia remain useful for gaining insight into the function of TNAP in humans.

1.2.7 Mesenchymal stromal cells (MSCs)

Both osteoblasts and adipocytes are derived from the same progenitor cells, namely mesenchymal stromal cells (MSCs). TNAP has been clearly defined as a highly necessary constituent for mineralisation (Whyte, 2010) and increased expression of TNAP in MSCs has been conventionally used as a marker for osteogenesis (Rebelatto *et al.*, 2008). More recently, it has been discovered that TNAP may also be involved in adipogenesis, prompting further investigation into the function of TNAP in MSC differentiation.

MSCs are defined according to their spindle shape, plastic-adherent nature, and their ability to differentiate into cells of tissues such as osteoblasts found in bone, adipocytes in fat tissue, myocytes in muscle tissue and chondrocytes, from cartilage, as well as into cells which have other functional properties, including the tempering of immuno-inflammatory functions and stromagenesis (Pittenger *et al.*, 1999; Covas *et al.*, 2008; Casteilla *et al.*, 2011). MSCs may also be able to differentiate towards neuronal and smooth muscle phenotypes (Fig. 1.2.7.1) (James, 2013). MSCs can be isolated from a variety of different tissues, including bone marrow, adipose tissue and umbilical cord blood, although these cells are most commonly derived from bone marrow or adipose tissue (Chen *et al.*, 2007; Gazit *et al.*, 2008). Interest in MSCs has been increasing greatly in recent years due to their possible uses in tissue

regenerative therapy, as well as for treatment of tumours (Horwitz *et al.*, 2007; Rebelatto *et al.*, 2008; Keating, 2012). The acronym MSC originally stood for mesenchymal stem cell, however it has been discovered that the plastic adherent cells isolated from various tissues mentioned earlier frequently exist as a heterogeneous population *in vitro*. Although the cells isolated and cultured in this way do exhibit multipotentiality, they may not meet the specific criteria to allow them to be designated as stem cells, such as the capacity for long-term self-renewal, as well as the ability to differentiate into multiple cell types *in vivo.* The existence of true mesenchymal stem cells is not in dispute, and it is likely that they form a sub-population of plastic-adherent cells. The issue remains that unless the cells in question have been thoroughly evaluated for the aforementioned stem cell characteristics, they should be designated as stromal cells, and thus eliminate any confusion about their exact nature (Horwitz *et al.*, 2005). These observations led investigators to propose that mesenchymal stem cells be renamed multipotent mesenchymal stromal cells, to allow for a more strict definition of stem cell characteristics (Horwitz *et al.*, 2005; Horwitz *et al.*, 2007). Despite this proposal, many researchers continue to use the name "mesenchymal stem cell" in publications, resulting in a situation where both names are frequently used in the literature to describe the same cells.

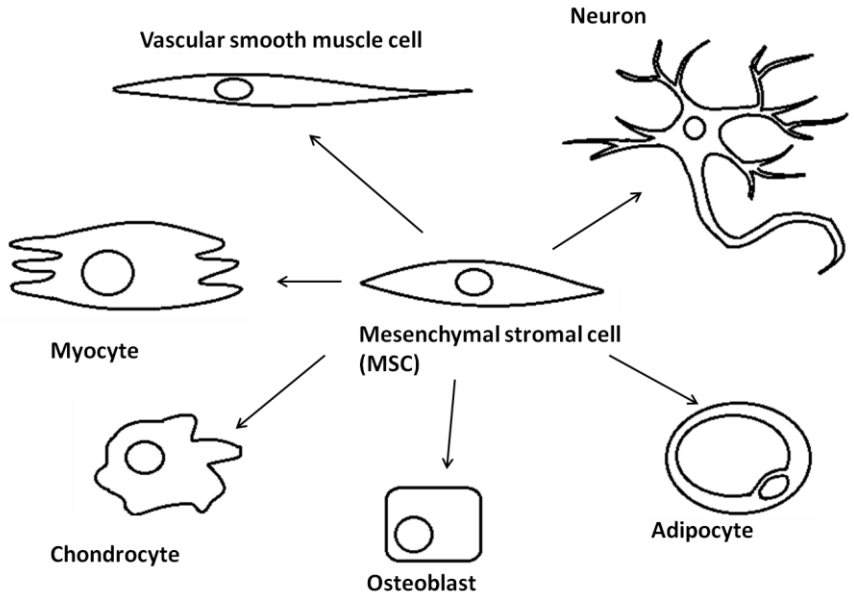

Figure 1.2.7.1: Representation of the multilineage differentiation potential of mesenchymal stromal cells (MSCs). MSCs are able to differentiate towards adipocytic, osteoblastic, chondrogenic, myogenic, neuronal as well as smooth muscle lineages. Adapted from (James, 2013).

Defining a set of characteristics that can be used to accurately and reliably identify MSCs has proven to be a challenging task for researchers, and as of yet there are no set criteria for identification of MSCs *in vivo.* However, basic *in vitro* purification allows MSC characteristics to be assessed (Chen *et al.*, 2007). According to the International Society for Cellular Therapy (ISCT), the three criteria for a population of cells to be defined as MSCs are the ability of the cells to differentiate into bone, fat and cartilage *in vitro*, plastic adherence, expression of the markers CD105, CD73 and CD90, plus a lack of expression of the haematopoietic marker, CD45 as well as CD11b or CD14, CD19 or CD79α and HLA-DR, in over 95% of the cell culture population (Brinchmann, 2008; Liu *et al.*, 2009; Gimble and Nuttall, 2012; Fernandez Vallone *et al.*, 2013). MSCs isolated from different tissues exhibit similar, but not identical properties to bone marrow-derived MSCs, such as variation in aspects related to their differentiation potential (Rebelatto *et al.*, 2008). Although much has been learnt about MSCs since their discovery in the 1960's, there is still much about the nature of these cells that remains unknown. For example, a paper by Qian *et al*. highlighted that CD44, a surface marker thought to be characteristic of MSCs, is in fact not expressed on primary MSCs, with CD44 expression proposed to be a result of prolonged *in vitro* culture (Qian *et al.*, 2012).

To date, the routine therapeutic use of MSCs is limited, with only bone marrow cells and umbilical cord blood cells being used in bone marrow transplants and umbilical cord cells for transplantation. All other therapeutic uses of MSCs and other stem cells remain mainly experimental, with clinical trials ongoing (Casteilla *et al.*, 2011; da Silva Meirelles and Nardi, 2011). Genomic instability of *in vitro* cultured rat bone marrow-derived mesenchymal stromal cells (bmMSCs) has been reported, whereas the genome of human MSCs has been found to be relatively stable in culture, indicating that caution should be taken when extrapolating data obtained using an animal MSC model for human MSC therapy (Foudah *et al.*, 2009). Research into the uses of MSCs in regenerative medicine is ongoing, with current investigations examining MSC therapy for regeneration of bone, fat and muscle and other somatic tissue (Horwitz, 2003; Derubeis and Cancedda, 2004; Rebelatto *et al.*, 2008).

The main source of MSCs for therapy has, up until recently, been limited to cells derived from bone marrow and stem cells from umbilical cord blood. The discovery of cells present in adipose tissue with similar properties to bmMSCs has had implications for therapy, as adipose tissue is more abundant and more easily- and less invasively obtained (Casteilla *et*

al., 2011). However, as stated earlier, differences in differentiation potential and other characteristics exist between MSCs derived from bone marrow and those derived from adipose tissue, and also between cells derived from different adipose tissue depots (Levi *et al.*, 2010). Many researchers use the term "MSC" to describe cells isolated from both bone-marrow and adipose tissue, however it has been put forward that the differences between the cells isolated from these tissues are so significantly large as to prompt some researchers to suggest that bone marrow-derived MSCs and adipose-derived MSCs be distinguished from one another in the literature, such that MSC refers specifically to bone marrow-derived cells and ADSC (adipose-derived stromal cell) refers to adipose-derived cells (Gimble *et al.*, 2007; Casteilla *et al.*, 2011). For this reason, it will be useful to discuss the characteristics of both bone marrow-derived mesenchymal stromal cells (bmMSCs) and adipose-derived stromal cells (ADSCs), including their similarities and differences.

1.2.7.1 Bone marrow-derived mesenchymal stromal cells (bmMSCs)

Bone marrow-derived MSCs reside *in vivo* in the bone marrow stroma, and are thought to be the precursor cells of osteoblasts. These bmMSCs are thought to occur in the vascular sinusoids of the bone marrow stroma, existing as CD146+ perivascular subendothelial cells. The CD146+ cells that reside in the bone marrow stroma are thought to be essential for the establishment of the haematopoietic microenvironment within the bone marrow, and interactions between bmMSCs and haematopoietic stem cells may play a role in the regulation of haematopoiesis (Sacchetti *et al.*, 2007; Kassem *et al.*, 2008). Bone-marrow derived MSCs from humans are often isolated from bone marrow samples aspirated from the periphery of large bones such as the femora or ilium. The aspirate is often processed by washing and density centrifugation to remove red blood cells where after the resulting bone marrow mononuclear cells (MNSCs) are seeded onto tissue culture plastic with the appropriate growth media. The bmMSCs are identified via plastic adherence and the ability of the cells to form colonies, and thus they are given the name colony forming unit-fibroblasts (CFU-F) (Song and Tuan, 2004; Kassem *et al.*, 2008; Rebelatto *et al.*, 2008). Bone marrow isolations frequently contain haematopoietic stem cells which although are less plastic adherent than bmMSCs, still results in the contamination of bmMSC cultures. Furthermore, bmMSC cultures are largely heterogeneous, meaning that the cells cultured in this way differ in their differentiation potential, with only a percentage of cells being true mesenchymal stem cells. Up until recently, the available markers have not been able to

distinguish true mesenchymal stem cells from the heterogenous population of bmMSCs to a greater degree than selection by plastic adherence (Kassem *et al.*, 2008). Additionally, prolonged *in vitro* culture of bmMSCs results in changes in the surface marker expression of these cells (Boiret *et al.*, 2005), making it difficult to identify *in vivo* characteristics of bmMSCs from *in vitro* studies. Recent research has identified two markers in humans and mice, platelet-derived growth factor receptor-α (PDGFR-α) and stem cell antigen-1 (Sca-1) which when expressed together in MSCs derived from bone-marrow or collagenase digested bone of mice, identify cells that have an enhanced self-renewal and the capacity for differentiation into osteoblasts, adipocytes and chondrocytes. These markers may be useful in identifying MSCs *in vivo* and will allow for a better understanding of the true nature and function of these cells *in vivo*, which will hopefully lead to advances in their use for therapy (Sacchetti *et al.*, 2007; Houlihan *et al.*, 2012; Mabuchi *et al.*, 2013) .

1.2.7.2 Adipose-derived mesenchymal stromal cells (ADSCs)

ADSCs have been found to reside in the vascular stroma of adipose tissue. In humans, ADSCs have been commonly isolated from the adipose tissue discarded from liposuction surgeries, known as lipoaspirates, as well as from surgical excision (Locke *et al.*, 2011). The adipose tissue obtained by either method is usually washed to remove blood and then digested with collagenase in order to break down the connective tissue. The cells that are released as a result of collagenase digestion are termed the stromal vascular fraction (SVF) and are able to be separated from the mature adipocytes via centrifugation on account of the buoyancy of the latter. The SVF is then seeded onto tissue culture grade plastic dishes with the appropriate growth medium (Casteilla *et al.*, 2011; Locke *et al.*, 2011). Researchers have over the years given various names to the cells derived from this method, including pre-adipocytes, processed lipoaspirate cells, stromal cells, and adipose-derived stromal cells (ADSCs), the latter being the definition used in this review (Locke *et al.*, 2011).

Before multipotential ADSCs can become adipocytes, they must first become committed to the adipocyte lineage, and once this commitment occurs, the cells are termed pre-adipocytes. *In vivo* commitment of multipotential ADSCs to the adipocyte lineage occurs when there is an excess of energy intake and increased transport of glucose into fat cells (Shepherd *et al.*, 1993). The exact mechanisms involved in adipocyte lineage commitment have yet to be determined, however several molecular factors have been discovered which activate lineage

adipocyte lineage commitment, including bone morphogenic protein (BMP) -4 (Tang *et al.*, 2004; Bowers *et al.*, 2006) as well as BMP-2 (Sottile and Seuwen, 2000; Huang *et al.*, 2009). The pre-adipocytes will then differentiate into adipocytes when stimulated, after first undergoing several rounds of mitotic cell division (Bowers and Lane, 2007; Tang and Lane, 2012). The full differentiation and clinical potential of ADSCs is unknown. Adipose tissue has a well established endocrine function, and is known to secrete hormones and adipokines (Wang *et al.*, 2008; Casteilla *et al.*, 2011). Thus far, the truly functional differentiation of ADSCs into a either the adipocytic, osteoblastic or chondrogenic lineage has not be conclusively demonstrated: It has been suggested that these cells are only expressing certain markers specific for the differentiated phenotype, while continuing to express other markers, indicating that the cells have not fully and functionally differentiated into the cell type which they may resemble phenotypically (Rose *et al.*, 2008; Casteilla *et al.*, 2011). Another possibility for the above observation may be that the marker expression pattern of each differentiated cell type as it appears *in vivo* is not yet fully understood, and differentiated cell types may share markers. The known plasticity between adipocytic and osteoblastic lineages may indicate that certain markers are indeed naturally common to both cell types (Kollmer *et al.*, 2013). A deeper, more thorough investigation into their biology is extremely important if these cells are going to be used clinically. More knowledge needs to be gained regarding the differentiation of ADSCs, as their potential for differentiation into lineages other than adipocytes is not fully understood. Furthermore, the differences in purity of cell populations and possibilities of contaminating cell types in ADSC cultures needs to be addressed (Locke *et al.*, 2011). A further consideration is that there are differences in the differentiation potential between ADSCs derived from different adipose tissue depots in the body, as observed in both humans and rats (Levi *et al.*, 2010; Sadie-Van Gijsen *et al.*, 2010).

1.2.8 MSC differentiation – osteoblastogenesis and adipogenesis

As previously stated, MSCs are capable of differentiating into multiple lineages, including osteoblasts, adipocytes, chondrocytes and myocytes, however, crosstalk is known to occur between adipose and skeletal tissue via molecules secreted by the cells of these tissues, which contributes to homeostasis (Gomez-Ambrosi *et al.*, 2008). The following section will discuss the mechanisms involved in MSC differentiation towards adipocytic and osteoblastic lineages.

1.2.8.1 Osteoblastogenesis

Osteoblastogenesis is the process whereby undifferentiated MSCs or osteoprogenitor cells differentiate into osteoblasts. The established markers for osteoblastogenesis include Cbfa-1/Runx2, Osterix, TNAP, bone sialoprotein and osteopontin (Post *et al.*, 2008). Runx2 is a key osteoblastic transcription factor that is expressed early during embryonic development, and activates progenitor cells to differentiate towards an osteoblastic lineage. In differentiated osteoblasts, Runx2 autoregulates it's own expression, and is the first transcriptional activator of a cascade of genes related to extracellular matrix (ECM) deposition, including osteopontin, osteocalcin and type I collagen. (Ducy *et al.*, 1999). Together with Runx2, other important transcription factors including transcription factor 7 (Sp7) and bone morphogeneic proteins (BMPs) function to direct naïve MSCs towards an osteoblastic lineage (Ding *et al.*, 2009; Tokuzawa *et al.*, 2010). Additional transcription factors supporting osteoblastogenesis include Msx2, tafazzin, Wnt5a and Wnt10b, CEPBβ and basic helix-loop-helix (bHLH) family member e40 (Bhlhe40). Recently, a transcription factor named Inhibitor of DNA binding 4 (Id4), belonging to the bHLH superfamily, has been identified in osteoblasts and functions to stabilise Runx2, thereby aiding its activity (Tokuzawa *et al.*, 2010). Another recently identified transcription factor, known as Maf (or c-Maf), of the basic leucine-zipper type, has been identified as important for osteoblastogenesis. The expression of Maf has been found to decrease as oxidative stress increases, which is common with aging. The study of Maf may be useful in understanding the causes of age-related bone loss and senile osteoporosis (McCauley, 2010; Nishikawa *et al.*, 2010).

The cyokines, tumour necrosis factor (TNF)-α and interleukin (IL)-1β are known to decrease bone formation and increase bone resorption in inflammatory diseases such as rheumatoid arthritis, and in contrast, evidence exists that these cytokines may stimulate the formation of ectopic bone in diseases such as type II diabetes and atherosclerosis (Ding *et al.*, 2009). TNFα and IL-1β together stimulated the expression of TNAP, resulting in increased mineralisation in human MSCs grown in osteoblastic differentiation medium, while the presence of the same cytokines caused a reduction Runx2 and COL1A2 (type I collagen) expression. The decrease in type I collagen synthesis caused by a reduction in Runx2 expression has been suggested as the reason for the decreased bone formation seen in rheumatoid arthritis, as osteoblasts are not able produce ECM, which consists predominantly of type I collagen, which needs to be laid down before mineralisation and bone formation can

occur. The ectopic mineralisation present in atherosclerosis is possibly facilitated by the increased expression of TNAP, stimulated by the inflammatory cytokines. It is proposed that an increased hydrolysis of the mineralisation inhibitor, PPi, results in ectopic bone formation. This also indicates that RUNX2 is not essential for mineralisation to occur, but rather only collagen-rich tissue and TNAP expression are necessary (Ding *et al.*, 2009). Additional protein markers of osteoblastogenesis include bone sialoprotein (BSP), as well as osteocalcin (OC) (Atmani *et al.*, 2003). BSP is present in osteoblasts, hypertrophic chondrocytes as well as osteoclasts, and its functional role in osteoblasts appears to be the initiation of hydroxyapatite crystal formation during mineralisation (Malaval *et al.*, 2008). OC is expressed exclusively by osteoblasts and is the most abundant protein in the ECM aside from collagen. Although OC is an osteoblast marker, it appears to inhibit osteoblast function, and in normal bone tissue acts as a negative regulator of bone formation (Ducy *et al.*, 1996).

An additional factor influencing osteogenesis is gravity, as it has been demonstrated that conditions of micro-gravity, as experienced by astronauts on prolonged space missions, leads to a loss in bone mineral density (Zayzafoon *et al.*, 2004). Human bone marrow-derived MSCs cultured for 7 days under micro-gravity simulations on earth, using the Rotary Cell Culture System (RCCS) after the initiation of osteogenesis at normal gravity, did not differentiate into osteoblasts, even after the cultures were returned to normal gravity and cultured for a further 30 days under osteogenic conditions. The investigators of the above experiment reported the complete inhibition of expression of the osteogenic markers, TNAP, COL 1A1, a major part of collagen type 1 and osteonectin, as well as suppression of Runx2 expression, after 7 days of micro-gravity culture (Zayzafoon *et al.*, 2004).

1.2.8.1.1 Basic biology of bone

Bone tissue deposition is performed by cells known as osteoblasts, which develop from preosteoblast precursor cells. Osteoblasts are responsible for depositing osteoid, or proteinatious, non-mineralised bone matrix consisting mainly of closely packed and highly crosslinked type I collagen, and shed extracellular matrix vesicles (MVs) which participate in bone matrix mineralisation by depositing calcium phosphate ($CaPO_4$) in the form of hydroxyapatite crystals into the matrix (Franz-Odendaal *et al.*, 2006; Blair *et al.*, 2007). During the progression of the osteoblasts life cycle, less active cells are buried in the bone matrix laid down by other more active osteoblasts. These buried osteoblasts then develop into

osteocytes, the predominant cell type found in bone, with long processes that travel throughout the bone matrix and connect the buried osteocytes to one another via gap junctions, forming an osteocyte network (Franz-Odendaal *et al.*, 2006; Blair *et al.*, 2007). Gap junctions also connect the buried osteocytes to a layer of osteoblasts on the bone surface, allowing for nutrients and minerals from the extracellular fluid to reach cells buried in the bone matrix. Gap junction-connected osteocytes and osteoblasts exist in groups separate from one another and each of these groups is referred to as an osteon (Blair *et al.*, 2007).

Osteoclasts are another cell type within bone, distinct from osteoblasts and osteocytes, and function in bone resorption in order to facilitate bone remodelling. Osteoclasts are members of the monocyte/macrophage family and are derived from haematopoietic precursors (Lacey *et al.*, 1998). Osteoclasts are able to liberate calcium from the mineralised bone matrix by attaching themselves closely to the bone surface and creating a micro-compartment called a resorption lacuna. The osteoclast transports H^+ ions into the resorption lacuna, which creates an acidic environment causing the hydroxyapatite crystals to dissolve, where after the Ca^{2+} is released into the extracellular fluid, where it may be used by cells throughout the body for calcium signalling and numerous other cellular regulation processes including attachment, motility and cell survival (Blair *et al.*, 2007). Ca^{2+} and PO_4^{3-} may also be released from the skeleton in order to counteract a pH imbalance in the body (Blair *et al.*, 2007). Interactions between osteoblasts, osteocytes and osteoclasts allow for a balance of bone deposition and resorption to be maintained at calcium homeostasis within the body (Franz-Odendaal *et al.*, 2006).

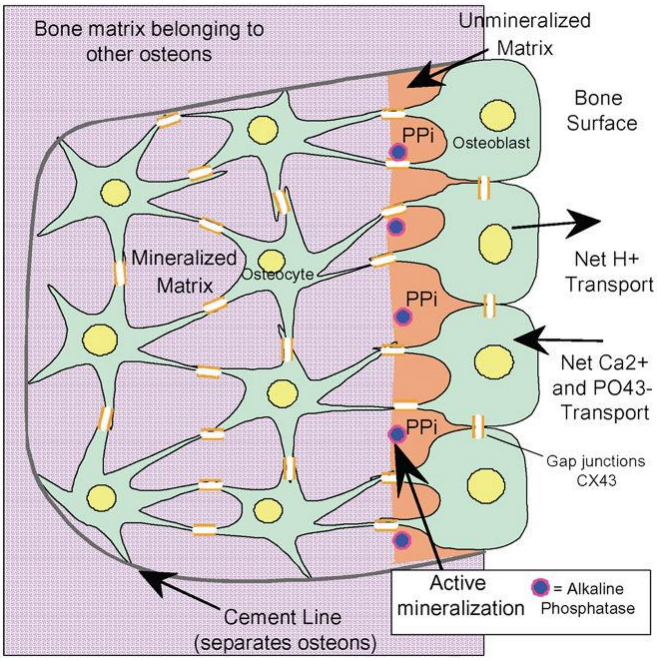

Figure 1.2.8.1.1: Organisation of osteoblasts and osteocytes in the osteon, depicting the process of mineralization. The osteocytes, which develop from osteoblasts, are buried in mineralized bone matrix, are connected to one another and to the osteoblasts on the bone surface by gap junctions containing connexin-43 (CX43). Mineralisation occurs at the interface between the mineralised and unmineralised matrix. The transportation of Ca^{2+} and PO^{-}_{4} ions is towards the site of mineralization, while H^{+} ions generated from the chemical formation of hydroxyapatite are transported away from the mineralization site. Taken from (Blair *et al.*, 2007).

1.2.8.1.2 Bone mineralisation

Mineralisation of endochondral bone, which is bone formed by the mineralisation of cartilage, is initiated by the formation of hydroxyapatite crystals within the extracellular matrix consisting of non-mineralised cartilage or osteoid surrounding osteoblasts and chondrocytes (Simao *et al.*, 2010). TNAP is highly expressed extracellularly on the plasma membrane of osteoblasts, hypertrophic chondrocytes and particularly highly on the surface of extracellular matrix vesicles, which are formed from the polarised budding of the cell membranes of osteoblasts, chondrocytes and odontoblasts, which are dentin-producing cells found in teeth (Millán *et al.*, 2006; Orimo and Shimada, 2008; Orimo, 2010). TNAP is thought to have several physiological substrates, these include inorganic pyrophosphate (PPi), pyridoxal 5'-phosphate (PLP) and phosphoethanolamine (PEA), although other substrates may still be identified (Orimo, 2010). TNAP also has ATPase activity (Muruganandan *et al.*, 2009). The known function of TNAP in bone mineralisation is to hydrolyse inorganic pyrophosphate (PPi) to form inorganic phosphate (Pi), which together with Ca^{2+} is needed for hydroxyapatite formation (Millán *et al.*, 2006; Orimo, 2010). PPi is generated in the extracellular space from adenosine triphosphate (ATP) by nucleotide pyrophosphatase

phosphodiesterase 1 (NPP1), a nucleotide triphosphate pyrophosphatase found on the surface of osteoblasts, chondrocytes and matrix vesicles (MVs) in close proximity to TNAP (Fig. 1.2.8.1.1), NPP1 was previously known as plasma cell glycoprotein-1 (PC-1). It has been found that osteoblast TNAP and NPP1 antagonise one another and are essential to maintain PPi at the correct levels for mineralisation (Johnson *et al.*, 2000; Hessle *et al.*, 2002; Millan, 2013). PPi generated from ATP by hydrolysis is also transported across the cell membrane to the extracellular space by the transmembrane PPi-channelling enzyme, ANK, the human homolog of the mouse progressive ankylosis (*ank*) gene product (Millán *et al.*, 2006). The correct balance of PPi to Pi is crucial for mineralisation to occur, as PPi is an inhibitor of mineralisation.

Figure 1.2.8.2.1 shows schematically the process of mineralisation accomplished by either an osteoblast, chondrocyte or odontoblast. The cell shown in figure 1.2.8.2.1 is in contact with the un-mineralised matrix, as depicted in figure 1.2.8.1.1, and from this cell a matrix vesicle buds off. The matrix vesicle is the main agent of mineralisation, and it is here that hydroxyapatite crystals are formed from $CaPO_4$ and deposited into the osteoid. For $CaPO_4$ to form within the matrix vesicle, a supply of Ca^{2+} and $H_2PO^-_4$ ions is needed.

Ca^{2+} ions enter the matrix vesicle from the extracellular fluid via calcium channels formed by annexins. Ca^{2+} is also liberated from calcium-binding phospholipids, such as phosphatidylserine and calcium-binding proteins, such as calbindin D_{9k} and bone sialoprotein (Orimo, 2010). Pi for mineralisation is produced in two steps. Firstly, ATP is hydrolysed by the ectoenzyme, nucleoside pyrophosphohydrolase 1 (NPP1), to produce inorganic pyrophosphate (PPi). PPi is subsequently hydroylsed to Pi by TNAP on the outside of the matrix vesicle. Pi produced in this way is then transported into the matrix vesicle from the extracellular fluid by the type III Na/Pi cotransporter, located on the both the cell and matrix vesicle membrane (Orimo, 2010). Pi is also produced inside the matrix vesicle by hydrolysis of phosphocholine (PCho) and phosphoethanolamine (PEA) by phosphatase orphan 1 (PHOSPHO1), a cytosolic phosphatase (Orimo, 2010). Once levels of Ca^{2+} and Pi exceed the solubility limit of $CaPO_4$ inside the matrix vesicle, hydroxyapatite crystals are formed. If the concentration of Ca^{2+} and Pi in the extracellular matrix are suitable, the membrane of the MV breaks down and allows the formed hydroxyapatite crystals to be released and deposited between collagen fibrils within the extracellular matrix (Orimo, 2010). Mineralisation is also pH dependent, and will only occur under alkaline conditions. The chemical formation of

hydroxyapatite results in the release of 1.4 H^+ ions for every Ca^{2+} ion that is deposited. H^+ ions released in this way must be removed from the site of mineralisation to prevent the pH from becoming acidic, which would halt the mineralisation process.

Mineralisation is therefore thought to be carefully controlled by the functioning of TNAP, NPP1, ANKH, PHOSPHO1 and also the mineralisation inhibitor, osteopontin (OPN), a glycoprotein rich in negatively charged phosphate groups. OPN, the expression of which is induced by PPi, is thought to inhibit mineralisation by binding to hydroxyapatite, due to the high affinity of its negatively charged phosphate groups for mineral (Johnson *et al.*, 2000; Hessle *et al.*, 2002; Millán *et al.*, 2006; Addison *et al.*, 2007; Orimo, 2010).

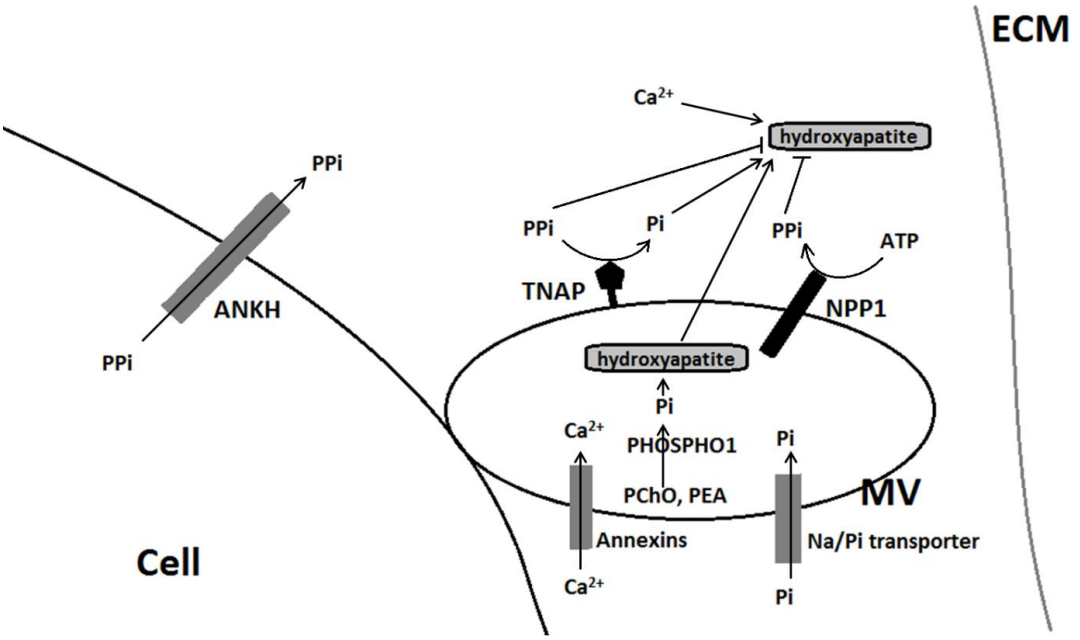

Figure 1.2.8.2.1: Schematic illustration of mineralisation. The cell depicted may be either an osteoblast, chondrocyte or ondontoblast. The matrix vesicle (MV) buds off from the cell membrane and is the main agent of mineralisation. Hydroxyapatite crystals form inside the MV from $CaPO_4$, which in turn is made from Ca^{2+} and Pi ions. Ca^{2+} is transported into the MV by annexins, whereas inorganic phosphate (Pi) ions are produced by hydrolysis of inorganic pyrophosphate (PPi) to Pi by TNAP and are transported into the MV via a Na/Pi transporter. PPi is produced by hydrolysis of ATP by nucleotide pyrophosphatase phosphodiesterase (NPP1). Additional Pi is produced by hydrolysis of phosphocholine (PCho) and phosphoethanolamine (PEA) by the cytosolic phosphatase, PHOSPHO1. When a suitable concentration of Ca^{2+} and Pi is present, hydroxyapatite crystals are formed and will move through the MV membrane into the extracellular matrix, where they are elongated and deposited (Adapted from Orimo, 2010).

1.2.8.2 Adipogenesis

Knowledge of the factors and mechanisms that play a role in adipogenic differentiation of MSCs are useful for gaining insights into the treatment possibilities for obesity as well as other diseases where adipose tissue is involved, such as osteoporosis and non-insulin dependent diabetes. The primary function of adipocytes is to store triglycerides for times when the body's need for energy is greater than the amount of energy available from the diet (Gregoire *et al.*, 1998). Adipocytes are derived from preadipocyte precursors which are themselves derived from a shared pool of MSC progenitors, capable of differentiation into multiple cell lineages (Covas *et al.*, 2008). Adipogenesis is the process that results in the development of a mature functional adipocyte from an undifferentiated MSC, due to changes in gene expression, and is exquisitely regulated by transcription factors (Tang and Lane, 2012). Cytidine-cytidine-adenosine-adenosine-thymidine (CCAAT)/enhancer binding proteins (C/EBPs) and peroxisome proliferator-activated receptor γ (PPARγ), are the major transcription factors which determine whether MSCs will become committed to the adipocyte lineage (MacDougald and Mandrup, 2002; Tang and Lane, 2012). The latter exists in the isoforms which are produced from one gene via alternative splicing and result in the proteins PPARγ1, PPARγ2 and PPARγ3. PPARγ is known as the master regulator of adipogenesis, with PPARγ2, the adipocyte specific isoform, also being more effective than PPARγ1 at causing cells to differentiate into adipocytes (Fujiki *et al.*, 2009). Activation of the sequence of adipogenic transcription factors that are required for adipogenesis starts with C/EBPβ and C/EBPδ, which stimulate the next wave of transcription factors, namely C/EBPα and PPARγ. The major transcription factors, C/EBPα and PPARγ, are able to propagate their own expression as well as the expression of each other, and together, along with the ligands of PPARγ, are the main drivers of the expression of adipocyte-specific genes (MacDougald and Mandrup, 2002). In *in vitro* cell culture, exogenous inducers of adipogenesis added to the culture medium initiate the activation of these adipogenic transcription factors. These inducers include: a glucocorticoid receptor agonist, such as the commonly used dexamethasone, a stimulator of insulin-like growth factor-I receptor (IGF-IR) accomplished by the addition of insulin to at high concentration, a factor which elevates intracellular cAMP, such as 3-isobutyl-1-methylxanthine (IBMX), and a PPARγ ligand, the latter consisting of derivatives of long-chain polyunsaturated acids, as well as the synthetic ligands such as thiazolidinediones (TZDs) (MacDougald and Mandrup, 2002; Vater *et al.*, 2011).

Recent data have suggested a role for the class B scavenger receptor and membrane glycoprotein known as CD36 in adipogenesis. CD36 expression has been detected in a variety of different cell types, including adipocytes, where it appears that CD36 has a number of different, cell type-specific functions (Christiaens *et al.*, 2012). Evidence has been put forward that CD36 is a lipid sensor, and may be involved in metabolism, behaviour, immunity as well as in diseases such as Alzheimer's disease, atherosclerosis and obesity (Martin *et al.*, 2011; Christiaens *et al.*, 2012). Experimental work by Christiaens *et al.* showed that CD36 has a functional role in adipogenesis, as silencing of CD36 in the murine preadipocyte cell line 3T3-F442A significantly reduced lipid accumulation after adipogenic induction *in vitro*, with a concurrent reduction in the expression of the adipocyte markers, aP2 and PPARγ (Christiaens *et al.*, 2012).

1.2.10 Bone morphogenetic proteins

Bone morphogenetic proteins (BMPs) have been found to play an important role in both osteoblastogenesis and adipogenesis of MSCs. BMPs are members of the transforming growth factor-β (TGF-β) superfamily and are signalling molecules involved in pathways important for the regulation of differentiation and proliferation of cells both during development of an organism as well as in stem cells present in adulthood (Kang *et al.*, 2009). In humans, 15 different BMPs have been identified. The osteogenic BMPs, such as BMP-2, -6 and -9 have been shown to strongly promote osteoblastogenesis, while BMP-2, along with BMP-4 and -7 are more involved with adipogenesis, when certain adipogenic cofactors and supplements are present (Kang *et al.*, 2009). Additionally, it has been discovered that BMPs and Wnt signalling pathways interact during development and this interaction varies between tissues, as well as temporally (Itasaki and Hoppler, 2010). Much still remains to be learnt about the precise function and role of BMPs within differentiation and whole body homeostasis, as well as about their interactions with other molecules and signalling pathways (Kang *et al.*, 2009; Itasaki and Hoppler, 2010).

1.2.11 Other factors influencing MSC differentiation

In addition to the various cellular signalling molecules involved in MSC differentiation already discussed, evidence exists for the involvement of several other factors in determining which differentiation pathway MSC take. Epigenetic regulation (Collas *et al.*, 2008; Delgado-

Calle *et al.*, 2011), micro RNA (miRNA) control of gene expression (Laine *et al.*, 2012), as well as reduction/oxidation (redox) potentials within the cell are all determinants of which differentiation pathway is taken (Imhoff and Hansen, 2010).

Epigenetic modifications are regulatory mechanisms for gene expression, which include methylation of DNA as well as modifications of chromatin, in the form of post-translational histone modifications. These modifications function to either facilitate or repress transcription of genes, by either opening the DNA strand or causing condensation of the strand, respectively (Teven *et al.*, 2011). Epigenetic modifications are heritable, and may be passed on to daughter cells produced via mitosis, as well as meiosis, where they may persist for several generations, even though they do not involve changes to the DNA sequence itself (Collas *et al.*, 2008). Epigenetic regulation of DNA involves the methylation of cytosine residues at position 5, at cytosine-phosphate-guanodine (CpG) sites, which functions to silence the genes downstream from the methylation site (Collas *et al.*, 2008). Histone modifications involve a variety of covalent modifications of the N-terminal tail of a translated histone protein, such as methylation or acetylation, which function to bring about gene regulation. Epigenetic regulation plays a major role in the life cycle of a cell, by either activating or repressing a variety of genes as the cell progresses from a progenitor to terminally differentiated phenotype (Teven *et al.*, 2011). An important role for epigenetic regulation in MSC lineage differentiation has been discovered, as epigenetic modifications have been found to affect the expression of several adipogenic and osteogenic markers, including osteocalcin, osteopontin and PPARγ (Teven *et al.*, 2011; Ozkul and Galderisi, 2016). The extent of epigenetic regulation in MSCs is not yet fully understood, and much work is required to elucidate the contribution of epigenetic regulation on MSC lineage commitment, maintenance of a stem cell phenotype as well as cellular aging and senescence (Ozkul and Galderisi, 2016).

MicroRNAs (miRNAs) are short, endogenous, non-coding RNA molecules, of around 19 to 24 nucleotides in length, which are able to regulate gene expression by binding to a complementary region on 3` untranslated region (UTR) of a messenger RNA (mRNA) molecule. The result of miRNA binding to an mRNA molecule is either repression of the gene or degradation of the mRNA molecule itself (Ambros, 2004). MiRNAs have been found in all metazoans studied to date, and form a large regulatory network, with between 40 – 90% of expressed human proteins being targets for miRNA regulation (Hu *et al.*, 2010). Studies

have shown that miRNAs may regulate stem cell pluripotency and differentiation (Singh *et al.*, 2008). The pattern of miRNAs present in MSCs alters as the cells progress from a progenitor to terminally differentiated cell. The pattern of miRNAs present in terminally differentiated MSCs is different from the pattern present in progenitor MSCs (Guo *et al.*, 2011). Several miRNAs involved in gene expression of MSCs have been identified and function to either inhibit or activate various genes involved in either the osteogenic or adipogenic differentiation pathway (Laine *et al.*, 2012). One gene may be targeted by several different miRNAs, and additionally, a single miRNA may target several different genes (Friedman *et al.*, 2009; Guo *et al.*, 2011). As an example, the endogenous miRNA-204 (miR-204) negatively regulates the expression of Runx2 in bmMSCs and mesenchymal progenitor cell lines ST2, C2C12 and C3H10T1/2. Overexpression of miR-204 was found to decrease the expression of Runx2, which resulted in the inhibition of osteogenesis and an increase in adipogenesis. When miR-204 was inhibited, osteogenesis was increased and adipogenesis was impaired (Huang *et al.*, 2010).

Oxidative stress in the form of oxidising extracellular reduction/oxidation (redox) potential results in a deregulation in the production of reactive oxygen species (ROS) within the cell. Low levels of ROS are necessary for cell function and survival, however high levels of ROS resulting from oxidative stress leads to cellular damage and dysfunction (Denu and Hematti, 2016). In MSCs, increased levels of ROS have been found to impair cellular proliferation, differentiation and self-renewal capacity (Alves *et al.*, 2010; Ko *et al.*, 2012; Alves *et al.*, 2013). MSCs are thought to be more sensitive to ROS than more differentiated cell types (Denu and Hematti, 2016). In general, increased oxidative stress and ROS production has been found to inhibit osteogenic differentiation of MSCs (Chen *et al.*, 2008), however, increased ROS and oxidative stress have been found to enhance adipogenesis in MSCs (Imhoff and Hansen, 2010). Tormos *et al*. discovered that ROS generated by mitochondrial metabolism during adipogenic differentiation of primary human MSCs were necessary for adipocyte differentiation to occur, rather than a by-product thereof (Tormos *et al.*, 2011). ROS levels were also found to increase during chondrogenesis, and stimulated chondrogenic hypertrophy (Denu and Hematti, 2016).

The overall aim of the current project was to provide a better understanding of the role of tissue-nonspecific alkaline phosphatase (TNAP) during the differentiation of primary

mesenchymal stromal cells (MSCs) towards an adipogenic phenotype, contrasted with the better known role of TNAP during osteogenesis. To this end, the first aim of the project was to establish the suitability of the model used for investigation, which consisted of primary rat MSCs derived from subcutaneous and perirenal visceral adipose, and bone marrow depots. This was achieved by assessing the surface marker expression, as well as adipogenic and osteogenic differentiation potential of MSCs derived from each depot, in order to verify that the cells used were MSC in nature. The second aim of the study was to investigate the effect of known TNAP inhibitor compounds, levamisole, L-homoarginine and histidine, on MSCs undergoing adipogenesis and osteogenesis, in order to determine if inhibiting TNAP activity would have an effect on the outcome of the differentiation process. The third aim of the project was to further characterise the TNAP present in rat-derived MSCs, by investigating the subcellular location of TNAP in MSCs undergoing adipogenesis, the TNAP mRNA transcript type present, as well as the glycosylation pattern differences of TNAP isoforms present in adipocyte and osteoblast phenotypes. Finally, the project aimed to investigate whether knocking down TNAP mRNA expression during adipogenic induction would inhibit lipid accumulation in scADSCs.

CHAPTER 2

Materials and Methods

2.1 Materials

Euthanasia was performed using sodium pentobarbitone (Eutha-naze) obtained from Bayer (Pty) Ltd. (Ref83/91, #22079248DJ, Isando, RSA). Dulbecco's modified Eagle's medium (DMEM) was purchased from BioWhittaker, (#BE12-604F, Lonza, Basel, Switzerland) and foetal bovine serum (FBS) was purchased from Biochrom (S0615, 0459B, Berlin, Germany). Collagenase type I was purchase from Worthington Biochemical Corporation (CLS1, #XOM12195J, Lakewood, New Jersey, USA). Trypsin (200 mg/l Versene EDTA, #BE171616, Lonza), penicillin/streptomycin solution (BioWhittaker, #DE17-6026, Lonza) and Hank's balanced salt solution (HBSS) (BioWhittaker, #10-508F, Lonza) were purchased from Lonza, BioWhittaker ® (Walkersville, MD, USA). Plastics for cell culture were purchased from either Greiner Bio-One (Cellstar ®, Frickenhausen, Germany) or Corning Incorporated (Corning ®, NY, USA) or Nest Biotech Co. Ltd. (China). Bovine serum albumin (BSA) was bought from Sigma-Aldrich BSA (#A4503-100G, Sigma–Aldrich). Levamisole (L tetramisole) (L9756-5G), histidine (H6034) and L-homoarginine (H1007-5G) were purchased from Sigma-Aldrich (St. Louis, MO, USA). The GoTaq® G2 Flexi DNA Polymerase kit (M7801) and ImProm-II™ reverse transcriptase (#M314A) were procured from Promega (Madison, WI, USA). The RNAeasy Mini kit for total RNA isolation was procured from Qiagen (#74106) (CA, USA). Primers were purchased from Integrated DNA Technologies Incorporated (IDT). All other chemicals were purchased from Sigma-Aldrich (St. Louis, MO, USA) and liquid solvents were procured from Merck Chemicals (Pty) Ltd (South Africa).

2.2 Methods

2.2.1 Isolation of rat mesenchymal stromal cells from subcutaneous and visceral adipose tissue depots.

Adipose-derived mesenchymal stromal cells (ADSCs) were isolated from the inguinal subcutaneous fat pad and peri-renal visceral depots of male Wistar rats, approximately 8 weeks of age, weighing 150 g. All the rats used for this study were housed in a facility at the University of Stellenbosch which is accredited by the AAALAC (Association for Assessment and Accreditation of Laboratory Animal Care), and animals were handled according to ethical guidelines of the University of Stellenbosch. Ethical clearance for the study was granted by the University of Stellenbosch with the clearance number given as (#SU-

ACUD15-00012). The rats were sacrificed by intraperitoneal injection with sodium pentobarbitone (Eutha-naze Ref83/91, #22079248DJ, Bayer) at 100 mg/kg body weight. As there are two inguinal subcutaneous and peri-renal visceral depots present in each animal, on each side of the groin or either kidney, adipose tissue from both sides were pooled together and used for the ADSC isolation. The tissue was excised using surgical scissors immediately after the animal was sacrificed, and rinsed after excision in 70% (v/v) ethanol to ensure sterility and briefly stored in high-glucose (4.5 g/l glucose: L-glutamine) Dulbecco's Modified Eagle's Medium (DMEM) (BioWhittaker, #BE12-604F, Lonza, Basel, Switzerland). All further processing was performed in a laminar flow biosafety cabinet (Laboratory and air purification systems cc., model LA1200BII, Midrand, RSA) under sterile conditions. The adipose tissue was placed in a sterile cell culture Petri dish, and finely macerated and teased apart with a sterile razor blade to loosen the connective tissue and increase the surface area. The tissue sample was placed in a sterile 50 ml Falcon™ tube (352070, BD, USA) containing 10 ml digestion mixture of Hank's balanced saline solution (HBSS) (BioWhittaker, #10-508F, Lonza) containing 0.075% (w/v) collagenase type 1 (CLS1, #XOM12195J, Worthington, Lakewood NJ, USA) and 1.5% (v/v) bovine serum albumin (BSA) (#A4503-100G, Sigma-Aldrich) followed by immersion of the tube containing the digestion mixture in a 37 °C water bath for 30 min with occasional agitation in order to aid the digestion of the connective tissue surrounding the MSCs. The digested tissue was subjected to centrifugation (250 x *g*, 10 min) to pellet cells freed from the tissue. Pelleted cells were transferred to a clean tube using a sterile Pasteur pipette and washed twice with phosphate buffered saline (PBS) pH 7.4. Cells were then pelleted by centrifugation (250 x *g*, 5 min) and resuspended in 2 ml DMEM with 1% penicillin/streptomycin (BioWhittaker, #DE17-6026, Lonza) containing 20% foetal bovine serum (FBS) (Biochrom, S0615, 0459B). The cell suspension, which constitutes the stromal vascular fraction (SVF) (Gimble *et al.*, 2007) was seeded at 1 ml into two 6 mm x 15 mm cell culture dishes (#430166, Corning, NY, USA) and the volume increased to 4 ml with DMEM containing 20% FBS with 1% penicillin/streptomycin. The cell cultures were maintained in a Forma Series II water jacketed CO_2 incubator (model 3111, Thermo Scientific) with 80-90% humidification at 37 °C with 5% CO_2 for 24 hr to allow the cells of the SVF, which contain ADSCs, to adhere to the surface of the dish. Cell cultures were visually evaluated after 24 hr using an Olympus light microscope (CKX41, CachN 10X/0.25 PhP objective, EOS600D Canon digital camera) to determine whether healthy cells were present, indicating that the isolation was successful. Cell cultures were then washed 2x with sterile PBS (pH 7.4, 37 °C) in order to remove debris

and any unattached cells and the medium was then replaced with standard growth medium (SGM) (DMEM with 1% penicillin/streptomycin, containing 10% FBS) and the cultures maintained at 37° C with 5 % CO_2 and constant humidity for further expansion.

2.2.2 Isolation of rat mesenchymal stromal cells from bone marrow.

Both femurs were excised from a 150 g male, Wistar rat directly after the animal was sacrificed by intraperitoneal injection of sodium pentobarbitone at 100 mg/kg body weight (Section 2.2.1). The femurs were rinsed briefly in 70 % (v/v) ethanol and placed in DMEM. In a sterile biosafety cabinet, the bones were manually denuded of adherent muscle tissue and ligaments by rubbing them with sterile gauze strips, after which the femurs were briefly rinsed in 70% (v/v) ethanol, and the ends of the bones severed using a surgical side cutter. Each bone shaft was flushed with 3 ml of DMEM containing 20% FBS and 1% penicillin/streptomycin by inserting a sterile syringe with an 18 G needle into the end of the bone shaft and flushing the bone marrow out with moderate force into a 6 mm x 15 mm cell culture dish. The bone marrow from each femur was flushed into a separate cell culture dish. The flushed marrow was then subjected to vigorous pipetting with a P1000 pipette to break up the large marrow cores, after which the volume of medium in the dish was adjusted to 4 ml and incubated at 37 °C and 5% CO_2 in a humidified incubator. After 24 hr of incubation, the plates were each washed 4 to 5 x with sterile PBS (pH 7.4) warmed to 37 °C in order to wash off non-adherent cells and debris, such as red blood cells and bone fragments, and the medium then replaced with 4 ml of SGM and incubation continued at 37 °C with 5 % CO_2. The cell culture at this time is at passage 0 (P0) and once the cell culture reached 80% confluence, typically after 5 to 7 days in culture, the cells were passaged (Section 2.2.3) to allow for further expansion of the cell number and to improve the homogeneity of the culture. Cells were passaged from P0 to P1 (passage 1) at roughly a 1:2 ratio, where cells from each 6 cm dish are pooled and split into two 10 cm Petri dishes, with a volume of 8 ml of SGM per dish. Further expansion was carried out in 10 cm Petri dishes and cells are passaged at a 1:2 ratio from P1 to P2 and at a 1:4 ratio for P2 to P3, at which passage cells are used for experimentation.

2.2.3 Cell culture maintenance and Passage

Naïve scADSCs, pvADSCs and bmMSCs from passages 0 to 3 (P0 – P3) were maintained in standard growth medium (SGM). Cells were incubated at 37° C in 5 % CO_2 under constant humidification, which allows for expansion of the cell number in culture as well as the maintenance of an undifferentiated phenotype.

Normal maintenance of cell cultures at less than 70% confluence in SGM was carried out by aspiration of spent medium after 2 to 3 days in culture, followed by replacement with fresh expansion medium and immediately placing cultures back into previous incubation conditions. Passaging was performed once cells had reached a confluence of 70-80%, by aspiration of SGM from culture dishes, followed by briefly washing the cells 2x with sterile PBS (37 °C, pH 7.2) in order to remove traces of SGM. Trypsin at 0.5 % (200 mg/l Versene EDTA, #BE171616, Lonza) was added to cells in a ratio of 1:10 trypsin solution: original medium volume, and incubated at 37 °C for 1 to 2 min to dislodge cells. Gentle tapping of the dish was done after incubation to encourage detachment of cells, and cells were briefly viewed under a light microscopy (CKX41, CachN 10X/0.25 PhP objective, EOS600D Canon digital camera) to confirm that detachment was complete and no cells remained adhered to the culture surface. SGM was added to the dish in order to neutralize the trypsin enzyme at a ratio of 2:1 SGM: trypsin solution. Volume of the SGM containing the detached cells was adjusted to the desired amount to allow cells to be split at the ratio of either 1:4 for scADSCs and pvADSCs or 1:2 for bmMSCs. Once the volume of SGM in the freshly passaged cultures was adjusted to the required level for the culture vessel, the vessels were swirled gently in order to ensure even distribution of the cell suspension and after which were immediately placed in the incubator to allow for the cells to settle and reattach to the culture dish surface.

2.2.4 Alkaline phosphatase (ALP) extraction and activity assay

Total alkaline phosphatase (ALP) activity in crude cell lysates (Section 2.2.4.1), as well as in semi-purified enzyme extracts (Section 2.4.2) was quantified using a colourimetric assay based on the hydrolysis of the substrate *para*-nitrophenylphosphate (*pNPP*) to yield a coloured product, *para*-nitrophenol (*p*NP), as outlined below.

2.2.4.1 Cell lysates preparation for alkaline phosphatase (ALP) activity assay

Cells from which ALP activity was to be measured were cultured in 24-well Cellstar® cell culture plates (#662160, Greiner bio-one, Germany) until required for assay. Medium was aspirated from the wells which were immediately washed 2x with Tris-buffered saline (TBS) (pH 7.2, RT) and plates immediately placed on ice. To each well, 250 µl of Lysis buffer (100 mM Tris-Cl, 0.001% Triton X-100, pH 7.4) was added and wells were scrapped using a standard 1000 µl pipette tip to dislodge cells from the well surface. Once the cells were detached, the lysates were transferred to a chilled 1.5 ml microcentrifuge tube (#509-GRD-Q, Quality Scientific Products). At this point cell lysates were either frozen at -20 °C and stored for later analysis or processed immediately.

Frozen lysate samples were thawed on ice before further processing. Thawed lysates were sonicated (at an amplitude of 20 microns peak to peak) for 3 x 5 sec bursts, while cooling the lysate on ice. The sonicated lysates were subjected to centrifugation (15 min, 15 000 x *g*, 4 °C) to pellet insoluble material. After centrifugation, the samples were placed on ice and the supernatant was transferred to a clean, chilled 1.5 ml microfuge tube. Samples were then frozen at -20 °C until needed or were used immediately for the ALP activity assay.

2.2.4.2 Alkaline phosphatase extraction

Alkaline phosphatase (ALP) extraction from cell lysates was necessary for scADSCs and pvADSCs to be used for glycosylation analysis, as these cell types do not possess sufficiently high ALP activity in crude cell lysates for glycosylation studies. The ALP extraction method was adapted from Merchant-Larios *et al*. (Merchant-Larios *et al.*, 1985). Cells were cultured in 10 cm Petri dishes until ready for ALP extraction. The medium was removed by aspiration and the cells washed 2 x with TBS (pH 7.2, RT) and immediately placed on ice. A 500 µl volume of ice-cold extraction buffer (100 mM Tris-Cl, 1% Triton X-100, pH 7.4) was added to the plate and the lysed cells dislodged from the plate by scraping using a cell scraper. The lysate was transferred to a chilled 1.5 ml microfuge tube and sonicated 3x 10 sec (at an amplitude of 20 microns peak to peak) while cooling the lysates on ice during sonication intervals. Lysates were subjected to centrifugation (15 000 x *g*, 15 min, 4° C) to pellet cell debris, and the supernatant transferred to a clean 1.5 ml microfuge tube and kept on ice. Ice-

cold butanol was added to the supernatant at a 1:5 ratio and the solution mixed by vortexing until it turned from clear to opaque/milky in appearance. The solution was then mixed using a tube rotator (G207378, Labnet Inc., USA) for 45 min at 4 °C, followed by centrifugation at 15000 x *g*, 1 hr, 4 °C. The lower aqueous phase was carefully removed and placed in a clean 1.5 ml microfuge tube, and a 0.6 volume ice-cold acetone added. The solution was vortexed for 5 sec followed by centrifugation (15 000 x *g*, 30 min, 4 °C). The resulting pellet was carefully resuspended in 20 µl of lysis buffer (100 mM Tris-Cl, 0.001 % Triton X-100, pH 7.2). To obtain a sufficient volume for glycosylation analysis, 6 to 10 ALP extraction samples were pooled together. Alkaline phosphatase activity was measured using 5 µl of sample. Semi-purified samples of ALP were stored at -20 °C.

2.2.4.3 Alkaline phosphatase activity assay

The alkaline phosphatase activity assay was adapted from the method of Sabokar *et al.* (Sabokbar *et al.*, 1994). Cell lysates or samples of semi-purified ALP were thawed on ice and either 5 µl for bmMSCs or 80 µl for scADSCs and pvADSCs, due to the higher ALP activity present in bmMSCs compared to ADSCs, of each internal replicate was added to wells of a 96-well plate and the total volume brought to 80 µl using lysis buffer (100 mM Tris, 0.001% Triton X-100, pH 7.4). Substrate solution was prepared immediately before use by adding 2 x 5 mg *para*-nitrophenylphosphate (*p*NPP) phosphatase substrate tablets (50942-50TAB, Sigma-Aldrich) into 5.4 ml of ice-cold DEA buffer (1 M diethanolamine, 0.5 mM $MgCl_2$, pH 9.8) protected from light and mixed by gentle shaking until the *p*NPP had dissolved. The substrate solution was added at a volume of 50 µl to each well, and the plate immediately incubated in a heating MultiskanGo plate reader (Thermo Scientific) with SkanIt Software version 3.2 (Thermo Scientific) at 37° C while absorbance at 405 nm was read at 2 min intervals for a total period of 20 to 40 min. Multiple readings were taken as the reaction progressed, as this allowed for a time point to be determined for which alkaline phosphatase activity in all samples was increasing in the linear phase of the reaction, as using a single endpoint reaction with one selected time would have resulted in some samples reaching a plateau in the reaction before others and the resultant incorrect ALP activity being calculated. A standard curve was constructed using known concentrations of *para*-nitrophenol (*p*NP) (1048-5G, Sigma Aldrich), which is the coloured product formed from the hydrolysis of *p*NPP. A stock solution of 25 mM *p*NP was made in ultrapure water and serial dilutions were made to give a concentration range of 0, 12.5, 25, 50, 100 and 200 µM, with 150 µl placed in

each well in triplicate. The amount of *p*NP in µmol for each concentration of the standards was calculated and used for a standard curve. From this curve the amount of product formed in the test samples was determined, an example of which is shown in figure 2.2.4.3.1. The amount of *p*NP calculated from the standard curve enabled the activity of the test samples to be measured using the following equation:

Activity (units/ml) = A/V/T

Where A is the amount of pNP (µmol) in the sample as determined from the standard curve.
V is the volume of lysate in ml.
T is the time of the reaction in minutes.

The specific activity of the samples was determined by the following equation:

$$\text{Activity (units/mg prot)} = \frac{\text{units/ml}}{\text{mg/ml prot (determined separately by Bradford protein assay)}}$$

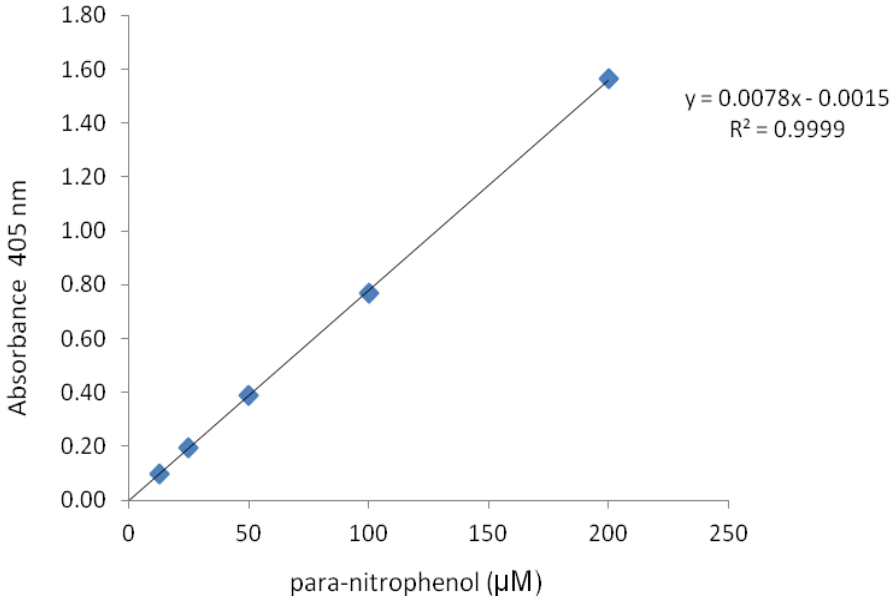

Figure 2.2.4.3.1: Standard curve example for para-nitrophenol with absorbance at 405 nm and standard concentrations of para-nitrophenol of 0, 12.5, 25, 50, 100 and 200 µM.

2.2.4.4 Protein concentration determination

Protein content in mg/ml was determined using the Bradford protein assay (Bradford, 1976). Bovine serum albumin (BSA) (#A4503-100G, Sigma-Aldrich, Germany) standards for use in the Bradford assay were made up in lysis buffer at concentrations of 1.4, 1.2, 1.0, 0.5, 0.25, 0.125 and 0 mg/ml. The Bradford assay was performed in a 96-well plate, where 5 µl of test sample or BSA standard were added to the well followed by 250 µl of Bradford reagent (10% (w/v) Coomassie Brilliant Blue G-250 10% (v/v), 85% Phosphoric acid, 5% (v/v) 95% EtOH). For the blank, lysis buffer with no Bradford reagent was used. Once the Bradford reagent was added, the plate was incubated for 5 min at RT to allow the colour to develop, after which the absorbance was read at 595 nm no longer than an hour after addition of the Bradford reagent, and the concentration of each sample calculated from the standard curve. Figure 2.2.4.4.1 shows an example of a standard curve for BSA. A BSA standard curve was included each time test samples were measured.

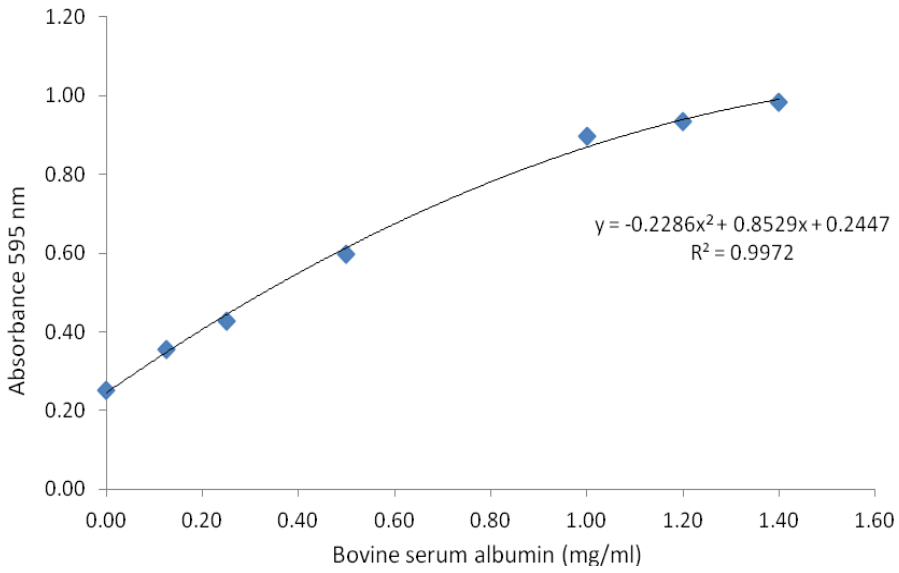

Figure 2.2.4.4.1: Example of standard curve for BSA with absorbance at 595 nm and standard concentrations of BSA from 0, 0.125, 0.25, 0.50, 1.0, 1.2 and 1.4 mg/ml.

2.2.5 Adipogenic differentiation

Adipogenic differentiation was adapted from the method of Ogawa *et al.* (Ogawa *et al.*, 2004). Adipogenesis was induced in scADSCs and pvADSCs while cells were in P2, whereas

bmMSCs were grown to P3 before induction. Cells that were 2 days post confluence were incubated in a cocktail consisting of standard growth medium (SGM) plus 0.5 mM 3-isobutyl-1-methylxanthine (IBMX) (STBC7632V, Sigma Life Sciences), 1 µM dexamethasone (Dex) (D4902-100MG, BCBK1265V, Sigma Life Sciences), 10 µM insulin (19278-5ML, SLBD5980, Sigma Life Sciences) and 56 µM indomethacin (17378-5G, 064K1207, Sigma Life Sciences), as well as 50 µM ascorbic acid (A4544-25G, SLBB4446V, Sigma Life Sciences). The concentrations of the components of this adipogenic differentiation media (AM) are given in Table A1, Addendum A. AM was prepared immediately before use and warmed to 37 °C, before being applied to cell cultures directly after the aspiration of expansion medium. Cell cultures undergoing adipogenic induction were incubated at 37 °C in 5 % CO_2 and constant humidity. AM was exchanged on cell cultures every 2 to 3 days for up to 14 days, by aspirating off spent medium and the immediate addition of fresh AM.

2.2.6 Oil Red-O staining

Oil Red-O (ORO) (O0625-100G, Sigma Aldrich) is a dye which binds lipids and is used to determine the quantity of intracellular lipid droplets present in a cell culture at specific time-points during adipogenic differentiation. ORO staining was performed according to the method of Laughton (Laughton, 1986). ORO stock solution (1% ORO dissolved in isopropanol (K44414134 315, Merck) was diluted to 70% ORO using ultrapure H_2O to make the working solution, which was filtered immediately before use using a Whatmann no. 1 filter paper. Culture medium was removed from cells cultured in a 24-well plate followed by direct addition of ~1 mL of ORO working solution and the cells incubated for 30 min at RT. A separate fixation step was not necessary as isopropanol in the ORO working solution fixes and stains the cells simultaneously. Wells were washed 3x with ultrapure H_2O followed by addition of phosphate buffered saline (PBS) at pH 7.4. The wells were then photographed for image analysis and lipid quantification (Section 2.2.9)

2.2.7 Osteogenic differentiation

Osteogenesis was induced in scADSCs and pvADSCs grown to P2 and bmMSCs while in P3 at 2 days post confluence using a cocktail consisting of standard expansion medium (DMEM+ 10% FBS) containing β-glycerophosphate (G5422-100G, 029K54241V, Sigma

Life Sciences), ascorbic acid and dexamethasone (Dex), and termed Osteogenic differentiation medium (OM), according to the method of Jaiswal *et al*. (Jaiswal *et al.*, 1997). OM was made immediately prior to use and warmed to 37 °C. OM used to induce osteogenic differentiation in scADSCs and pvADSCs contained 100 nM Dex, compared to 10 nM Dex in the OM cocktail used for bmMSCs, as the ADSCs were found to require a higher concentration of Dex in order to differentiate. Osteogenic differentiation was induced in cell cultures by aspirating off expansion medium, followed by immediate addition of OM, and incubation of the cells at 37 °C in 5% CO_2 and constant humidity. OM was changed every 3 to 4 days by aspiration of spent medium and the immediate addition of fresh OM followed by incubation for up to 21 days for scADSCs and pvADSCs and 14 days for bmMSCs (See Addendum A, Section A2 for OM components).

2.2.8 Alizarin red staining for mineralisation

Mineralisation on the cell culture plate surface after cells were cultured in OM was visualised by staining with Alizarin red S (#9436, Amresco, Solon, OH, USA) (Reinholz *et al.*, 2000). Alizarin red dye solution was made up in ultrapure water to a concentration of 100 mM and adjusted to pH 4.0 using 10 mM ammonium phosphate solution, and stored at RT protected from light. Medium from cell cultures to be stained with Alizarin red S, was aspirated off and plates were gently washed 2 x with PBS (pH 7.4) to avoid dislodging any formed mineral deposits, followed by fixing of the cells by addition of 70% (v/v) ethanol for 5 min at RT. The plates were then washed 2 x with ultrapure H_2O and incubated with Alizarin red dye solution (pH 4.0) for 16 hr at RT in the dark. Following staining, plates were washed 3 x with ultrapure H_2O to remove unbound Alizarin red S. PBS (pH 7.4) was then added to the stained wells, which were immediately photographed for image analysis and quantification of mineralisation (Section 2.2.9).

2.2.9 Quantification of lipid accumulation and mineralisation by image analysis

Images acquired for image analysis and quantification were taken with an Olympus light microscope (CKX41, CachN 10X/0.25 PhP objective, EOS600D Canon digital camera). Three replicates for each experimental condition were performed and four images (one in

each quarter) were taken per replicate well. The images were analysed using ImageJ software (version 1.46, nih.gov) and area of positively stained lipid accumulation or mineralisation present was expressed as a percentage area of each well.

2.2.10 Surface marker expression of MSCs by FACS analysis

Subcutaneous ADSCs and pvADSCs in passage 2 (P2) and bmMSCs in P3 were expanded in SGM until 80% confluence was reached in 10 cm cell culture dishes. The cells were harvested through trypsinisation (Section 2.2.2) and after neutralisation with 2 ml DMEM + 10% FBS per dish, cells were subjected to centrifugation (250 x *g*, 5 min, RT) and resuspended in 10 ml PBS containing 1% BSA. A 30 µl aliquot of the cell suspension was then taken for cell counting, and the remainder of cell suspension was again subjected to centrifugation (250 x *g*, 5 min, RT) and resuspended in PBS containing 1% BSA (#A4503-100G, Sigma-Aldrich, Germany) at a concentration of 1 x 10^6 cells/ml. A 100 µl aliquot of cell suspension (containing 100 000 cells) was transferred to a FACS tube (BD Biosciences, CA USA) at RT. Cell suspensions at a concentration of 1 × 10^5 cells per 100 µL were co-labelled with mouse anti-rat fluorescent antibodies against progenitor cell- (CD90 (Thy-1) FITC, #554897, BD Biosciences; CD106 Alexa Fluor 647, # MCA4633A647T, AbD Serotech), fibroblast- (CD26 PE, #559641, BD Biosciences) and leukocyte- (CD45 V450, #561587, BD Biosciences) associated surface markers. Refer to table 3.2.2.1 for antibody information. After addition of the antibody cocktail specific for each cell type analysed, cell suspensions were gently vortexed and incubated in the dark at RT for 30 min. After incubation, 200 µl of 0.5 % paraformaldehyde in PBS containing 1% BSA was added to each sample tube and the tube vortexed briefly to resuspend the cells. The cells were immediately analysed by flow cytometry. Flow cytometric analysis was performed using a FACS Canto II (BD) and FACSDiva software (BD). Since a multicolour cytometric analysis was carried out, fluorescent compensation settings were established through a compensation experiment and regions of positive and negative staining were determined through a fluorochrome minus one (FMO) experiment. An unstained sample was used as a negative control for gating purposes. A total of 30 000 events were recorded for each sample and data was analysed using Flow Jo Vx (Treestar) software. (See figure A in Addendum A for compensation controls).

Table 2.2.10.1 Flow cytometry antibodies to determine expression marker pattern of isolated MSCs.

Specificity (Mouse anti-rat)	Conjugate	Concentration per 10^6 cells	Isotype	Manufacturer
CD106	Alexa Fluor 647	5µL	IgG1	AbD Serotech, Cat # MCA4633A647T
CD26	PE	5µL	Mouse (BALB/c) IgG2a,κ	BD Pharmingen, Cat # 559641, Lot #10178
CD90	FITC	5µL	Mouse (BALB/c) IgG1,κ	BD Pharmingen, Cat # 554897, Lot # 2195904
CD45	V450	2.5µL	Mouse (BALB/c) IgG1,κ	BD Horizon, Cat # 561587, Lot # 2223891

2.2.11 5-bromo-2'-deoxyuridine (BrdU) assay for cellular proliferation

The BrdU assay for cellular proliferation is based on the incorporation of BrdU into newly synthesized DNA in cells undergoing proliferation, and is measured colourimetrically where absorbance values obtained are proportional to the amount of cellular proliferation occurring. The Cell Proliferation ELISA, BrdU (colourimetric) kit (#11647229001, Roche Diagnostics Corporation, IN, USA) was used and the assay was performed according to manufacturer's instructions. scADSCs and pvADSCs at P2 or bmMSCs at P3 were seeded at 10^4 cells per well in 96-well plates and incubated in standard expansion medium at 100 µl/well overnight at 37 °C in 5% CO_2 and constant humidity. The following day the cell cultures were serum starved in order to synchronize the cell cycle, this was done by exchanging the expansion medium with starvation medium (DMEM + 1% FBS), at 100 µl/well and incubated for a further 16 hours. After synchronization of the cell cycle was complete, starvation medium was aspirated and replaced with expansion medium. Treatments which may affect cellular proliferation were given to the cells at this time. Cells, in expansion medium, with or without treatment, were incubated at 37 °C in 5 % CO_2 and constant humidity for a further 22 hr, followed by addition of 10 µl of BrdU labeling solution (1:100 dilution of BrdU labeling stock in DMEM) to each well containing cells, and the plate was incubated for a further 2 hr to allow for the BrdU to be incorporated. Medium containing BrdU labeling solution was then removed by aspiration and the plate either allowed to air-dry followed by storage at 4 °C for up to 7 days before further processing, or the assay was carried out immediately.

To perform the BrdU assay, the wells were incubated with 200 µl/well FixDenat solution for 30 min at RT. After removal of FixDenat, the cells were incubated with 100 µl/well anti-BrdU-POD [monoclonal antibody from mouse-mouse hybrid cells (clone BMG 6H8, Fab fragments) conjugated with peroxidase] working solution (1:10 anti-BrdU-POD: Antibody

dilution solution) for 90 min at RT. After 90 min, the anti-BrdU-POD was removed and wells washed with Washing solution (PBS) at 200 µl/well x 3. Substrate solution (tetramethyl-benzidine) was then added at 100 µ/well and colour allowed to develop for 5 min before reading the absorbance at 370 nm (reference wavelength 492 nm). For the blank, the assay was performed in wells containing no cells. Background was controlled for by performing the BrdU assay on wells which contained cells that were not labeled with BrdU labeling solution.

2.2.12 Nucleic acid methods

Confirmation of the expression of genes associated with adipogenesis and osteogenesis are necessary to ensure that a true adipogenic or osteogenic phenotype has been achieved with adipogenic or osteogenic induction. Adipogenic marker genes that were quantified were PPARγ2, aP2 and adipsin, while the osteogenic marker genes that were quantified were alkaline phosphatase, RunX2 and bone sialoprotein (BSP) (Sadie-Van Gijsen *et al.*, 2012). This section details the procedures used to isolate total RNA from naïve cells or cells differentiated with AM or OM, followed by synthesis of cDNA from the isolated total RNA, and finally semi-quantitative real time PCR to quantify relative gene expression levels using the synthesized cDNA.

2.2.12.1 Total RNA isolation

Subcutaneous ADSCs and pvADSCs at P2 and bmMSCs at P3, to be used for RNA isolation, were cultured in 6-well plates (Nest Biotech Co., Ltd, China) under various conditions until RNA was harvested at the required time point. RNA was isolated from cells using the RNeasy® RNA isolation kit (Qiagen, #74106) as recommended by the manufacturer. At the required time point, medium was aspirated from the wells followed by immediate addition of 350 µl of RLT (rapid lysis treatment) buffer supplied in the kit. Gentle pipetting was used to dislodge the cells from the well surface and the lysate was transferred to an RNAse-free 1.5 ml microfuge tube. RNA lysates were stored at -80 °C before RNA isolation was carried out.

The RNA isolation procedure was carried out on thawed previously prepared RNA lysates. A volume of 350 µl of 70% EtOH was added to each tube containing RNA lysate and gently mixed by pippeting. A 700 µl volume of the EtOH/lysate mixture was transferred to an RNeasy mini column, inserted into a 2 ml collection tube, followed by centrifugation (8 000

x *g*, 15 sec, RT). The flow through was discarded, and a volume of 700 µl of wash buffer RW1 was applied to the column, the column and collection tube were centrifuged (8000 x *g*, 15 sec, RT), and the flow through was again discarded. 500 µl of buffer RPE was applied to the column, which was centrifuged (8000 x *g*, 15 sec, RT) and the flow through discarded. A final 500 µl volume of buffer RPE was applied to the column and this was again centrifuged (8000 x *g*, 2 min, RT) for a longer period of time in order to dry the column. The column was carefully removed from the collection tube, so as not to make contact with any flow through, and placed in a clean 1.5 ml microfuge tube. A volume of 30 µl of RNAse-free water was applied directly to the membrane of the column, and the column and collection tube were centrifuged (8000 x *g*, 1 min, RT) in order to elute the RNA from the column. Isolated RNA was stored at -80 °C before cDNA synthesis was carried out.

2.2.12.2 cDNA synthesis

Samples of total RNA isolated using the RNeasy® RNA isolation kit (Section 2.2.12.1) were thawed on ice and heated at 65 °C for 10 min and immediately placed on ice. The optical density (OD) of the RNA was measured using a NanoDrop 2000 spectrophotometer (Thermo Scientific, DE, USA) to determine the concentration of RNA in µg/ml. The absorbance ratio of 260/280 nm which was also measured to determine the purity of the RNA, with a value of ~ 2.0 indicating pure RNA and a value of ~1.8 indicating pure DNA. Values for 260/230 nm provide a secondary measure of RNA purity, and a ratio of 2.0 is considered to be indicative of pure RNA (Wilfinger *et al.*, 1997).

Once the concentration of the RNA and purity of the RNA as shown by the A260/280 and A260/230 ratios had been determined, 1.1 µg of RNA was transferred to an RNAse-free 0.6 ml PCR tube (QSP) and the volume of each sample made up to 8 µl with RNAse-free H_2O.

A 1:1 mixture of 10 x DNase reaction buffer (Promega, Madison, WI, USA) and RQ1 DNase (Promega, Madison, WI, USA) was made and 2 µl of this mixture was added to each sample, which were then incubated at 37 °C for 30 min in a PCR Express thermocycler (22962, Hybaid, UK) in order to digest any DNA present in the sample. The DNase reaction was stopped by the addition of DNase stop solution (Promega, Madison, WI, USA) and the DNase enzyme inactivated by incubation of the samples at 65 °C for 10 min in the thermocycler.

A volume of 10 µl of the DNase-treated RNA, containing approximately 1 µg of RNA, was transferred to a clean RNAse-free 0.6 ml PCR tube, and a volume of 1.7 µl of 100 µM oligo(dT) primer (IDT) was added to each sample. Samples were incubated in a thermocycler at 70 °C for 5 min for RNA denaturation, and placed on ice immediately after to prevent the primers from annealing to one another. To each sample, 7.8 µl of the following cocktail was added:

- 4 µl of RT buffer consisting of 80% ImProm-II™ reaction buffer (Promega, Madison, WI, USA) and 20% M-MLV™ reaction buffer (Promega, Madison, WI, USA)
- 0.5 µl of 10 mM dNTPs (Sigma-Aldrich)
- 1.8 µl RNAse-free H_2O
- 0.5 µl RNAsin (Promega, Madison, WI, USA)
- 1 µl ImProm-II™ reverse transcriptase (RT) (Promega, Madison, WI, USA)

After the addition of the above cocktail, samples were incubated at 25° C for 5 min, followed by 42 °C for 1 hr, in a 2-step RT reaction. Finally, the RT was inactivated by incubation of the samples at 70 °C for 15 min. Samples containing synthesized cDNA were stored at -20 °C.

2.2.12.3 Conventional PCR

Brun-Heath *et al*. designed and published primers that were able to distinguish between bone-type and liver-type TNAP mRNA transcripts in rat, as each forward primer was specific for a region on the 5′-untranslated region which varies between bone or liver transcripts, and a single common reverse primer, complimentary to a protein-coding region of the mRNA (Brun-Heath *et al.*, 2011). The sequence of the bone-type forward primer is 5′ GCCGGGACAGACCCTCCCCAC 3′, the liver-type forward primer is 5′ GCTGAAGGTTGAGCATTCTAGTGCAGG 3′ and the reverse primer is 5′ GGCGTATGCCTCCTGCATTGG 3′. The expected PCR products from the use of the bone or liver primer sets are 1595 and 1607 bp respectively. PCR template samples included cDNA synthesized from RNA isolated from AM- or OM-treated bmMSCs, scADSCs and

pvADSCs, as well as from RNA isolated from rat liver for use as a positive control (Section 3.2.12.2). PCR was performed using the GoTaq® G2 Flexi DNA polymerase kit (Promega, Madison, WI, USA) according to manufacturer instructions, with a PCR reaction volume of 50 µl [10 µl of GoTaq® Flexi Buffer, 2 µl $MgCl_2$ (25 mM), 1 µl dNTP mixture (10 mM), 0.25 µl GoTaq® Flexi DNA Polymerase (5 U/µl), 1 µl of forward primer (10 µM) and 1 µl of reverse primer (10 µM), 2 µl template cDNA, volume made up to 50µl with nuclease-free water]. PCR reactions were carried out using a PCR Express thermocycler (Hybaid, UK). Amplification conditions for the bone-type primer set were as follows: Denaturation at 94 °C for 5 min, followed by 40 cycles at 94 °C for 1 min, 60 °C for 1 min and 72 °C for 2 min, followed by a final extension of 72 °C for 15 min. Amplification conditions for the liver-type primer set were as follows: Denaturation at 94 °C for 5 min, followed by 40 cycles at 94 °C for 1 min, 57 °C for 1 min and 72 °C for 2 min, followed by a final extension of 72 °C for 15 min. For analysis, amplicons were subjected to electrophoresis on a 1% agarose gel containing 0.5 µg/ml ethidium bromide (EtBr), run at 80 V for 45 min. The DNA bands were visualised by the fluorescence of the EtBr dye under UV light, using a ChemiDoc imaging system (Bio-Rad Laboratories, CA, USA).

2.2.12.4 Quantitative real-time PCR (RT-qPCR)

RT-qPCR was performed using a Rotor-Gene Q 2-Plex (Qiagen) and data was analysed using Rotor-Gene Q series software version 2.2.3 (Build 11) to quantify relative gene expression. Synthesized cDNA samples (Section 2.2.12.2) were diluted 1:125 with nuclease-free water in order to assess levels of the reference gene (RG), acidic ribosomal phosphoprotein (*Arbp*) (*Rplp0*) (van Wijngaarden *et al.*, 2007). For evaluation of the various genes of interest (GOIs), cDNA samples were diluted 1:5 with nuclease-free water. Quantification of the expression of the various GOIs was achieved by normalization of the relative expression of each GOI to the relative expression of the RG. Three biological repeats were employed for each experiment, where the individual repeats were assayed in duplicate.

RT-qPCR reaction components for a single PCR sample (total volume of 10 µl) included:

- 0.1 µl forward primer (10 µM)
- 0.1 µl reverse primer (10 µM)
- 5.0 µl 2x Sensimix SYBR No Rox (Bioline, London, UK)
- 3.8 µl nuclease-free H_2O

- 1 µl cDNA template diluted 1:5 with nuclease-free water

Primer sets used for detection of the various GOIs are given in Table 2.2.12.4.1.

Table 2.2.12.4.1: Primer sequences used for semi-quantitative real-time PCR (RT-qPCR).

Transcripts **(reference)**	Primer sequences **(5' -3')**	Product size **(bp)**
Pparγ2 (Pparg2) **(Tanabe *et al.*, 2004b)**	F: ACT GCC TAT GAG CAC TTC AC R: CAA TCG GAT GGT TCT TCG GA	448
Ap2 (Fabp4) **(Fukuen *et al.*, 2005)**	F: TGA AAT CAC CCC AGA TGA CAG R: CTC ATG CCC TTT CAT AAA CT	194
Adipsin (Adps) **(van de Vyver *et al.*, 2014)**	F: CAC GTG TGC GGT GGC ACC CTG R: CCC CTG CAA GTG TCC CTG CGG T	476
Alkaline phosphatase (*Alp*) (Kuroda *et al.*, 2005)	F: GAG CAG GAA CAG AAG TTT GC R: GTT GCA GGG TCT GGA GAG TA	202
RunX2 (Liu *et al.*, 2004)	F: GAT GAC ACT GCC ACC TCT GA R: ATG AAA TGC TTG GGA ACT GC	118
Bone Sialoprotein (BSP) (Tanabe *et al.*, 2004a)	F: GAT AGT TCG GAG GAG GAG GG R: CTA ACT CCA ACT TTC CAG CG	172
Arbp (Rplp0) **(van Wijngaarden *et al.*, 2007)**	F: AAA GGG TCC TGG CTT TGT CT R: GCA AAT GCA GAT GGA TCG	91

Thermal cycling conditions varied slightly according the primer set used, with the steps commonly used including an initial denaturation of 95 °C for 10 min, followed by a sequence cycle starting with a short denaturation step of 95 °C for 3 sec, a variable annealing step, and a variable extension step, repeated 35 x, and lastly, a final extension step of 72 °C for 5 min. Table 2.2.12.4.2 gives the thermal cycling conditions for the primer sets used to amplify the various GOs.

Table 2.2.12.4.2: Thermal cycling conditions for the primer sets used to amplify the various genes of interest (GOIs).

Transcripts	Annealing temperature (°C)	Annealing time (sec)	Extension temperature (°C)	Extension time (sec)
PPARγ2 (Pparg2)	53	10	72	20
Ap2 (Fabp4)	50	5	72	6
Adipsin (Adps)	60	3	72	15
Adiponectin	54	7	72	5
Alkaline phosphatase (*Alp*)	52	5	72	8
Bone sialoprotein	52	10	72	8
RunX2	52	8	72	6
Arbp (Rplp0)	52	10	72	8

2.2.13 Fluorescence microscopy – optimization of perilipin A staining in subcutaneous and visceral adipose derived stromal cells.

ScADSCs and pvADSCs at passage 2 (P2) and bmMSCs at passage 3 (P3) were seeded at 30 000 cells/well into a sterile Lab-Tek Chambered #1.0 Borosilicate coverglass system 8-well chamber dish (120177LE 1007, Nunc, NY,USA) and incubated with SGM at 37° C in 5% CO_2 until two days post confluence. Thereafter, cells were induced with adipogenic differentiation media (AM) as previously described (Section 2.2.5), and cultured for a further 5 days for ADSCs and for 14 days for bmMSCs in AM with media changes every third day.

2.2.13.1 Immuno-fluorescent Perilipin A staining

Once cells were ready for staining, at either day 5 or 14, as described above, the medium was aspirated off and cells were fixed with 4% paraformaldehyde in PBS (pH 7.4, 100 µl/well, 10 min, 4 °C). The wells were then washed 1 x for 30 sec with 200 µl/well PBS (pH 7.4), followed by the addition of 100 µl/well Triton X-100 (10 min at 4 °C). Wells were again washed 1 x with 200 µl/well PBS for 30 sec and 100 µl/well of blocking serum (FBS) was added and the plate incubated for 20 min at RT. Blocking serum was drained and not washed, followed by addition of 100 µl/well of primary antibody [Rabbit polyclonal Perilipin A (1.00 mg/ml) (#ab3526, Abcam, UK) at a 1:50 dilution with PBS] and the dish was incubated

overnight at 4 °C in the dark. The wells were then washed with 200 µl/well PBS (pH 7.4) for 30 sec and 100 µl/well of the secondary antibody [goat polyclonal secondary antibody to rabbit IgG – H&L (Alexa Fluor® 594) (2.00 mg/ml) (#ab150080, Abcam, UK) at 1:250 dilution in PBS] was added and the dish incubated for 1hr at RT in the dark. The wells were washed 2x with 200 µl/well PBS (pH 7.4) and either a single drop of Dako fluorescent mounting medium (S3023, North America Inc., CA, USA) was applied to the wells to preserve integrity of the cells, or the wells were co-stained for endogenous alkaline phosphatase activity using the ELF® 97 endogenous phosphatase detection kit (Roche Diagnostics Corporation, IN, USA).

2.2.13.2 Alkaline phosphatase activity detection using a fluorescent probe.

The ELF® 97 endogenous phosphatase detection kit (#E6601, Molecular Probes™, Invitrogen, Leiden, The Netherlands) was used to detect alkaline phosphatase activity, and was performed according to manufacturer instructions. The ELF 97 phosphatase substrate was diluted 20 x in detection buffer and filtered with a 0.2 µm pore size filter immediately before use. The diluted substrate was applied to the wells at 50 µl/well for a period of 5 min in the dark at RT. The reaction was stopped by washing the wells 3 x with 200 µl/well wash buffer (PBS containing 25 mM EDTA, 5 mM levamisole, pH 8.0) for 5 min each wash. The wash buffer was removed by aspiration with a pipette, as much as possible without drying the sample, and a drop of ELF 97 mounting medium was applied to the well. The dish was then covered in foil to protect it from light and stored at -20 °C until ready to view. Images were acquired using a A Zeiss LSM780 Elyra S1 confocal microscope with ZEN 2011 software (Carl Zeiss, Jena, Germany) using a standard Hoeschst/DAPI longpass filter set, as the maximum emission of the ELF alcohol product is 530 nm.

2.2.14 Knockdown of tissue-nonspecific alkaline phosphatase (TNAP) gene (*Alp1*) using the MISSION® viral transduction system (Sigma)

Knockdown of the alkaline phosphatase (*Alp1)* gene was performed in scADSCs undergoing adipogenic differentiation using the MISSION® viral transduction system (Sigma) according to the manufacturer recommendations, in order to determine the contribution of TNAP on lipid accumulation and adipogenesis. Confirmation of knockdown was performed by RT-

qPCR (Section 2.2.12). The MISSION viral transduction system is based on RNA interference (RNAi), where the short hairpin RNA (shRNA) specific for a particular gene is inserted into a viral vector (amphotropic lentiviral particles), which is transfected into the cells of interest. Once integrated into the cellular genome, the shRNA are expressed and processed intracellularly into siRNA. Selection of transfected cells is based on resistance to the antibiotic puromycin, as the puromycin resistance gene is expressed from the viral vector. Figure 2.2.14.1 presents the vector diagram of the lentiviral plasmid pLKO.1-puro used in this study.

Subcutaneous ADSCs in P1 were transfected with MISSION pLKO.1-puro Non-Target shRNA Control Transduction Particles (SHC016V) or MISSION® Lentiviral Transduction particles (SHCLNV) targeting TNAP at a ratio of 2:1 particles to cells. Roughly 40 000 cells/well were grown in a 6-well plate before transfection commenced with polybrene being also added at a final concentration of 8 µg/ml to the standard expansion medium. The cells were incubated at 37 °C in 5 % CO_2 and constant humidity for 24 hr to allow for viral transfection to occur. After 24 hours, the medium containing viral particles and polybrene was aspirated off and the medium was replaced with SGM. The cells were incubated for a further 24 hr before the addition of puromycin (#P8833, Sigma-Aldrich) at 2 µg/ml. Puromycin was also added to untransfected cells as a control, in order to confirm the efficacy of antibiotic selection. The antibiotic-containing medium on the wells containing the transfected cells was replaced with SGM without antibiotic and cells were incubated for a further 24 hr at 37 °C, 5% CO_2 with constant humidity. After 24 hr, the transfected cells were passaged (into P2) for experimentation and incubated for a further 24 hr at 37 C, 5% CO_2 with constant humidity (Section 2.2.3). After this step, the SGM on the cells was replaced with SGM containing 2 µg/ml puromycin, and cells were maintained in this medium until the time that adipogenic induction was initiated (Section 2.2.5). During adipogenic differentiation of the transfected cells, no puromycin was added to the AM. At day 5 of adipogenic differentiation, cells were harvested for RNA isolation and RT-qPCR to assess knockdown of the *Alp1* gene (Section 2.2.12.3).

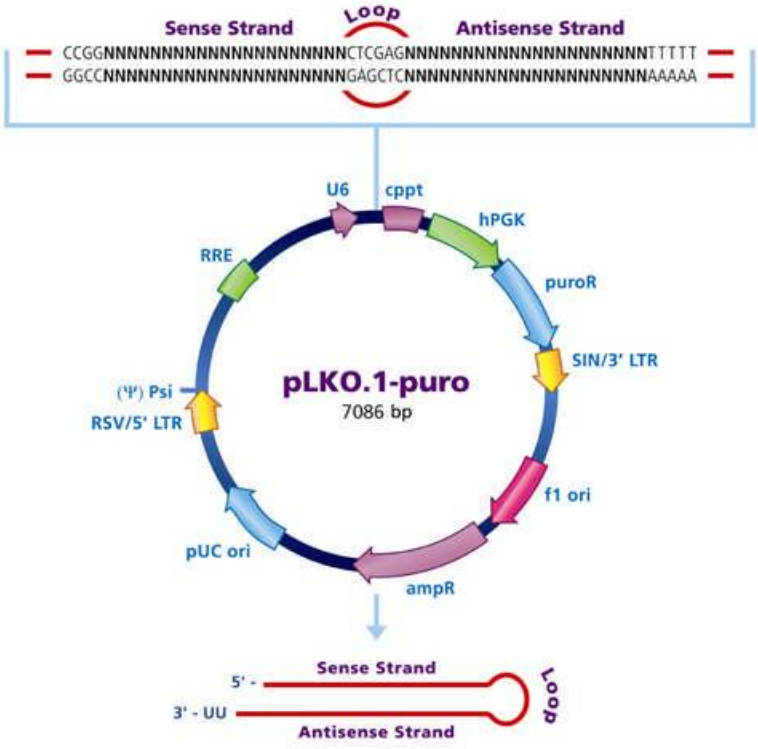

Figure 2.2.14.1: Vector diagram of the TRC1 and TRC1.5 Lentiviral Plasmid Vector pLKO.1-puro features (Taken from, MISSION® shRNA control transduction particles, Technical bulletin, Sigma-Aldrich,http://www.sigmaaldrich.com/content/dam/sigma-aldrich/docs/Sigma/Bulletin/1/shc016vbul.pdf, Accessed: 6 July 2016).

2.2.15 Glycosylation analysis of TNAP

Samples for glycosylation analysis were cell lysates (bmMSCs) (Section 2.2.4.1) and alkaline phosphatase extraction samples (scADSCs and pvADSCs) (Section 2.2.4.2). ALP isozymes present in the samples were separated by wheat germ lectin (WGL) affinity electrophoresis on a 1% agarose gel buffered to an alkaline pH of 9.4 (HYRAGEL 7, ISO-PAL kit), using a Hydrasys semi-automated electrophoresis system (Sebia, France) according to manufacturer instructions. Samples were run in duplicate in adjacent wells, with 10 µl of sample applied per well, and with the addition of 10 µl of lectin solution in one well of each duplicate pair. Each sample was run at an ALP concentration of 200U/L, as determined by ALP activity assay (Section 2.2.4.3). The migration was carried out for approximately 30 minutes, at 10 W constant power at 30 °C. Following migration, 2.5 ml of ISO-PAL substrate solution [2 ml BCIP (5-Bromo-4-Chloro-3-Indolyl Phosphate) in Aminomethyl Propanol buffer (AMP) pH 10.1 ± 0.5 + 0.5 ml chromogen (Nitro Blue Tetrazolium) in water] is applied to the gel and incubated at 37 °C for 45 min. Following substrate incubation, the remaining substrate solution is removed and the gel is blotted with filter paper at 45 °C for 3 min. The filter paper

was discarded after blotting and the gel remained in the Hydrasys instrument for drying at 60 °C for 2 min. The final washing and processing of the gel was performed by the Hydrasys instrument, and the final dried, processed gel was visually evaluated.

2.2.16 Statistical analysis

Variables were subjected to unpaired t-tests (for comparing two groups) or analysis of variance (ANOVA) (for comparing 3 or more groups) followed with Tukey's *post hoc* test to compare all groups where appropriate. Biological repeats of a minimum of n=3 were performed per experiment, with three technical repeats performed per n=1, unless otherwise stated. Values are expressed as mean ± SEM. Statistical significance was denoted using asterisks (*). Results were considered statistically significant where $P < 0.05$. GraphPad Prism 5 software (GraphPad Software, Inc.) as well as Statistica software (StatSoft, version 10) were used to perform statistical analysis.

CHAPTER 3

Characterisation of mesenchymal stromal cells (MSCs) from adipose and bone marrow depots.

3.1 Introduction

Mesenchymal stromal cells (MSCs) were first isolated from bone marrow tissue by Friendenstein *et al*. in the 1960s, when it was discovered that these cells were plastic-adherent and capable of spontaneous bone formation (Friedenstein *et al.*, 1970). These bone marrow-derived MSCs were also found to have stem cell-like characteristics, in that they were able to undergo several rounds of expansion in culture and could be differentiated towards various mesenchymal cell types, including osteoblasts, adipocytes and chondrocytes (Chen *et al.*, 2007; Galderisi and Giordano, 2014). MSC-like cells were later found in various other tissues, including adipose and umbilical cord tissue, and were characterised based on their ability to differentiate into the various mesenchymal lineages (Dominici *et al.*, 2006; Peng *et al.*, 2008).

Interest in MSCs has grown in recent years due to the potential clinical use of these cells for regeneration of damaged tissue, such as bone, cartilage and adipose tissue, damaged either as a result of injury, cancer or a congenital defect (Arrigoni *et al.*, 2009; Shah *et al.*, 2014). A greater understanding of the biology and mechanisms underlying the differentiation of MSCs into the various lineage phenotypes is necessary in order that the full therapeutic potential of these cells is realised, as well as for understanding the development of certain metabolic diseases, such as those brought about by osteoblast and adipocyte dysfunction, including osteoporosis and obesity (Nuttall and Gimble, 2004; Yu *et al.*, 2010; Czekanska *et al.*, 2012).

Immortalized cell lines are often derived from cancers or other malignancies, and have been extensively utilized as models to study cellular differentiation due to their ease of use. Immortalized cell lines can be expanded extensively in culture and are more phenotypically stable than primary-derived cells. There are however, drawbacks to using various immortalized cell lines, including a limited differentiation profile, an aberrant cell cycle, chromosome abnormalities, lack of growth inhibition, as well as findings that suggest a lack of homogeneity between cells from earlier and later passages (Czekanska *et al.*, 2014). For the above reasons, the present study selected to use primary-derived MSCs as a model for studying adipogenesis and osteoblastogenesis, as the characteristics of primary cells are known to be closer to those of cells *in vivo* than immortalized cell lines (Marko *et al.*, 1995).

Rats provide a well-established immunocompetent small animal model for studying MSC biology. MSCs have been successfully harvested from a variety of rat tissues, including bone marrow, as well as inguinal subcutaneous and peri-renal visceral adipose depots. While rat MSCs provide a suitable model for investigation into the mechanisms of mesenchymal differentiation, a limitation exists in the form of a paucity of reagents for surface marker characterisation, a situation which may improve as more of these products become available (Arrigoni *et al.*, 2009; Lopez and Spencer, 2011).

Despite the ability of MSCs isolated from various tissues to differentiate into osteoblastic, adipocytic and chondrocytic lineages, as well as having similar surface marker expression, several differences exist between MSCs isolated from various sources, including variations in proliferation and differentiation capability, and gene expression profiles (Noel *et al.*, 2008; Casteilla *et al.*, 2011). For the above reason, it is necessary to characterise MSCs from various depots with regards to phenotype, proliferation rate, as well as differentiation capability, in order to establish the suitability of those particular MSCs as a model for the cellular differentiation pathway of interest.

The present study utilised rat MSCs derived from bone marrow (bmMSCs) as well as the inguinal subcutaneous and peri-renal visceral adipose-derived MSCs (scADSCs and pvADSCs, respectively) as models for both adipogenesis and osteoblastogenesis. Previous studies have shown differences in the response of rat scADSCs and pvADSCs when induced towards adipogenic and osteogenic differentiation, particularly that scADSCs have a greater osteogenic potential than pvADSCs, while pvADSCs had a greater potential for lipid accumulation during adipogenic induction than scADSCs (Arrigoni *et al.*, 2009; Sadie-Van Gijsen *et al.*, 2012). Additionally, rat-derived bmMSCs have been reported to have a greater osteogenic differentiation potential in comparison to scADSCs, while the adipogenic differentiation potential of scADSCs is superior to bmMSCs (Yoshimura *et al.*, 2007; Hayashi *et al.*, 2008).

The *in situ* identification of MSCs has proven to be difficult, as no single marker is available which is able to identify undifferentiated naive MSCs within intact tissue (Baer and Geiger, 2012). Immunohistochemistry and cell sorting techniques have identified populations of

perivascular cells in various human organs, which share many characteristics with cultured MSCs, suggesting that MSCs may originate from a perivascular niche (Corselli *et al.*, 2010). MSC characterisation is still most often retrospective rather than prospective, where MSCs isolated from various tissues and cultured *in vitro* are characterised by plastic adherence, surface marker expression and the ability to differentiate into osteoblasts, adipocytes and chondrocytes. There is at present a lack of standardization in cell culture techniques, media composition and other reagents used for cell culture between different investigators, and this has led to difficulties in making direct comparisons between the results obtained from different studies (Baer and Geiger, 2012). It is therefore necessary to characterise the MSCs isolated for this study in terms of surface marker expression, proliferation and differentiation potential, in order to verify that the isolated cells are indeed MSCs.

One of the drawbacks of using primary-derived MSCs is that primary cell cultures are known to be heterogeneous, and may contain several different progenitor sub-populations. MSCs also have a limited lifespan in culture, and as such for each experiment cells must be isolated from fresh tissue, so that experiments can be performed consistently with cells at a specified passage (Bianco *et al.*, 2001; Sethe *et al.*, 2006; Brinchmann, 2008; Baer and Geiger, 2012).

In order to compare MSCs from different anatomical locations, the MSCs isolated from bone-marrow and adipose depots were characterised in terms of their morphology, which is based on qualitative visual evaluation, as MSCs typically have a fibroblastic or spindle-shaped appearance in culture, but may also appear as random polygonal. Differences in morphological appearances of MSCs may be a consequence of the inherent heterogeneity observed in primary-derived MSC cultures (Bianco *et al.*, 2001; Kollmer *et al.*, 2013). We have also performed flow cytometry on the MSCs isolated from different depots, which provided a more rigorous measure of cellular morphology and allowed for individual cells within a sample population to be characterised based on the size and internal complexity, termed granularity, of the cells. Flow cytometry analysis also allows for the presence of different populations of cells with a sample population to be identified.

We have evaluated the MSC populations isolated from bone-marrow and adipose tissue for expansion rate in culture, which was assessed by cellular proliferation rate, as this allowed us

to gain a better understanding of the behaviour of the cells in culture, and to identify which culture conditions would be suitable for cells from each MSC depot, such as cell density prior to passage. The MSCs isolated were further characterised using cell surface markers and flow cytometry, to allow positive confirmation of the MSC phenotype and exclude the possibly that the cell types isolated were of the hematopoietic or fibroblastic lineage. Adipogenic and osteogenic differentiation capabilities were also assessed, by treating cells from adipose- and bone-marrow depots with either adipogenic or osteogenic differentiation media followed by staining and quantification of lipid and mineral content, respectively. Differentiation of MSCs into either adipogenic or osteoblastic lineages was confirmed using reverse-transcription semi-quantitative PCR (RT-qPCR) to detect the presence of adipogenic or osteoblastic gene marker (mRNA) expression levels, and differences in the relative expression of the various markers between MSC depots were compared to the housekeeping gene, *Arbp*.

3.2 Results

3.2.1 Mesenchymal stem cell (MSC) morphology

MSCs from subcutaneous (scADSCs) and visceral (pvADSCs) adipose depots, as well as bone-marrow (bmMSCs), were cultured with DMEM and 10% foetal bovine serum at 37° C with 5% CO_2 in a humidified environment (Section 2.2.3). The morphology of the cells was fibroblastic, i.e. elongated and spindle-shaped, for all three cell types at passage 0 (P0). The adipose-derived MSCs (ADSCs) appeared to be evenly spaced from one another at 24 to 48 hr after seeding at P0 (Fig. 3.2.1.1, A and D) and proliferated to form clusters of cells with sparsely populated gaps between the clusters after 4-6 days and then a confluent lawn. In contrast, bone-marrow derived MSCs (bmMSCs) were observed as loose clusters one to two days after initial seeding at P0, and subsequently spread out from these regions to form a confluent lawn after 4-6 days in culture (Fig. 3.2.1.2, A).

After the first passage (P1), the ADSCs became slightly broader and less elongated in appearance while still retaining a fibroblastic morphology, and were generally homogenous in appearance (Fig. 3.2.1.1, B and E). Cells proliferated rapidly in P1 and typically reached confluence within three to four days after seeding. Morphology of ADSCs after passage 2

(P2) was highly similar to cells in P1, where cells formed a confluent lawn after seeding after 3-5 days. ADSCs were used for experimentation at P2. Cells at P2 which had reached confluence appeared as a lawn, where individual cells were not easily distinguishable (Fig. 3.2.1.1, C and D).

Bone marrow-derived MSCs were more heterogeneous in appearance at P0 than ADSCs, and were used at passage 3 (P3) for experimentation. Bone marrow-derived MSCs were observed to become more homogenous in appearance with increased passaging (Fig. 3.2.1.2, B, C and D), while cells maintained a polygonal/fibroblastic morphology throughout all passages.

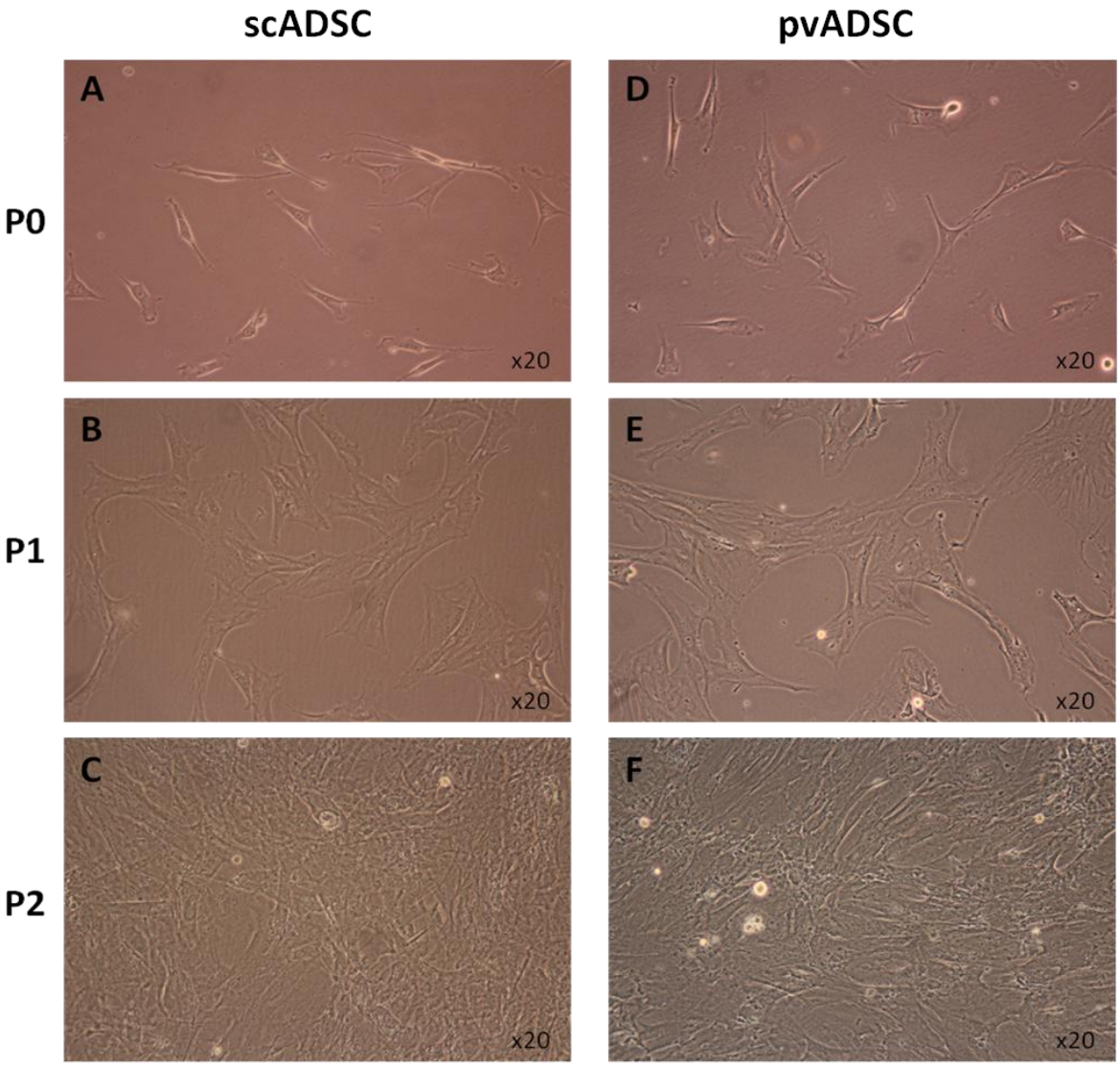

Figure 3.2.1.1: Morphology of adipose tissue-derived MSCs. Images of scADSC (A, B and C) and pvADSC (D, E and F) at P0 (A, D), P1 (B, E) and P2 (C, F). Cells at P2 are shown at confluence on the first day of treatment. Images were taken using an Olympus (CKX41) microscope at x20 magnification.

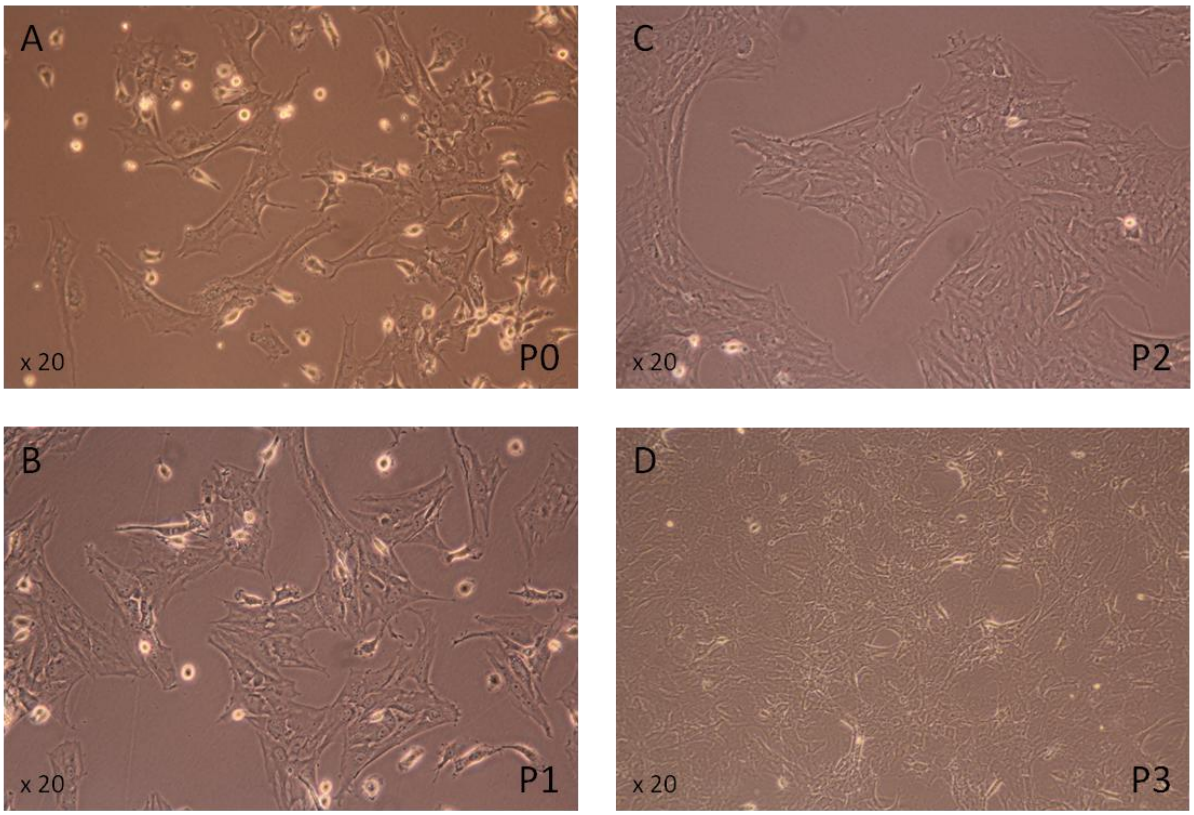

Figure 3.2.1.2: Morphology of bone marrow-derived MSCs (bmMSCs). Images of bmMSCs at P0 (A), P1 (B), P2 (C) and P3 (D). P3 cells are shown at confluence on the first day of treatment. Images were taken using an Olympus (CKX41) microscope at x 20 magnification.

3.2.2 Mesenchymal stem cell (MSC) surface marker expression

In order to determine the purity of the isolated MSC populations, flow cytometry was performed to assess surface marker expression. ADSCs at P2 and bmMSCs at P3 were harvested by trypsinisation and re-suspended in PBS containing 1% BSA. Cell suspensions at a concentration of 1×10^5 cells per 100 µL were co-labelled with mouse anti-rat fluorescent antibodies against progenitor cell (CD90 (Thy-1)) (Dominici *et al.*, 2006), fibroblast- (CD26) (Sgodda *et al.*, 2007) and leukocyte- (CD45) (Dominici *et al.*, 2006) associated surface markers as well as vascular cell adhesion molecule 1 (VCAM1) (CD106) (Cappellesso-Fleury *et al.*, 2010) (Refer to Section 2.2.10 for antibody information).

The scADSC and pvADSC populations were expected to be positive for CD90, as this is an established marker for mesenchymal stromal progenitor populations (Dominici *et al.*, 2006). The International Society for Cellular Therapy (ISCT) also defines MSCs as negative for the surface marker CD45, which is a haematopoietic cell marker (Dominici *et al.*, 2006). The

surface marker, CD26 is a fibroblast marker, and therefore was not expected to be present on the surface of MSCs (Sgodda *et al.*, 2007). The bmMSC populations were expected to be CD90 positive, as well as CD106 positive, as CD106 has been identified as a marker expressed in bmMSCs (Cappellesso-Fleury *et al.*, 2010) and negative for CD45 and CD26. Results see Table 3.2.2.1 and Figure 3.2.2.1.

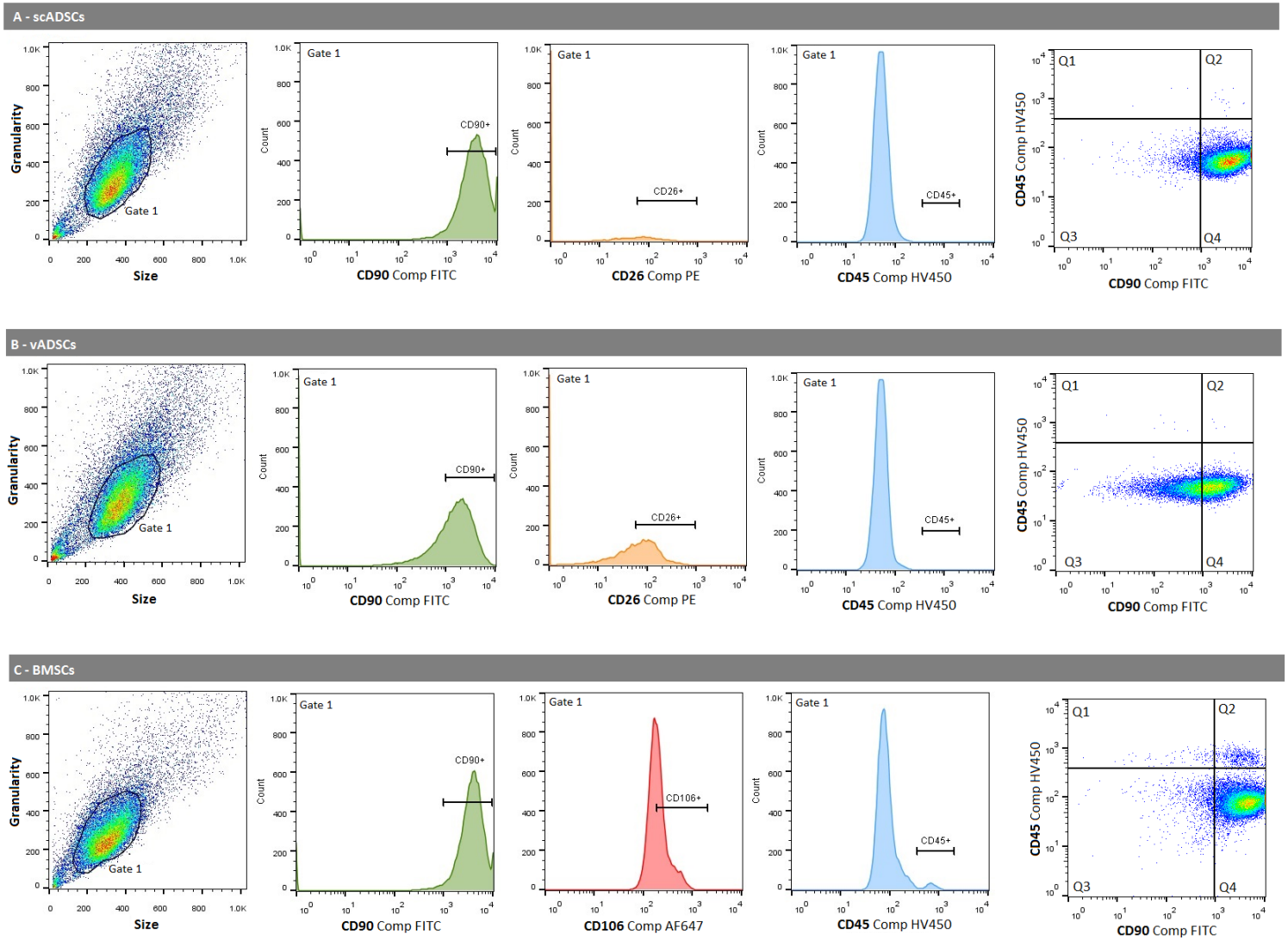

Figure 3.2.2.1: Surface marker expression profile of scADSCs, pvADSCs and bmMSCs. Flow cytometry on scADSCs (A), pvADSCs (B) and bmMSCs (C) was performed on a FACS Canto II instrument using FACSDiva software with a total of 30 000 gated events recorded prior to data analysis. Q1 – $CD90^{-}CD45^{+}$ (Leukocytes); Q2- $CD90^{+}CD45^{+}$ (haematopoietic progenitors); Q3 – $CD90^{-}CD45^{-}$; Q4 – $CD90^{+}CD45^{-}$ (MSCs). The x axis describes the size of the cell, while granularity on the y-axis describes the internal complexity of the cell.

Flow cytometry revealed that cells from all scADSC, pvADSC and bmMSC samples analysed contained a single population (Fig. 3.2.2.1) which were all positive for CD90, and negative for CD26 and CD45 (Table 3.2.2.1). The scADSCs samples had a greater percentage of cells positive for CD90, as compared to the pvADSCs, with CD90 percentage mean values of 85.7% and 57.32%, respectively (Table 3.2.2.1). In the bmMSC samples, 81.7% of cells were positive for CD90. Subcutaneous ADSCs and bmMSCs had a similarly low percentage of cells positive for CD26, with a mean value of 6.4% and 6.3%, respectively, while pvADSCs had a CD26 positive population of 22.1% (Table 3.2.2.1). ADSC samples were virtually devoid of CD45 positive cells, with similar percentages of CD45 cells at 0.2% for scADSCs and 0.3% for pvADSCs, while bmMSC samples had a low level of CD45 expression, as 6.4% of the sample population were positive. bmMSC samples analysed were 54.1% positive for CD106 (Table 3.2.2.1).

Table 3.2.2.1: Percentage of positive staining for cell surface markers CD90, CD26, CD45 and CD106 in scADSCs, pvADSCs and bmMSCs.

Cell type	$CD90^+$	$CD26^+$	$CD45^+$	$CD106^+$
scADSCs (n=4)	85.7 ± 3.8	6.4 ±3.3	0.2 ± 0.1	n.a
pvADSCs (n=4)	57.32 ±4.0	22.1 ±5.9	0.3 ± 0.1	n.a
bmMSCs (n=5)	81.7 ± 3.79	6.3 ±2.2	6.4 ±2.6	54.1 ±17.3

Footnote: Values are presented as the percentage (%) of analysed cells which were positively stained (mean ± SE).

3.2.3 Proliferation

Cellular proliferation was measured in MSCs from adipose and bone marrow depots as part of the characterisation of the various cell types. Cellular proliferation was quantified by a colourimetric immunoassay, measuring the amount of 5-bromo-2'-deoxyuridine (BrdU) incorporated into the cells during DNA synthesis, using the BrdU Cell Proliferation ELISA kit (Roche) (Section 2.2.11). Briefly, proliferation is measured by the incorporation of BrdU, an analogue of thymidine, into the DNA strands during DNA replication prior to cell division. After fixing and denaturing the DNA, an anti-BrdU monoclonal antibody conjugated to peroxidase is used to bind to the incorporated BrdU in the newly synthesized

DNA strands. Cleavage of a substrate by the peroxidase produces a coloured product, which is quantified by absorbance using an ELISA plate reader.

Subcutaneous ADSCs and pvADSCs at P2 and bmMSCs at P3 were seeded at 10^4 cells per well in a 96-well plate and serum-starved overnight to synchronise the cell cycle, where after standard growth medium conditions were restored, and proliferation then quantified at 24 and 48 hours. The absorbance reading was higher at both 0 and 24hr time points for the scADSCs and pvADSCs, when compared to bmMSCs; however by 48hr the absorbance measurement for the scADSCs and pvADSCs had dropped below initial starting levels, while the bmMSCs continued to increase from levels seen at 24hr. The drop in absorbance measurement observed in scADSCs and pvADSCs is likely due to a contact inhibition, where by 48hrs after initiation, the cells had reached confluence and as a result experienced a drop in proliferation (Leontieva *et al.*, 2014). The bmMSCs exhibit a lower absorbance measurement at 0 and 24hrs compared to the ADSCs, and as these cells had not reached confluence by 48hr, cellular proliferation continued. This may be due to the ADSCs having a higher initial rate of proliferation and reaching the exponential phase of proliferation between 24 and 48 hrs, while the bmMSCs experience a slower initial rate and therefore reach exponential proliferation at a later time point than the ADSC samples.

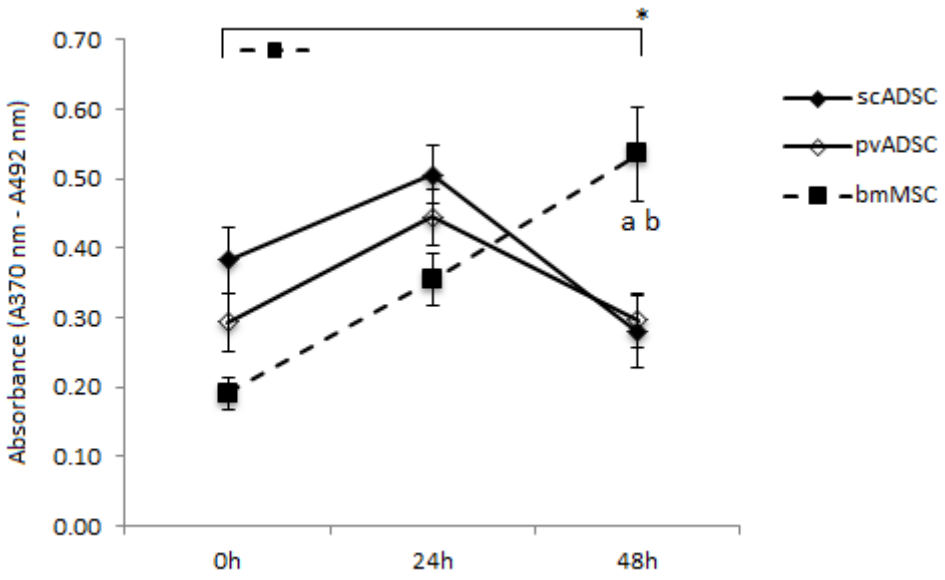

Figure 3.2.3.1: Quantification of BrdU incorporation to provide a comparison of the increase in cell number of MSCs derived from each of the different depots over a 48hr period. Statistical analysis: Factorial ANOVA with Tukey post hoc test. A significant effect of time within each cell type is indicated with *. Significant difference between cell types at the same time point is indicated with **a** (scADSC vs bmMSC) or **b** (pvADSC vs bmMSC). Level of significance was accepted at $p < 0.05$.

3.2.4 Differentiation

The adipogenic and osteogenic differentiation potential of the ADSCs and bmMSCs was assessed by culturing each cell type in the presence of adipogenic (AM) or osteogenic (OM) differentiation medium for specific amounts of time (Section 2.2.5 and 2.2.7 for detailed methodology on culturing conditions). Differentiation was assessed in order to confirm that the cells isolated from adipose and bone marrow depots were mesenchymal progenitor cells and able to undergo differentiation into both adipogenic and osteogenic lineages. This also allowed the differences in differentiation potential between cell types to be qualitatively and quantitatively compared.

3.2.4.1 Adipogenic differentiation

ADSCs and bmMSCs were cultured for up to 14 days in the presence of AM in order to induce adipogenesis. The presence of lipid droplets within the cells provided a visual indication that adipogenesis had occurred. Cell cultures were stained with the dye, Oil Red O which stains lipid red, in order to visualise and quantify the amount of lipid accumulation during adipogenesis. Differentiated cells from scADSC, pvADSC and bmMSC cultures in

AM contained lipid droplets stained red with Oil Red O after 14 days of culture (Fig. 3.2.4.1.1, D, E and F), in contrast to control cells cultured in standard growth medium (DMEM + 10% FBS + vehicle) which do not contain any visible lipid droplets (Fig. 3.2.4.1.1, A, B and C). bmMSC control cultures were observed to form dense clusters of cells during long term culture, which when stained with Oil Red O were observed to trap dye and give rise to aberrant staining (Fig. 3.2.4.1.1, C. indicated by arrows). The aberrant staining present in the bmMSC day 14 controls is indicated in the increase in positive staining during quantification, at 1.5 ±0.5%, compared to the controls for scADSCs of 0.4 ±0.04% and pvADSCs of 0.3 ±0.05% at the same time point (Fig. 3.2.4.1.1, A,B and C).

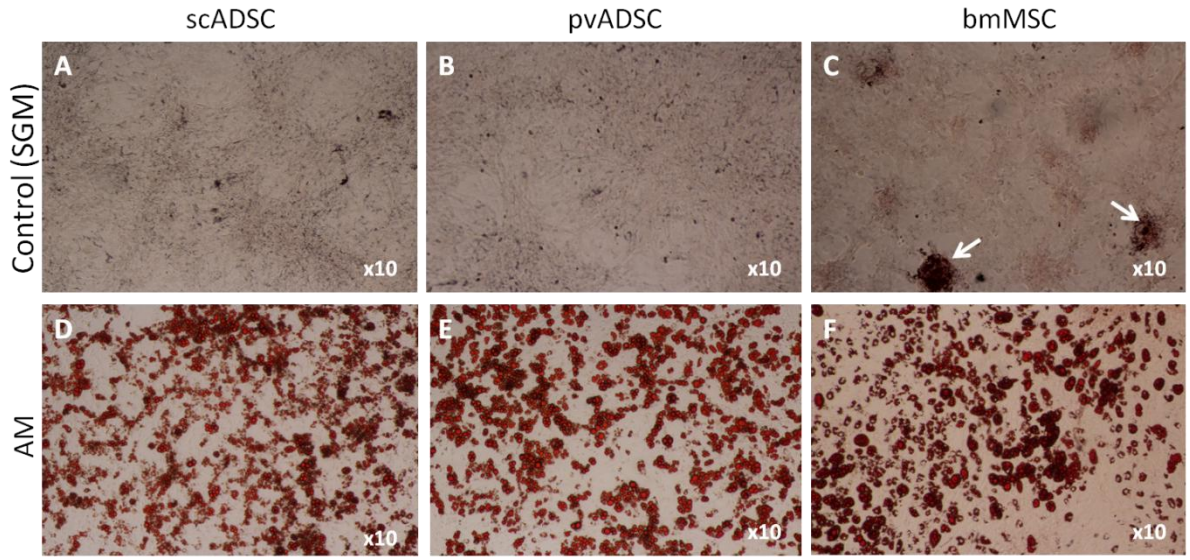

Figure 3.2.4.1.1: Adipogenic differentiation of scADSCs, pvADSCs and bmMSCs. Subcutaneous ADSCs (A and D), pvADSCs (B and E) and bmMSCs (C and F) were cultured for 14 days in standard growth medium (SGM) as control (A, B and C) or adipogenic differentiation medium (AM) (D, E and F) and stained with Oil Red O to visualise lipid droplets. Arrows indicate areas of aberrant staining in control bmMSCs due to formation of cell clusters during culture. Images were taken using an Olympus CKX41 inverted microscope at x10 magnification.

Lipid accumulation in ADSCs and bmMSCs was quantified by image analysis, and the results expressed as the percentage area containing lipid droplets stained with Oil Red O. Analysis commenced at day 5 after induction of adipogenesis, as this was the time point when the first lipid droplets became visible. In addition to analysis at day 5, lipid accumulation was quantified on days 7, 10 and 14 for all cell types. Oil Red O staining increased for all cell types over the 14 day differentiation period, with the highest percentage of staining achieved in the pvADSCs, followed by the scADSCs, with the lowest percentage

of staining in the bmMSC cultures (Fig. 3.2.4.1.2). Data showed that lipid accumulation increased significantly between day 5 and days 7, 10 and 14 for pvADSCs, and days 10 and 14 for scADSC and bmMSCs (Fig. 3.2.4.1.2). Staining showed that lipid accumulation increased most rapidly between days 7 and 10 for scADSCs and pvADSCs, with only a slight increase observed between days 10 and 14 for pvADSCs, while lipid accumulation in scADSCs appeared to plateau between these time points. bmMSCs showed the greatest amount of lipid accumulation between the day 10 and 14 time points, which was however significantly lower than either the scADSCs or pvADSCs at both day 10 and 14 (Fig. 3.2.4.1.2.).

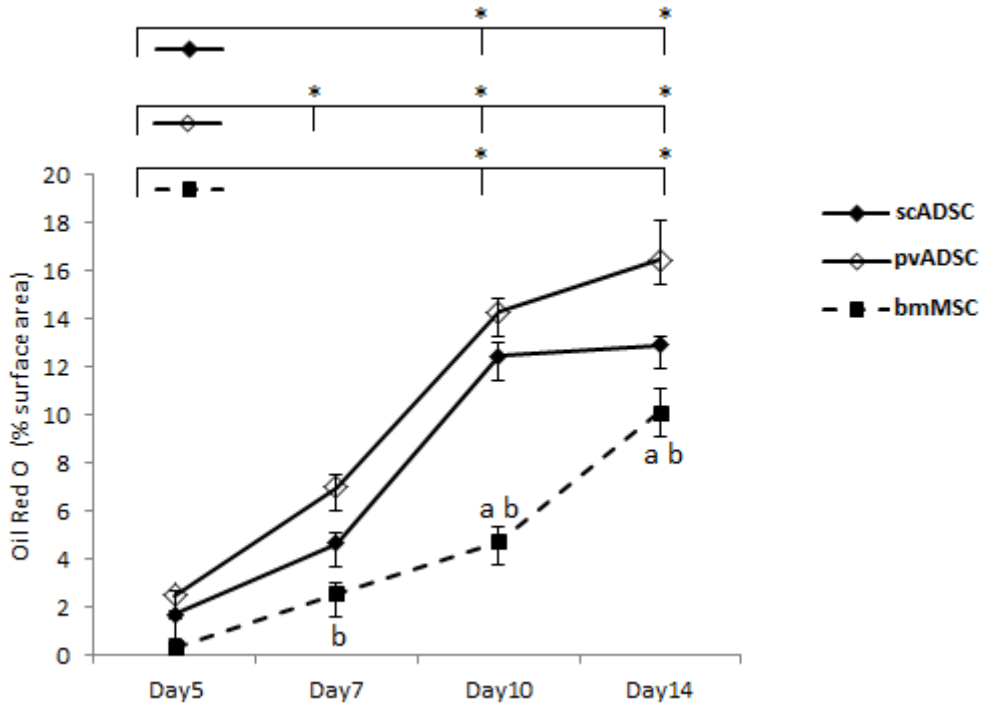

Figure 3.2.4.1.2: Quantification of Oil Red O staining of differentiated MSCs derived from bone-marrow, subcutaneous adipose and peri-renal visceral adipose depots. Values are presented as percentage of positively stained surface area (mean ± SE). Statistical analysis: Factorial ANOVA with Tukey post hoc test. A significant effect of time within each cell type is indicated with *. Significant difference between cell types at the same time point is indicated with **a** (scADSC vs bmMSCs) or **b** (pvADSC vs bmMSCs). Level of significance was accepted at $p < 0.05$.

ADSCs and bmMSCs were treated with AM, and RNA isolated at days 3, 5, 7, 10 and 14 for RT-qPCR analysis of mRNA expression of the adipogenic markers, PPARγ, aP2 and adipsin (Fig. 3.2.4.1.3). RT-qPCR was performed as per Chapter 2, Section 2.2.12.4. Levels of mRNA expression were presented as relative to the house-keeping gene, *Arbp* (van

Wijngaarden *et al.*, 2007). PPARγ, and specifically the PPARγ2 isoform in adipocytes, is the master regulator of adipogenesis, and is expressed early in adipocyte lineage commitment (MacDougald and Mandrup, 2002; Fujiki *et al.*, 2009). Adipsin, a serine protease, is the mouse homolog of complement factor D, and is expressed at an increasing rate during adipogenic differentiation (Wilkison *et al.*, 1990). Another adipose-specific product is a fatty acid binding protein named aP2, also known as 422, which was first identified in murine 3T3-L1 cells and is activated by PPARγ during adipogenesis (Bernlohr *et al.*, 1984; Gregoire *et al.*, 1998).

Relative expression of PPARγ, aP2 and adipsin were found to increase significantly in scADSCs, over the course of the differentiation period (day 3 to day 10), as compared to time-matched controls under standard growth media conditions (Fig 3.2.4.1.3, A – F), whereas the increase was not statistically significant for either pvADSCs or bmMSCs. Subcutaneous ADSCs showed significantly higher expression of all adipogenic markers at day 10, compared to pvADSCs or bmMSCs (Fig. 3.2.4.1.3, A, C, and E). No significant increase in the relative expression of any of the adipogenic marker genes was found when comparing scADSCs with either pvADSCs or bmMSCs by day 10 of adipogenic differentiation (Fig. 3.4.2.4.1.3, A – F).

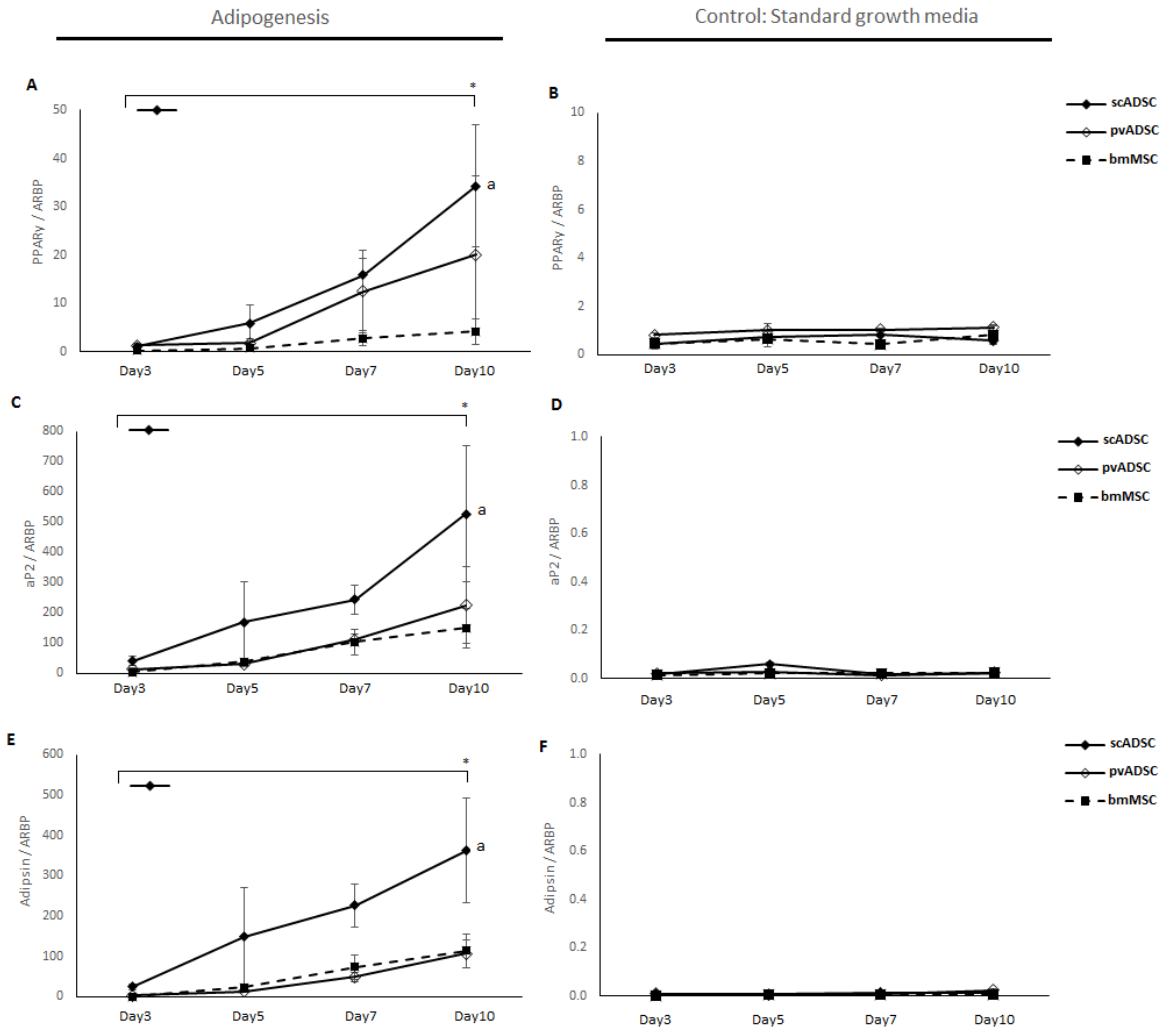

Figure 3.2.4.1.3: RT-qPCR comparing the expression of adipogenic genes in MSCs derived bone-marrow, subcutaneous adipose and peri-renal visceral adipose depots under standard growth media conditions and during adipogenic differentiation. The relative expression of PPARγ (A and B), aP2 (C and D) and Adipsin (E and F) is shown in scADSCs, pvADSCs and bmMSCs. Values (mean ± SE) are presented as relative expression compared to the expression of the housekeeping gene (ARBP). Statistical analysis: Factorial ANOVA with Tukey post hoc test. A significant effect of time within each cell type is indicated with *. Significant difference between cell types at the same time point is indicated with **a** (scADSC vs bmMSCs). Level of significance was accepted at $p<0.05$.

3.2.4.2 Osteogenic differentiation

Cells were cultured in the presence of osteogenic differentiation medium for a period of 21 days for ADSCs and 14 days for bmMSCs in order to induce osteogenesis. At the desired time points, cell cultures were stained with Alizarin Red dye which stains calcium mineral deposits red. The presence of calcium mineral deposits indicates that osteogenic differentiation has taken place. Mineral deposits were observed as early as day 5 for bmMSCs, with mineralisation being complete by day 14, however mineral deposits were only observed at day 21 for scADSCs and pvADSCs (Fig. 3.2.4.2.1, D, E and F). ADSCs cultured

in standard growth medium (DMEM+10% FBS+ vehicle) as a control did not stain positively by day 21, with scADSCs and pvADSCs exhibiting only 0.8 ± 0.1% and 1.25 ±0.1% area positively stained, respectively (Fig. 3.2.4.2.1, A and B, and Fig. 3.2.4.2.2). The bmMSC controls had a low percentage of the well area stained positively with Alizarin Red at day 14 of 2.1 ±0.2%, a value slightly higher than that of ADSC controls. The slight positive stain in the bmMSC controls is a result of aberrant staining due to the clustering phenomenon observed in these cells after prolonged periods in culture, which has previously been observed in controls during experiments where bmMSCs were differentiated into adipocytes (Fig. 3.2.4.2.1, C and Fig. 3.2.4.2.2).

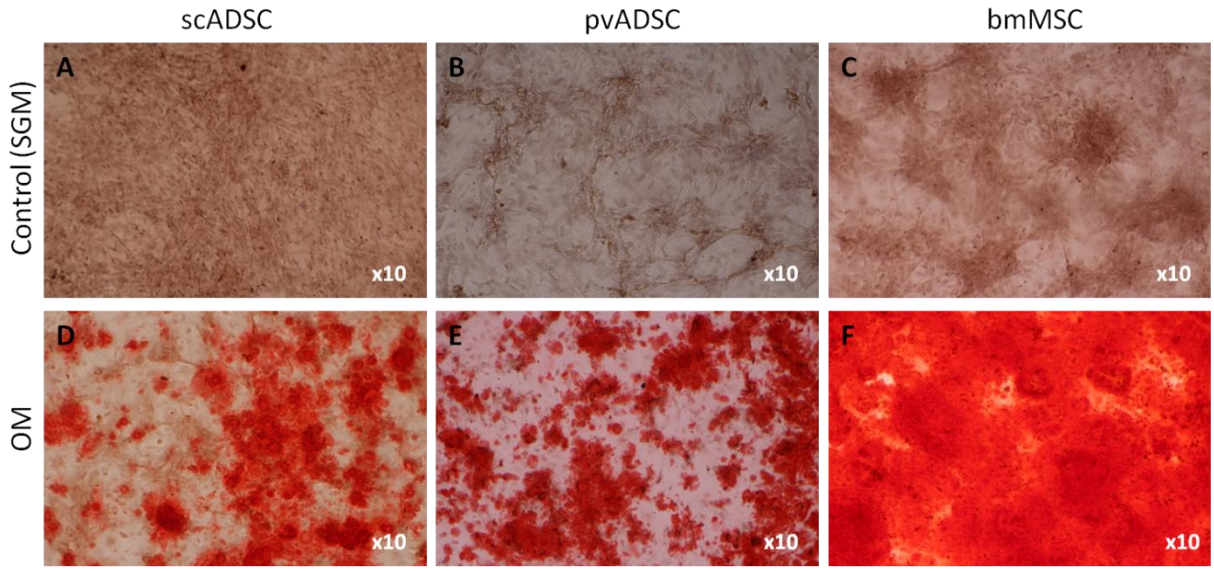

Figure 3.2.4.2.1: Osteogenic differentiation of scADSCs, pvADSCs and bmMSCs. Subcutaneous ADSCs (A and D), pvADSCs (B and E) and bmMSCs (C and F) were cultured for 21 Days for scADSC and pvADSC and 14 days for bmMSC in either standard growth medium (SGM) as control (A, B and C) or osteogenic differentiation medium (OM) (D, E and F) and stained with Alizarin Red to visualise calcified mineral deposits (red colour). Images were taken using an Olympus CKX41 inverted microscope at x10 magnification.

Mineralised surface area, as visualised by Alizarin Red staining and quantified by image analysis with values expressed as percentage positively stained area, was over 10% on day 7 for bmMSC cultures and increased significantly at both day 10 and 14 time points. Positive staining for both scADSC and pvADSC cultures was only significantly greater from day 7 to day 21, with no significant difference observed between either ADSC types. Mineralisation in bmMSCs was significantly greater than either scADSCs or pvADSCs on days 7 10 and 14, and showed a steady increase in percentage of mineralised surface area throughout all time points measured (Fig. 3.2.4.2.2).

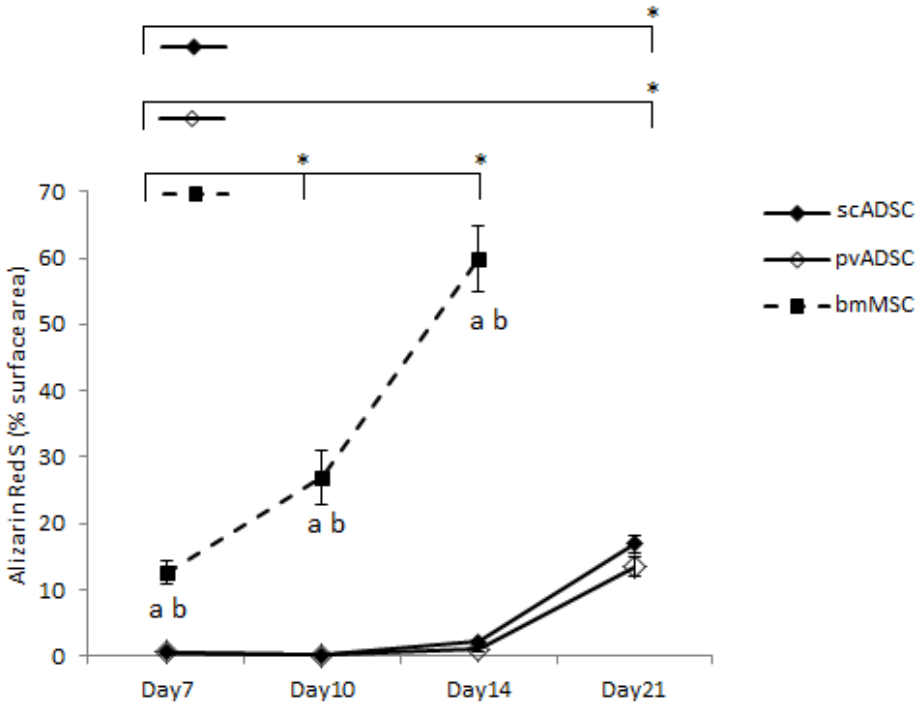

Figure 3.2.4.2.2: Quantification of Alizarin Red S staining comparing the osteogenic differentiation of MSCs derived from bone marrow (bmMSC), as well as subcutaneous adipose (scADSC) and peri-renal visceral adipose (pvADSC) depots. Values are presented as percentage of positively stained surface area (mean ± SE). Statistical analysis: Factorial ANOVA with Tukey post hoc test. A significant effect of time within each cell type is indicated with *. Significant difference between cell types at the same time point is indicated with **a** (scADSC vs bmMSCs) or **b** (pvADSC vs bmMSCs). Level of significance was accepted at $p<0.05$.

ADSCs and bmMSCs were treated with OM and RNA from ADSCs was collected at days 0, 3, 5, 7, 10 and 21 for gene expression analysis, and at days 0, 3 and 5 for bmMSCs (Fig. 3.2.4.2.3). RNA concentration in bmMSCs undergoing osteogenesis was too low to be measured from day 7 onwards, possibly due to excessive mineralisation. The expression of the osteogenic marker genes Runx2, bone sialoprotein (BSP) and alkaline phosphatase (ALP) were measured and presented as relative expression compared to the housekeeping gene *Arbp*. The transcription factor Runx2, also known as Cbfa1, is the key regulator of osteoblast differentiation and in mature osteoblasts also functions to regulate mineral deposition in bone matrix (Ducy, 2000). BSP is, apart from collagen, one of the major proteins found in mineralised bone matrix, and is almost exclusively found in this tissue where it is involved with cell adhesion (Tanabe *et al.*, 2004a). ALP is a common marker for identification of an osteoblastic phenotype, and has been used extensively to for this purpose (Kuroda *et al.*, 2005; Sadie-Van Gijsen *et al.*, 2012).

A significant effect of time in ALP expression compared to control was observed by day 5 in bmMSCs, when compared to day 0. ALP expression was significantly higher at day 5 for bmMSCs as compared to scADSCs or pvADSCs. No significant increase in ALP over time was observed for scADSCs and pvADSCs (Fig. 3.2.4.2.3, A, B and C). Runx2 expression peaked at day 3 in scADSCs undergoing osteogenesis, whereas no significant differences in Runx2 expression were observed in other cell types or controls (Fig. 3.2.4.2.3, D, E and F). Expression of BSP was significantly higher at day 3 and 5 compared to day 0 for bmMSCs with no effect of time observed for scADSCs or pvADSCs. BSP expression was also significantly higher in bmMSCs compared to scADSCs and pvADSCs at day 3 and 5 of osteogenic differentiation (Fig. 3.2.4.2.3, G, H and I).

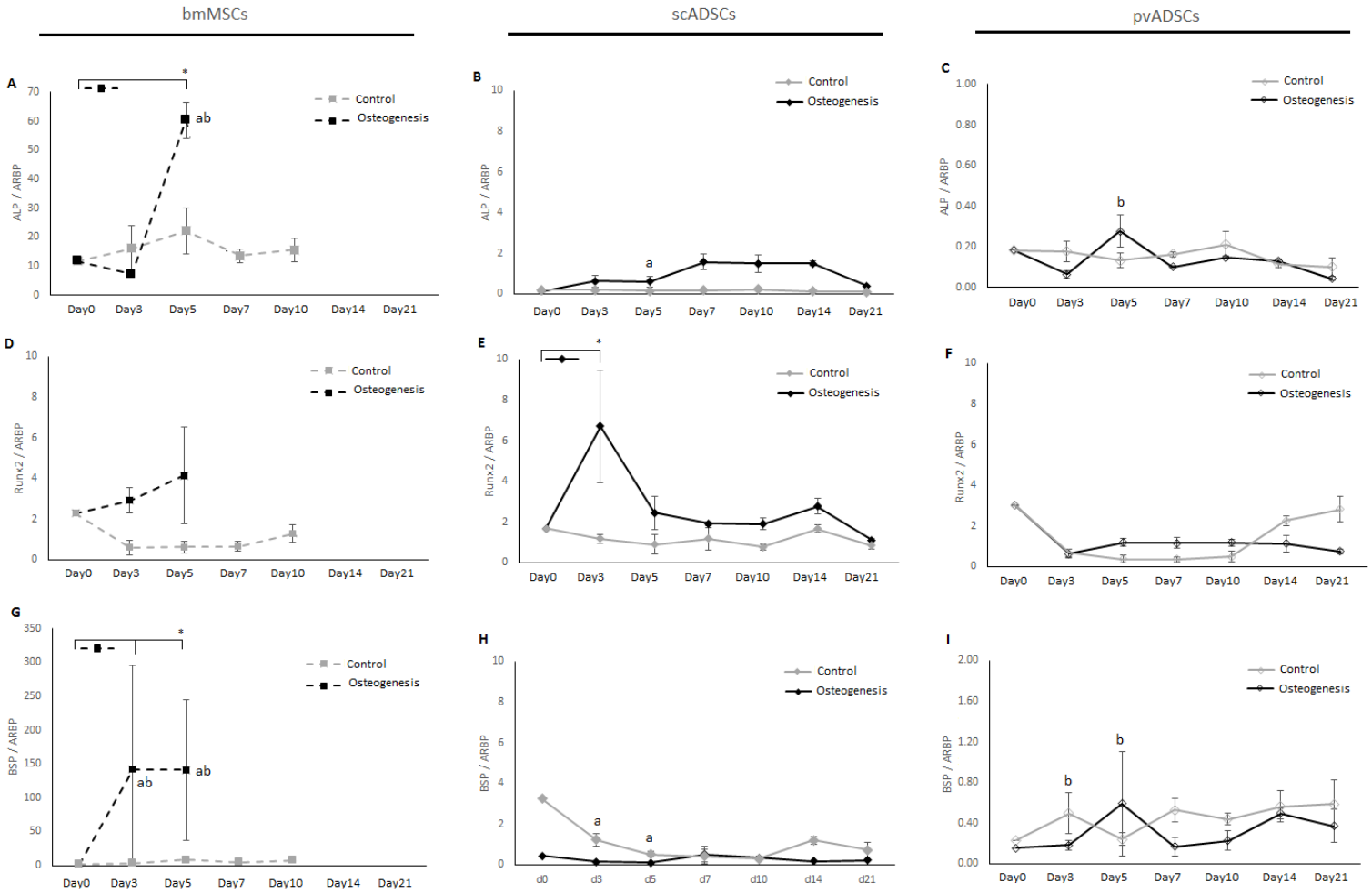

Figure 3.2.4.2.3: RT-qPCR comparing the expression of osteogenic genes in MSCs derived from each of the different depots under standard growth media conditions and during ostegenic differentiation. The relative mRNA expression of ALP, (A, B and C), Runx2 (D, E and F) and BSP (G, H and I) in bmMSCs, scADSCs, and pvADSCs**.** Values (mean ± SE) are presented as relative expression compared to the expression of the housekeeping gene, *Arbp*. Statistical analysis: Factorial ANOVA with Tukey post hoc test. A significant effect of time within each cell type is indicated with *. Significant difference between cell types at the same time point is indicated with **a** (scADSC vs bmMSCs) or **b** (pvADSC vs bmMSCs). Level of significance was accepted at $p<0.05$.

3.3 Discussion

In this chapter, MSCs were isolated from bone-marrow (bmMSCs), subcutaneous adipose (scADSCs) and peri-renal visceral adipose (pvADSCs) depots and were compared to one another by examining morphology, proliferation rate, surface marker expression, and osteogenic and adipogenic differentiation. Adherence to plastic was the main selection criteria used for isolation of bmMSCs, scADSCs and pvADSCs, and this proved to be sufficient to obtain morphologically homogenous populations of cells with MSC characteristics. Cells derived from all three MSC depots appeared morphologically similar, with cell shapes commonly observed to vary between elongated and spindle-shaped cells as well as random polygonal-shaped cells and cells with a broad flattened appearance (Fig. 3.2.1.1 and Fig. 3.2.1.2), consistent with observations of MSC morphology found in the literature (Bianco *et al.*, 2001; Kollmer *et al.*, 2013).

The isolation of the ADSCs and bmMSCs used in this study was by the use of a common technique, with selection by plastic adherence (Bunnell *et al.*, 2008; Peng *et al.*, 2008; Lopez and Spencer, 2011; Mendez-Ferrer *et al.*, 2015). ADSCs are isolated by collagenase digestion of adipose tissue to break down the fibrous collagen network, followed by a centrifugation step which allows for the ADSCs and other released cells to be collected as a pellet, consisting of a heterogeneous mixture known as the stromal vascular fraction (SVF) (Bunnell *et al.*, 2008; Baer and Geiger, 2012; Bassi *et al.*, 2012). A limitation with this technique is that the SVF may contain a combination of different cell types, including ADSCs with true multipotential characteristics, as well as fibroblasts, immune regulatory monocytes/macrophages and vascular endothelial cells (Bunnell *et al.*, 2008; Baer and Geiger, 2012; Bassi *et al.*, 2012). The heterogeneous appearance that was observed in bmMSC cultures selected by plastic adherence is also consistent with the literature, as these cultures typically may contain a small population of primitive stem cells, and cells which are already partially or fully lineage committed, such as fibroblasts (Mendez-Ferrer *et al.*, 2015).

The proliferation rate of bmMSCs was observed to be lower than that of both scADSCs and pvADSCs, which agrees with the finding by Yoshimura *et al*. using cells from Sprague-Dawley rats, and Hayashi *et al*. using Fischer 344 rats (Yoshimura *et al.*, 2007; Hayashi *et al.*, 2008). An earlier study using bmMSCs isolated from Lewis rats found that rat bmMSCs had almost twice the maximal expansion rate of human bmMSCs, when plated at low density

of approximately 2 cell/cm^2 (Javazon *et al.*, 2001), while Yoshimura *et al*. reported that in their own experiments, the expansion rate of rat bmMSCs was lower than that of human bmMSCs (Yoshimura *et al.*, 2007). The present study made use of Wistar rats, and did not subject the bone marrow to density gradient centrifugation during the isolation procedure, but rather plated the bone marrow directly onto the culture surface. Culture medium also differed between the present study and that used by others; in this study cells were cultured in DMEM with 10% FBS, while Yoshimura *et al.* and Javazon *et al*. made use of αMEM with 20% FBS, and Hayashi *et al*. used MEM with 15% FBS (Javazon *et al.*, 2001; Yoshimura *et al.*, 2007; Hayashi *et al.*, 2008). Batch-to-batch variation of FBS and the resulting variation in the suitability for cell culture is a well-known phenomenon, and this may also have played a role in observed cellular expansion rates observed. Yoshimura *et al*. noted that FBS selected for rapid growth of human bmMSCs may not necessarily provide the most favourable growth conditions for rat bmMSCs (Yoshimura *et al.*, 2007). A further difference between the present study and previous work is that bmMSCs proliferation was measured at P3, while previous work measured expansion capability by colony forming unit-fibroblast (CFU-F) assay in cells from P0 or P1 (Javazon *et al.*, 2001; Yoshimura *et al.*, 2007; Hayashi *et al.*, 2008). The data, however, indicates that the lower expansion rate of bmMSCs compared to scADSCs was not a strain-specific effect, and was also independent of the use of density gradient centrifugation, or culture medium composition, between cells from Sprague-Dawley, Fischer 344 and Wistar rats. The differences noted above between the present study and previous studies underlines the well-known lack of standardisation of methods for isolation and culture conditions for MSCs, which greatly complicates any attempts to compare results from different laboratories. Subtle difference in cell culture conditions have been known to support the expansion of different subsets of the culture population, which may result in greater differences in the results obtained (Ho *et al.*, 2008).

Subcutaneous ADSCs at P2 had a higher rate of proliferation than pvADSCs, which is in agreement with the results obtained by Arrigoni *et al*., who reported a shorter doubling time for rat-derived scADSCs compared to pvADSCs with increasing passage number. The doubling times reported by Arrigoni *et al*. for scADSCs and pvADSCs appeared to be similar at P2 and P3, while the present study found a small difference in proliferation rate between scADSCs and pvADSCs at P2 (Fig. 3.2.3.1), a discrepancy which may be due to differences in the methods used for evaluating the expansion rate of the cells (Arrigoni *et al.*, 2009).

The proliferation rate of both scADSCs and pvADSCs dropped rapidly after 48 hours in culture, while the rate of bmMSCs increased at 48 hours compared to earlier time points. The decrease in proliferation of scADSCs and pvADSCs is likely to be due to growth arrest, observed in cell cultures upon reaching high density, as a result of the phenomenon of contact inhibition (CI) (Leontieva *et al.*, 2014). Due to the slower rate of proliferation observed in bmMSCs at earlier time points compared to the ADSCs, cell numbers had not yet reached a high enough density by the 48 hour time point for CI to substantially retard proliferation.

Subcutaneous ADSCs, pvADSCs and bmMSCs were positive for CD90 (Thy1.1), which was expected based on previous reports in the literature, as CD90 is a well-established MSC surface marker (Javazon *et al.*, 2001; Dezawa *et al.*, 2005; Yoshimura *et al.*, 2007; van de Vyver *et al.*, 2014). Subcutaneous ADSCs and pvADSCs were negative for CD45 (leukocyte common antigen), however, a small population of CD45 positive cells were present in bmMSC samples. The presence of CD45 positive cells in bmMSCs has been previously reported, along with the markers CD34 and c-Kit, while the majority of the population remains negative for these markers (Dezawa *et al.*, 2005). A small percentage of all MSC types expressed the ectopeptidase dipeptidylpeptidase type IV (CD26), known to be a hepatocyte (Sgodda *et al.*, 2007) and fibroblast (Cappellesso-Fleury *et al.*, 2010) marker, with the highest expression in pvADSCs at 22% positive. The expression of CD26 in human bmMSCs is known to be variable (40-78%), while Sgodda *et al*. found expression of CD26 in rat adipose-derived MSCs after 7 days of hepatocyte induction, indicating that CD26 is absent in naïve rat adipose-derived MSCs (Sgodda *et al.*, 2007; Cappellesso-Fleury *et al.*, 2010). The increased percentage of CD26 postive cells in the pvADSC population compared to the other cell types suggests that pvADSCs may contain a small population of fibroblasts (22%). However, the presence of CD26 postive cells may not be indicative of the presence of fibroblasts, as fibroblasts are reported to not able to differentiate towards an adipocyte or osteoblast phenotype (Cappellesso-Fleury *et al.*, 2010), while pvADSCs were observed to have higher lipid accumulation than scADSCs, which had a lower fraction of CD26 positive cells (Fig. 3.2.2.1). Since expression of CD26 in bmMSCs has been reported to be variable, it may be possible that variable expression of CD26 also occurs in pvADSCs, and possibly scADSCs. In order to confirm the identity of the CD26 positive population of pvADSCs as either MSC or fibroblast in nature, the CD26 population may be sorted via fluorescence activated cell sorting (FACS) analysis and induced to differentiate towards either an osteogenic or adipogenic phenotype. Human bmMSCs are known to be positive for CD106

(vascular cell adhesion molecule 1, VCAM1) (Pittenger *et al.*, 1999; Cappellesso-Fleury *et al.*, 2010), however one study reported that two stem cell clones derived from rat bmMSCs were negative for CD106 (Schwarz *et al.*, 2014). The results from the present study, 77% of the population of rat bmMSCs sampled were positive for CD106, indicating that some CD106 negative cells may be present in the rat bmMSC population. This is consistent with the literature findings in that bmMSCs are largely positive for CD106, and also indicates that rat derived bmMSCs may contain a mixed population of CD106 positive and negative cells.

All three MSC types exhibited adipogenic and osteogenic differentiation potential *in vitro*, however, variation in differentiation capability between depots was observed. Adipogenic differentiation potential was lower in bmMSCs compared to either scADSCs or pvADSCs. This observation is consistent with previous findings, which indicated that scADSCs have a greater adipogenic differentiation potential than bmMSCs (Yoshimura *et al.*, 2007). The *in vitro* adipogenic differentiation, assessed by lipid accumulation, of pvADSCs was greater than that of scADSCs, which is also consistent with findings in the literature (Sadie-Van Gijsen *et al.*, 2012; van de Vyver *et al.*, 2014).

In contrast to adipogenic differentiation, bmMSC mineralisation was much more rapid and extensive *in vitro* compared with either scADSCs or pvADSCs, a finding which is confirmed by previous studies. Yoshimura *et al*. found that bmMSCs from Sprague-Dawley rats had a greater osteogenic differentiation potential in comparison to scADSCs, when mineralisation was measured by Alizarin Red staining and alkaline phosphatase (ALP) activity assay (Yoshimura *et al.*, 2007). Hayashi *et al*. also reported that *in vitro* osteogenic differentiation capability was higher in bmMSCs than scADSCs, by quantification of mineralised matrix, ALP activity and osteocalcin levels (Hayashi *et al.*, 2008). Mineralisation in scADSCs and pvADSCs was only detectable after 21 days of culture, which is in range of values obtained in the literature (Yoshimura *et al.*, 2007; Hayashi *et al.*, 2008). The levels of mineralisation observed in scADSCs and pvADSCs under osteogenic conditions were found to be similar to one another, which is in keeping with previous findings (Arrigoni *et al.*, 2009; van de Vyver *et al.*, 2014).

Weiser *et al*. found that ascorbic acid enhanced adipogenesis in the bmMSCs isolated from Sprague-Dawley rats, and they proposed that the mechanism by which ascorbic acid enhanced lipid accumulation in these cells was due to an increase in collagen synthesis

(Weiser *et al.*, 2009). Analysis of the expression of the adipogenic marker genes, PPARγ, aP2 and Adipsin in scADSCs, pvADSCs and bmMSCs showed an increase in the relative expression of these genes throughout adipogenic induction, in comparison to time-matched control samples. PPARγ is expressed early on in the adipocyte differentiation pathway, as mentioned in Section 3.2.4.1, is the master regulator of adipogenesis, and along with C/EPBα, are the main drivers of expression of adipocyte-specific genes (MacDougald and Mandrup, 2002). In contrast to lipid accumulation data, which indicated that lipid accumulation was slightly higher in pvADSCs compared to scADSCs, scADSCs appeared to have the highest levels expression of adipogenic markers, followed by pvADSCs and lowest levels overall were found in bmMSCs. Expression of PPARγ in rat bmMSCs and scADSCs after four days of *in vitro* adipogenic induction has previously been reported (Yoshimura *et al.*, 2007). An increase in PPARγ expression was also found in human bmMSCs and scADSCs after 21 days incubation in adipogenic differentiation medium, where PPARγ expression levels were similar for MSCs from both depots (Noel *et al.*, 2008). In contrast to the results reported with ADSCs from rat subcutaneous and visceral depots, a study comparing human ADSCs derived from various adipose depots including subcutaneous and visceral (omental) depots, found that subcutaneous ADSCs were more adipogenic than visceral ADSCs (Russo *et al.*, 2014). The difference between the adipogenic potential of human and rat scADSCs and visceral ADSCs may be related to the precise source of the visceral ADSCs, as the rat pvADSCs were derived from the fat pad surrounding the kidney, while human visceral ADSCS in the study by Russo *et al*. (2014) were derived from the omentum. Van de Vyver *et al*. also reported an increase in the relative expression of aP2 and adipsin in rat scADSCs and pvADSCs between days 7 and 10 of adipogenic induction, which is consistent with the present findings as expression of all adipogenic markers increased most notably between days 7 and 10 of adipogenic induction (van de Vyver *et al.*, 2014). Taken together, the literature reports an increase in the expression of adipogenic marker genes PPARγ, aP2 and adipsin in MSCs during adipogenic induction, which is consistent with the findings in the present study, indicating that adipogenesis is occurring.

Osteogenic differentiation was evaluated by measuring the relative expression of the osteogenic marker genes, Runx2, BSP and ALP. Runx2, as mentioned in Section 3.2.4.2, is a key regulator of osteoblast differentiation and also functions in mature osteoblasts. BSP is also found almost exclusively in mineralised bone matrix, and is product of mature osteoblasts (Ducy, 2000). Increased ALP expression is also characteristic of osteoblast

differentiation (Kuroda *et al.*, 2005). Expression of osteogenic markers was significantly higher in bmMSCs compared to time-matched controls, confirming that osteogenesis was taking place in these cells.. Mineralisation proceeded rapidly in bmMSCs during osteogenic differentiation, resulting in an overabundance of mineral deposits by day 7 of differentiation, which prevented sufficient quantities of RNA to be obtained from these samples. Expression of osteogenic markers in scADSCs and pvADSCs was not significantly different compared to undifferentiated time-matched control samples, and no trends were apparent. This finding is supported by previous studies, one of which found no significant differences in relative Runx2 expression between time-matched undifferentiated controls and cells incubated in osteogenic differentiation medium for both rat scADSCs and pvADSCs (Sadie-Van Gijsen *et al.*, 2012). A later study also found no statistically significant increase in relative ALP expression levels in rat scADSCs and pvADSCs between day 7 and 10 of osteogenic induction, and also reported that there was no increase in expression mRNA levels of the osteogenic markers Msx2 and collagen I between days 7 and 10 in the same cells (van de Vyver *et al.*, 2014). It is therefore proposed that the osteogenic differentiation capacity in rat scADSCs and pvADSCs is lower than that of bmMSCs, despite the observation that these cells have the ability to form mineralised calcium deposits under osteogenic induction conditions.

The results from the present study are supportive of the conclusion that the cells isolated from bone marrow, subcutaneous and peri-renal visceral adipose depots are mesenchymal stromal cells. Surface marker expression is consistent with the literature for rat-derived MSCs and the cells isolated from all three depots studied have been shown to exhibit bipotentiality *in vitro*. The data also suggest that cells isolated from adipose and bone-marrow tissue retain characteristics of the tissue of origin. Both scADSCs and pvADSCs were observed to have a greater capacity for adipogenic differentiation than bmMSCs, as quantified by both lipid accumulation and relative expression levels of adipogenic marker genes. Conversely, bmMSCs differentiated more readily towards an osteogenic phenotype, with more rapid and extensive formation of mineralised matrix, as well as higher relative expression of osteogenic marker genes, compared to ADSCs, where mineralisation required more than double the amount of time to occur and was marginal in comparison to that observed for bmMSCs. Osteogenic induction did not significantly increase expression of osteogenic marker genes in either scADSCs or pvADSCs, indicating that osteogenesis may be poorly or incompletely induced in these cells, under the differentiation conditions assessed. Taken together, rat

bmMSCs, scADSCs and pvADSCs provide adequate *in vitro* cellular models for gathering insight into the interplay between adipogenesis and osteogenesis. Due to MSCs from each depot retaining characteristics of the tissue of origin, MSCs from a single depot may not provide the best model for investigating both osteogenic and adipogenic differentiation pathways, as demonstrated by the limited capacity for osteogenic differentiation in scADSCs and pvADSCs compared to bmMSCs as well as the limited capacity for adipogenic differentiation in bmMSCs compared to either scADSCs and pvADSCs. Increased understanding of the differences in the behaviour of MSCs from various depots provides better insight into choice of model for future investigations, and for possible clinical use with regards to tissue-engineering.

CHAPTER 4

Effects of TNAP inhibitors on lipid accumulation, mineralisation and ALP activity levels of MSCs undergoing adipogenic or osteogenic induction.

4.1 Introduction

Tissue non-specific ALP is highly expressed in skeletal, hepatic and renal tissues, and also at low levels in most other tissues. TNAP has a well established role in skeletal mineralisation, however very little is known about the function of TNAP in other tissues. The presence of TNAP in a variety of different tissues, and the existence of multiple isoforms of TNAP, indicates that there may be a variety of physiological roles for this enzyme (Sharma *et al.*, 2014). TNAP has also been identified as a mesenchymal stem cell marker and is also known as Mesenchymal stem cell antigen-1 (MSCA-1), which further indicates the possible diverse roles for this enzyme (Sobiesiak *et al.*, 2010).

Recent research has indicated a role for TNAP during adipogenesis in the 3T3-L1 murine preadipocytic cell line. Ali *et al*. (2005) noted that ALP activity increased over the course of adipogenic induction in these cells, while the addition of either of the TNAP inhibitors, levamisole or histidine during adipogenesis was found to significantly reduce lipid accumulation within the cells. The research also found that alkaline phosphatase activity was spatially associated with the lipid membrane which surrounds these lipid droplets that are characteristically present in adipocytes. Similar results were obtained using primary human preadipocytes, derived from mammary tissue, where the presence of histidine during adipogenic induction resulted in a concomitant drop in lipid accumulation and ALP activity, compared to samples where histidine was absent (Ali *et al.*, 2006).

A further study by Ali *et al*. (2013) using human adipose-derived preadipocytes found that the addition of levamisole during adipogenic induction produced a decrease in lipid accumulation compared to control samples, while an increase in ALP activity was observed (Ali *et al.*, 2013). It was proposed that in human preadipocytes that levamisole blocked adipogenesis at a point downstream from TNAP (Ali *et al.*, 2013).

TNAP expression has previously been identified in rat adipose tissue (Wallach and Ko, 1964), and we questioned whether inhibition of TNAP had a similar effect on lipid accumulation during adipogenesis in rat-derived MSCs, as seen in 3T3-L1 and human preadipocytes. Consequently, rat MSCs were harvested from bone-marrow as well as visceral and subcutaneous adipose depots and expanded *in vitro*. Bone marrow-derived MSCS (bmMSCs) are able to readily differentiate into either osteoblasts or adipocytes within the marrow cavity,

and the age-related disease, osteoporosis, is thought to be due, at least in part, to the skewing of the differentiation of marrow-derived MSCs from an osteogenic towards the adipocytic lineage (Bruedigam *et al.*, 2010). This results in a reduction in the number of bone-forming osteoblasts, a subsequent imbalance in bone turnover and loss of bone. For this reason, investigation into the role of TNAP in bmMSCs undergoing adipogenic induction may provide insight into the mechanisms of osteoporosis.

Differences between MSCs derived from different tissues, as well as between adipose-derived stromal cells (ADSCs) from different adipose depots, have been well documented (Sadie-Van Gijsen *et al.*, 2010; Strioga *et al.*, 2012; Elahi *et al.*, 2016). Differences between adipocytes from different adipose depots can be illustrated by the finding that in humans, increased visceral adiposity, as opposed to subcutaneous adiposity, is related to a greater risk for metabolic disorders such as diabetes (Boyko *et al.*, 2000). In Chapter 3 of this study it was shown that differences exist between scADSC and pvADSC differentiation in both levels of adipogenic marker genes expressed during adipogenic differentiation as well as in lipid accumulation levels. As TNAP has been previously shown to be involved in adipogenesis, the question may be asked whether TNAP is differentially expressed in the various adipose depots, as TNAP expression differences may contribute to the depot specific differences in differentiation.

ALP activity levels in bmMSCs, scADSCs and pvADSCs during both osteogenesis and adipogenesis were investigated, with the addition of TNAP-specific inhibitors levamisole, L-histidine and L-homoarginine, added separately or in combination, during either osteogenic or adipogenic induction. Three inhibitors were used because each inhibitor is not specific for TNAP alone, and may have other off-target effects within the cell. Combinations of each inhibitor allowed for any additive effects of the inhibitors to be observed. The resulting mineralisation or lipid accumulation was measured over the course of the differentiation period, as well as the corresponding levels of ALP activity for each treatment.

Certain L-amino acids have commonly been found to selectively inhibit TNAP, among these are L-homoarginine and L-histidine (Bodansky and Schwartz, 1963; Kozlenkov *et al.*, 2004; Ali *et al.*, 2005). L-homoarginine is found in circulation and can function as a substrate for nitric oxide synthesis by nitric oxide synthases in brain and other tissues (Bernstein *et al.*, 2015). Histidine is an essential amino acid which is involved in the biosynthesis of proteins.

Other TNAP inhibitor compounds, not related to amino acids, exist, such as levamisole and theophylline (Kozlenkov *et al.*, 2004). Levamisole, the L-isomer of tetramisole, is used as an antihelmintic, targeting the nicotinic acetylcholine receptors of parasitic nematodes, and is also an allosteric modulator of human nicotinic acetylcholine receptors in the brain (Levandoski *et al.*, 2003), but is also a potent selective inhibitor of TNAP (Kozlenkov *et al.*, 2004). Levamisole, as well as L-homoarginine, are uncompetitive inhibitors of TNAP, and although levamisole is close to one hundred times more potent than L-homoarginine, both inhibitors have a weak binding affinity for TNAP and have other off-target effects (Kozlenkov *et al.*, 2004). The exact mechanism and binding sites for levamisole and L-homoarginine inhibition of ALP are currently unknown (Kozlenkov *et al.*, 2004).The mechanism of inhibition for L-histidine is considered to be mixed (Bodansky and Schwartz, 1963).

The levels of TNAP mRNA expression in all three cell types above, during adipogenesis and osteogenesis and in the presence of the TNAP inhibitors, levamisole, L-histidine and L-homoarginine, were measured. This was done in order to assess what effect TNAP inhibition during differentiation has on the gene expression. Biological repeats of between n=3 to n=5 were performed for each set of experiments, where each experiment consisted of 3 technical (internal) repeats.

4.2 Results

Due to the large number of treatment conditions assessed, Table 4.2.1 is presented to summarise the statistically significant results obtained for the treatment of bmMSCs, scADSCs and pvADSCs with levamisole, histidine or L-homoarginine, both alone or in combination with one another, while the cells were undergoing either adipogenic or osteogenic induction. The response to each treatment was assessed by measurement of the change in percentage area of mineralisation or lipid accumulation for each treatment, relative to untreated control cells, in cells cultured in either OM or AM. No significant response in mineralisation or ALP activity in the presence of any of the inhibitors was observed in pvADSCs undergoing osteogenic induction. Briefly, treatment with levamisole, alone or in combination, was able to decrease mineralisation significantly in bmMSCs and scADSCs, while histidine and L-homoarginine had no effect on mineralisation during osteogenic

induction. No significant effect on ALP activity, in the presence of any of the inhibitors, was observed in either bmMSCs or scADSCs undergoing osteogenic induction.

During adipogenesis, levamisole treatment alone did not decrease lipid accumulation in any cell type tested. A significant decrease in lipid accumulation compared to control was observed with treatment of all cell types with either L-homoarginine alone or in combination with histidine or levamisole. Histidine was only able to decrease lipid accumulation in bmMSCs. ALP activity was only decreased significantly in bmMSCs treated with levamisole alone or in combination with histidine. Levamisole in combination with L-homoarginine significantly increased ALP activity in scADSCs and pvADSCs, while treatment with L-homoarginine alone or in combination with histidine resulted in a significant increase in ALP activity in scADSCs only.

Table 4.2.1: Summary of statistically significant effects of levamisole (Lev), histidine (His) and L-homoarginine (Arg) on lipid accumulation, mineralisation and alkaline phosphatase (ALP) activity in bmMSCs, scADSCs and pvADSCs undergoing either osteogenic or adipogenic induction.

Cell type	Differentiation	Inhibitor	Mineralization or lipid accumulation response to inhibitor compared to control	ALP activity response to inhibitor compared to control
bmMSC	Osteogenic	Lev	Decreased	-
		His	-	-
		Arg	-	-
		Lev + His	Decreased	-
		Lev + Arg	Decreased	-
		His + Arg	-	-
	Adipogenic	Lev	-	Decreased
		His	Decreased	-
		Arg	Decreased	-
		Lev + His	-	Decreased
		Lev + Arg	Decreased	-
		His + Arg	Decreased	-
scADSC	Osteogenic	Lev	Decreased	-
		His	-	-
		Arg	-	-
		Lev + His	Decreased	-
		Lev + Arg	Decreased	-
		His + Arg	-	-
	Adipogenic	Lev	-	-
		His	-	-
		Arg	Decreased	Increased
		Lev + His	-	-
		Lev + Arg	Decreased	Increased
		His + Arg	Decreased	Increased
pvADSC	Osteogenic	All inhibitors tested	No significant response	No significant response
	Adipogenic	Lev	-	-
		His	-	-
		Arg	Decreased	-
		Lev + His	-	-
		Lev + Arg	Decreased	Increased
		His + Arg	Decreased	-

Responses to treatment in either the relative percentage area of mineralisation or lipid accumulation, as well as ALP activity, in treated compared to control untreated cells. Statistical significance was assumed when $p < 0.05$. Only statistically significant results are shown. Quantification is shown in subsequent graphs.

4.2.1 Selection of TNAP inhibitor concentrations

The proliferation rate of bmMSCs, scADSCs and pvADSCs cultured in in the presence of the TNAP inhibitors, levamisole (Lev), histidine (His) and L-homoarginine (Arg) was assayed using the BrdU cell proliferation ELISA kit (Roche) to determine the maximum concentration of each inhibitor which would not hinder cellular proliferation. All inhibitors were reconstituted in SGM, at stock concentrations of 100 mM (Lev), 200 mM (His) and 500 mM (Arg). Briefly, proliferation is measured by incorporation of BrdU, an analogue of thymidine, into the new DNA strands during DNA replication prior to cell division. After fixing and denaturing the DNA, an anti-BrdU monoclonal antibody conjugated to peroxidase is used to bind to the incorporated BrdU in the newly synthesized DNA strands. Cleavage of a substrate by the peroxidase produces a coloured product, which is quantified by absorbance using an ELISA plate reader. Proliferation in bmMSCs, scADSCs and pvADSCs was measured at 24 and 48 hr time points (Fig. 4.2.1.1). Ali *et al*. (2005) used a concentration of 2.5 mM levamisole and 50 mM histidine with 3T3-L1 cells to study the effects of TNAP inhibitors on lipid accumulation and ALP activity (Ali *et al.*, 2005). However, these concentrations proved to be toxic to the rat-derived MSCs used in the present study, and so a lower range of concentrations were compared. At the time of writing we are aware of only one study that has used L-homoarginine applied to live cells, where it was reported that long term cellular proliferation was inhibited at a concentration of 22.3 mM L-homoarginine (Kikuchi *et al.*, 1982). Proliferation in the presence of levamisole was measured with inhibitor concentrations of 0.1, 0.5 and 1.0 mM. In all cell types, at both 24 and 48 hr time points 1.0 mM levamisole appeared to reduce cell proliferation when compared to control sample. The only statistically significant effect for levamisole was observed in scADSCs treated with 1.0 mM levamisole compared to untreated controls, at 24 hr (Fig. 4.2.1.1 A, D and G). A concentration of 0.5 mM levamisole was chosen for further experiments as this was the highest concentration which did not inhibit cell proliferation in either bmMSCs, scADSCs or pvADSCs. At the highest concentration measured (20 mM) for both histidine and L-homoarginine, no significant decrease in proliferation after either 24 and 48 hr in all three cell types was observed (Fig 4.2.1.1 B, C, E, F, H and I), however the presence of histidine or L-homoarginine at 20 mM did result in observable morphological differences in all cell types during longer periods of culture such as during treatment with AM or OM. For this reason, histidine and L-homoarginine were each used at a concentration of 10 mM for further experiments, as this

concentration did not inhibit cellular proliferation or result in apparent morphological changes of the cells.

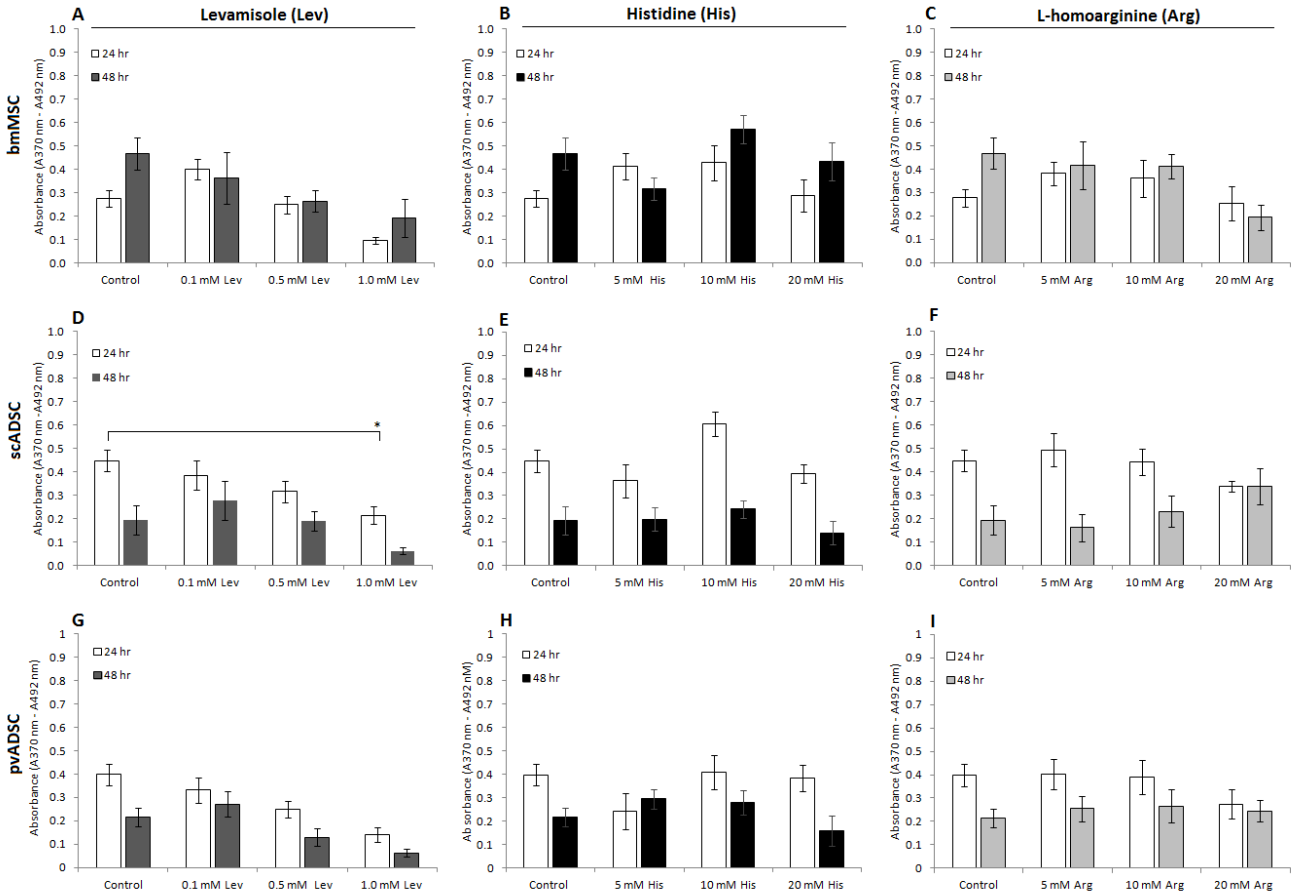

Figure 4.2.1.1: BrdU cell proliferation ELISA of bmMSCs, scADSCs and pvADSCs in the presence of TNAP inhibitors. Cells were either cultured in SGM, as controls (no inhibitors), or in the presence of levamisole (Lev) at 0.1, 0.5 or 1.0 mM (A, D and G), histidine (His) at 5, 10 or 20 mM (B, E and H) and L-homoarginine (Arg) at 5, 10 or 20 mM (C, F and I). n=3. Statistical analysis was performed using one-way ANOVA and Tukey post-test to determine statistical differences where $p < 0.05$ (* represents $p < 0.05$). Error bars are representative of standard error (SE).

4.2.2 Evaluation of the effect TNAP inhibitors on bmMSC osteogenesis and adipogenesis

Bone marrow-derived MSCs were induced to differentiate into either an osteogenic or adipogenic phenotype as previously described (Sections 2.2.5 and 2.2.7), in the presence of the TNAP inhibitors levamisole (0.5 mM), histidine (10 mM) and L-homoarginine (10 mM), added separately or in combination with one another. Inhibitors were added to cell cultures at the start of osteogenic or adipogenic induction and maintained throughout the differentiation

period. Table 4.2.2.1 provides a summary of the overall effects of TNAP inhibitors on the percentage of mineralisation, lipid accumulation and ALP activity levels on bmMSCs induced towards an osteogenic or adipogenic phenotype.

Table 4.2.2.1: Overall effects of tissue nonspecific alkaline phosphatase (TNAP) inhibitors on percentage mineralisation, lipid accumulation and alkaline phosphatase (ALP) activity on bmMSCs induced towards an osteogenic or adipogenic phenotype.

	Osteogenic phenotype		Adipogenic phenotype	
Inhibitor	**Mineralisation**	**ALP activity**	**Lipid accumulation**	**ALP activity**
Lev	Decreased ++	Increased	No effect	Decreased++
His	No effect	Increased	Decreased ++	Increased
Arg	No effect	No effect	Decreased ++	Decreased
Lev+His	Decreased ++	Increased	Decreased	Decreased++
Lev+Arg	Decreased ++	Decreased	Decreased ++	Decreased
His+Arg	No effect	Increased	Decreased ++	Decreased

Inhibitors used include levamisole (Lev) (0.1 mM), histidine (His) (10 mM) and L-homoarginine (Arg) (10 mM), and the differentiation period was 10 and 14 days for osteogenic and adipogenic differentiation, respectively. Where a possible trend was noticed, it is indicated by either "Increased" or "Decreased", "++" statistically significant $p<0.05$. Quantification is shown in subsequent graphs.

4.2.2.1 Bone marrow MSC osteogenesis

In bmMSCs, mineralisation was typically first observed by day 5 of osteogenic induction, although this varied from between day 3 to 7 in some instances, and was typically complete by day 10 (Fig. 4.2.2.1.1). No mineralisation was observed in bmMSCs cultured in SGM with vehicle controls (the addition of an equal volume of inhibitor solvent into the control cells) throughout the differentiation period (Fig. 4.2.2.1.1 A, B and C), however dense clusters of cells were observed by day 10 on control samples (Fig. 4.2.2.1.1C). Image analysis results show that mineralisation in OM reaches a mean value of 50% of the cell culture surface by day 10, significantly higher than day 5 in OM, with a mean of 15% (Fig. 4.2.2.1.3 A), however individual biological repeats displayed considerable variation of mineralisation by day 10, ranging from approximately 12 to 77% (See Addendum B, Fig. B1, F and I).

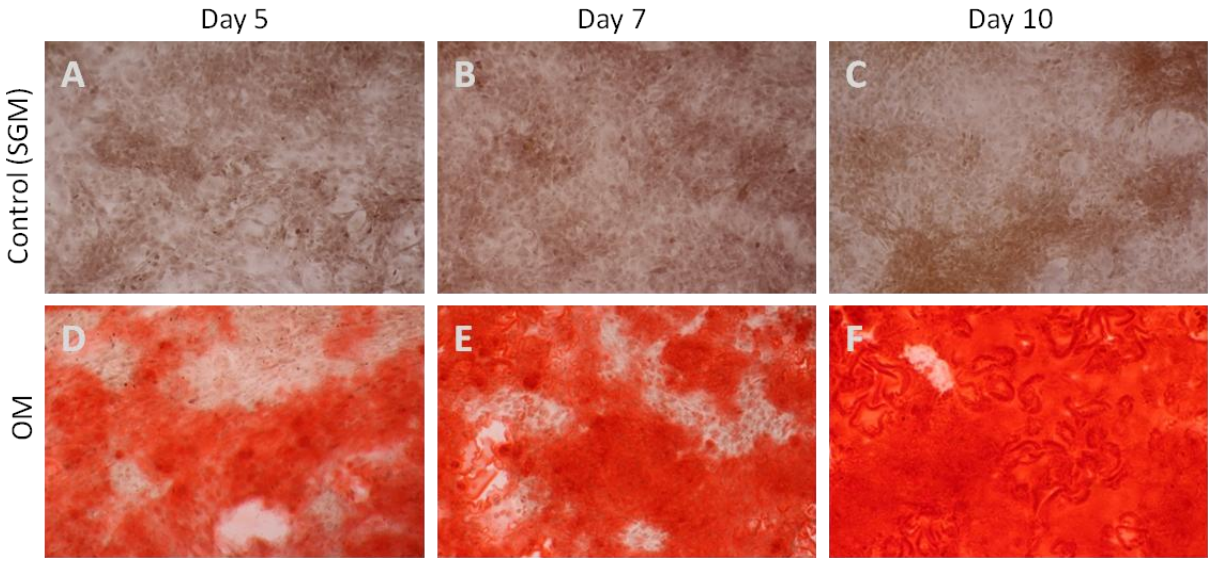

Figure 4.2.2.1.1: Osteogenic differentiation of bmMSCs. Bone marrow-derived MSCs were cultured in standard growth medium (SGM) (A, B and C) and osteogenic differentiation medium (OM) (D, E and F), and differentiation progression is shown on day 5 (A and D), day 7 (B and E) and day 10 (C and F). Cells were stained with Alizarin Red S to visualise mineralisation (Red). These images were acquired using an Olympus (CKX41) microscope at x10 magnification.

By day 10 of osteogenic induction, no mineralisation was observed in bmMSCs cultured in the presence of levamisole alone (Fig 4.2.2.1.2 A) or when used in combination with either histidine (Fig. 4.2.2.1.2 D) or L-homoarginine (Fig. 4.2.2.1.2 E). Image analysis confirmed that the presence of levamisole was sufficient to block mineralisation completely in all samples by day 10 (Fig. 4.2.2.1.3 F and G). The presence of histidine or L-homoarginine, alone or in combination with one another during osteogenic induction resulted in mineralisation which was frequently indistinguishable from control at day 10 (Fig 4.2.2.1.2, B, C and F). No significant differences in mineralisation were detected in the presence of histidine and/or L-homoarginine by the end (day 10) of the osteogenic induction period (Fig. 4.2.2.1.3 F and G).

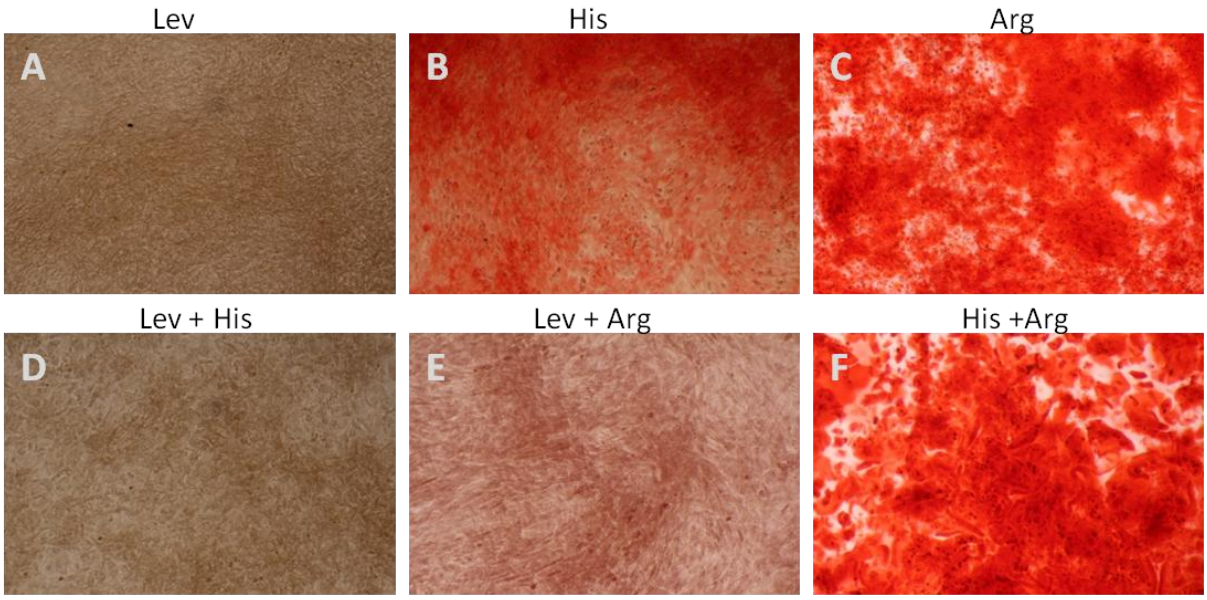

Figure 4.2.2.1.2: Osteogenic differentiation of bmMSCs in the presence of TNAP inhibitors. Bone marrow-derived MSCs cultured in osteogenic differentiation medium containing levamisole (Lev) (A), histidine (His) (B), L-homoarginine (Arg) (C), Lev+His (D) Lev+Arg (E) and His+Arg (F) for 10 days and stained with Alizarin Red S to visualise mineralisation. See Fig. 4.2.2.1.1 (F) for control osteogenic differentiation image. These images were acquired using an Olympus (CKX41) microscope at x10 magnification.

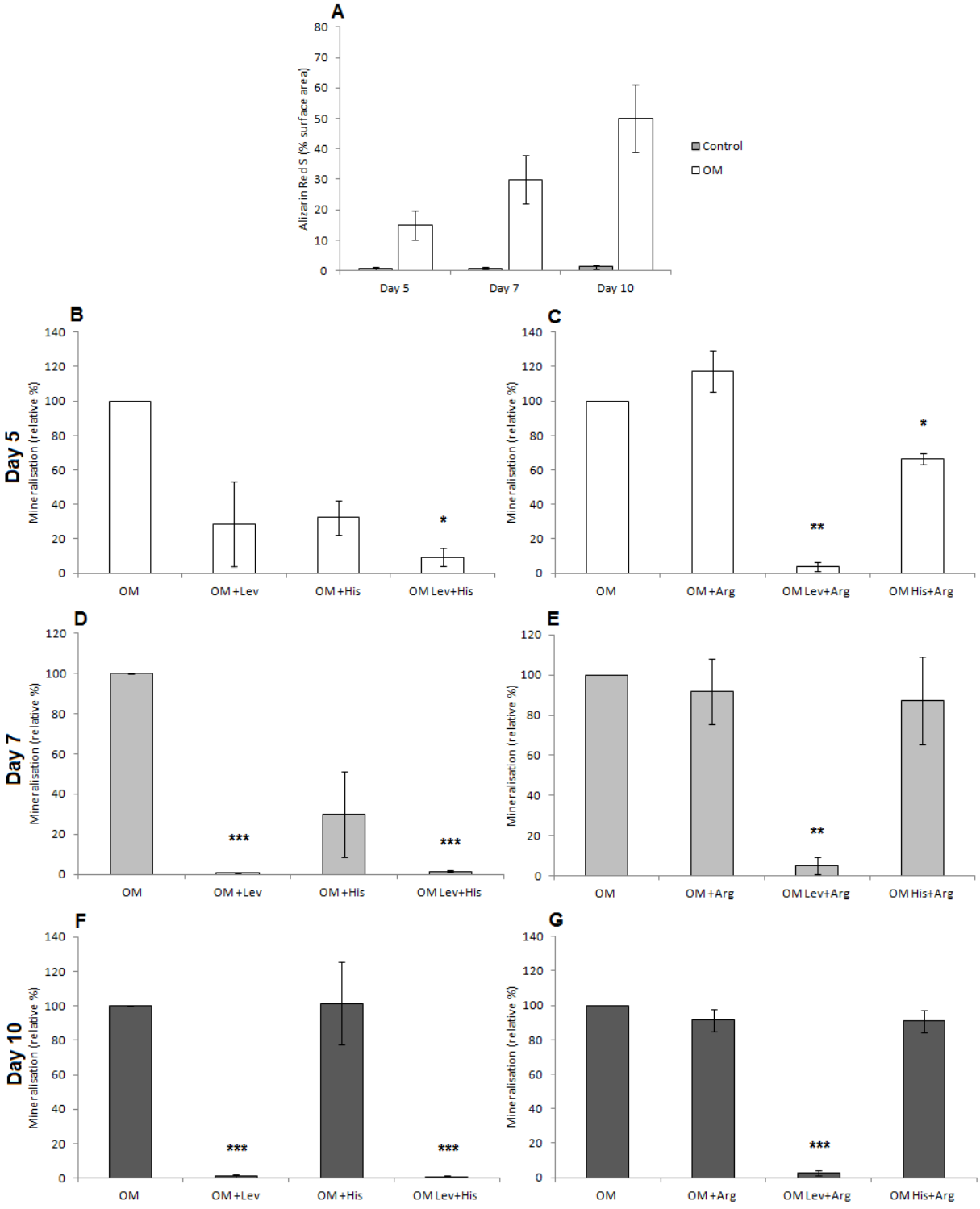

Figure 4.2.2.1.3: Image analysis to determine percentage area of mineralisation of bmMSCs cultured in osteogenic differentiation medium (OM) in the presence and absence of levamisole (Lev), histidine (His) and L-homoarginine (Arg). Percentage mineralisation of cells cultured in standard growth medium (SGM) (Control) or OM, at day 5, 7 and 10, animal 1 – 6, n=6 (A). Pooled data for animals 1 – 3 is shown in panel B, D and F, with relative % mineralisation at day 5, 7 and 10 in the presence of Lev, His or Lev+His. Pooled data for animal 4 – 6 are shown in panels C, E and G, with relative % mineralisation at day 5, 7 and 10 in the presence of Arg, Lev+Arg and His+Arg. Statistical analysis was performed using Student's t test, and Bonferroni's correction, where $p < 0.05$ (* represents $p < 0.05$, ** represents $p < 0.01$, *** represents $p < 0.001$). Error bars are representative of standard error (SE). Control OM was set to 100% for each inhibitor experiment.

TNAP is essential for mineralisation during osteogenesis. The effect of the addition of TNAP inhibitors, levamisole, histidine and L-homoarginine on total ALP activity of bmMSCs undergoing osteogenic induction was investigated. The question was asked whether a decrease or increase in percentage mineralisation observed upon addition of TNAP inhibitors would result in a corresponding decrease or increase in ALP activity. This would confirm the role of TNAP in mineralisation and allow for the effects of the various inhibitors to be compared with one another.

ALP activity levels remained fairly constant throughout the osteogenic induction period, with no significant difference between control samples and those cultured in OM (Fig. 4.2.2.1.4 A). Addition of levamisole and histidine resulted in a non-significant increase in ALP activity compared to only treated with OM (control OM) in samples taken at day 5, 7 and 10. A combination of levamisole and histidine appeared to produce an additive effect on ALP activity at day 5 and 7, but the effect was lost by day 10 (Fig. 4.2.2.1.4 B, D and F). L-homoarginine had no statistically significant effect on ALP activity levels compared to control OM at days 5, 7 and 10 (Fig. 4.2.2.1.4 C, E and G). The combination of levamisole and L-homoarginine had no effect on ALP activity at days 5 and 7, however, by day 10 a decrease in activity was observed which was not significantly different to control OM. The combination of L-homoarginine and histidine produced an increase in ALP activity above control OM in day 5, 7 and 10 samples, and appeared to have an additive effect compared to the effect of either L-homoarginine or histidine alone. Overall, histidine appeared to increase activity when used in combination with either levamisole or L-homoarginine, although statistical significance was not observed.

While the presence of levamisole alone, or in combination, was able to block mineralisation during osteogenic induction, total cell ALP activity was slightly increased in the presence of levamisole or when in combination with histidine. Histidine and L-homoarginine alone had no effect on mineralisation or total cell ALP activity compared to control OM samples. The combination of L-homoarginine with levamisole blocked mineralisation and produced a concomitant decrease in ALP activity at day 10, while L-homoarginine in combination with histidine had no effect on mineralisation but an increase in ALP activity was observed in comparison to untreated controls.

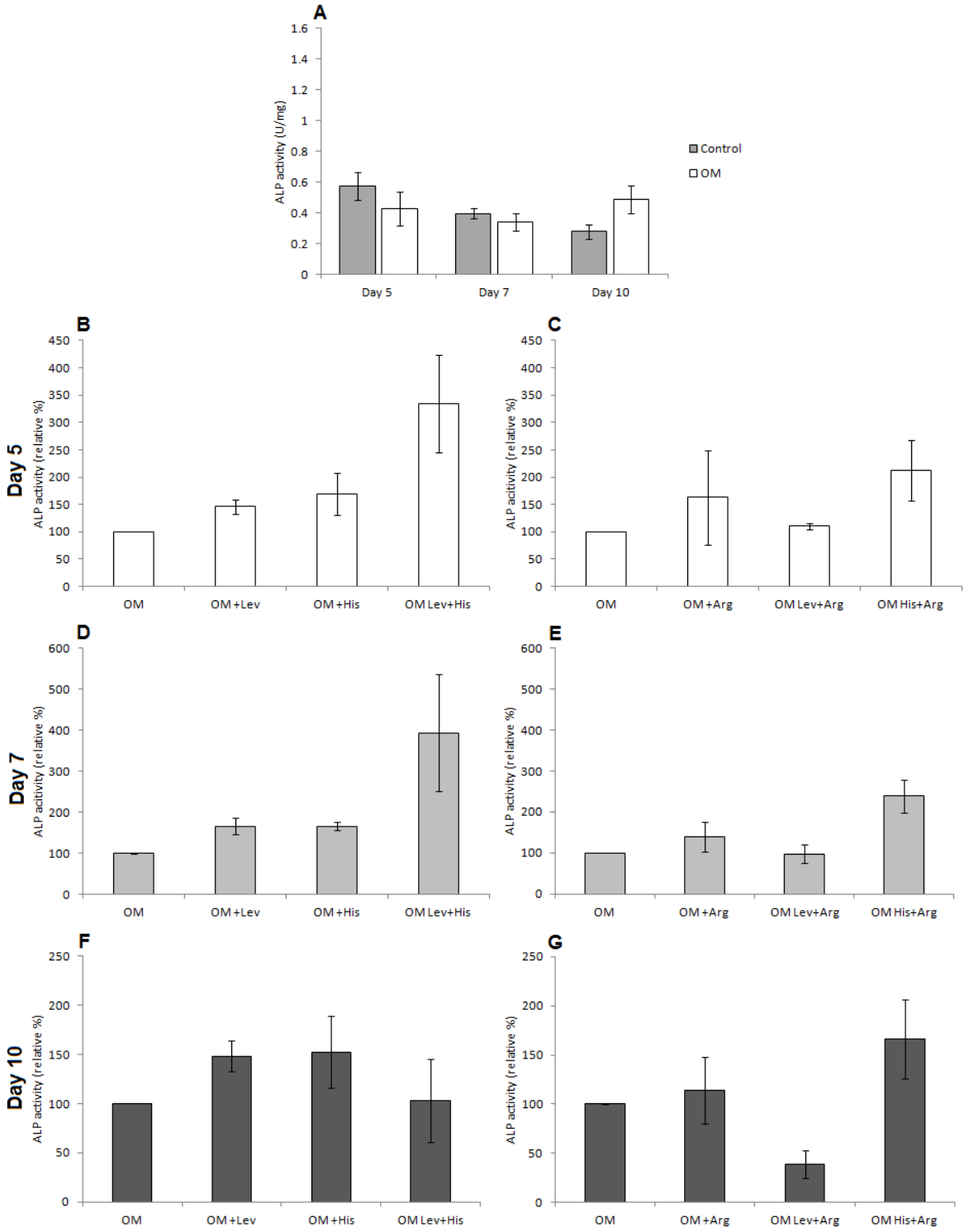

Figure 4.2.2.1.4: Alkaline phosphatase (ALP) assay to determine total cell ALP activity of bmMSCs cultured in osteogenic differentiation medium (OM) in the presence and absence of levamisole (Lev), histidine (His) and L-homoarginine (Arg). ALP activity (U/mg) of cells cultured in standard growth medium (SGM) (Control) or OM, at day 5, 7 and 10, n=6 (A). Pooled data for animals 1 – 3 are displayed in panel B, D and F, showing relative % ALP activity at days 5, 7 and 10 in the presence of Lev, His or Lev+His. Pooled data for animals 4 – 6 are displayed in panels C, E and G, showing relative % ALP activity at day 5, 7 and 10 in the presence of Arg, Lev+Arg and His+Arg. Statistical analysis was performed using Student's t test, and Bonferroni's correction, where $p < 0.05$. Error bars are representative of standard error (SE). Control OM was set to 100% for each inhibitor experiment.

4.2.2.2 Bone marrow MSC adipogenesis

Cells containing lipid droplets were typically visible by day 7 of adipogenic induction and increased in number and size throughout the differentiation period (Fig. 4.2.2.2.1 D – F). bmMSCs cultured in SGM with solvent vehicle as a control did not produce any visible lipid accumulation throughout the differentiation period, however dense clusters of cells were visible by day 14 (Fig. 4.2.2.2.1 A – C). Results from image analysis showed that cells containing lipid droplets reached a mean value of 10.1% of the culture surface area by day 14, a significant increase from day 7, with a mean value of 2.6% (Fig, 4.2.2.2.3 A). Maximum lipid accumulation by day 14 of adipogenic induction varied considerably between animals, with a range of between 2.5% and 30.7% (n=9) (Addendum B, Fig. B2, F and I).

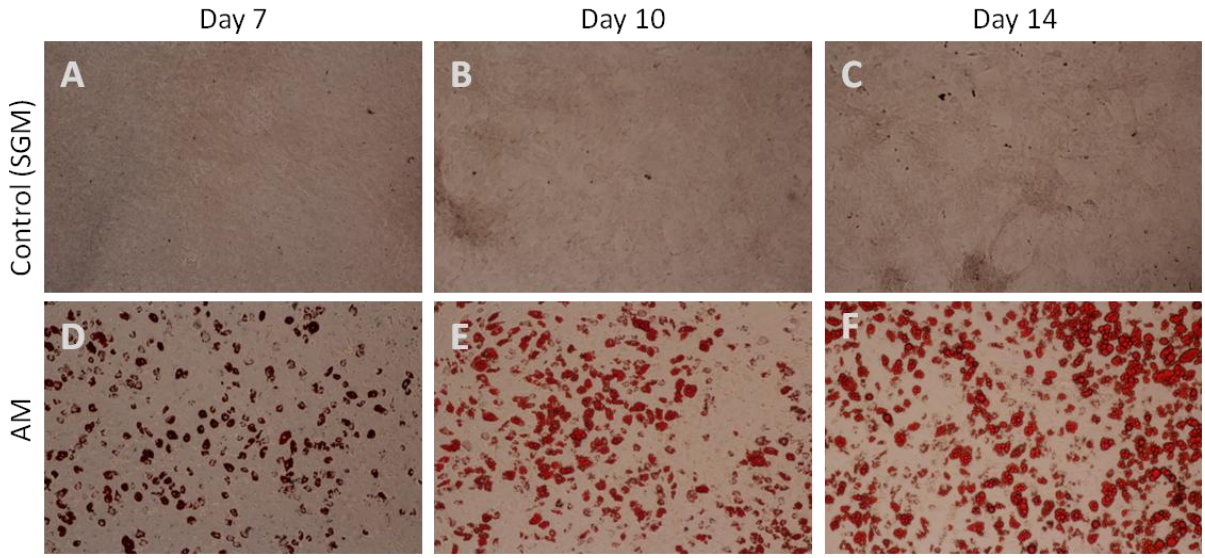

Figure 4.2.2.2.1: Adipogenic differentiation of bmMSCs. Bone marrow-derived MSCs were cultured in standard growth medium (SGM) (A, B and C) and adipogenic differentiation medium (AM) (D, E and F), and differentiation progression is shown on day 7 (A and D), day 10 (B and E) and day 14 (C and F). Cells were stained with Oil Red O to visualise lipid droplets (Red). These images were acquired using an Olympus (CKX41) microscope at x10 magnification.

The addition of levamisole to bmMSCs undergoing adipogenic induction had no discernible effect on lipid accumulation, as the lipid droplets were visually observable (Fig. 4.2.2.2.2 A) and image analysis results showed no significant differences between AM control (cells grown in AM without inhibitors) and levamisole samples at days 7, 10 and 14 (Fig. 4.2.2.2.3 B, D and F). The presence of histidine during adipogenic induction resulted in a statistically significant decrease in the number of cells containing lipid droplets compared to AM control or cells cultured with levamisole (Fig. 4.2.2.2.2 B). The combination of levamisole and

histidine during adipogenic induction resulted in a visually observable decrease in the number of cells containing lipid droplets compared to AM control (Fig. 4.2.2.2.2 D). Image analysis showed that the decrease in lipid accumulation produced by the combination of levamisole and histidine was intermediate between the effects of histidine or levamisole alone by day 14 but similar to the effect of histidine alone at days 7 and 10 (Fig. 4.2.2.2.3 B, D and F). L-homoarginine alone was sufficient to block adipogenesis by day 14 (Fig. 4.2.2.2.2 C), as few to no cells containing lipid droplets were visible. The combination of L-homoarginine with either histidine or levamisole (Fig. 4.2.2.2.2 E and F) had a similar effect to treatment with L-homoarginine alone, as confirmed by image analysis (Fig. 4.2.2.2.3 C, E and G) which shows a statistically significant reduction in lipid accumulation compared to control AM in all samples where L-homoarginine was present (Fig. 4.2.2.2.3 C, E and G).

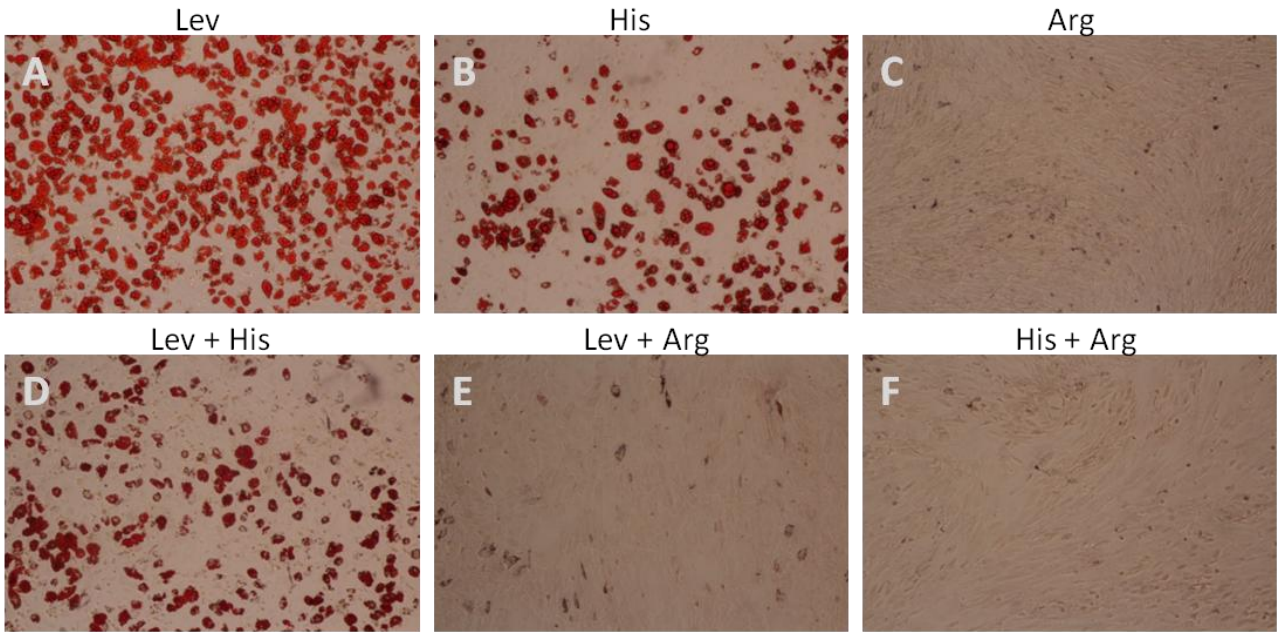

Figure 4.2.2.2.2: Adipogenic differentiation of bmMSCs in the presence of TNAP inhibitors. Bone marrow-derived MSCs cultured in Adipogenic differentiation medium (AM) containing levamisole (Lev) (A), histidine (His) (B), L-homoarginine (Arg) (C), Lev+His (D) Lev+Arg (E) and His+Arg (F) for 14 days and stained with Oil Red O to visualise lipid droplets (red). See Fig. 4.2.2.2.1 (F) for control adipogenic differentiation image. These images were acquired using an Olympus (CKX41) microscope at x10 magnification.

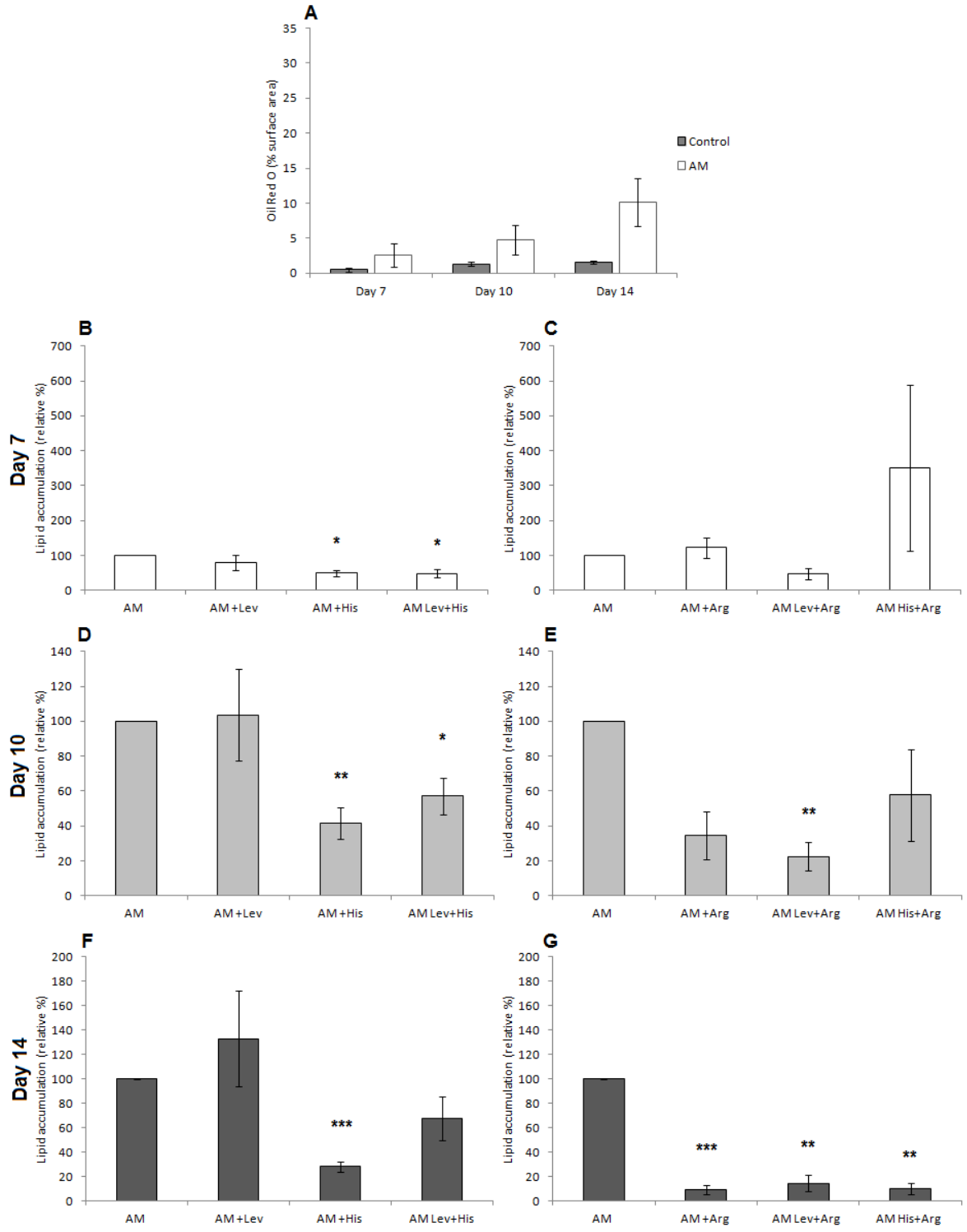

Figure 4.2.2.2.3: Image analysis to determine percentage area of lipid accumulation in bmMSCs cultured in adipogenic differentiation medium (AM) in the presence and absence of levamisole (Lev), histidine (His) and L-homoarginine (Arg). Percentage area of lipid accumulation of cells cultured in standard growth medium (SGM) (Control) or AM, at day 7, 10 and 14, n=9 (A). Pooled data for animals 1 – 5 are displayed in panel B, D and F, showing relative % lipid accumulation at days 7, 10 and 14 in the presence of Lev, His or Lev+His. Pooled data for animal 6 - 9 are displayed in panels C, E and G, showing relative % lipid accumulation at day 7, 10 and 14 in the presence of Arg, Lev+Arg and His+Arg. Statistical analysis was performed using Student's t test, and Bonferroni's correction, where $p < 0.05$ (* represents $p < 0.05$, ** represents $p < 0.01$, *** represents $p < 0.001$). Error bars are representative of standard error (SE). Control AM was set to 100% for each experiment.

Total cell ALP activity increased in bmMSCs undergoing adipogenic induction throughout the differentiation period, while that of bmMSCs maintained in SGM with vehicle (control) experienced a slight decrease in activity over the same period (Fig. 4.2.2.2.4 A). The ALP activity of cells cultured in AM was significantly higher than that of control cells by day 14 of adipogenic induction, with mean values of 1.4 U/mg and 0.31 U/mg respectively (Fig. 4.2.2.2.4 A).

In the presence of levamisole, a progressive decrease in ALP activity, in both absolute and relative values, was observed over days 10 and 14, with the greatest difference present at day 14 of adipogenic induction (Fig. 4.2.2.2.4 B, D and F and Addendum B, Fig. B4). The decrease in ALP activity in the presence of levamisole was observed in all biological repeats (Addendum B, Fig. B4, D – F). Addition of histidine resulted in a slight, non-statistically significant increase in ALP activity compared to AM control samples, observed across all time points (Fig. 4.2.2.2.4 B, D and F). The combination of levamisole and histidine resulted in partial rescue of ALP activity by histidine, but ALP activity was still significantly reduced compared to control AM by day 14 (Fig. 4.2.2.2.4 F). L-homoarginine resulted in a slight but non-significant reduction of ALP activity compared to control AM, however ALP activity appeared to be similar to control AM when L-homoraginine was present in combination with levamisole or hisitidine (Fig. 4.2.2.2.4 C, E and G).

Results show that the presence of levamisole during adipogenic induction in bmMSCs does not decrease lipid accumulation, but does result in a decrease of total cell ALP activity compared to untreated controls. Conversely, the addition of histidine during adipogenic induction results in a decrease in lipid accumulation and a slight increase in total cell ALP activity, compared to untreated controls. In contrast to both levamisole and histidine, the presence of L-homoarginine during adipogenic induction, alone or in combination, results in significant decrease in lipid accumulation, as well as a slight decrease in total cell ALP activity (Addendum B, Fig. B4).

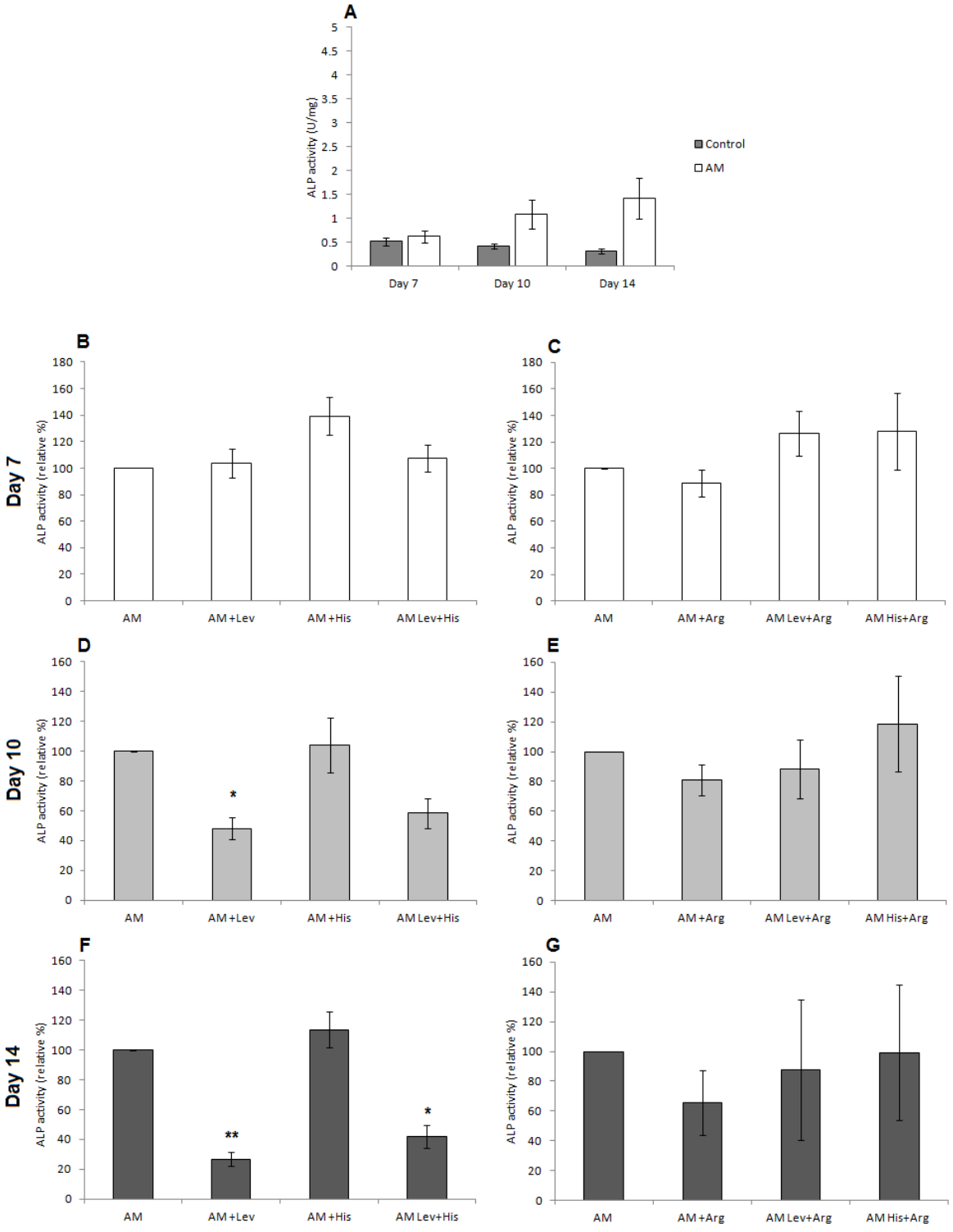

Figure 4.2.2.2.4 Alkaline phosphatase (ALP) assay to determine total cell ALP activity of bmMSCs cultured in adipogenic differentiation medium (AM) in the presence and absence of levamisole (Lev), histidine (His) and L-homoarginine (Arg). ALP activity (U/mg) of cells cultured in standard growth medium (SGM) (Control) or AM, at day 7, 10 and 14, n=7 (A). Pooled data for animals 1 – 4 are displayed in panels B, D and F, showing relative % ALP activity at days 7, 10 and 14 in the presence of Lev, His or Lev+His. Pooled data for animal 5 – 7 are displayed in panels C, E and G, showing relative % ALP activity at days 7, 10 and 14 in the presence of Arg, Lev+Arg or His+Arg. Statistical analysis was performed using Student's t test, and Bonferroni's correction, where $p < 0.05$ (* represents $p < 0.05$, ** represents $p < 0.01$). Error bars are representative of standard error (SE). Control AM was set to 100% for each experiment.

4.2.3 Evaluation of TNAP inhibitors on scADSC osteogenesis and adipogenesis

Subcutaneous ADSCs were induced to differentiate into either an osteogenic or adipogenic phenotype as previously described (Chapter 2, Sections 2.6 and 2.8), in the presence of the TNAP inhibitors levamisole (0.5 mM), histidine (10 mM) and L-homoarginine (10 mM), added separately or in combination with one another. Inhibitors were added to cell cultures at the start of osteogenic or adipogenic induction and maintained throughout the differentiation period.

Table 4.2.3.1: Overall effects of tissue nonspecific alkaline phosphatase (TNAP) inhibitors on percentage mineralisation, lipid accumulation and alkaline phosphatase (ALP) activity on subcutaneous adipose derived stromal cells (scADSCs) induced towards an osteogenic or adipogenic phenotype.

	Osteogenic phenotype		Adipogenic phenotype	
Inhibitor	**Mineralisation**	**ALP activity**	**Lipid accumulation**	**ALP activity**
Lev	Decreased ++	No effect	No effect	Decreased
His	Increased	No effect	Decreased	No effect
Arg	Decreased	No effect	Decreased++	Increased++
Lev +His	Decreased ++	Increased	No effect	No effect
Lev +Arg	Decreased ++	Increased	Decreased ++	Increased ++
His+Arg	No effect	Increased	Decreased ++	Increased ++

Inhibitors used include levamisole (Lev) (0.1 mM), histidine (His) (10 mM) and L-homoarginine (Arg) (10 mM), and the differentiation period was 21 and 10 days for osteogenic and adipogenic differentiation, respectively**.** Where a possible trend was noticed, it is indicated by either "Increased" or "Decreased", "++" statistically significant $p<0.05$. Quantification is shown in subsequent graphs.

4.2.3.1 Subcutaneous ADSC osteogenesis

Mineralisation was typically first detectable by staining with Alizarin Red S at day 14 of osteogenic induction in scADSCs and reached quantifiable levels by day 21, although morphological changes were already visible in cells at day 7 of osteogenic induction, in comparison to time-matched controls maintained in SGM with vehicle (Fig. 4.2.3.1.1). No mineralisation was detected in time-matched controls throughout the differentiation period (Fig. 4.2.3.1.1 A – C). Image analysis showed that scADSCs had a mean 17.7% surface area mineralisation by day 21 of osteogenic induction, significantly higher in comparison to mean values of only 2.4% and 0.5% at days 14 and 7, respectively (Fig. 4.2.3.1.3 A). The

percentage of mineralisation at day 21 ranged from 8.4% to 30.8% between biological repeats (Addendum B, Fig. B5, F and I).

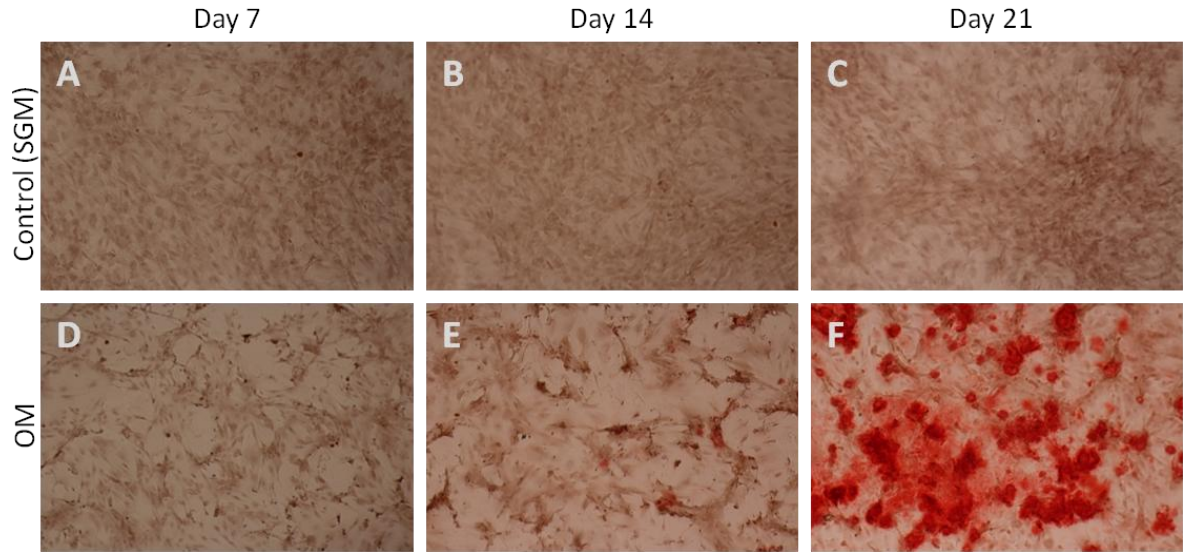

Figure 4.2.3.1.1: Osteogenic differentiation of scADSCs. Subcutaneous ADSCs were cultured in standard growth medium (SGM) (A, B and C) and osteogenic differentiation medium (OM) (D, E and F), and differentiation progression is shown on day 7 (A and D), day 14 (B and E) and day 21 (C and F). Cells were stained with Alizarin Red S to visualise mineralisation (red). These images were acquired using an Olympus (CKX41) microscope at x10 magnification.

Subcutaneous ADSCs undergoing osteogenic induction in the presence of levamisole formed cell clusters which appeared darker than surrounding areas upon staining with Alizarin Red S (Fig. 4.2.3.1.2 A), in contrast to the more homogenous appearance of untreated control cells (Fig. 4.2.3.1.1 C). Similar darkly staining cell clusters were observed when levamisole was added in combination with histidine or L-homoarginine (Fig. 4.2.3.1.2 D and E). Mineralisation was completely inhibited in all samples where levamisole was present, as evidenced by the lack of red staining in these samples (Fig 4.2.3.1.2 A, D and E). While visual analysis confirmed a lack positively stained mineralisation in samples containing levamisole, image analysis detected a small percentage of positive staining for these groups (Addendum B, Fig. B5, B, D – F). This appears to be a false positive result due to the darker stained cell clusters present in these samples. The stained cell clusters are considered to be false positives, as these have a brown appearance after staining, in contrast to the red colour present in OM treated cultures, which identifies the presence of calcified mineral.

The addition of histidine alone had the surprising effect of increasing mineralisation in scADSCs compared to OM controls. The increased mineralisation in the presence of histidine was confirmed by visual observation (Fig. 4.2.3.1.2 B) as well as image analysis, which showed an increase in percentage mineralisation at all time points, with a significant increase observed on day 7 (Fig. 4.2.3.1.3 B, D and F). Image analysis data showed that a mean value of 55.2% mineralisation was observed in samples containing histidine in comparison to 16.5% for OM samples at day 21 (Addendum B, Fig. B5, B, D – F). L-homoarginine alone was sufficient to inhibit mineralisation in scADSCs, with no mineralisation observed at day 21 (Fig. 4.2.3.1.2 C). The combination of L-homoarginine with histidine during osteogenic induction resulted in a slight increase in mineralisation compared to control OM at day 14, however by day 21 percentage mineralisation in the presence of L-homoarginine and histidine were approximately equal to control OM (Fig. 4.2.3.1.3 C, E and G).

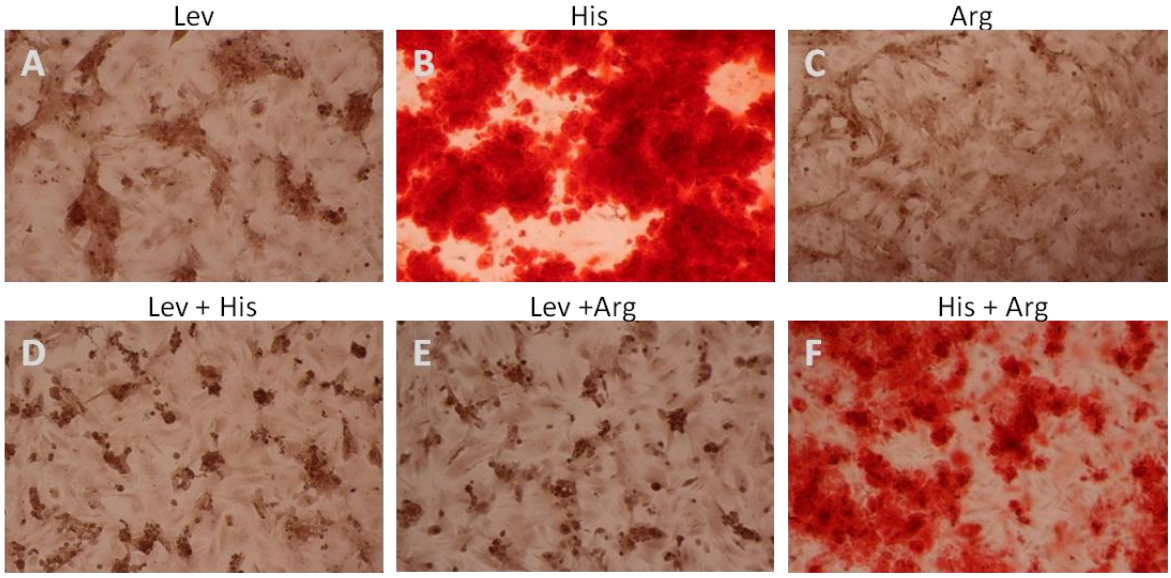

Figure 4.2.3.1.2: Osteogenic differentiation of scADSCs in the presence of TNAP inhibitors. Subcutaneous ADSCs were cultured in osteogenic differentiation medium (OM) containing levamisole (Lev) (A), histidine (His) (B), L-homoarginine (Arg) (C), Lev+His (D) Lev+Arg (E) and His+Arg (F) for 21 days and stained with Alizarin Red S to visualise mineralisation (red). See Fig. 4.2.3.1.1 (F) for control osteogenic differentiation image. These images were acquired using an Olympus (CKX41) microscope at x10 magnification.

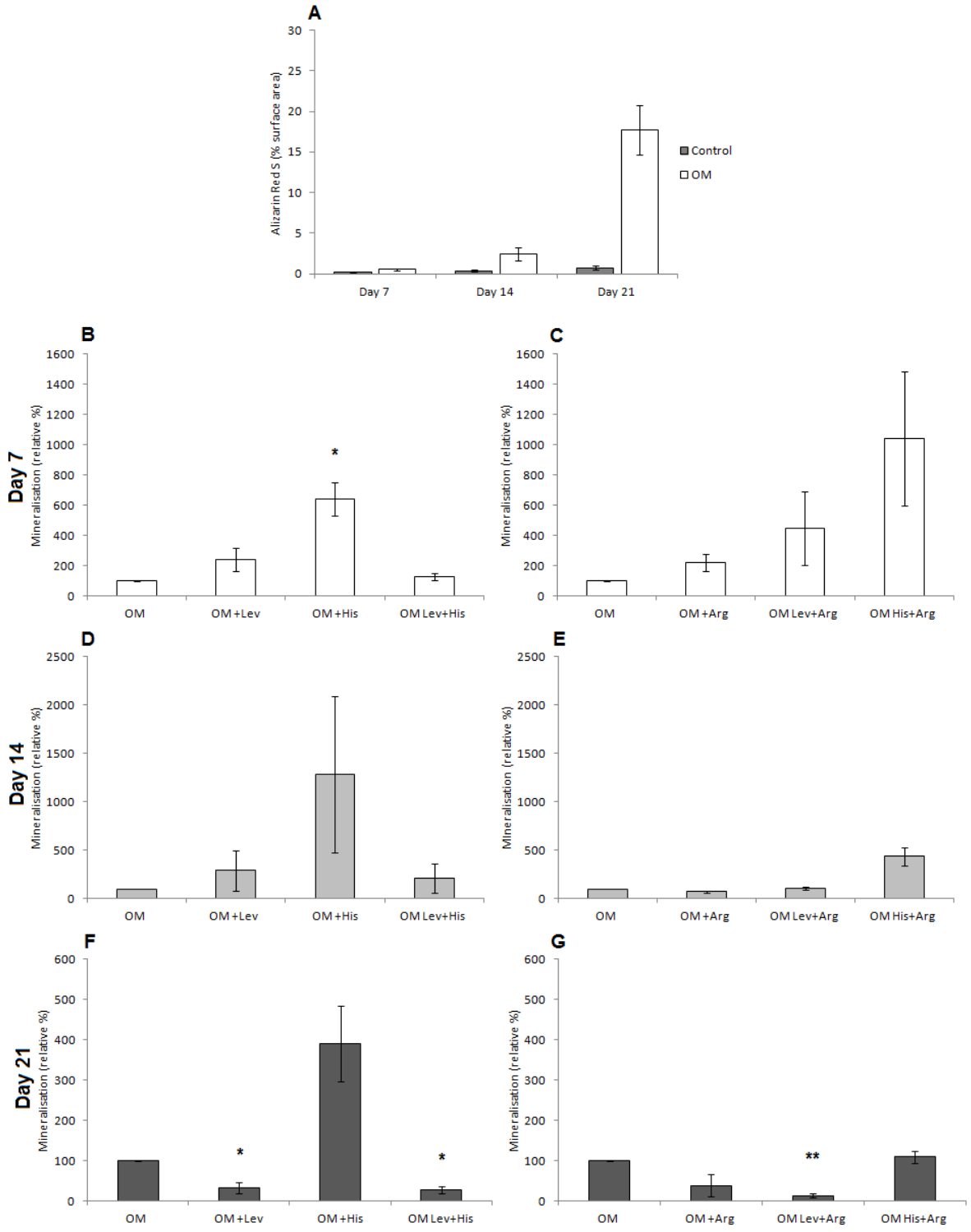

Figure 4.2.3.1.3: Image analysis to determine percentage area of mineralisation of scADSCs cultured in osteogenic differentiation medium (OM) in the presence and absence of levamisole (Lev), histidine (His) and L-homoarginine (Arg). Percentage mineralisation of cells cultured in standard growth medium (SGM) (Control) or OM, at day 7, 14 and 21, n=7 (A). Pooled data for animals 1 – 4 are displayed in panels B, D and F, showing relative % mineralisation at days 7, 14 and 21 in the presence of Lev, His or Lev+His. Pooled data for animal 5 – 7 are shown in panels C, E and G, showing relative % mineralisation at days 7, 14 and 21 in the presence of Arg, Lev+Arg or His+Arg. Statistical analysis was performed using Student's t test, and Bonferroni's correction, where $p < 0.05$ (* represents $p < 0.05$, ** represents $p < 0.01$). Error bars are representative of standard error (SE). Control OM was set to 100% for each inhibitor experiment.

Considerable variation in total cell ALP activity was detected between biological repeats in scADSCs undergoing osteogenic induction. ALP activity in cells undergoing osteogenic induction displayed no significant difference compared to time-matched controls maintained in SGM with OM vehicle. Total cell ALP activity of OM treated cells appeared to peak at day 14, with the lowest levels observed at day 21 (Fig. 4.2.3.1.4 A).

The addition of levamisole, histidine or L-homoarginine did not decrease ALP activity levels, but rather resulted in a slightly discernible increase in ALP activity levels, most noticeable by day 14 of osteogenic induction (Fig. 4.2.3.1.4 B – G). The combination of histidine with levamisole, levamisole and L-homoarginine and histidine with L-homoarginine resulted in a more noticeable increase in ALP activity compared to control OM, most noticeably at day 14, where the combination of levamisole and L-homoarginine was statistically significant (Fig. 4.2.3.1.4 B - G).

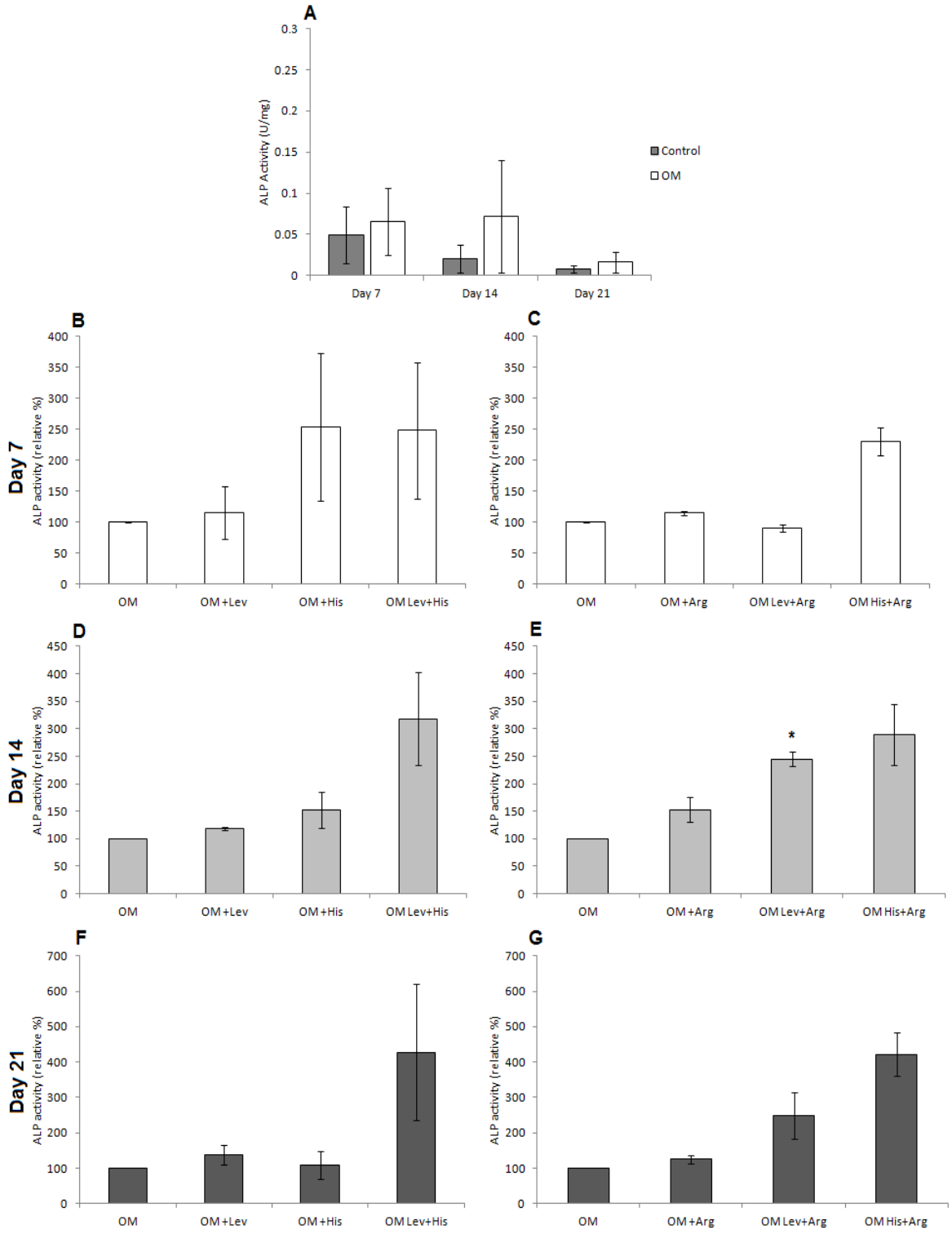

Figure 4.2.3.1.4: Alkaline phosphatase (ALP) assay to determine total cell ALP activity of scADSCs cultured in osteogenic differentiation medium (OM) in the presence and absence of levamisole (Lev), histidine (His) and L-homoarginine (Arg). ALP activity (U/mg) of cells cultured in standard growth medium (SGM) (Control) or OM, at day 7, 14 and 21, n=6 (A). Pooled data for animals 1 – 3 are displayed in panel B, D and F, showing relative % ALP activity at days 7, 14 and 21 in the presence of Lev, His or Lev+His. Pooled data for animal 4 – 6 are displayed in panels C, E and G, showing relative % ALP activity at day 7, 14 and 21 in the presence of Arg, Lev+Arg or His+Arg. Statistical analysis was performed using Student's t test, and Bonferroni's correction, where $p < 0.05$ (* represents $p < 0.05$). Error bars are representative of standard error (SE). Control OM was set to 100% for each inhibitor experiment.

4.2.3.2 Subcutaneous ADSC adipogenesis

Cells containing lipid droplets were typically visible by day 5 of adipogenic induction, where after lipid accumulation increased steadily and was typically complete by day 10, where most cells present had visible intracellular lipid droplets (Fig. 4.2.3.2.1 D – F). By day 10 of adipogenic induction, scADSCs had an average value of 12.4% of surface area positively stained for lipid with Oil Red O (Fig. 4.2.3.2.3 A), however this ranged from 6.9% to 24.0% between biological repeats (n=8) (Addendum B, Fig. B7). Subcutaneous ADSCs maintained in SGM with vehicle control did not produce any visible lipid droplets throughout the differentiation period (Fig. 4.2.3.2.1 A – C).

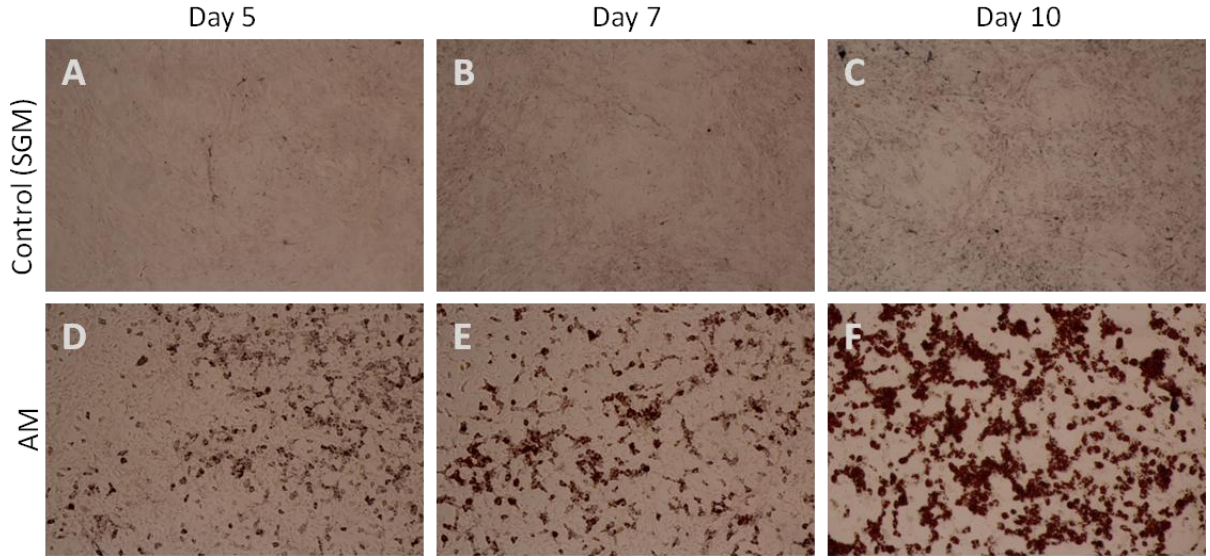

Figure 4.2.3.2.1: Adipogenic differentiation of scADSCs. Subcutaneous ADSCs were cultured in standard growth medium (SGM) (A, B and C) and adipogenic differentiation medium (AM) (D, E and F), and differentiation progression is shown on day 5 (A and D), day 7 (B and E) and day 10 (C and F). Cells were stained with Oil Red O to visualise lipid droplets (red). These images were acquired using an Olympus (CKX41) microscope at x10 magnification.

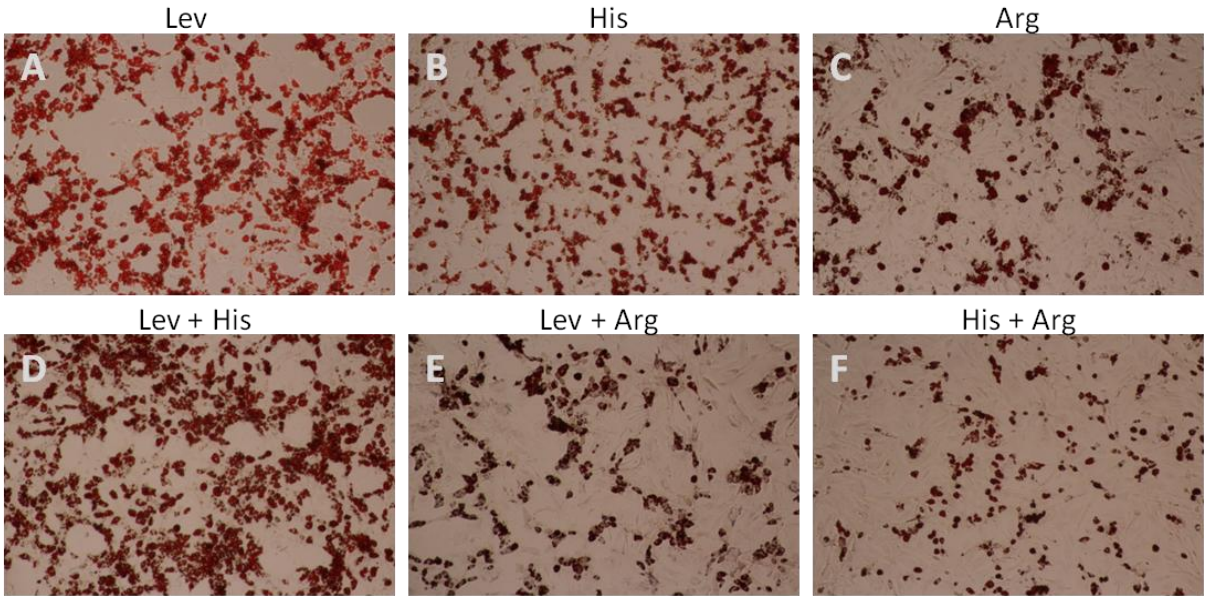

Figure 4.2.3.2.2: Adipogenic differentiation of scADSCs in the presence of TNAP inhibitors. Subcutaneous ADSCs were cultured in adipogenic differentiation medium (AM) containing levamisole (Lev) (A), histidine (His) (B), L-homoarginine (Arg) (C), Lev+His (D) Lev+Arg (E) and His+Arg (F) for 10 days and stained with Oil Red O to visualise lipid droplets (red). See Fig. 4.2.3.2.1 (F) for control adipogenic differentiation image. These images were acquired using an Olympus (CKX41) microscope at x10 magnification.

The addition of levamisole to scADSCs undergoing adipogenic induction had no apparent visible effect on lipid accumulation compared to control AM samples (Fig. 4.2.3.2.2 A). Image analysis results confirmed that the presence of levamisole had little effect on lipid accumulation, as percentage surface area of lipid in samples containing levamisole was only slightly below that of control AM at days 5, 7 and approximately equal to control AM at day 10 (Fig. 4.2.3.2.3 B, D and F). The presence of histidine during adipogenic induction produced a slight drop in lipid accumulation, a trend present in all biological repeats (n=3). The combination of histidine and levamisole resulted in lipid accumulation at similar levels to those observed in control AM and levamisole (Fig. 4.2.3.2.3 B, D and F).

In the presence of L-homoarginine, a slight decrease in lipid accumulation was noticeable by day 7 and statistically significant by 10 (Fig. 4.2.3.2.3 C, E and G). The decrease in lipid accumulation was visibly apparent by day 10 in comparison to control AM samples (Fig. 4.2.3.2.3 A). The combination of L-homoarginine with levamisole had a similar effect to L-homoarginine alone, while the combination of L-homoarginine with histidine resulted in an even greater decrease in lipid accumulation compared to L-homoarginine alone, when viewed in comparison to lipid accumulation in control AM cells by day 10 (Fig. 4.2.3.2.3 C, E and G).

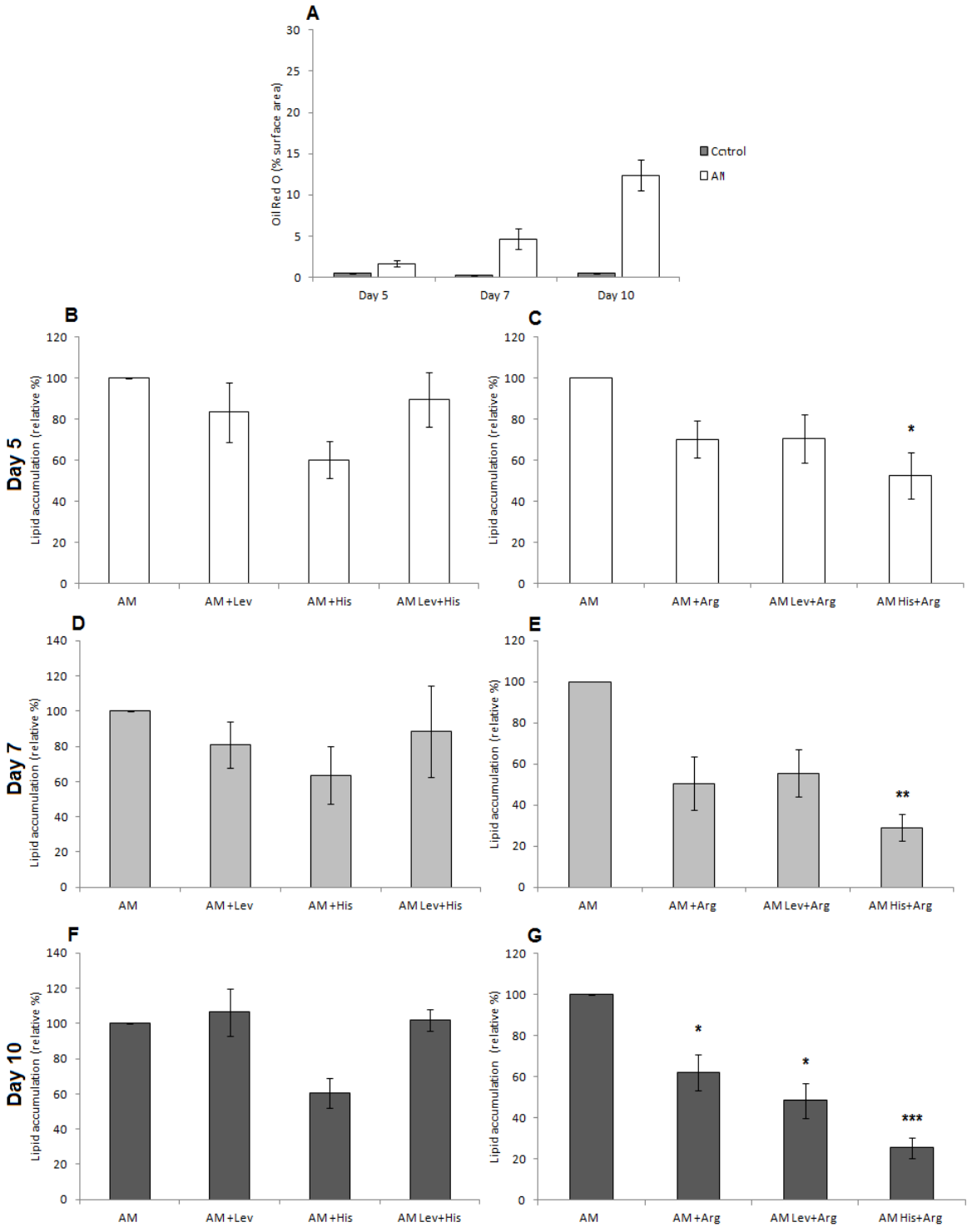

Figure 4.2.3.2.3: Image analysis to determine percentage area of lipid accumulation in scADSCs cultured in adipogenic differentiation medium (AM) in the presence and absence of levamisole (Lev), histidine (His) and L-homoarginine (Arg). Percentage area of lipid accumulation of cells cultured in standard growth medium (SGM) (Control) or AM, at day 5, 7 and 10, n=8 (A). Pooled data for animals 1 – 3 are displayed in panels B, D and F, showing relative % lipid accumulation at days 5, 7 and 10 in the presence of Lev, His or Lev+His respectively. Pooled data for animal 4 – 8 are displayed in panels C, E and G, showing relative % lipid accumulation at days 5, 7 and 10 in the presence of Arg, Lev+Arg or His+Arg. Statistical analysis was performed using Student's t test, and Bonferroni's correction, where $p < 0.05$ (* represents $p < 0.05$, ** represents $p < 0.01$, *** represents $p < 0.001$). Error bars are representative of standard error (SE). Control AM was set to 100% for each inhibitor experiment.

The highest level of total cell ALP activity in scADSCs undergoing adipogenic induction was observed at day 5, at a mean value of 0.0271 U/mg, and decreased significantly with time until the lowest level was reached at day 10, where the average ALP activity was 0.0080 U/mg, approximately equal to ALP activity levels in time-matched controls maintained in SGM with vehicle, at an average of 0.0078 U/mg (Fig. 4.2.3.2.4 A). The ALP activity detected in time-matched controls, was slightly lower than in cells undergoing adipogenic induction at days 5 and 7, but showed a similar decreasing trend over time (Fig. 4.2.3.2.4 A).

The ALP activity of scADSCs undergoing adipogenic induction in the presence of levamisole was slightly lower in comparison to AM control samples at days 5 and 10 and significantly lower at day 7 only (Fig. 4.2.3.2.4 B, D and F). The presence of histidine alone resulted in a slight increase in ALP activity compared to control AM at days 5 and 7, however by day 10 it was similar to control AM. Histidine in combination with levamisole had no apparent effect on ALP activity when compared to AM controls at all time points measured (Fig. 4.2.3.2.4 B, D and F). ALP activity in the presence of levamisole, histidine and in combination decreased similarly to that of control AM over the differentiation period (Addendum B, Fig. B8).

The presence of L-homoarginine during adipogenic induction resulted in a significant increase in ALP activity in comparison to control AM samples, visible over all time-points investigated (Fig. 4.2.3.2.4 C, E and G). The combination of L-homoarginine with either levamisole or histidine resulted in increasing levels of ALP activity over the differentiation period, exceeding that for L-homoarginine alone, indicating an additive effect (Fig. 4.2.3.2.4 C, E and G). The combination of L-homoarginine and histidine resulted in a significantly greater amount of ALP activity in comparison to control AM at day 10 (Fig. 4.2.3.2.4 C, E and G).

The combined image analysis and ALP activity results show that levamisole did not inhibit lipid accumulation in scADSCs undergoing adipogenic induction, whereas a slight inhibition of ALP activity was observed. Conversely, the presence of histidine produced a slightly lower percentage of lipid accumulation, while ALP activity levels were not affected when compared to control AM samples. L-homoarginine resulted in a decrease in lipid accumulation and a concomitant increase in ALP activity, and effect which was intensified when L-homoarginine was combined with levamisole or histidine, with the combination with histidine having the greatest effect on lipid accumulation and ALP activity.

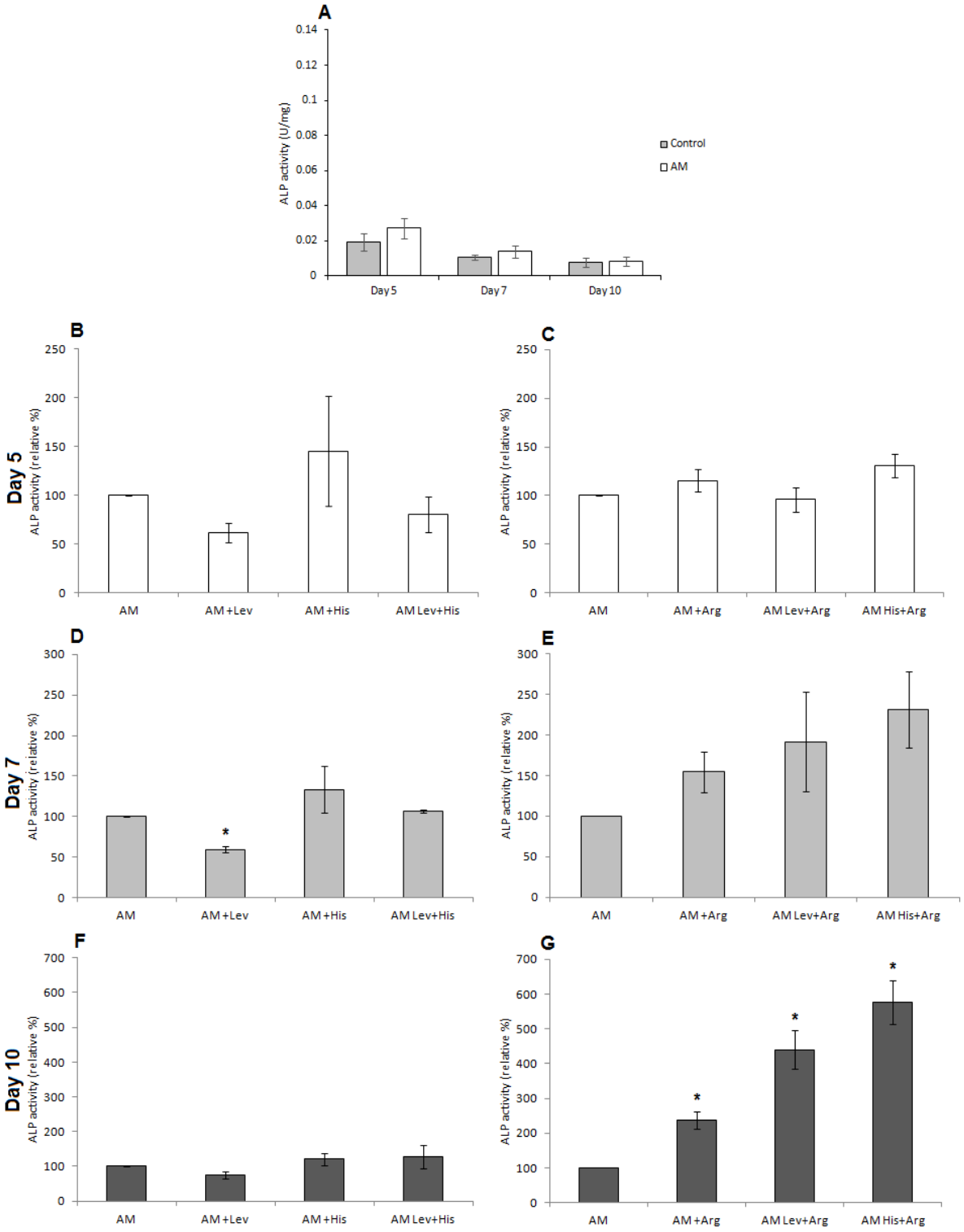

Figure 4.2.3.2.4: Alkaline phosphatase (ALP) assay to determine total cell ALP activity of scADSCs cultured in adipogenic differentiation medium (AM) in the presence and absence of levamisole (Lev), histidine (His) and L-homoarginine (Arg). ALP activity (U/mg) of cells cultured in standard growth medium (SGM) (Control) or AM, at day 5, 7 and 10, n=7 (A). Pooled data for animals 1 – 3 are displayed in panels B, D and F, showing relative % ALP activity at days 5, 7 and 10 in the presence of Lev, His or Lev+His. Pooled data for animal 4 – 7 are displayed in panels C, E and G, showing relative % ALP activity at days 5, 7 and 10 in the presence of Arg, Lev+Arg or His+Arg. Statistical analysis was performed using Student's t test, and Bonferroni's correction, where $p < 0.05$ (* represents $p < 0.05$). Error bars are representative of standard error (SE). Control AM was set to 100% for the inhibitor experiments.

4.2.4 Evaluation of TNAP inhibitors on pvADSC osteogenesis and adipogenesis

Peri-renal visceral ADSCs were induced to differentiate into either an osteogenic or adipogenic phenotype as previously described (Chapter 2, Sections 2.6 and 2.8), in the presence of the TNAP inhibitors levamisole (0.5 mM), histidine (10 mM) and L-homoarginine (10 mM), added separately or in combination with one another. Inhibitors were added to cell cultures at the start of osteogenic or adipogenic induction and maintained throughout the differentiation period.

Table 4.2.4.1: Overall effects of tissue nonspecific alkaline phsosphatase (TNAP) inhibitors on percentage mineralisation, lipid accumulation and alkaline phosphatase (ALP) activity on peri-renal visceral adipose-derived stromal cells (pvADSCs) induced towards an osteogenic or adipogenic phenotype.

	Osteogenic phenotype		Adipogenic phenotype	
Inhibitor	**Mineralisation**	**ALP activity**	**Lipid accumulation**	**ALP activity**
Lev	Decreased	No effect	No effect	Decreased
His	No effect	Increased	Decreased	Decreased
Arg	Decreased	No effect	Decreased ++	Increased
Lev +His	Decreased	Increased	No effect	No effect
Lev +Arg	Decreased	No effect	Decreased ++	Increased ++
His+Arg	Increased	Increased	Decreased ++	Increased

Inhibitors used include levamisole (Lev) (0.1 mM), histidine (His) (10 mM) and L-homoarginine (Arg) (10 mM), and the differentiation period was 10 and 14 days for osteogenic and adipogenic differentiation, respectively**.** Where a possible trend was noticed, it is indicated by either "Increased" or "Decreased", "++" statistically significant $p<0.05$. Quantification is shown in subsequent graphs.

4.2.4.1 Peri-renal visceral ADSC osteogenesis.

Mineralisation in pvADSCs was typically only apparent by day 21 of osteogenic induction, although the presence of a small amount of mineralisation was detectable by day 14 in some samples (Fig. 4.2.4.1.1 D – F). Mineralisation was not detected in pvADSCs maintained in SGM with vehicle as control after 21 days in culture (Fig. 4.2.4.1.1 A – C). Successful mineralisation of pvADSCs was variable, with mineralisation ranging from a maximum of 35.8% to a minimum of 1.35% – similar to levels measured in control samples, at day 21 (Fig. 4.2.4.1.3 A and Addendum B, Fig. B9).

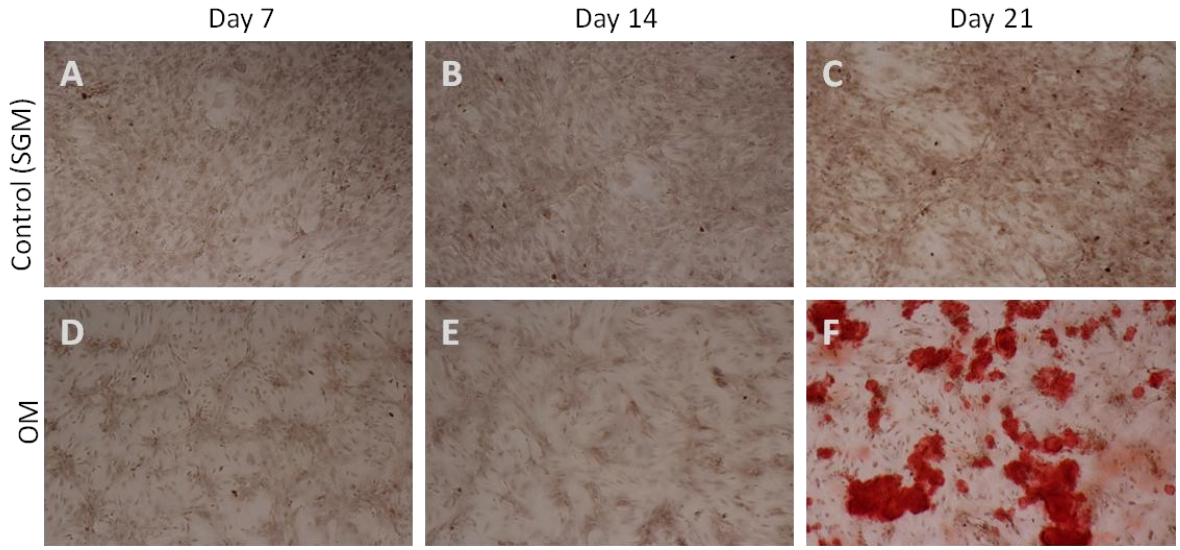

Figure 4.2.4.1.1: Osteogenic differentiation of pvADSCs. Peri-renal visceral ADSCs were cultured in standard growth medium (SGM) (A, B and C) and osteogenic differentiation medium (OM) (D, E and F), and differentiation progression is shown on day 7 (A and D), day 14 (B and E) and day 21 (C and F). Cells were stained with Alizarin Red S to visualise mineralisation (red). These images were acquired using an Olympus (CKX41) microscope at x10 magnification.

The addition of levamisole to pvADSCs, alone or in combination with histidine and L-homoarginine, prevented mineralisation from occurring by day 21 of osteogenic induction (Fig. 4.2.4.1.2 A, D and E). Similar to the observation in scADSCs, clusters of cells which appeared darker than surrounding areas when stained with Alizarin Red S were apparent in samples where levamisole was present, and resulted in a slight false postive result for mineralisation during image analysis. (Fig. 4.2.4.1.3 B, D and F; Addendum B, Fig. B9).

Histidine alone, or in combination with L-homoarginine, resulted in an increase in mineralisation in comparison to OM control cells by day 21 of osteogenic induction (Fig. 4.2.4.1.2 B and F, and Fig. 4.2.4.1.3 F and G), although this trend was not present in all biological repeats (Addendum B, Fig. B9, F and I). Mineralisation in the presence of histidine and L-homoarginine was higher than with L-homoarginine alone. L-homoarginine appeared to inhibit mineralisation in pvADSCs during osteogenic induction, however this inhibition was not as complete as that observed for levamisole, due to the observeration of slight red-stained mineral present in these samples (Fig 4.2.4.1.2 C).

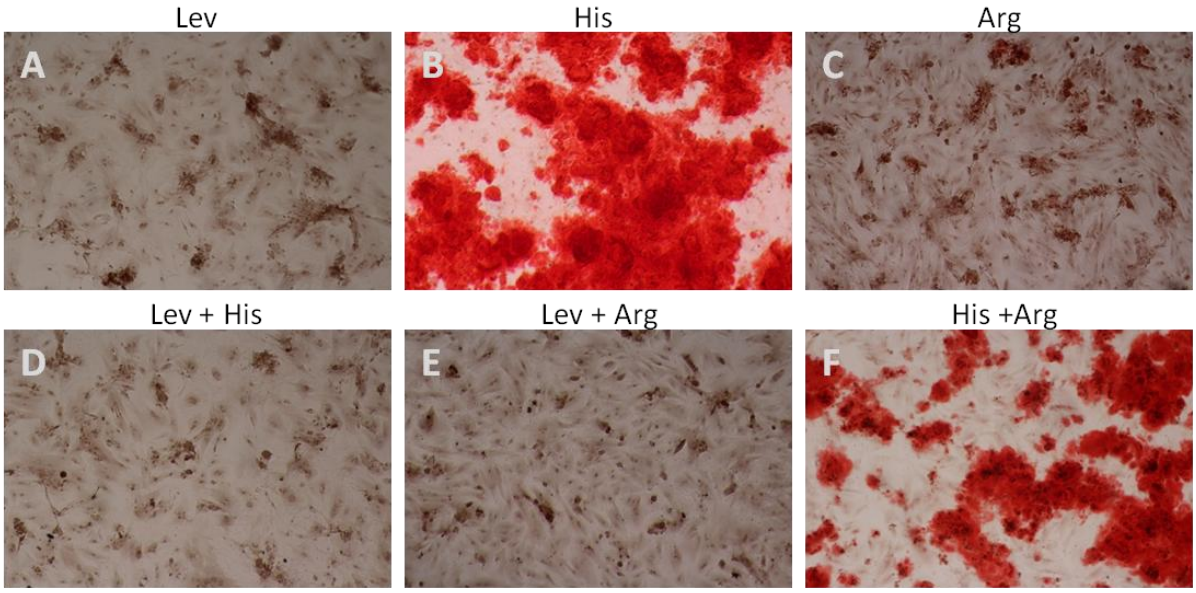

Figure 4.2.4.1.2: Osteogenic differentiation of pvADSCs in the presence of TNAP inhibitors. Peri-renal visceral ADSCs were cultured in osteogenic differentiation medium (OM) containing levamisole (Lev) (A), histidine (His) (B), L-homoarginine (Arg) (C), Lev+His (D) Lev+Arg (E) and His+Arg (F) for 21 days and stained with Alizarin Red S to visualise mineralisation (red). See Fig. 4.2.4.1.1 (F) for control osteogenic differentiation image. These images were acquired using an Olympus (CKX41) microscope at x10 magnification.

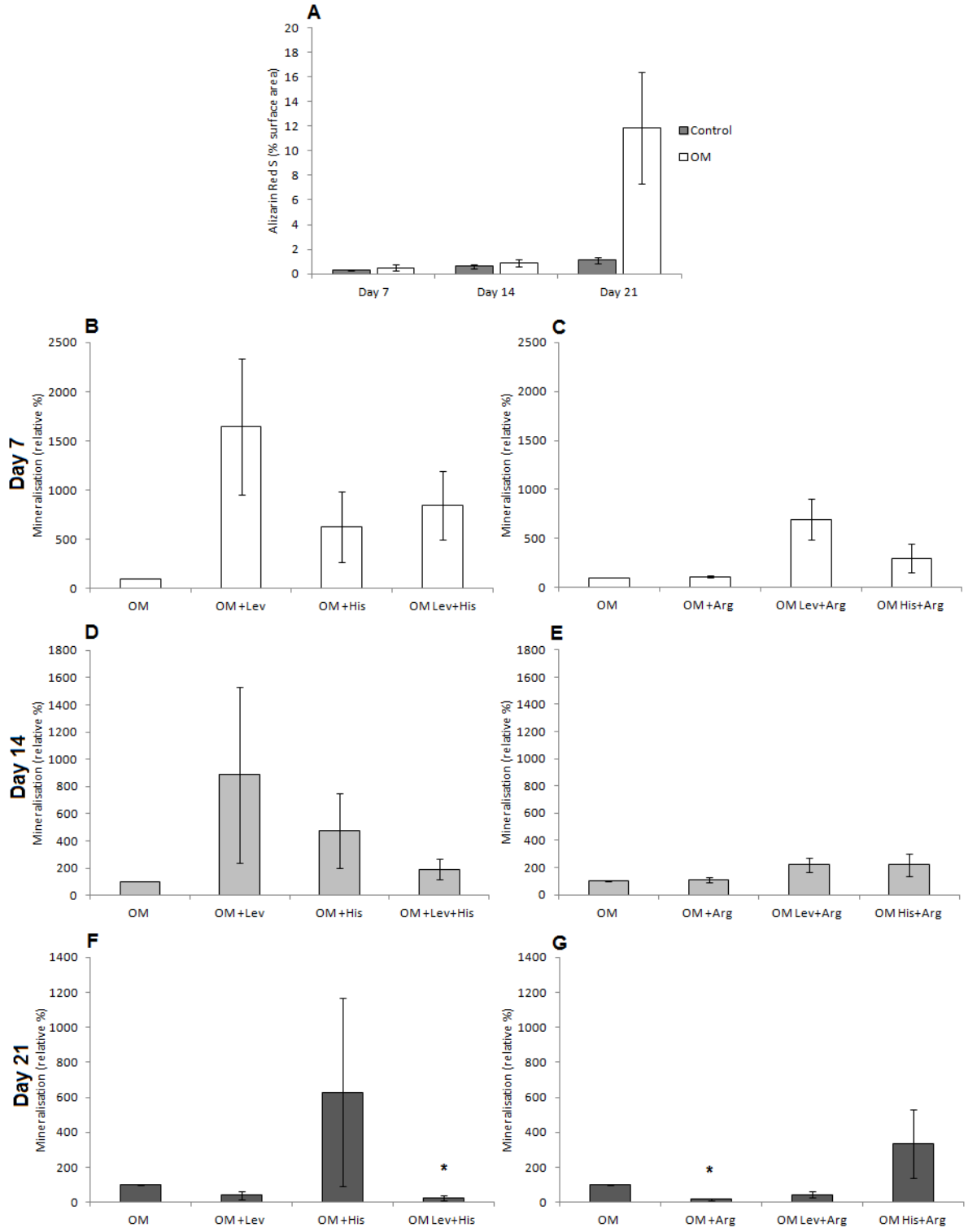

Figure 4.2.4.1.3: Image analysis to determine percentage area of mineralisation of pvADSCs cultured in osteogenic differentiation medium (OM) in the presence and absence of levamisole (Lev), histidine (His) and L-homoarginine (Arg). Percentage mineralisation of cells cultured in standard growth medium (SGM) (Control) or OM, at day 7, 14 and 21, n=7 (A). Pooled data for animals 1 – 4 are displayed in panels B, D and F, showing relative % mineralisation at days 7, 14 and 21 in the presence of Lev, His or Lev+His. Pooled data for animal 5 – 7 are displayed in panels C, E and G, showing relative % mineralisation at days 7, 14 and 21 in the presence of Arg, Lev+Arg or His+Arg. Statistical analysis was performed using Student's t test, and Bonferroni's correction, where $p < 0.05$ (* represents $p < 0.05$, ** represents $p < 0.01$). Error bars are representative of standard error (SE). Control OM was set to 100% for the inhibitor experiments.

Similarly to scADSCs, the total cell ALP activity of pvADSCs undergoing osteogenic induction was observed to decrease over the differentiation period of 21 days. The total cell ALP activity of cells maintained in SGM with vehicle control was higher than that of cells undergoing osteogenic induction for all time points measured (Fig. 4.2.4.1.4 A). The lowest ALP activity levels were observed in pvADSCs in comparison to scADSCs and bmMSCs, with a maximum average value of 0.0015 U/mg (1.5 mU/mg) at day 7 in cells undergoing osteogenic induction, and dropping to an average of 0.00085 U/mg (0.85 mU/mg) on day 21 (Fig. 4.2.4.1.4 A). The biological variation in ALP activity of pvADSCs undergoing osteogenic induction was not as pronounced as that of scADSCs, however a day 14 sample (animal 1) did have markedly higher ALP activity compared to other samples at the same time point, where control OM had 0.0043 U/mg (4.3 mU/mg) compared to values of less than 0.001 U/mg for the remaining 5 biological repeats at the same time point (Addendum B, Fig. B10, E and H).

The addition of levamisole or histidine to cells undergoing osteogenic induction did not have any apparent effect on ALP activity levels compared to OM control, however the combination of levamisole and histidine resulted in a slightly higher ALP activity, indicating an additive effect in pvADSCs undergoing osteogenic induction (Fig. 4.2.4.1.4 B, D and F). L-homoarginine alone, or in combination with levamisole had little discernible effect on ALP activity, whereas the combination of L-homoarginine with histidine resulted in an increase in ALP activity compared to control OM for all three time points sampled, with statistical significance on day 7 and 21 (Fig. 4.2.4.1.4 C, E and G).

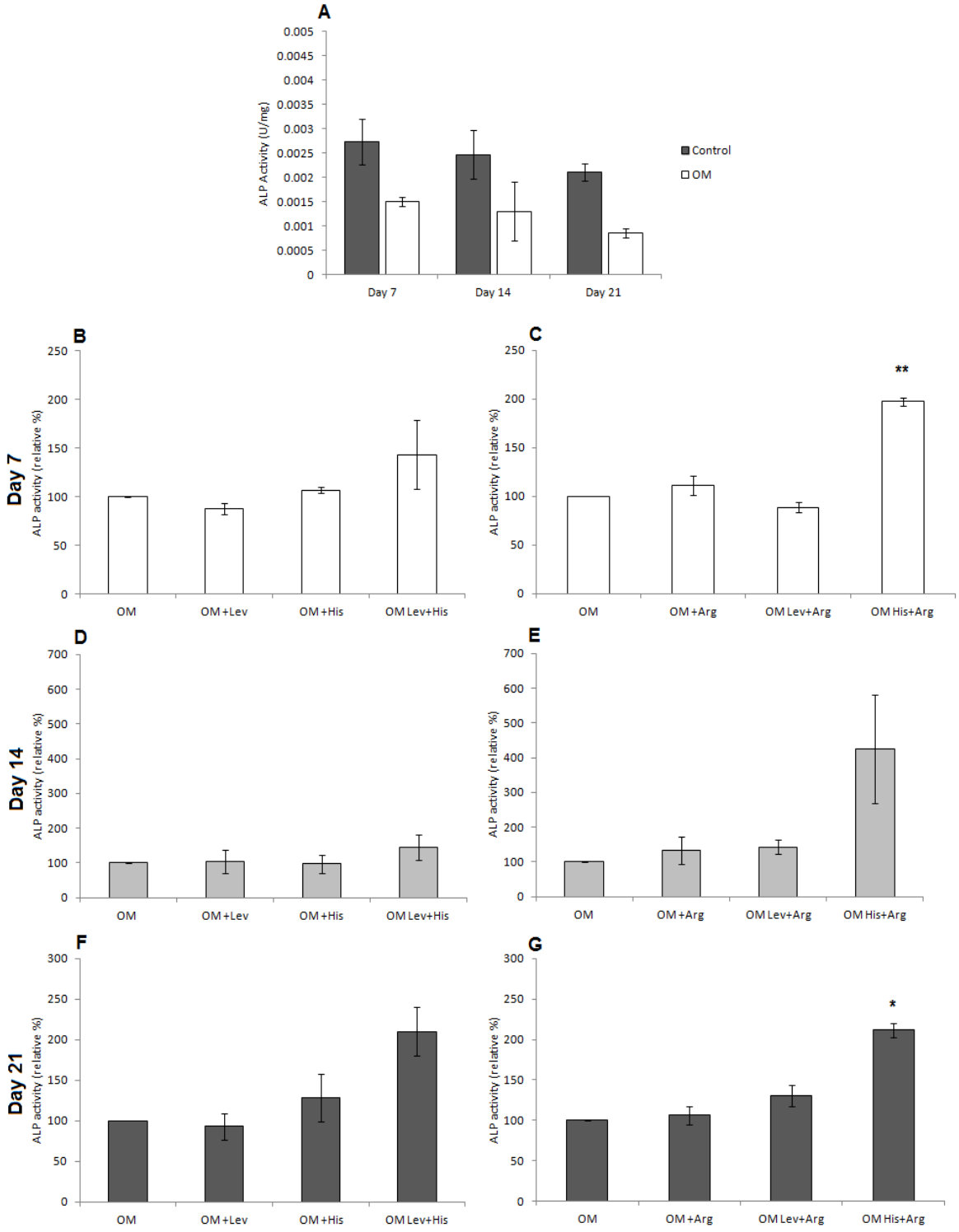

Figure 4.2.4.1.4: Alkaline phosphatase (ALP) assay to determine total cell ALP activity of pvADSCs cultured in osteogenic differentiation medium (OM) in the presence and absence of levamisole (Lev), histidine (His) and L-homoarginine (Arg). ALP activity (U/mg) of cells cultured in standard growth medium (SGM) (Control) or OM, at day 7, 14 and 21, n=6 (A). Pooled data for animals 1 – 3 are displayed in panela B, D and F, showing relative % ALP activity at days 7, 14 and 21 in the presence of Lev, His or Lev+His. Pooled data for animal 4 – 6 are displayed in panels C, E and G, showing relative % ALP activity at days 7, 14 and 21 in the presence of Arg, Lev+Arg and His+Arg. Statistical analysis was performed using Student's t test, and Bonferroni's correction, where $p < 0.05$ (* represents $p < 0.05$, ** represents $p < 0.01$). Error bars are representative of standard error (SE). Control OM was set to 100% for the inhibitor experiments.

4.2.4.2 Peri-renal visceral ADSC adipogenesis

By day 5, pvADSCs undergoing adipogenic induction typically produced visible intracellular lipid droplets, where after lipid droplets increased in size and number until day 10 where the majority of cells contained droplets (Fig. 4.2.4.2.1 D – F). No lipid accumulation was visible in cells maintained in SGM with vehicle control over the differentiation period, and instead maintained a homogenous lawn appearance (Fig. 4.2.4.2.1 A – C). By day 10, pvADSCs reached an average of 14.3 % surface area lipid when stained with Oil Red O, however, the maximum lipid accumulation achieved varied between biological repeats, with a range from 5.9% to 22.6% (Addendum B, Fig. B11, F and I).

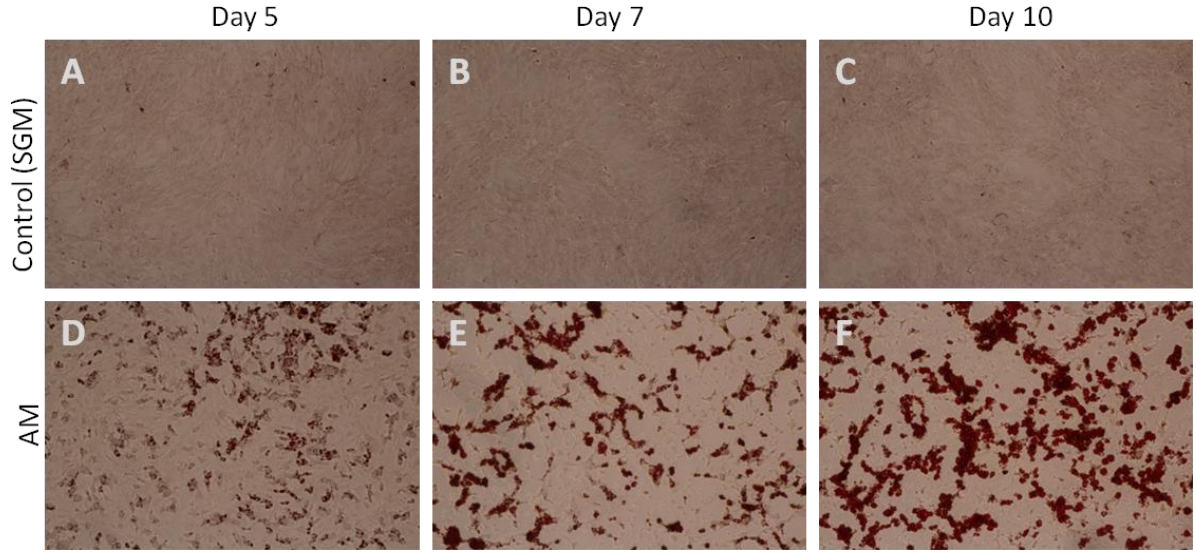

Figure 4.2.4.2.1: Adipogenic differentiation of pvADSCs. Peri-renal visceral ADSCs were cultured in standard growth medium (SGM) (A, B and C) and adipogenic differentiation medium (AM) (D, E and F), and differentiation progression is shown on day 5 (A and D), day 7 (B and E) and day 10 (C and F). Cells were stained with Oil Red O to visualise lipid droplets (red). These images were acquired using an Olympus (CKX41) microscope at x10 magnification..

By day 10 of adipogenic induction, it could be seen that the presence of levamisole, alone or in combination with histidine, did not appear to visibly inhibit lipid accumulation in pvADSCs (Fig. 4.2.4.2.2 A and D), and image analysis data showed that the percentage surface area of lipid was slightly higher in these samples than for control AM (Fig. 4.2.4.2.3 F). Histidine alone resulted in a very slight visible decrease in lipid accumulation (Fig. 4.2.4.2.2 B), an observation that was confirmed by image analysis data (Fig. 4.2.4.2.3 B and D).

The presence of L-homoarginine alone, or in combination with either levamisole or histidine resulted in a significant decrease in lipid accumulation compared to AM control, with the greatest reduction observed with L-homoarginine was combined with histidine (Fig. 4.2.4.2.3 C, E and G).

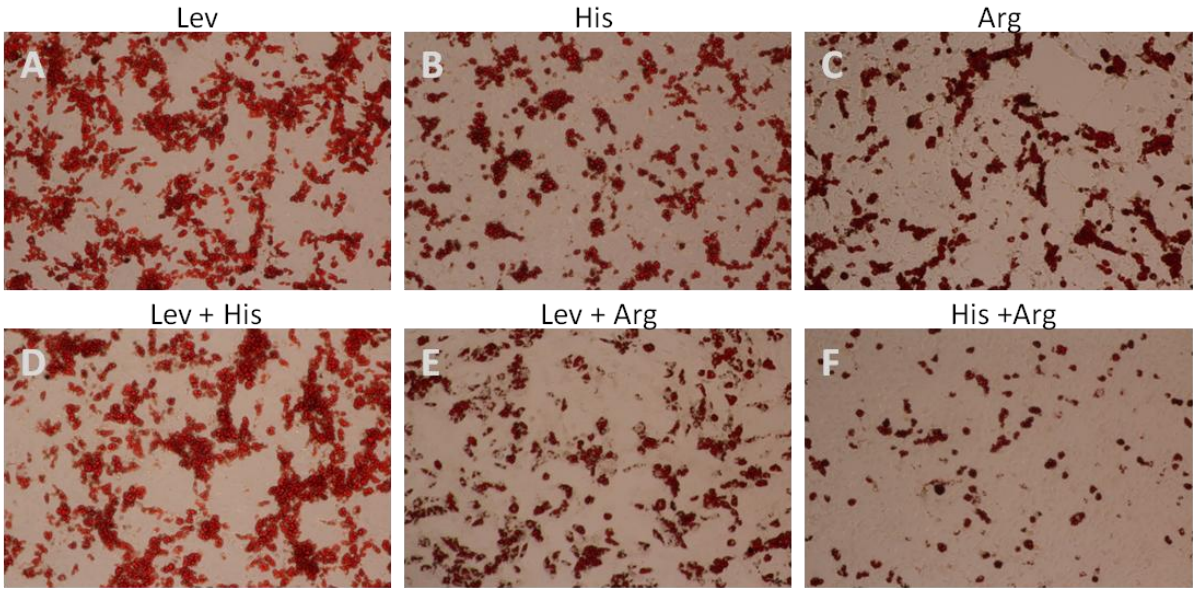

Figure 4.2.4.2.2: Adipogenic differentiation of pvADSCs in the presence of TNAP inhibitors. Peri-renal visceral ADSCs were cultured in adipogenic differentiation medium (AM) containing levamisole (Lev) (A), histidine (His) (B), L-homoarginine (Arg) (C), Lev+His (D) Lev+Arg (E) and His+Arg (F) for 10 days and stained with Oil Red O to visualise lipid droplets (red). See Fig. 4.2.4.2.1 (F) for control adipogenic differntiation image. These images were acquired using an Olympus (CKX41) microscope at x10 magnification.

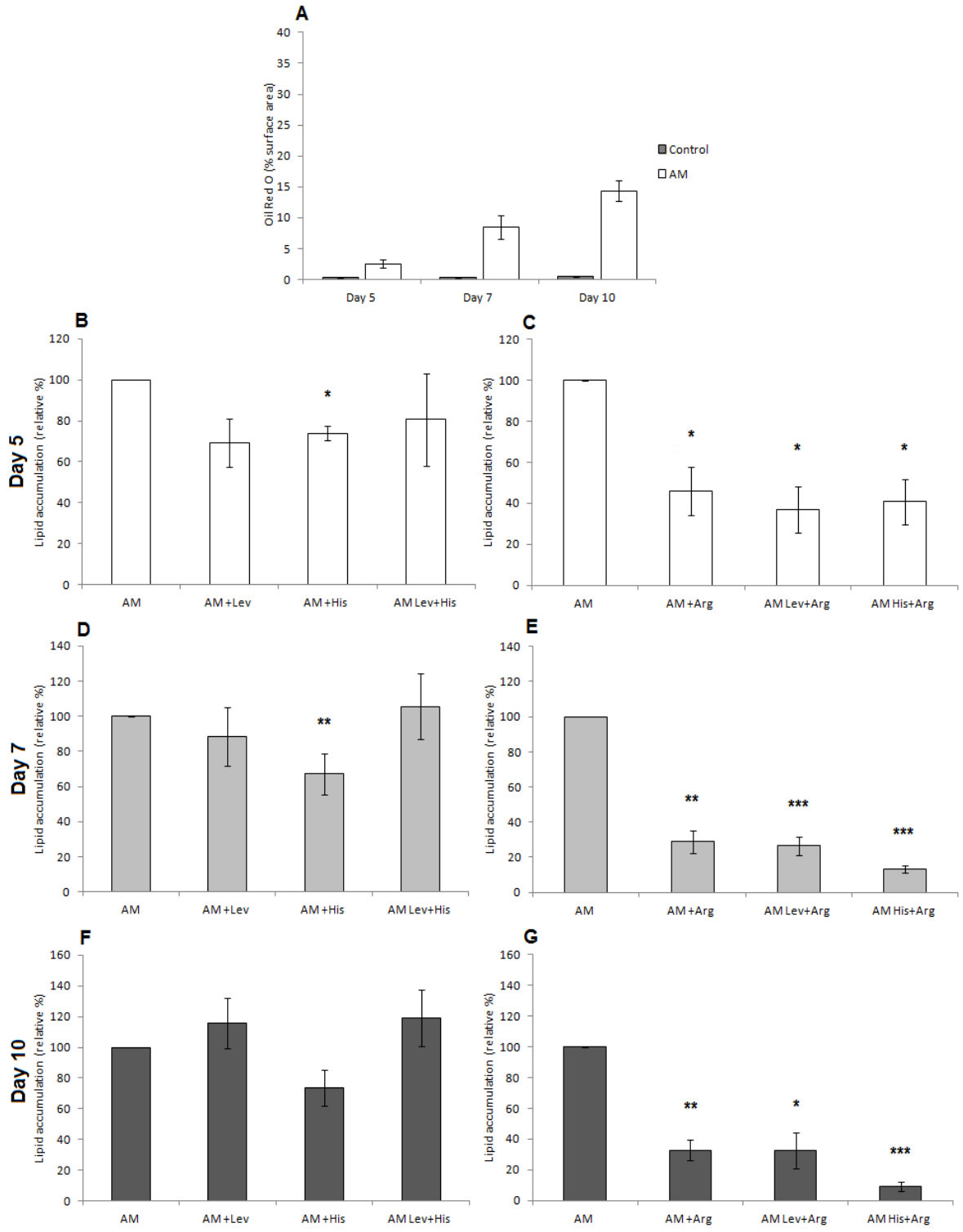

Figure 4.2.4.2.3: Image analysis to determine percentage area of lipid accumulation in pvADSCs cultured in adipogenic differentiation medium (AM) in the presence and absence of levamisole (Lev), histidine (His) and L-homoarginine (Arg). Percentage area of lipid accumulation of cells cultured in standard growth medium (SGM) (Control) or AM, at day 5, 7 and 10, n=9 (A). Pooled data for animals 1 – 4 are displayed in panels B, D and F, showing relative % lipid accumulation at days 5, 7 and 10 in the presence of Lev, His or Lev+His. Pooled data for animal 5 – 9 are displayed in panels C, E and G, showing relative % lipid accumulation at days 5, 7 and 10 in the presence of Arg, Lev+Arg or His+Arg. Statistical analysis was performed using Student's t test, and Bonferroni's correction, where $p < 0.05$ (* represents $p < 0.05$, ** represents $p < 0.01$, *** represents $p < 0.001$). Error bars are representative of standard error (SE). Control AM was set to 100% for the inhibitor experiments.

The total cell ALP activity of pvADSCs undergoing adipogenic induction was highest at day 5 at 0.0060 U/mg and decreased over the course of the differentiation period, to levels of 0.0022 U/mg at day 10, while the total cell ALP activity of cells maintained in SGM with vehicle control remained fairly constant over the same period (Fig. 4.2.4.2.4 A). In contrast to pvADSCs undergoing osteogenic induction, ALP activity in cells undergoing adipogenic induction was significantly higher than control cells at day 5, and also significantly higher at day 5 than at day 7 or 10 of differentiation (Fig. 4.2.4.2.4 A).

The presence of levamisole or histidine alone during adipogenic induction appeared to decrease ALP activity very slightly compared to control AM at days 5 and 7 but were similar to control AM by day 10. The combination of levamisole and histidine resulted in levels of ALP activity very similar to control AM at all time points sampled (Fig. 4.2.4.2.4 B, D and F).

The addition of L-homoarginine alone or in combination with levamisole and histidine resulted in either similar or higher ALP activity levels compared to control AM at all time points investigated. The combination of L-homoarginine with levamisole resulted in the highest levels of ALP activity at day 7 and 10, and were significantly higher than control AM at day 10, while ALP activity levels of L-homoarginine alone or in combination with histidine were largely similar to one another (Fig. 4.2.4.2.4 C, E and G). The ALP activity of both L-homoarginine combinations were found to increase over time compared to control AM, which was observed to decrease over the same period.

In pvADSCs, levamisole alone or in combination with L-homoarginine or histidine seemed to be able to block mineralisation, but this was not statistically significant. Levamisole had no effect on lipid accumulation. The presence of histidine alone, or and in combination with L-homoarginine, had no significant effect on mineralisation in comparison to control OM. However, a trend towards an increase was noticeable. Levamisole or histidine alone did not decrease ALP activity in cells undergoing osteogenic induction; however the combination of the two inhibitors resulted in a slight increase in ALP activity, although again this was not statistically significant. L-homoarginine in combination with levamisole was seen to inhibit mineralisation, and resulted in a slight increase in ALP activity, while L-homoarginine in combination with histidine resulted in an increase in mineralisation during osteogenic induction, and a concomitant increase in ALP activity in these samples.

Levamisole alone, or in combination with histidine had little to no effect on lipid accumulation or ALP activity, while histidine alone resulted in a slight reduction in lipid accumulation with a similar slight reduction on ALP activity. L-homoarginine, alone or in combination with levamisole or histidine, resulted in a significant reduction in lipid accumulation compared to control AM samples, while conversely, causing a significant increase in ALP activity in comparison on control AM samples.

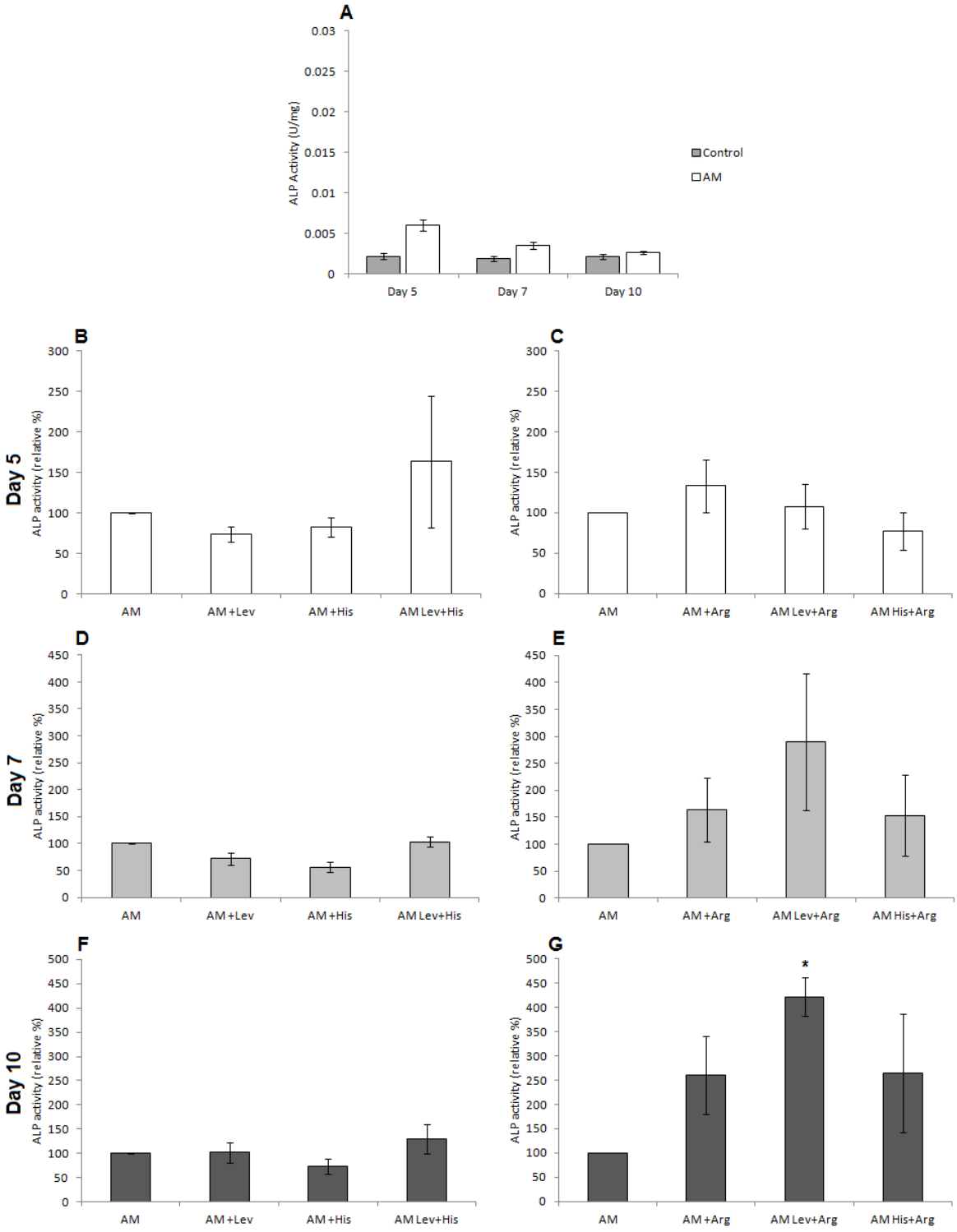

Figure 4.2.4.2.4: Alkaline phosphatase (ALP) assay to determine total cell ALP activity of pvADSCs cultured in adipogenic differentiation medium (AM) in the presence and absence of levamisole (Lev), histidine (His) and L-homoarginine (Arg). ALP activity (U/mg) of cells cultured in standard growth medium (SGM) (Control) or AM, at day 5, 7 and 10, n=7 (A). Pooled data for animals 1 – 4 are displayed in panels B, D and F, showing relative % ALP activity at days 5, 7 and 10 in the presence of Lev, His or Lev+His. Pooled data for animal 5 – 7 are displayed in panels C, E and G, showing relative % ALP activity at days 5, 7 and 10 in the presence of Arg, Lev+Arg or His+Arg. Statistical analysis was performed using Student's t test, and Bonferroni's correction, where $p < 0.05$ (* represents $p < 0.05$). Error bars are representative of standard error (SE). Control AM was set to 100% for the inhibitor experiments.

4.2.5 ALP mRNA levels during osteogenesis and adipogenesis in the presence of TNAP inhibitors

The mRNA expression levels of TNAP in bmMSCs, scADSCs and pvADSCs undergoing either adipogenic or osteogenic induction in the presence of TNAP inhibitors levamisole, histidine and L-homoarginine were investigated. The question posed was whether the presence of the various inhibitors would alter TNAP mRNA during adipogenic or osteogenic induction, and whether this change would correspond to the changes in lipid accumulation or mineralisation and ALP activity previously observed. Time points used for gene expression analysis corresponded to the time points previously found to have the overall highest TNAP mRNA expression, this being days 5 and 7 for both adipogenic and osteogenic induction, except for bmMSCs where day 3 and 5 time points were investigated, as insufficient RNA could be extracted from later time points. The highest relative TNAP expression levels were observed in bmMSCs, in which the average expression levels were never below 75 fold, followed by scADSCs and finally pvADSCs, in which TNAP mRNA expression was comparatively extremely low, where no samples were observed to reach even a 2-fold increase.

The relative expression of TNAP mRNA compared to the housekeeping gene, ARBP, in bmMSCs between days 3 and 5 of osteogenic induction remained fairly stable, with average values of 83 and 75 fold, respectively. Levamisole resulted in a slight drop in TNAP mRNA, to levels of 76 and 56 fold on days 3 and 5 of osteogenic induction, respectively. The presence of histidine and L-homoarginine resulted in an increase in TNAP mRNA expression, with the greatest increase being that of L-homoarginine with an average level of 186 fold on day 3 and 167 fold on day 5. This data is in contrast to ALP activity data, where treatment with levamisole resulted in a slight increase in ALP activity, while L-homoarginine had no apparent effect compared to control OM samples. Treatment with histidine resulted in an increase in ALP activity and TNAP mRNA expression (Fig. 4.2.2.1.4 B – G).

During adipogenic induction of bmMSCs, relative TNAP mRNA expression more than doubled, from an average level of 89 fold to 242 fold on days 5 and 7, respectively. On both days 5 and 7, the presence of levamisole resulted in a decrease in TNAP mRNA expression compared to AM control, with a significant decrease on day 7 at an average level of 76 fold (Fig. 4.2.5.1 B). The presence of histidine and L-homoarginine resulted in an increase in

TNAP mRNA compared to control AM samples, peaking on day 7 at 343 and 297 fold, respectively. The mRNA data for levamisole and histidine correspond to ALP activity data, which showed a decrease and an increase in ALP activity in the presence of levamisole and histidine respectively. L-homoarginine resulted in a decrease in ALP activity, compared to the increase in TNAP mRNA expression observed under the same conditions (Fig. 4.2.5.1 B).

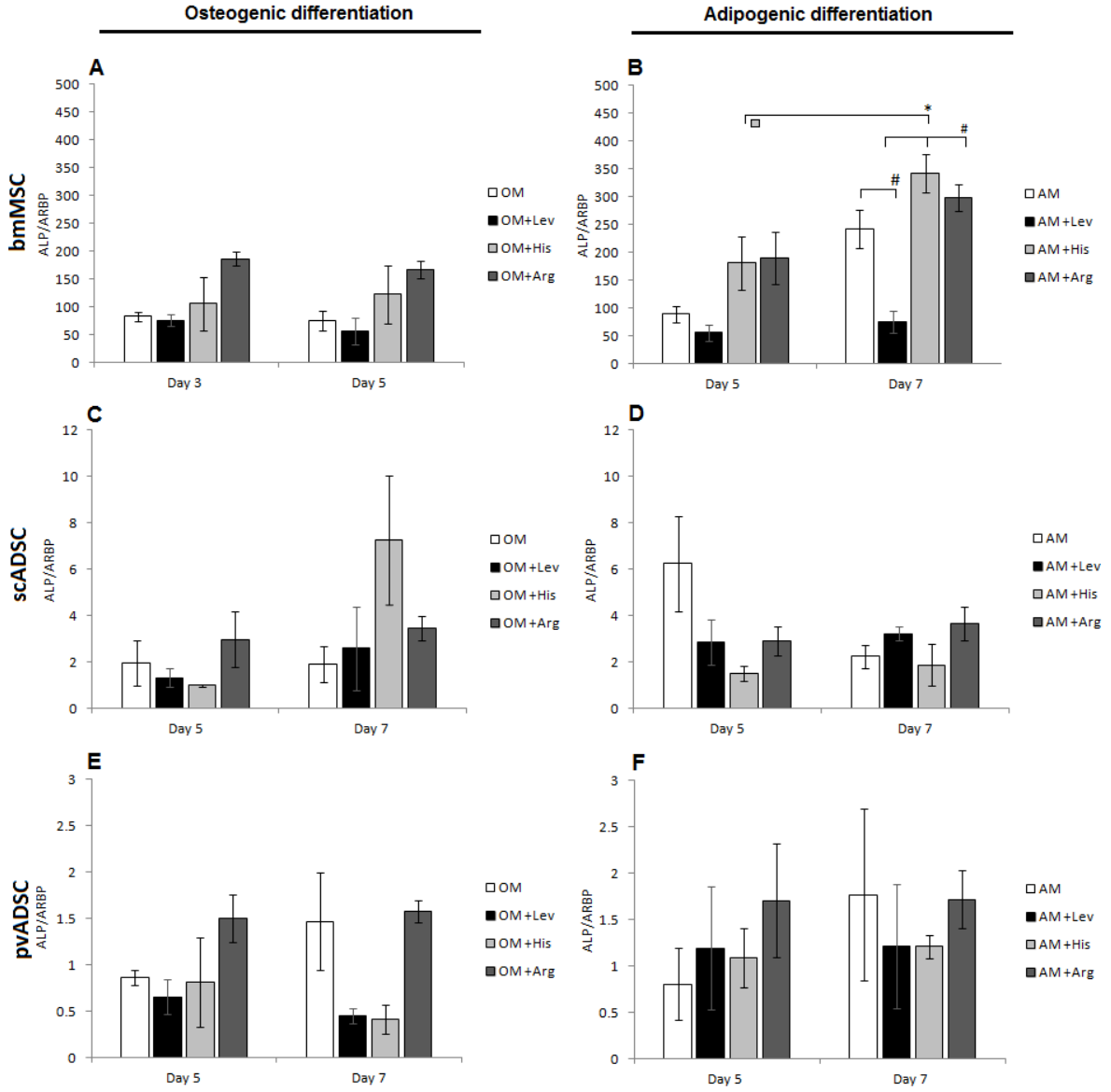

Figure 4.2.5.1: Relative expression of TNAP mRNA in bmMSCs, scADSCs and pvADSCs during osteogenic or adipogenic induction in the presence of TNAP inhibitors. TNAP mRNA expression relative to house-keeping gene *Arbp*, in cells cultured in either adipogenic differentiation medium (AM) or osteogenic differentiation medium (OM) in the presence of the TNAP inhibitors levamisole (Lev), histidine (His) and L-homoarginine (Arg). Statistical analysis was performed using one-way ANOVA and Tukey post-test to determine statistical differences where statistical significance was given when $p < 0.05$ (* represents $p < 0.05$, # represents $p < 0.05$ differences between treatments at the same time point). Error bars are representative of standard error (SE). (n=3).

TNAP mRNA levels in scADSCs undergoing osteogenic differentiation in OM were fairly similar at day 5 and 7, with average expression levels of 1.94 and 1.89-fold, respectively. TNAP mRNA levels in samples where levamisole and histidine were present were both lower than control OM on day 5, and higher than control OM on day 7. Samples containing L-homoarginine had similar TNAP mRNA levels at day 5 and 7, both of which were slightly higher than control OM (Fig. 4.2.5.1 C). The ALP activity data for scADSCs suggested that neither the presence of levamisole, histidine nor L-homoarginine had any effect on ALP activity during osteogenic induction.

The levels of TNAP mRNA expression in scADSCs during adipogenesis were higher on day 5, and dropped on day 7, similar to that observed with ALP activity data for scADSCs. The levels of TNAP mRNA in levamisole, histidine and L-homoarginine samples were similar on both day 5 and 7, with all three at lower levels than control AM samples on day 5 and levamisole and L-homoarginine being higher than control AM on day 7 (Fig. 4.2.5.1 D). ALP activity data indicated that the presence of levamisole resulted in a decrease in ALP activity, while histidine had no effect, and L-homoarginine increased ALP activity during adipogenic induction.

The relative expression of TNAP mRNA appeared to increase from day 5 to day 7 in samples of pvADSCs undergoing osteogenic induction; however this increase was only from an average level of 0.86 to 1.47-fold, respectively. At both day 5 and 7 time points, the presence of levamisole and histidine resulted in a decrease in TNAP mRNA compared to control OM, while L-homoarginine presented a slight increase in comparison to controls in OM (Fig. 4.2.5.1. E). ALP activity data for pvADSCs indicated that levamisole and L-homoarginine had no effect of ALP activity levels, while the presence of histidine increased ALP activity during osteogenic induction.

TNAP mRNA expression levels during adipogenic induction of pvADSCs increased between the day 5 and 7 time points assessed, and were similarly low, with average values of 0.08 and 1.77-fold, respectively. The average TNAP mRNA expression levels of levamisole, histidine and L-homoarginine remained fairly similar between day 5 and 7 time points, and were all higher than controls in AM at day 5, while only L-homoarginine was higher than control at day 7 (Fig. 4.2.5.1 F). The TNAP mRNA expression data at day 7 of adipogenic induction

most closely compare to the ALP activity data for the same conditions, where levamisole and histidine decreased ALP activity, and L-homoarginine was found to increase it.

4.2.6 Alkaline phosphatase activity assay after osteogenic or adipogenic induction in the presence of TNAP inhibitors

Previous experiments investigated whether the addition of TNAP inhibitors to cells undergoing adipogenic or osteogenic induction would inhibit differentiation, as assessed by either lipid accumulation or mineralisation, respectively, as well as the resulting effect on ALP activity. The question was asked whether the ALP activity of the cells would be inhibited when the various inhibitors were added to samples of total cell lysate from control cells maintained in SGM, or cells that had undergone adipogenic or osteogenic induction. Samples were collected at time points where ALP activity was previously found to be highest, namely day 5 and 14 for ADSCs and bmMSCs during adipogenic induction and days 5 and 7 for ADSCs and bmMSCs during osteogenic induction. Cell lysate samples from control cells were taken at day 7 from the point where differentiation was initiated. The inhibitors were added to the cell lysate prior to the addition of substrate, at 0.5 mM for levamisole and 10 mM each for histidine and L-homoarginine, which were the same concentrations of the inhibitors applied to live cell cultures. The reason for this was to investigate the effectiveness of the inhibitors used at these concentrations to inhibit ALP activity under ALP activity assay conditions, as opposed to cell culture conditions.

ALP activity assay confirmed that levamisole was able to inhibit ALP activity in bmMSCs, scADSCs and pvADSCs, in control, adipogenic and osteogenic samples, although inhibition was not statistically significant in some bmMSC and scADSC samples (Fig. 4.2.6.1 A – I).

Histidine partially inhibited ALP activity in scADSCs and pvADSCs in control, adipogenic and osteogenic samples, and in the bmMSC osteogenic group. Surprisingly, in bmMSC control and adipogenic samples, histidine appeared to increase ALP activity in comparison to the untreated controls in each group (Fig 4.2.6.1 A and C). This corresponds to the increased ALP activity observed in bmMSCs undergoing adipogenesis and osteogenesis where histidine was present during the differentiation period (see Section 4.2.2).

L-homoarginine was able to inhibit ALP activity in bmMSCs and scADSCs, when added to control, adipogenic and osteogenic samples, to an equal or greater extent than levamisole (Fig. 4.2.6.1). Conversely, in pvADSCs levamisole inhibited more strongly than L-homoarginine (Fig. 4.2.6.1 G – I).

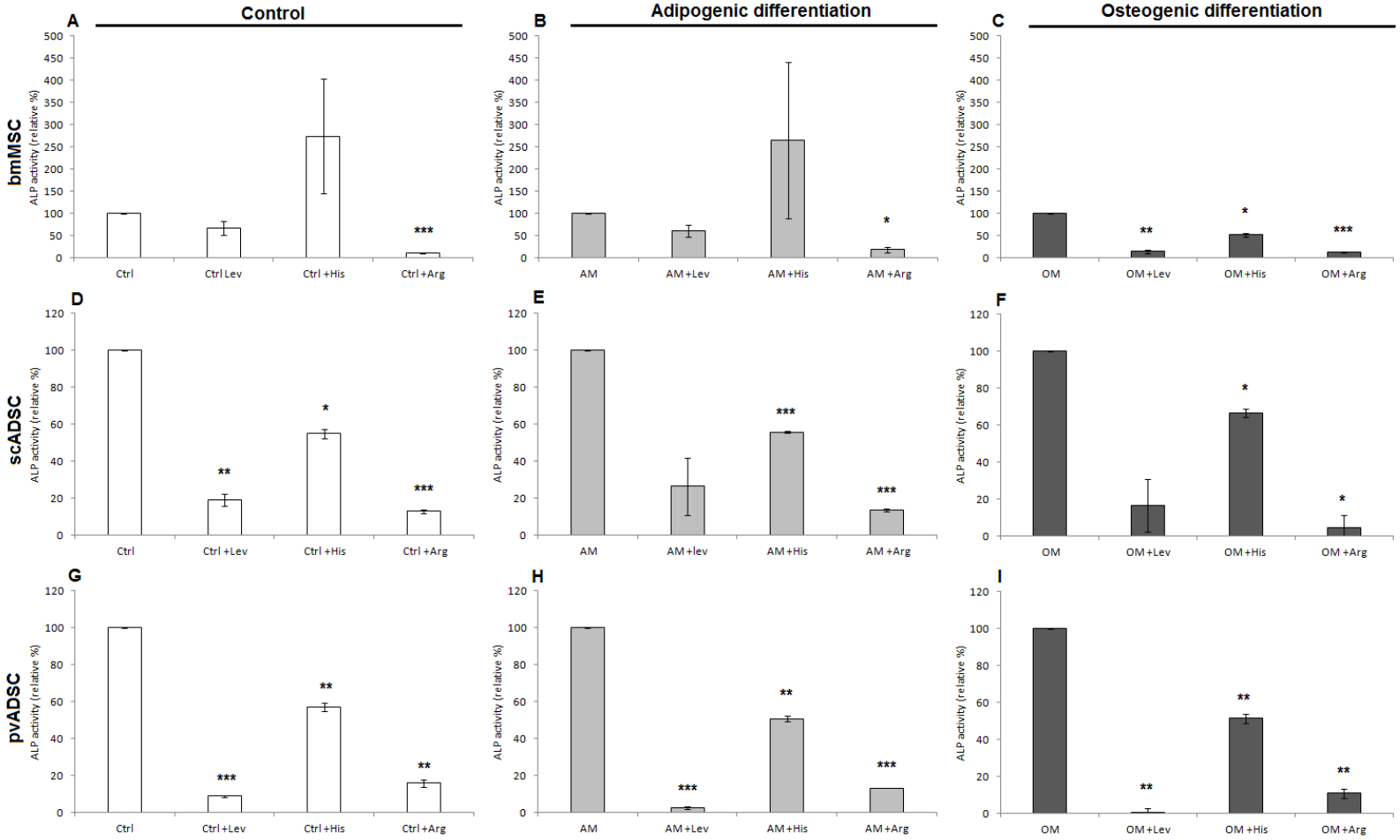

Figure 4.2.6.1: ALP activity in lysates of naïve undifferentiated control cells (Ctrl) and cells after having undergone adipogenic (AM) and osteogenic (OM) differentiation in the presence of TNAP inhibitors levamisole (Lev), histidine (His) and L-homoarginine (Arg). Control (ctrl) samples were taken from day 7 cell cultures, while OM samples were taken at day 5 for bmMSCs and day 7 for scADSCs and pvADSCs. AM samples were taken from day 14 for bmMSCs and day 5 for scADSCs and pvADSCs. ALP activity is presented as U/mg of total cell protein. n =3. Statistical analysis was performed using Student's t test and Bonferroni's correction to determine statistical differences where $p < 0.05$ (* represents $p < 0.05$, ** represents $p < 0.01$, *** represents $p < 0.001$). Error bars are representative of standard error (SE). Controls were set to 100%.

4.3 Discussion

In order to determine the effect that TNAP inhibitors would have on differentiation of MSCs from bone marrow and adipose tissue, the maximum, non-cytotoxic, concentration of each inhibitor was assessed for each cell type. In contrast to previous studies using 3T3-L1 and primary cultured human mammary preadipocytes, the rat-derived MSCs used in this study were noted to be more sensitive to both levamisole and histidine. Previous studies found that 3T3-L1 cells could tolerate levamisole at 2.5 mM (Ali *et al.*, 2005), while the data presented here showed that rat-derived MSCs were not able to tolerate greater than 0.5 mM levamisole over the course of the differentiation period, which ranged from 10 to 21 days. Similarly, histidine was not well tolerated above 10 mM in rat-derived MSC cultures, while 3T3-L1 cells were able to tolerate 50 mM histidine (Ali *et al.*, 2005). We found that rat MSCs were able to tolerate an L-homoarginine concentration of 10 mM during culture. Under ALP activity assay conditions, 8 mM L-homoarginine was previously found to be sufficient to inhibit ALP activity by 80%, where pH was also found to have no effect on inhibition (Lin and Fishman, 1972). Since *in vitro* ALP assay conditions are typically at an alkaline pH (Section 2.2.4.3) and are optimised for ALP activity where cell lysates or extracts are used, the percentage of ALP inhibition in these conditions may be different to that when the inhibitors are added exogenously to intact cells at concentrations optimised for cell survival. In spite of this, previous data showing that 8 mM L-homoarginine is sufficient to inhibit 80% of ALP, and that pH did not affect the ability of L-homoarginine to inhibit ALP activity, indicates that some inhibition can be expected at a concentration of 10 mM L-homoarginine in live cell culture.

During osteogenic induction, the presence of levamisole, alone or in combination with histidine or L-homoarginine successfully inhibited mineralisation in bmMSCs, scADSCs and pvADSCs, and resulted in slightly increased ALP activity in bmMSCs and no apparent effect on activity in either scADSCs or pvADSCs. Increased ALP activity in cells undergoing osteogenic differentiation in the presence of levamisole has been observed before in a rat-derived bone marrow stromal cell model where mineralisation was simultaneously inhibited (Klein *et al.*, 1993). It was proposed by Klein *et al*. that levamisole may prevent mineralisation by inhibition of calcium accumulation. This may be by a mechanism other than by the inhibition of ALP activity, as the D-isomer of levamisole has been observed to inhibit mineralisation, but does not inhibit ALP activity (Klein *et al.*, 1993). The increase in

ALP activity observed by Klein *et al*. was hypothesized to be due to a compensatory mechanism, where the cells are increasing synthesis of TNAP in response to the inhibition by levamisole. A similar compensatory mechanism may be present here in bmMSCs where increased ALP activity was observed in the presence of levamisole, while mineralisation was simultaneously inhibited.

Levamisole alone had no apparent effect on lipid accumulation, but resulted in a decrease in ALP activity in all three cell types during adipogenic induction, compared to AM controls. This is in contrast to the effect of levamisole observed on cells undergoing osteogenic induction, and also in a separate study, the effect of levamisole on human preadipocytes, where levamisole significantly reduced lipid accumulation and increased ALP activity (Ali *et al.*, 2013). Another recent study reported that adipogenic potential in human adipocyte precursor cells derived from subcutaneous adipose tissue was highest in a subset of the population that expressed TNAP on the surface membrane, and this subset of cells also had the highest ALP activity in comparison to the subset of adipocyte precursors which did not express TNAP as a cell surface marker (Esteve *et al.*, 2015). In the TNAP-positive subset, lipid accumulation was inhibited and adipocytic marker gene expression was lowered in the presence of tetramisole, a racemate of L-tetramisole (levamisole) and D-tetramisole, as well as with RNA interference against TNAP. This same study concluded that TNAP activity was necessary for triglyceride accumulation in human white and brite (Browned white) preadipocytes (Esteve *et al.*, 2015). It is worthwhile to note that only levamisole is known to have an inhibitory effect on TNAP, while D-tetramisole has no effect (Borgers, 1973; Nowak *et al.*, 2015). It is possible that tetramisole and levamisole have effects beyond inhibition of TNAP in living MSCs, as experiments examining the inhibition of TNAP in cells from mouse brain cortex by tetramisole and levamisole found that the effects were not stereospecific, and that tetramisole had at least four other targets in the nervous system apart from TNAP (Nowak *et al.*, 2015). The same authors cautioned the use of levamisole and tetramisole in living excitable cells for the sole aim of inhibiting TNAP, due to the numerous off-target effects (Nowak *et al.*, 2015).

Levamisole has also be found to reduce lipid accumulation in the murine preadipocyte cell line, 3T3-L1, along with a reduction in ALP activity (Ali *et al.*, 2005). The lack of response of lipid accumulation to levamisole observed in rat-derived MSCs found here may be due to several factors, including possible heterogeneity of the cell cultures, compared to the more

homogenous 3T3-L1 cell line, or the human adipocyte precursors, which were selected for specific surface markers. The human adipocyte precursors were selected using cell depletion kits to select for markers CD31, CD45 and immuno-magnetic selection kits for CD34, CD271 and MSCA-1 (TNAP), followed by flow cytometry analysis to analyse purity of populations (Ali *et al.*, 2005; Esteve *et al.*, 2015). The effect of levamisole may also be obscured in rat-derived MSCs, as a 5 x lower concentration of levamisole was used in comparison to that used on 3T3-L1 cells. We also suggest that the different responses in ALP activity to levamisole treatment observed between human adipocyte precursors (Ali *et al.*, 2013) where ALP activity increases, and the murine 3T3-L1 cells (Ali *et al.*, 2005) and rat-derived MSCs, where ALP activity decreased, may be the result of species-specific differences, as rat and mouse are more closely biologically related to one another than to humans. Levamisole also resulted in a slight decrease in TNAP mRNA levels during adipogenic induction of bmMSCs, while levamisole had no apparent effect on TNAP mRNA in scADSCs and pvADSCs

Histidine did not inhibit mineralisation or ALP activity during osteogenic induction in bmMSCs, scADSCs and pvADSCs. The inability of histidine to inhibit ALP activity and consequentially mineralisation may be related to the observation that at pH 7.5, approximately the pH of cell culture media, the inhibitory effect of histidine on the hydrolysis of adenosine 5`-phosphate by ALP was negligible, while the inhibition of ALP activity by histidine was maximal at pH 9.5 (Bodansky and Schwartz, 1963). This may indicate that at physiological pH, the inhibitory effect of histidine at 10 mM on rat-derived TNAP during in *vitro* cell culture is low or nonexistent, which may explain the lack of inhibition of ALP activity or mineralisation by histidine. The lack of inhibition of TNAP by histidine may be due in some part to the sub-optimal conditions of the cell culture environment, such as lower pH, for histidine binding to TNAP.

The mechanism by which histidine inhibits TNAP is described as mixed type, that is, the inhibitor may bind to the enzyme both when the substrate is bound and when it is not (Bodansky and Schwartz, 1963), however inhibition by histidine may possibly be uncompetitive (where the inhibitor is only able to bind to the enzyme when the substrate is also bound), due to the observation that other L-amino acids inhibit TNAP by this method (Kozlenkov *et al.*, 2004). Inhibition assay data using cell lysates showed that histidine was the weakest of the three inhibitors examined here, and surprisingly, even increased ALP

activity in bmMSC control and adipogenic samples, but not osteogenic samples. TNAP mRNA expression data indicated that histidine increased TNAP mRNA levels compared to OM control in bmMSCs and scADSCs, but not in pvADSCs. In cells treated with AM, histidine resulted in an increase in TNAP mRNA levels compared to control AM in bmMSCs only. Although during osteogenic induction the substrate for TNAP is β-glycerophosphate, the primary substrate for TNAP is not known for cells undergoing adipogenic induction. It may be possible, as previously described for levamisole, that inhibition of TNAP by histidine causes the cells to compensate, by increasing synthesis of TNAP enzyme molecules. The increased amount of TNAP in the cells may then be enough to overcome the partial inhibition by histidine, allowing mineralisation to proceed, albeit at a slower rate. This appears to be confirmed by the observation that while the percentage mineralisation of bmMSC samples containing histidine lags behind OM control samples at days 5 and 7, the levels are approximately equal to OM control by day 10. The ALP activity levels of bmMSCs in the presence of histidine are found to increase over time in comparison to OM control, such that the increased enzyme activity in the presence of histidine was able to overcome the partial inhibition of TNAP by histidine.

Similarly, in all three cell types, the combination of levamisole and histidine resulted in an increase in ALP activity, even though mineralisation was still completely inhibited, which may further indicate that a compensatory mechanism is occurring, as TNAP mRNA expression levels increased in the presence of histidine, in comparison to control OM, for bmMSCs and scADSCs, but was not observed in pvADSCs, where TNAP mRNA expression levels were lowest.

Histidine treatment during adipogenic induction was able to decrease lipid accumulation in all three cell types, although this decrease was only statistically significant in bmMSCs. Histidine treatment resulted in a very slight increase in ALP activity in bmMSCs, and no apparent effect in scADSCs or pvADSCs. Previous research has found that histidine causes a significant decrease in lipid accumulation and in ALP activity in both 3T3-L1 cells and human preadipocytes (Ali *et al.*, 2005; Ali *et al.*, 2013). The discrepancy may be due to the lower concentration of histidine used in this study (10 mM) compared to the higher concentrations of 50 and 20 mM used on 3T3-L1 and human preadipocytes, respectively. However, due to the sensitivity of the rat-derived MSCs to histidine concentrations above 10 mM, higher concentrations could not be used under the current experimental conditions. Due

to the observation that histidine is a weak inhibitor of TNAP in comparison to levamisole and L-homoarginine (Fig. 4.2.6.1), future studies on TNAP from rat-derived MSCs may wish to exclude this inhibitor, although the effect of histidine on adipogenesis is still of great interest.

The combination of levamisole and histidine in bmMSCs undergoing adipogenic induction appeared to have an intermediate effect, as lipid accumulation and ALP activity decreased to levels between that observed for either inhibitor, indicating that levamisole and histidine have different effects to one another during adipogenic differentiation, and that levamisole may be able to partially rescue the inhibition of lipid accumulation by histidine. In scADSCs and pvADSCs, the combination of levamisole and histidine during adipogenic induction had no effect when compared to AM control, while histidine alone resulted in a small decrease in lipid accumulation, indicating that here again levamisole may be able to rescue the histidine-induced decrease in lipid accumulation, which may be a consequence of depot specific differences between rat-derived MSCs from bone marrow and adipose tissue. It appears that under adipogenic conditions, levamisole decreases ALP activity, and enhances lipid accumulation; while histidine has the opposite effect in rat-derived MSCs. Histidine has been reported to have mixed inhibition towards TNAP, while levamisole has uncompetitive inhibition. Histidine may be more inhibitory towards TNAP as it is able to bind to TNAP both when the substrate is bound in the active site, as well as when no substrate is bound, while levamisole is only able to bind to TNAP when the substrate is bound at the active site. It is presently unclear how the presence of levamisole is able to rescue the inhibition of lipid accumulation by histidine.

At the time of writing, we are aware of only one study that looked at the effects of L-homoarginine on ALP activity of live cells in culture. In murine osteosarcoma (OS) cells, L-homoarginine at 44.5 mM was able to inhibit the cellular proliferation, as measured by a reduction in [^{3}H]thymidine uptake, to 9% of untreated controls at 24 hr, and 17% of untreated controls at 48hr. At 22.3 mM L-homoarginine, proliferation of OS cells was not affected at 24 and 48 hr, but proliferation in long-term OS cell cultures was inhibited (Kikuchi *et al.*, 1982). No inhibition of proliferation was detected in rat MSCs incubated with 20 mM L-homoarginine in the study presented here, in comparison to untreated controls in a short-term proliferation assay (Fig. 4.2.1.1). This is similar to the findings of Kikuchi *et al*. using OS cells treated with L-homoarginine at 22.3 mM for 25 and 48 hr, who reported no significant reduction in cell viability or proliferation during these time periods (Kikuchi *et al.*, 1982).

Kikuchi *et al*. also reported that L-homoarginine at 11.2 mM was capable of inhibiting ALP activity substantially during ALP activity assay, consistent with the inhibition of ALP activity in rat MSCs in the presence of 10 mM L-homoarginine found here (Fig. 4.2.6.1) (Kikuchi *et al.*, 1982).

L-homoarginine, like histidine, was not able to block mineralisation or decrease ALP activity in bmMSCs undergoing osteogenic induction. In bmMSCs the percentage of mineralisation in the presence of L-homoarginine was similar to OM control at all time points sampled, unlike histidine which caused a lag in mineralisation compared to OM control samples. In scADSCs and pvADSCs however, L-homoarginine appeared to inhibit mineralisation. In bmMSCs, scADSCs and pvADSCs, the addition of L-homoarginine during osteogenic induction resulted in ALP activity that was noted to be similar to – or marginally higher than, OM control samples, and again this may be due to a compensation reaction by the cell to TNAP inhibition. Inhibition assay data indicated that L-homoarginine was a more potent inhibitor of ALP activity than histidine under assay conditions, which may explain why mineralisation as impaired in scADSCs and pvADSCs but not in bmMSCs, in the presence of L-homoarginine.

In the presence of histidine alone, an increase in mineralisation of scADSCs, and no effect on mineralisation of pvADSCs, in comparison to OM control was observed. L-homoarginine was able to block mineralisation in scADSCs and pvADSCs, however when L-homoarginine was in combination with histidine, mineralisation was similar to, or higher than control, respectively. In all three cell types the combination of histidine with L-homoarginine resulted in an increase in ALP activity, above levels observed for either histidine or L-homoarginine separately. This observation appears to confirm that L-homoarginine and histidine partially inhibit TNAP. L-homoarginine and histidine may also cause the cell to compensate by increasing TNAP synthesis, as TNAP mRNA levels were approximately equal to or higher than control levels in all three MSC cell types cultured in either OM or AM (Fig. 4.2.5.1).

In the presence of levamisole, L-homoarginine blocked mineralisation in all cell types, with a variable effect on ALP activity. As levamisole or L-homoarginine alone had no discernible effect on ALP activity, it was expected that the combination of the two inhibitors would similarly have little effect on ALP activity. In line with expectations, the combination of levamisole and L-homoarginine resulted in only a slight increase in ALP activity in scADSCs

and pvADSCs, and unexpectedly, a decrease in ALP activity in bmMSCs, where levamisole and L-homoarginine separately had produced a slight increase in ALP activity. Levamisole and L-homoarginine cannot act simultaneously on TNAP, as a common amino acid residue binds them in the binding site pocket, with His-434 and Tyr-371 binding levamisole, while the residues at position 108 as well as Tyr-371 are necessary for L-homoarginine binding, and yet the effects of the two inhibitors have been found to be additive (Kozlenkov *et al.*, 2004). It is also known that levamisole is a more potent inhibitor than L-homoarginine, by nearly 100 times, and the higher potency of levamisole has been confirmed by enzyme assay data (Fig. 4.2.6.1) (Kozlenkov *et al.*, 2004). Further work will be needed to confirm this result; however, this data may suggest depot-specific differences between MSCs derived from bone marrow and adipose tissue with regards to TNAP isozyme expression.

L-homoarginine was able to significantly inhibit lipid accumulation across all cell types undergoing adipogenic induction, but surprisingly, decreased ALP activity compared to AM control in bmMSCs and increased ALP activity compared to AM control in scADSCs and pvADSCs. The combination of L-homoarginine with levamisole resulted in decreased lipid accumulation similar to that observed with L-homoarginine alone; along with increased ALP activity in scADSCs and pvADSCs, however no effect on ALP activity was observed in bmMSCs. This data may indicate that TNAP activity is linked to lipid accumulation during adipogenesis, and that differences exist between the isoform of TNAP present in bmMSCs and ADSCs, which leads to different effects of L-homoarginine and other inhibitors of TNAP in these cells.

The combination of L-homoarginine with histidine showed the greatest reduction in lipid accumulation of all inhibitors and their combinations, in all three cell types. Similar to the combination of L-homoarginine with levamisole, the combination of L-homoarginine with histidine resulted in an increase, which was not statistically significant in all cases, in ALP activity in scADSCs and pvADSCs, and no apparent effect on ALP activity in bmMSCs. In each cell type the increased ALP activity for the combinations with L-homoarginine was higher than for L-homoarginine alone, with the highest activity mainly observed in combination with histidine. During adipogenic induction, an additive effect was observed between L-homoarginine and either histidine or levamisole, and a decrease in lipid accumulation and an increase in ALP activity is observed. These observations confirm that L-homoarginine, levamisole and histidine have different effects to one another when applied to

live rat-derived MSCs, and these effects may be due to interactions of the inhibitors with TNAP, but may also be due to other currently unknown off-target effects.

A major difficulty in interpreting the data lay in the biological variation detected between experimental batches, most notably being the large variation observed in ALP activity in scADSCs during osteogenic induction. Heterogeneity of MSCs cultured *in vitro* has been discussed and is a well-known feature of these cells (Section 3.3) with several precursor cell populations possibly present in the initial cultures. Ho *et al*. observed that slight variations in culture conditions may preferentially support the growth of certain subsets of the culture population, and this may result in genetic instability of the cell culture or malignant transformation (Ho *et al.*, 2008). A study investigating the genomic stability of rat bmMSCs discovered a high degree of chromosome instability during *in vitro* culture in comparison to mouse and human MSCs, although the rat bmMSCs were still capable of differentiation into osteoblast, adipocyte and chondrocyte phenotypes (Foudah *et al.*, 2009). Therefore, factors such as heterogeneity, minor variations in cell culture conditions between experiments, and possible chromosomal abnormality may have contributed to the observed biological variation. Together with biological variation, and low repeat number of between n=3 and n=5 for each experiment makes it difficult to draw clear conclusions from the statistical analyses in all experiments. Thus, future work should include a higher number of repeats in order to firmly establish the current findings.

In addition to increased biological repeats, the effects of biological variation may be reduced by stricter selection criteria, which may involve the selection of surface markers in rat-derived MSCs which identify cells that will reliably differentiate towards an adipogenic or osteogenic phenotype *in vitro*, as the current method of plastic adherence, while commonly used to select for MSC populations, is known to possibly result in heterogeneous cell populations (Bianco *et al.*, 2008; Strioga *et al.*, 2012).

Bone marrow-derived MSCs cultured in OM had fully mineralised by day 10. In bmMSC samples where mineralisation had occurred, deposited mineral was prone to detach or wash off the culture surface during media changes, or during staining and sample preparation for the ALP assay. Therefore, later time points experience variations that are difficult to control for. For this reason, multiple time points are necessary for a more accurate assessment of the effect of inhibitors on osteogenic differentiation, and day 7 may give a more accurate

assessment in bmMSC samples. Similar behaviour between scADSCs and pvADSCs was observed during osteogenic induction, but as discussed previously, together had a far more limited capacity for mineralisation than bmMSCs (Wu *et al.*, 2015).

The ALP activity of control undifferentiated pvADSCs was markedly higher than the ALP activity of osteogenic differentiated pvADSC samples. Peri-renal visceral ADSCs also displayed the lowest levels of ALP activity and low levels of mineralisation. Subcutaneous ADSCs displayed a slightly higher percentage area of mineralisation at day 21, ALP activity levels and TNAP mRNA expression compared to pvADSCs; however, both were still far less than the levels observed in bmMSCs. We therefore put forward that rat-derived pvADSCs and scADSCs are a less efficient model for *in vitro* osteogenesis in comparison to bmMSCs; however, the *in vivo* osteogenesis of scADSCs and pvADSCs compared to bmMSCs should be ideally investigated. This data also highlights the need to screen various depots for suitability if cells are going to be used for bone tissue engineering, due to existing depot specific differences.

Interestingly, while treatment with the various inhibitors and their combinations during both osteogenic or adipogenic induction resulted in similar effects across the three rat-derived MSCs with regards to either mineralisation or lipid accumulation percentage, differences were noted in mainly between the bmMSCs and the ADSCs (scADSCs and pvADSCs) regarding ALP activity. Noticeably, under adipogenic conditions, histidine and L-homoarginine, alone or in combination with one another and levamisole, produced an opposite response in either bmMSCs or ADSCs. This may indicate that the TNAP isozyme present in bmMSCs and ADSCs undergoing adipogenic induction may be different depending on the tissue depot from where the cells were isolated. The existence of differences between TNAP isoforms from bone, liver and kidney is well established, and various TNAP bone isoforms have also been discovered (Halling Linder *et al.*, 2009). Therefore, it may be possible that differences observed between cell types under the same conditions are due to the expression of different TNAP isoforms intrinsic to these cell types. ALP activity was found to vary between MSCs from the same depot, in the presence of the same inhibitors, depending on whether the cells were undergoing adipogenic or osteogenic induction, which may also indicate that different isoforms of TNAP may be expressed in MSCs from the same source, depending on whether the cells are induced to differentiate towards either an osteogenic or adipogenic phenotype. This conclusion may be verified by

investigating whether TNAP enzymes isolated from cells from a single MSC source, when undergoing adipogenic and osteogenic differentiation, had differing glycosylation patterns which would indicate the existence of different TNAP isoforms.

CHAPTER 5

Sub-cellular localisation and characterisation of tissue-nonspecific alkaline phosphatase (TNAP) transcript and glycosylation differences, as well as knockdown of TNAP in rat-derived mesenchymal stromal cells (MSCs) undergoing differentiation.

5.1 Introduction

That alkaline phosphatase (ALP) is present in adipose tissue and adipocyte precursors from various species, including human and rat, has been known for many years (Wallach and Ko, 1964; Okochi *et al.*, 1987; Bianco *et al.*, 1988). The ALP expressed in adipose tissue has been identified as TNAP, and while the role of TNAP in mineralisation and its presence in osteoblasts and osteoblast progenitors is well known, the function of TNAP in adipocytes and adipocyte progenitors is less well established (Ali *et al.*, 2005; Ali *et al.*, 2013). Much work remains to elucidate the function of TNAP in adipocytes, as well as other cell types where TNAP is expressed.

In osteoblasts, TNAP is known to be an ectoenzyme, attached to the outer layer of the plasma membrane of cells or vesicles by GPI anchors (Millán *et al.*, 2006). The presence of ALP has been detected in rat adipose tissue as early as 1964 (Wallach and Ko, 1964) as well as in adipocytes found in human bone marrow (Bianco *et al.*, 1988). Kodama *et al.* identified ALP activity in mouse bone marrow-derived fibroblasts, converted to adipocytes *in vitro* (Kodama *et al.*, 1983). A later study using the murine preadipocyte cell line, 3T3-L1, found that ALP activity was exclusively present on the lipid droplet membrane, while no ALP activity was detected on the plasma membrane after these cells were induced towards adipogenesis. The same study proposed that ALP on the lipid droplet membrane would be involved with either altering the phosphorylation state of other proteins and enzymes anchored to the lipid droplet membrane, or in the hydrolysis of ATP, as TNAP is known to have adenosine triphosphatase (ATPase) activity (Ali *et al.*, 2005). Ali *et al*. identified the ALP in differentiated 3T3-L1 cells as TNAP, as the ALP activity in these cells was only inhibited in the presence of the TNAP-specific inhibitors levamisole and histidine, and not the tissue-specific ALP inhibitor, Phe-Gly-Gly (Ali *et al.*, 2005). We hypothesized that the subcellular location of TNAP present in primary rat-derived MSCs differentiated towards adipocytic phenotype *in vitro* would also be on the surface of the lipid droplet membrane, similar to that found in 3T3-L1 cells (Ali *et al.*, 2005; Ali *et al.*, 2013).

Several isoforms of TNAP exist, and are preferentially expressed in various tissues such as bone, liver and kidney. These isoforms consist of the same primary amino acid sequence, but differ to one another based on various posttranslational modifications, in the form of N- and O-linked glycosylations (Nosjean *et al.*, 1997). Differences in glycosylation pattern are

thought to be the main factor contributing to the differences that exist between the various TNAP isoforms (Nosjean *et al.*, 1997; Millán *et al.*, 2006). Initially, it was thought there was one TNAP isoform specific to each tissue, however it appears that further variations exist within each tissue-specific TNAP isoform, as four different bone-specific TNAP isoforms have been discovered in humans (Halling Linder *et al.*, 2009) along with several liver-specific TNAP isoforms in rat (Dziedziejko *et al.*, 2005). The glycosylation pattern of the TNAP present in adipocytes is to the best of our knowledge, currently unknown, and an understanding of this may help to further establish the function of TNAP in adipose tissue.

The TNAP gene in rats, designated *Alp1*, is found on a single locus, and consists of 13 exons – 11 protein-coding exons and 2 non-coding exons in the 5'-untranslated region (UTR), designated as 1a or 1b, with each having different promoter regions (Toh *et al.*, 1989a). The mature TNAP mRNA therefore consists of 11 coding exons, and either exon 1a or 1b, which are incorporated into the mRNA sequence via alternative transcription initiation (Toh *et al.*, 1989b; Brun-Heath *et al.*, 2011). In bone, transcription is preferably initiated with the 1a exon, while in liver and kidney the 1b exon is preferred. In rat liver, it has been found that both bone and liver TNAP mRNA transcripts are present, with the bone transcript predominating (Brun-Heath *et al.*, 2011). It is currently unclear as to which TNAP mRNA transcript is preferentially expressed in rat-derived MSCs from bone-marrow (bmMSCs,), subcutaneous adipose (scADSCs) and peri-renal visceral adipose (pvADSCs) depots, when differentiated towards an adipogenic phenotype. Brun-Heath *et al*. were able to amplify both rat TNAP mRNA transcripts by designing forward PCR primers specific for either the 1A or 1B exon, which allowed them to determine which exon was preferentially expressed in rat brain tissue (Brun-Heath *et al.*, 2011). We have used the same primers designed by Brun-Heath *et al*. to amplify a reverse transcribed TNAP cDNA sequence from rat-derived bmMSCs, scADSCs and pvADSCs, which were differentiated towards either an osteogenic or adipogenic phenotype. Conventional PCR amplification of the TNAP cDNA using the primers specific for either bone or liver-type TNAP transcripts was performed in order to determine the leader exon preferentially expressed in these cells, as well as to determine whether the leader exon usage changes when cells are differentiated between an osteogenic or adipogenic phenotype.

RNA interference (RNAi) is a process used naturally by cells to regulate the expression of targeted mRNA molecules, and is used as a cellular mechanism to protect the genome from

aberrant or harmful RNA resulting from viral infections or transposons. It may also be a mechanism for regulating post-transcriptional gene expression. RNAi involves the cleavage of double-stranded RNA (dsRNA) by the enzyme Dicer, into dsRNA of approximately 21 to 23 nucleotides in length, with 3′ overhangs of 1 to 2 nucleotides, which are termed short interfering RNA (siRNA). Double-stranded RNA may be exogenous, in the form of viral RNA or introduced into the cell in the laboratory, or it may be endogenous, in the form of microRNA (miRNA) or certain types of transposable elements. Double-stranded RNA produced endogenously is formed from stem-loop structures which are further processed into dsRNA by Dicer. The double-stranded siRNA molecules bind to Argonaute proteins, where the dsRNA is denatured into single-strands, with the antisense strand, also known as the guide strand, remaining bound to the Argonaute protein, now known as the RNA-induced silencing complex (RISC), while the remaining sense strand, also known as the passenger strand, is degraded by the RISC complex. This complex is then targeted to a region on the native mRNA molecule complementary to the antisense RNA strand in the RISC. Once the RISC binds to the complementary region of the mRNA target, the enzyme Argonaute, which is part of the RISC, degrades the mRNA, thus preventing translation of the mRNA and effectively silencing gene expression. If the guide strand incorporated into the RISC is not completely complementary to the target mRNA molecule to which it is bound, the RISC cannot degrade the target mRNA and translation is only repressed instead of silenced (Tuschl *et al.*, 1999; Elbashir *et al.*, 2001; Nakanishi, 2016).

RNAi has been utilised as a way to study gene function; by delivering exogenous double-stranded siRNA molecules specific to a target gene within a cell, the target gene is silenced by the endogenous RNAi silencing system and the effects of gene knockdown on the cell can be analysed (Moore *et al.*, 2010). Cells may be transfected with siRNA molecules, using either reagent- or instrument-based methods, however many cell types are resistant to transfection, or have low transfection efficiency (Luft and Ketteler, 2015). siRNA transfected into the cell cytoplasm has only transient effects, and is therefore often only useful for short term, *in vitro* studies (Moore *et al.*, 2010).

Another technique which makes use of the RNAi mechanism involves the introduction into the cell of short hairpin RNAs (shRNAs), and usually mediated by infection with viral or plasmid vectors. In order to produce the shRNA, a DNA sequence is inserted into the vector consisting of two complementary strands of DNA of approximately 20 nucleotides in length,

connected to one another by a short stretch of four to eleven nucleotides, which when expressed will produce the shRNA molecule (Moore *et al.*, 2010). The vector construct is delivered into the cell either by transfection, in the case of plasmids, or by infection of the cell with the viral vectors containing the construct. The viral-mediated transfection is also known as transduction. Once inside the cell, the construct DNA is stably integrated into the host cell genome, leading to transcription of the encoded shRNA molecule. Once transcribed, the shRNA sequence forms the dsRNA hairpin structure, due to the inbuilt complementarity of the sequence. The double-stranded shRNA is recognized by the enzyme Dicer, which cleaves off the interconnecting nucleotides to form a siRNA molecule. The siRNA produced from the cleavage of the shRNA is then bound to an Argonaute protein, leading to formation of the RISC complex, and to the degradation of the target mRNA (Moore *et al.*, 2010). This allows for a stable long-term knockdown of the target mRNA, as opposed to short-term knockdown which results from transfection of the cell directly with siRNA molecules.

As TNAP in adipocytes is thought to play a role in lipid accumulation, reducing the levels of TNAP expression during adipogenic induction by RNAi should produce a concomitant reduction in lipid droplet formation. Transduction of MSCs with shRNA targeting TNAP mRNA should allow for a stable knock-down of TNAP expression, and test the hypothesis that TNAP is involved in lipid accumulation.

The aim of this chapter was to further characterise the expression of alkaline phosphatase (ALP) in rat-derived MSCs, in particular when these cells were differentiated towards an adipogenic phenotype. The sub-cellular localisation of TNAP in bmMSCs, scADSCs and pvADSCs differentiated towards an adipogenic phenotype was investigated using confocal microscopy and the endogenous phosphate substrate ELF-97, in order to visualise ALP activity within the cell. PCR amplification was used to determine whether the bone- or liver-specific TNAP mRNA transcript is present in bmMSCs, scADSCs and pvADSCs when differentiated towards either an osteogenic or adipogenic phenotype. Differences in glycosylation between the ALP molecules from undifferentiated bmMSCs or those differentiated towards either an osteogenic or adipogenic phenotype was investigated and compared to the ALP from scADSCs differentiated towards an adipogenic phenotype, by means of agarose electrophoresis in the presence of wheat germ lectin (WGL), which binds selectively to sialic acid residues. As the bone-specific TNAP isoform is known to have the highest degree of sialation of the various ALP isozymes, WGL is able to bind preferentially

to this isozyme, allowing it to be identified. Finally, we attempted to knock-down TNAP expression by transduction of scADSCs with shRNA molecules targeting TNAP mRNA, and assessed the levels of lipid accumulation and TNAP mRNA during adipogenic differentiation of these cells.

5.2 Results

5.2.1 Subcellular localisation of ALP activity in rat-derived MSCs undergoing adipogenesis.

It was hypothesized that the TNAP present in adipocytes is localised on the lipid droplet membrane, where it may play a role in lipid transport. A suitable anti-TNAP antibody to detect the presence of TNAP within adipogenically induced cells is not currently commercially available; therefore ALP activity in the cell was measured using a fluorescent substrate for ALP. The subcellular localisation of ALP in bmMSCs, scADSCs and pvADSCs was investigated using the endogenous phosphatase substrate, ELF-97, where cells were also immunolabelled for Perilipin A, a protein associated with the lipid droplet membrane. Labelling with Perilipin A allows the lipid droplet membrane to be easily identified, and provides a frame of reference when looking at the location of ALP activity. According to the hypothesis that TNAP within lipid-containing cells is localised to the lipid droplet membrane, as seen in 3T3-L1 cells (Ali *et al.*, 2005), the fluorescent signal resulting from the cleavage of the ELF-97 substrate by ALP enzyme activity was expected to localise in the same area as perilipin A.

Cells were fixed and labelled with the perilipin A primary antibody, and the signal (red) detected using Alexa Fluor 594 conjugated goat anti-rabbit secondary antibody, as previously described (Section 2.2.13.1). Perilipin A was positively detected in bmMSCs, scADSCs and pvADSCs undergoing adipogenic induction, where perilipin A staining corresponded with the outline of lipid droplets visible in phase contrast images. Perilipin A appeared to be more strongly detected in scADSCs and pvADSCs in comparison to bmMSCs (Fig. 5.2.2.1, 5.2.1.2 and 5.2.1.3). Cells that contained lipid droplets, or were in the process of forming lipid droplets, were observed to have the most positive perilipin A signal, with cells that did not have any visible lipid droplets having little to no perilipin A signal. Primary antibody controls, which were stained with only the secondary antibody and ELF-97, yielded faint nonspecific background staining (Fig. 5.2.1.4 K – O).

The ELF-97 fluorescent signal appeared as small bright yellow/green dots, indicating the position of ALP activity. ELF-97 signal was observed in bmMSCs, scADSCs and pvADSCs, but most abundantly in bmMSCs. ELF-97 signal was observed most strongly in association with perilipin A staining, where it appeared to be associated with the surface of the lipid droplet in all cell types. In bmMSCs, ELF-97 signal was also observed within the cell cytoplasm, although the signal here was less bright than the ELF-97 signal associated with lipid droplets. Interestingly, ELF-97 signal was not uniformly present across all lipid droplet-containing cells, but appeared to be more abundant on some cells and on some lipid droplets compared to others, appearing as distinct, bright green points in the location of the lipid droplet membrane. The outer cell plasma membrane was not stained for visualisation; therefore the presence of ELF-97 signal at this region could not be defined, however, in scADSCs and pvADSCs, ELF-97 signal was not observed apart from surrounding lipid droplets.

As a negative control for ELF-97, the TNAP-specific inhibitor, levamisole, was included during the incubation with the ELF-97 substrate, resulting in a near total reduction in ELF-97 signal within this sample (Fig. 5.2.1.4 A – E). An additional negative control, from which ELF-97 substrate was excluded, resulted in no ELF-97 signal detected, indicating that the positive signal observed was not the result of background staining (Fig. 5.2.1.4 F – J)

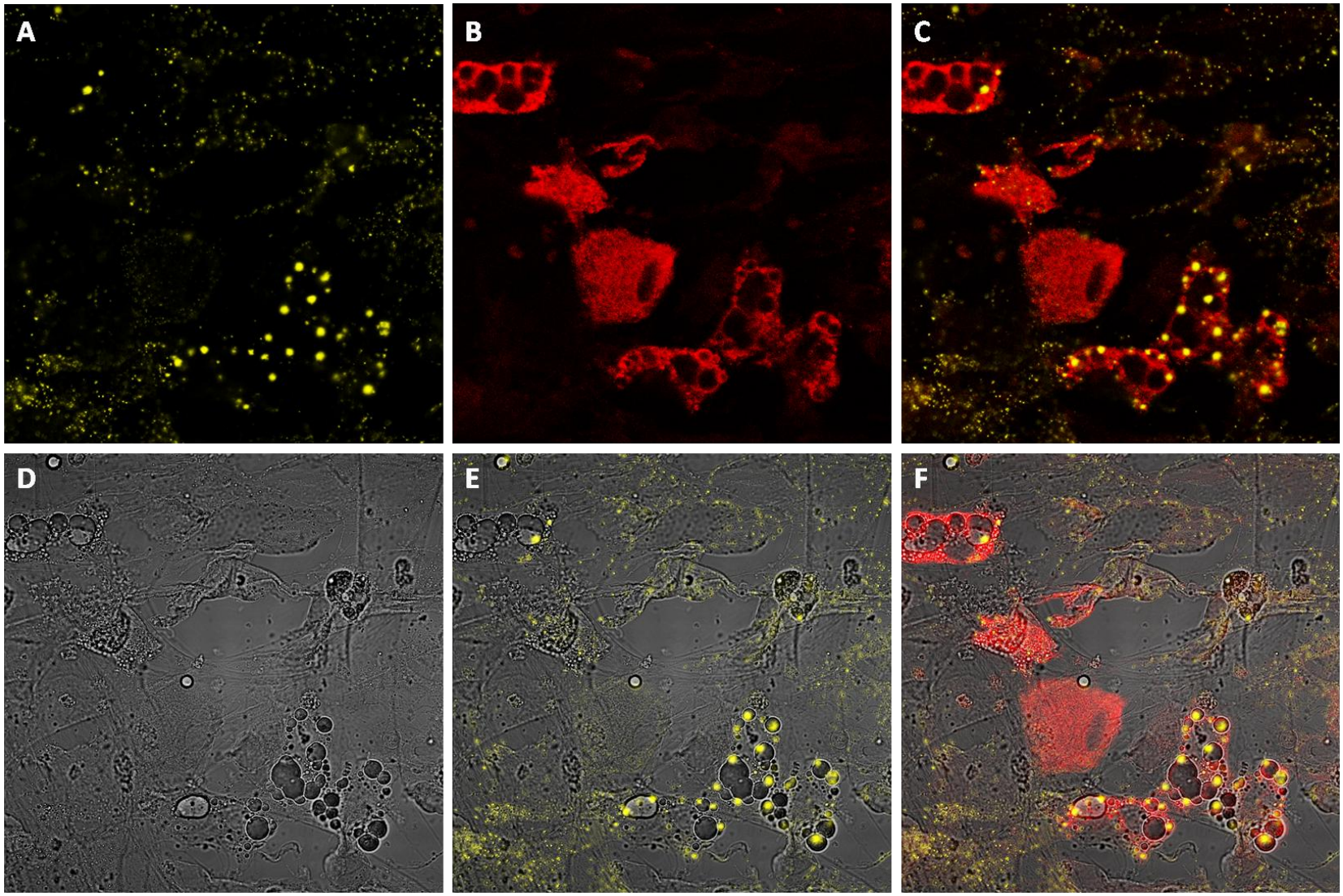

Figure 5.2.1.1: Confocal microscopy images of bmMSCs after 14 days of adipogenic induction, showing lipid droplets and staining with ELF-97 and perilipin ASingle and merged images for each channel are shown. Single channels for ELF-97 (yellow) (A), and Perilipin A (red) (B), and phase contrast (D) are shown, while panel (C) is a merged image of (A) and (B), (E) is merged channel D and A and panel F is merged image of panels A, B and D. Magnification x60.

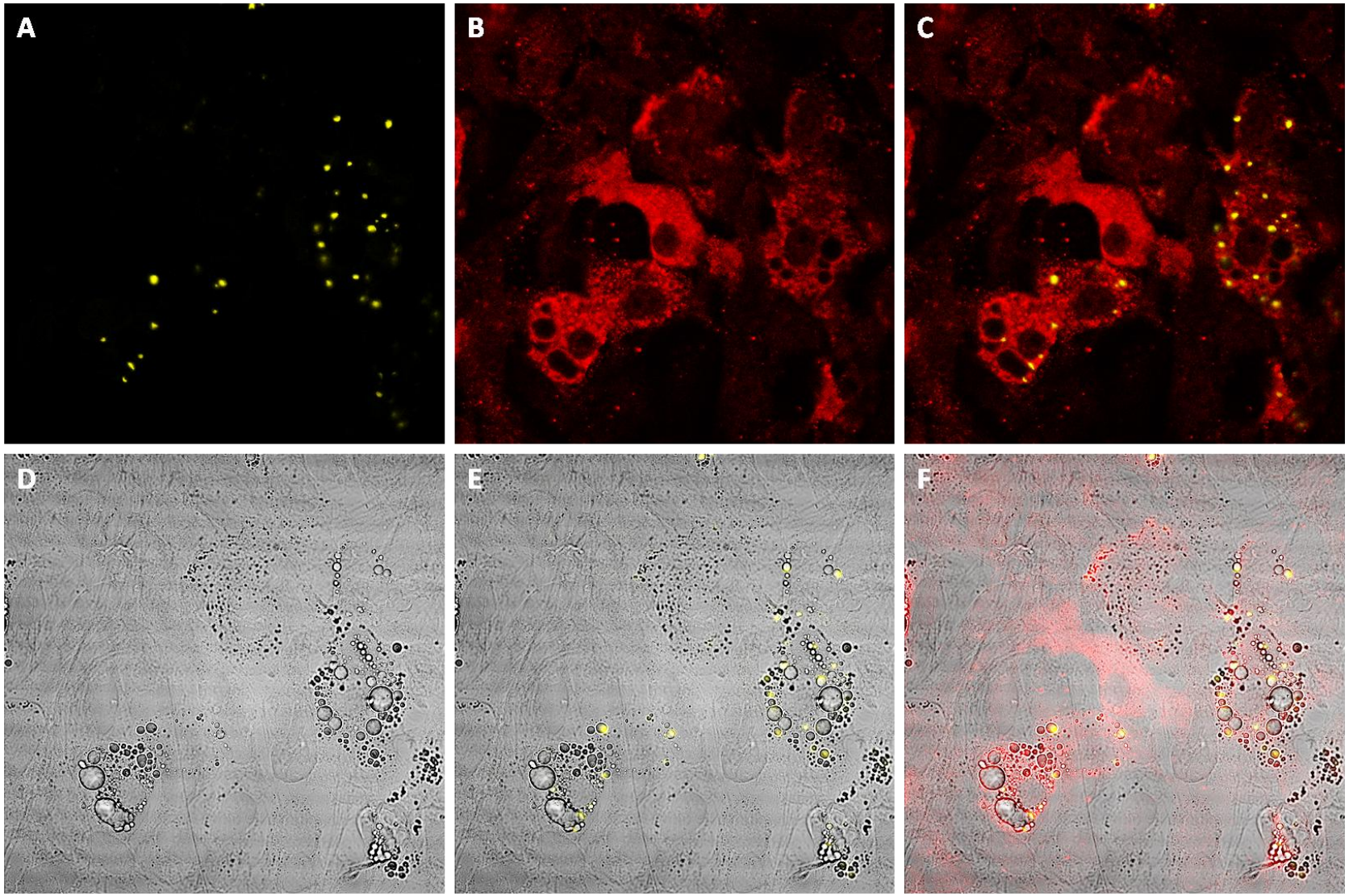

Figure 5.2.1.2: Confocal microscopy images of scADSCs after 5 days of adipogenic induction, showing lipid droplets and staining with ELF-97 and perilipin A. Single and merged images for each channel are shown. Single channels for ELF-97 (yellow) (A), and Perilipin A (red) (B), and phase contrast (D) are shown, while panel (C) is a merged image of (A) and (B), (E) is merged channel D and A and panel F is merged image of panels A, B and D. Magnification x60.

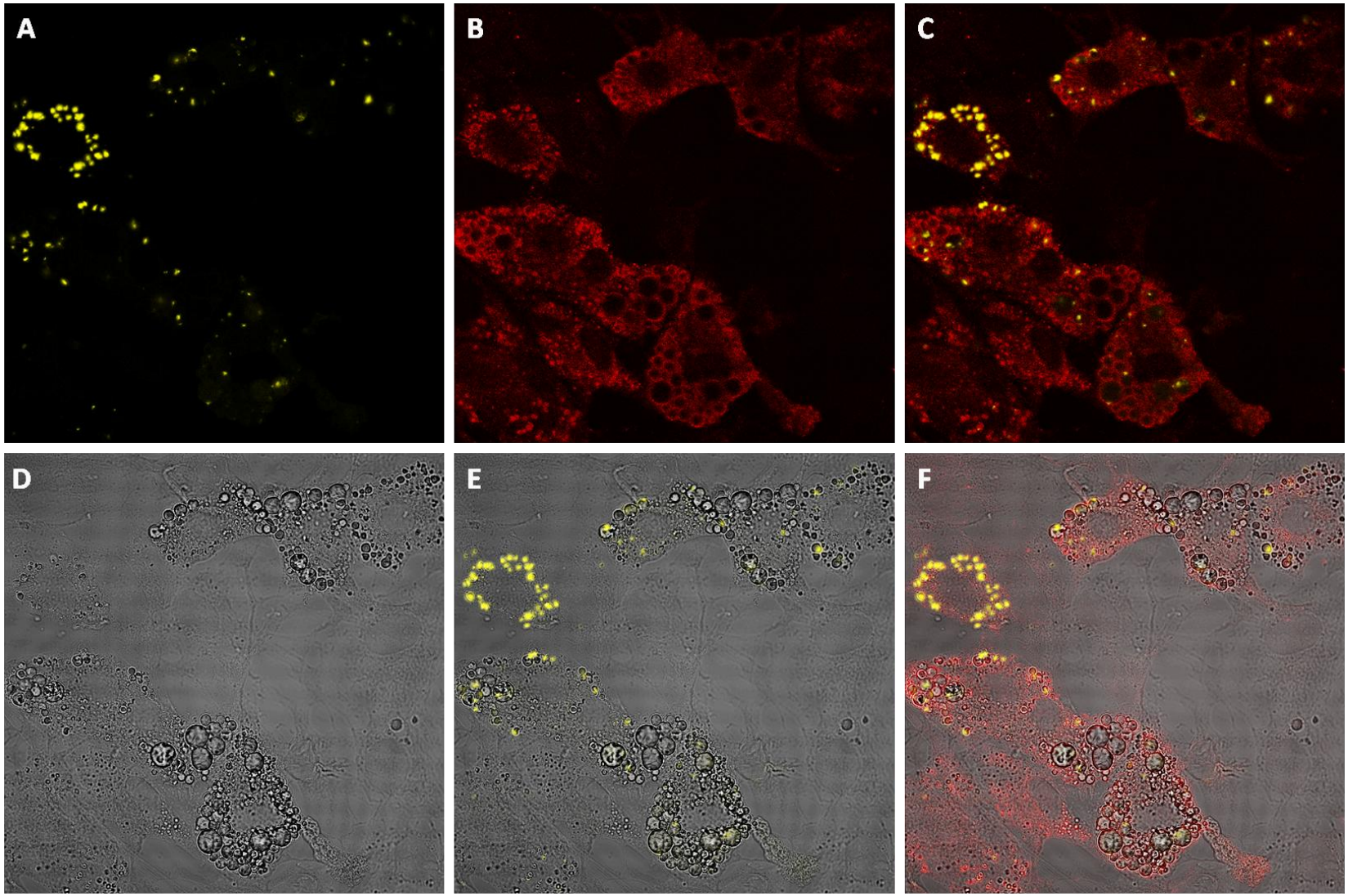

Figure 5.2.1.3: Confocal microscopy images of pvADSCs after 5 days of adipogenic induction, showing lipid droplets and staining with ELF-97 and perilipin A. Single and merged images for each channel are shown. Single channels for ELF-97 (yellow) (A), and Perilipin A (red) (B), and phase contrast (D) are shown, while panel (C) is a merged image of (A) and (B), (E) is merged channel D and A and panel F is merged image of panels A, B and D. Magnification x60.

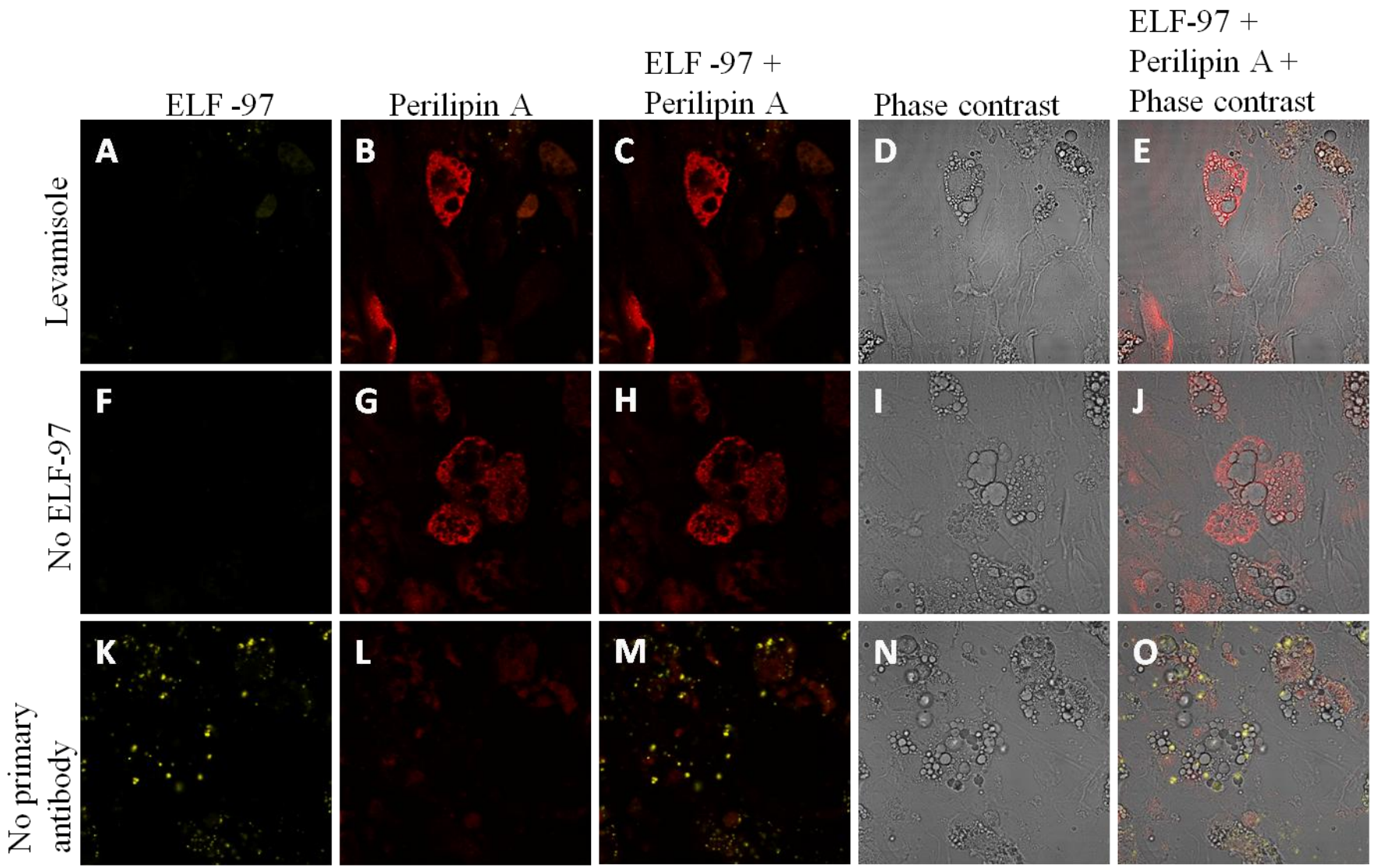

Figure 5.2.1.4: Control samples for ELF-97 and perilipin A staining. Panel A – E, ELF-97+ and perilipin A primary and secondary antibody staining in the presence of the TNAP inhibitor, levamisole; F – J, perilipin A staining, and ELF-97- control; K – O, ELF-97+ and primary antibody control. Magnification x60.

5.2.2 Identification of the TNAP mRNA transcripts expressed in bmMSC, scADSC and pvADSCs

Either the 1A or 1B untranslated leader exons are preferred in TNAP mRNA transcripts from cells of different tissues. TNAP mRNA molecules containing exon 1A are preferentially transcribed in osteoblasts, as well as in neural tissue, and is designated as bone-type TNAP mRNA, while the 1B exon has been found in TNAP mRNA transcripts from liver tissue, and is designated as liver-type TNAP mRNA (Brun-Heath *et al.*, 2011). To the best of our knowledge, no information is available for which exon, 1A or 1B, is preferably incorporated into the TNAP mRNA from rat-derived MSCs when differentiated into an adipogenic phenotype. Using PCR primer sets specific for either bone- or liver-type TNAP mRNA, we attempted to determine the preferred TNAP mRNA type using cDNA isolated from rat-derived MSCs, which had been treated with OM or AM.

PCR primers were synthesized using previously published sequences for forward primers specific for regions on either the bone- or liver-specific non-coding exons, as well as a single reverse primer corresponding to a coding region on TNAP mRNA, which would be common to all TNAP mRNA sequences (Brun-Heath *et al.*, 2011). These primer sequences were used as query sequences in a database search, and two separate entries for rat TNAP mRNA sequences were identified, with accession numbers, NM_013059.1 and XM_006239136.2, which were identified as the bone and liver mRNA isoforms, respectively. A sequence alignment was constructed using the two identified TNAP mRNA sequences (Addendum C, Fig. C1) in order to determine the non-coding exon/coding exon boundary, as well as to confirm that the forward primers did indeed correspond to regions which were not common to both bone and liver mRNA transcripts.

The expected lengths of the bone and liver amplicons were 1595 bp and 1607 bp, respectively. Amplification of TNAP from bmMSCs using the bone isoform-specific primers yielded a band at approximately 1600 bp, which corresponded to the expected length of the product, in adipogenic samples from three separate animals (n=3) (Fig. 5.2.2.1, lane 5 – 7), while a band corresponding to the expected size was detected in only one osteogenic sample (Fig. 5.2.2.1, lane 2 – 4). Rat liver RNA was isolated and reverse transcribed into cDNA for use as a positive control for the detection of the liver transcript in mRNA isolated from rat-derived MSCs. As predicted, the amplification of rat liver cDNA with the bone type-specific

primer set did not produce any bands (Fig. 5.2.2.1, lane 8). Multiple non-specific bands were observed in all test samples, which could not be resolved by adjusting PCR conditions (Addendum C, Fig C2). A control reaction using the bmMSC OM sample 1 as template, which came up as positive for TNAP when used as the template in the presence of bone forward and reverse primers in lane 2, along with only the forward primer resulted in the detection of several bands (Fig. 5.2.2.1, lane 9), indicating that the forward primer was able to act as a forward and reverse primer, allowing for the formation of nonspecific products, whereas the reverse primer alone did not have this effect (Fig. 5.2.2.1, lane 10). Bone marrow-derived MSC OM sample 1 was used as a positive control for subsequent PCR amplifications using the bone-type primer set with either scADSC or pvADSC samples, because although nonspecific bands were present in this sample, a band at the predicted size for the bone-type transcript was present.

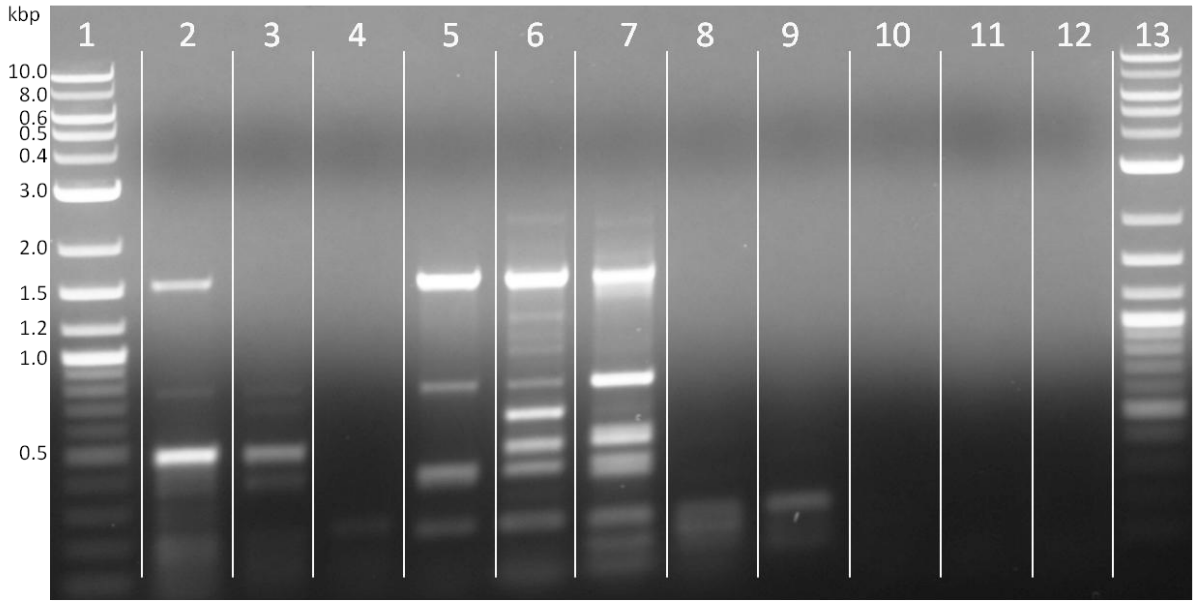

Figure 5.2.2.1: PCR amplification of bone-type TNAP cDNA in bmMSCs differentiated towards an (OM) osteogenic or adipogenic (AM) phenotype. Lane 1 and 13, molecular size marker (NEB, 1kb DNA ladder); lanes 2 – 4, bmMSC OM samples 1 – 3; lanes 5 – 7, bmMSC AM samples 1 – 3; lane 8, rat liver cDNA; lane 9, bmMSC OM sample 1 with forward primer only; lane 10, bmMSC OM sample 1 with reverse primer only; lane 11, no cDNA control; lane 12, no cDNA control with forward primer only.

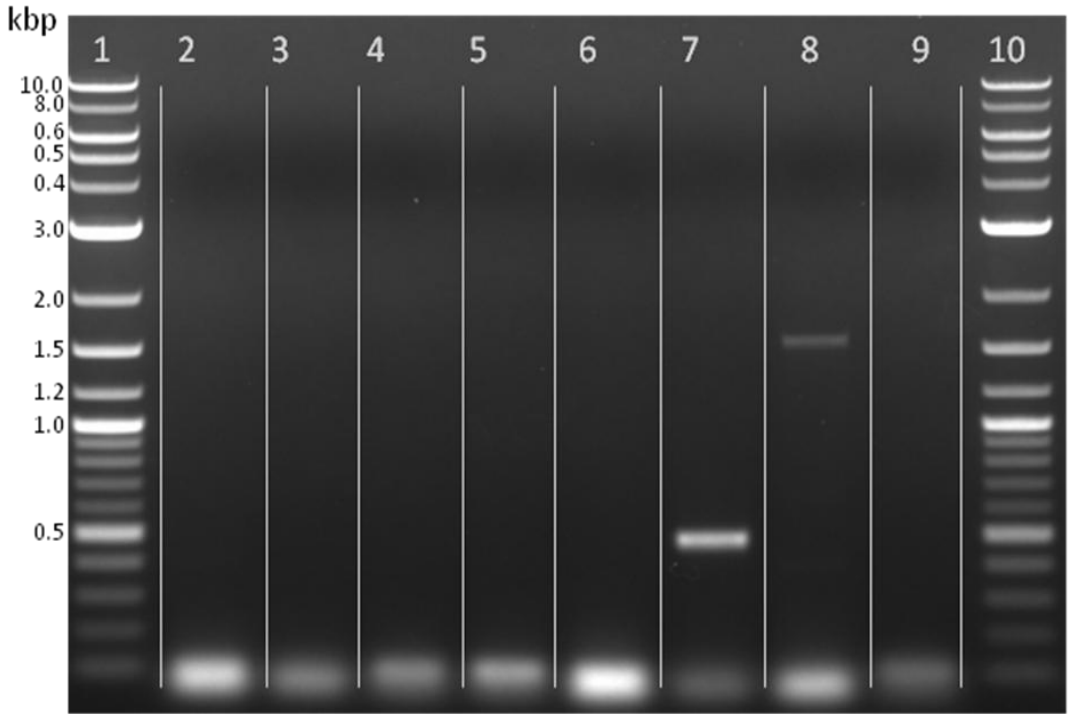

Figure 5.2.2.2: Amplification of the liver-type TNAP cDNA in bmMSCs differentiated towards either an osteogenic (OM) or adipogenic (AM) phenotype. Lanes 1 and 10, molecular size marker (NEB, 1kb DNA ladder); lanes 2 – 4, bmMSC OM samples 1 – 3; lanes 5 – 7, bmMSC AM samples 1 – 3; lane 8, rat liver cDNA; lane 9, no cDNA control.

Neither adipogenic nor osteogenic bmMSC samples produced any bands when template was amplified using the TNAP liver isoform-specific PCR primer set. A single non-specific band was observed in adipogenic sample 3, while no other bands were detected in any other test samples (Fig.5.2.2.2). A single band of the expected size was observed in the rat liver cDNA sample, which served as a positive control (Fig. 5.2.2.2, lane 8).

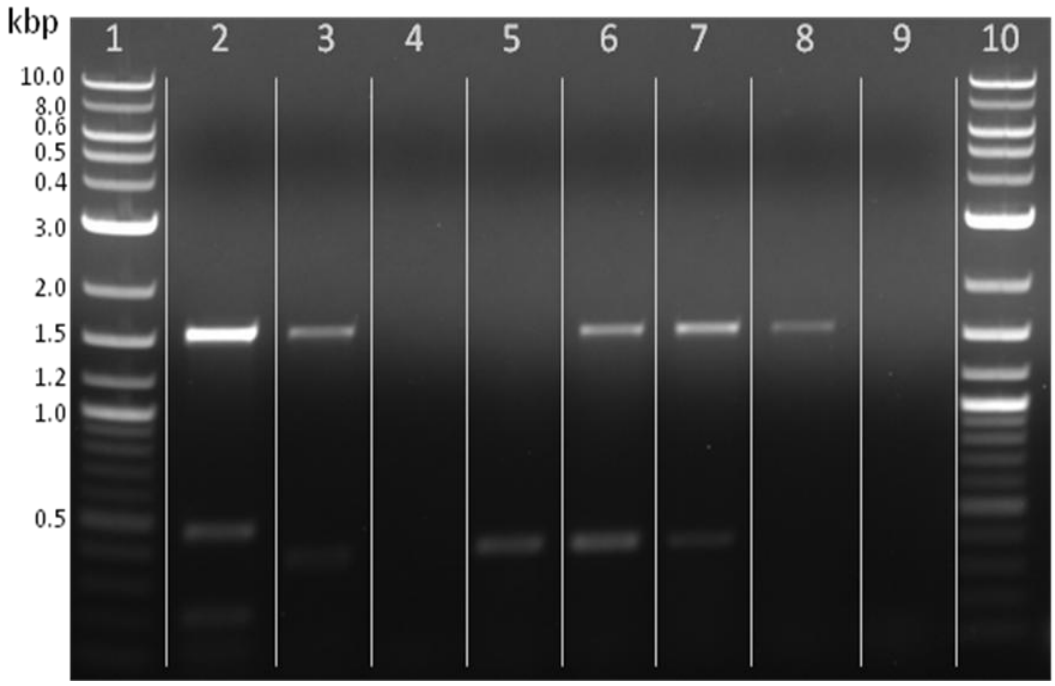

Figure 5.2.2.3: Amplification of bone-type TNAP cDNA in scADSCs differentiated towards either an osteogenic (OM) or adipogenic (AM) phenotype. Lanes 1 and 10, molecular weight marker (NEB, 1kb DNA ladder); lane 2; bmMSC OM sample 1; lane 3 – 5, scADSC OM samples 1 – 3; lanes 6 – 8, scADSC AM samples 1 – 3; lane 9, no cDNA control.

The amplification of the bone-type transcript of TNAP was performed in scADSCs differentiated towards either an osteogenic or adipogenic phenotype. Similar to bmMSCs, a band at the expected size was amplified in all three adipogenic samples (Fig. 5.2.2.3, lane 6 – 8) and only one osteogenic sample (Fig. 5.2.2.3, lane 3 – 5). Nonspecific bands were also detected with this bone isoform primer set, however these bands were fewer in comparison to those observed in the bmMSC samples.

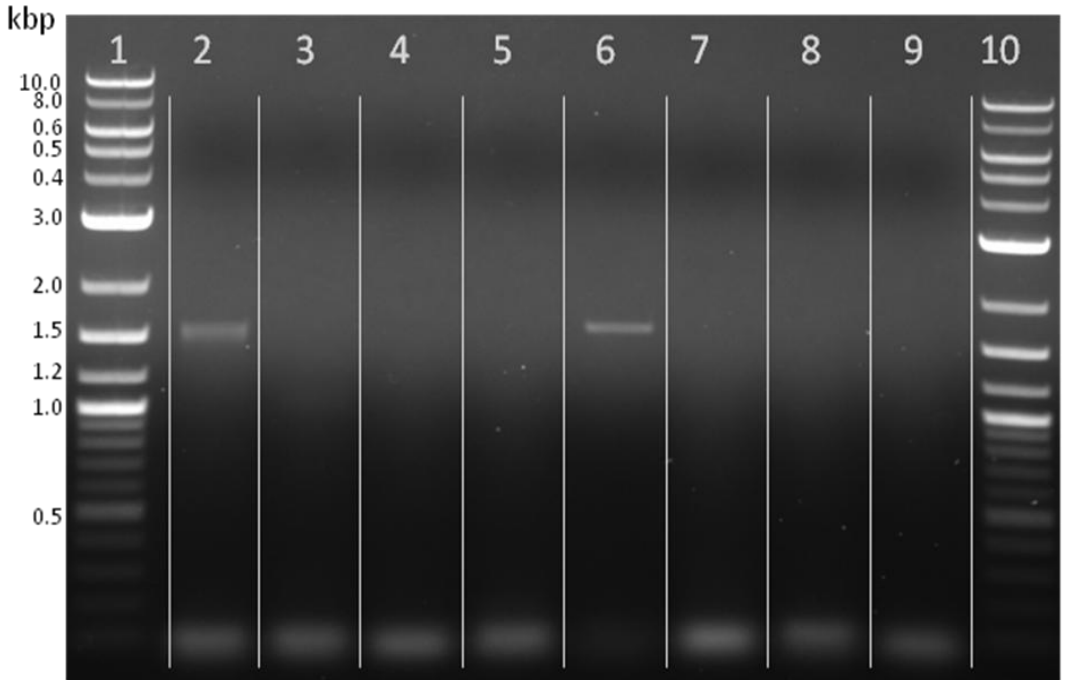

Figure 5.2.2.4 Amplification of the liver-type TNAP cDNA in scADSCs differentiated towards either an osteogenic (OM) or adipogenic (AM) phenotype. Lanes 1 and 10, molecular weight marker (NEB, 1kb DNA ladder); lane 2, rat liver cDNA; lane 3 – 5, scADSC OM; lanes 6 – 8, scADSC AM; lane 9, no cDNA control.

The liver isoform primer set was not able to amplify any bands in the scADSC samples differentiated into an osteogenic phenotype, however a single band of the expected product size was observed in scADSC adipogenic sample 1 (Fig. 5.2.2.4, lane 6), which may have been due to contamination as it was not reproducible in subsequent PCR reactions.

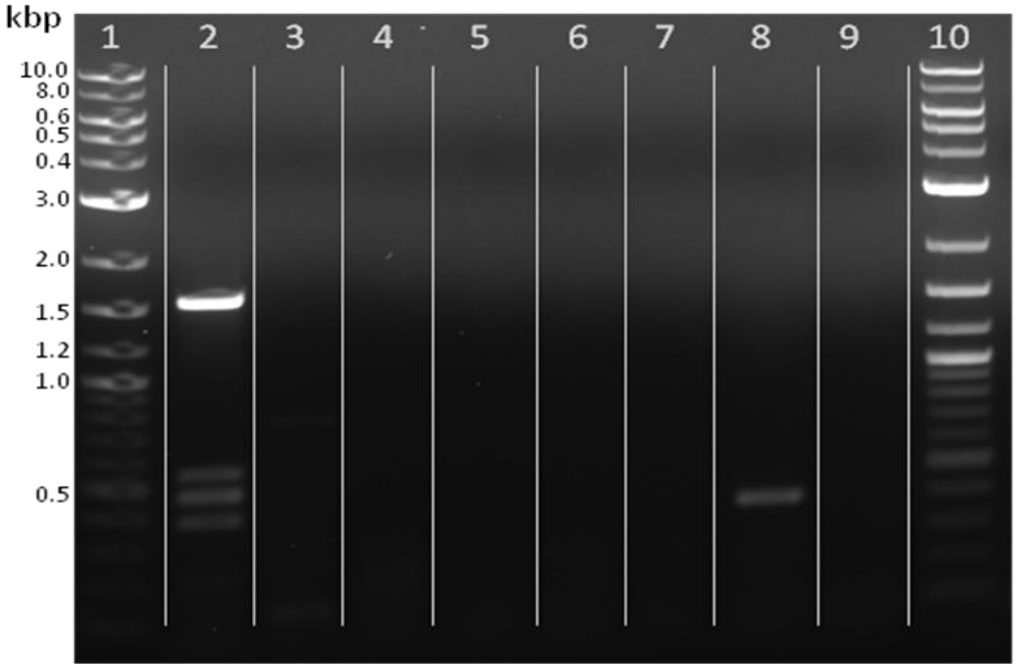

Figure 5.2.2.5: Amplification of the bone-type TNAP cDNA in pvADSCs differentiated towards either an osteogenic (OM) or adipogenic (AM) phenotype. Lanes 1 and 10, molecular weight marker (NEB, 1kb DNA ladder); lane 2; bmMSC OM; lane 3 – 5, pvADSC OM samples 1 – 3; lanes 6 – 8, pvADSC AM samples 1 – 3; lane 9, no cDNA control.

PCR amplification using both the bone and liver isoform PCR primer sets with pvADSC samples did not yield any bands at the expected sizes (Fig. 5.2.2.5 and Fig 5.2.2.6). Nonspecific faint bands were observed for pvADSC osteogenic sample 1 and adipogenic sample 2 with the bone isoform primer set (Fig. 5.2.2.5, lane 3 and 8).

Due to the multiple nonspecific bands observed with the bone-type primers, it was deemed necessary to confirm the identity of the band located at the expected size for the product amplified using this primer set. The band corresponding to the expected product size for bmMSC adipogenic sample 1 was excised, sequenced and used as a query sequence for a database search. The database search aligned the sequenced fragment to a region on to the published rat *Alp*l gene sequence NM_013059.1, confirming the identity of the product as TNAP (Addendum C, Fig. C3).

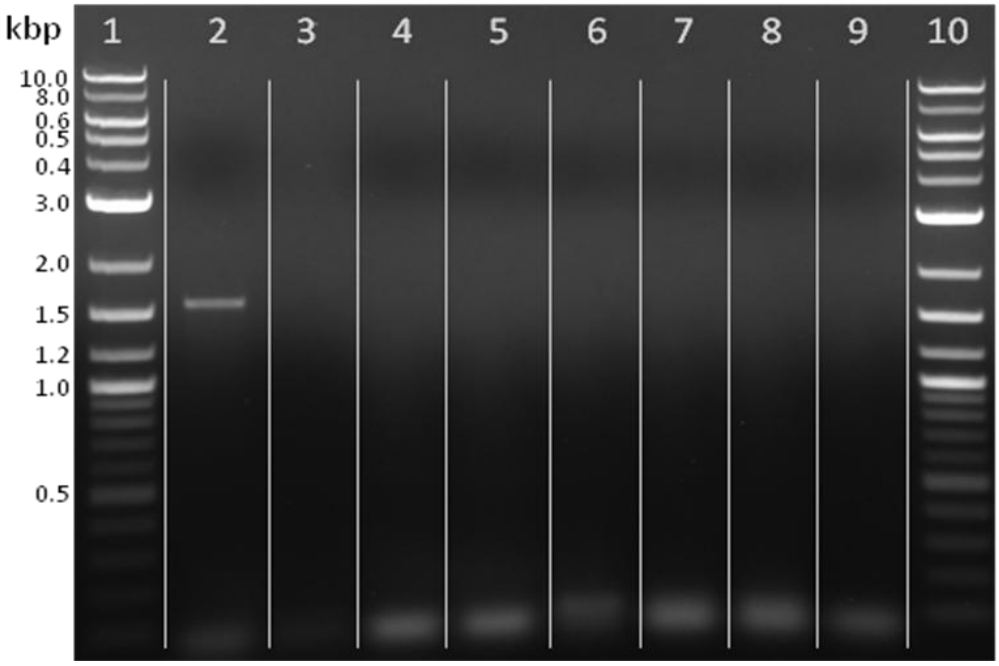

Figure 5.2.2.6: Amplification of the liver-type TNAP cDNA in pvADSCs differentiated towards either an osteogenic (OM) or adipogenic (AM) phenotype. Lanes 1 and 10, molecular weight marker (NEB, 1kb DNA ladder); lane 2, rat liver cDNA; lane 3 – 5, pvADSC OM samples 1 – 3; lanes 6 – 8, pvADSC AM samples 1 – 3; lane 9, no cDNA control.

5.2.3 Analysis of the glycosylation pattern of TNAP from bmMSCs and scADSCs differentiated towards an adipogenic or osteogenic phenotype.

Isoforms of TNAP, which all have the same primary amino acid sequence, are differentiated from one another by the amount and type of post-translational modifications, in the form of O- and N-linked glycosylations, which are present. The glycosylations present are responsible for the variation in the properties of the TNAP isoforms, such as heat stability and sensitivity to various inhibitors, as well as differences in electrophoretic migration and sensitivity to neuraminidase (Nosjean *et al.*, 1997; Dziedziejko *et al.*, 2005). The glycosylation pattern of the TNAP isoform present in rat-derived MSCs differentiated towards an adipogenic phenotype is unknown. Glycosylation differences between the various isozymes of ALP may be detected by agarose electrophoresis, as electrophoretic mobility is directly related to the molecular weight, which is altered by the amount of glycosylation of the enzyme. Once the enzymes have been subjected to electrophoresis, detection is achieved via the cleavage of a substrate by ALP enzyme activity to yield a coloured product in this zymogram.

Serum was collected from male Wistar rats (150 g) for use as a control, as serum ALP in rats is known to contain bone and intestinal ALP isoforms (Dziedziejko *et al.*, 2005). Total cell ALP was prepared from bmMSCs, scADSCs and pvADSCs that were induced towards either adipogenic or osteogenic differentiation, as well as from undifferentiated naïve cells, as previously described (Section 2.2.4.1). In order for adequate detection within the zymogram, an activity of 150 mU/ml for ALP was required, a level which could not be achieved using the available ALP extraction method for either scADSCs or pvADSCs, treated with either AM, OM or naïve undifferentiated cells, with the exception of scADSCs treated with AM. Crude total cell lysates of bmMSCs contained sufficient ALP activity for glycosylation analysis to be performed, and therefore only the crude total cell lysates were used for glycosylation analysis of bmMSC samples of AM or OM treated, as well as naïve undifferentiated cells. Normal human serum was used as a running control for electrophoresis.

Rat serum ALP was separated into bands which were identified as either bone or intestinal ALP, as well as a third band which may be the slow migratory (SM) band identified by Dziedziejko *et al*. (Fig. 5.2.3.1, A). In agreement with earlier reports, the bone ALP band appeared diffuse, while the intestinal ALP band was the most dominant band observed (Dziedziejko *et al.*, 2005). The addition of wheat germ lectin (WGL) to the sample resulted in the precipitation of the bone ALP isoform at the anode, while the intestinal ALP isoform was not affected. Precipitation of the bone ALP isoform, but not the intestinal ALP isoform, with WGL has been previously reported (Dziedziejko *et al.*, 2005). Human serum was used as a control for the reaction, and showed a similar precipitation of the bone isoform in the presence of WGL, however the banding pattern between human and rat differs markedly, as previously found (Dziedziejko *et al.*, 2005).

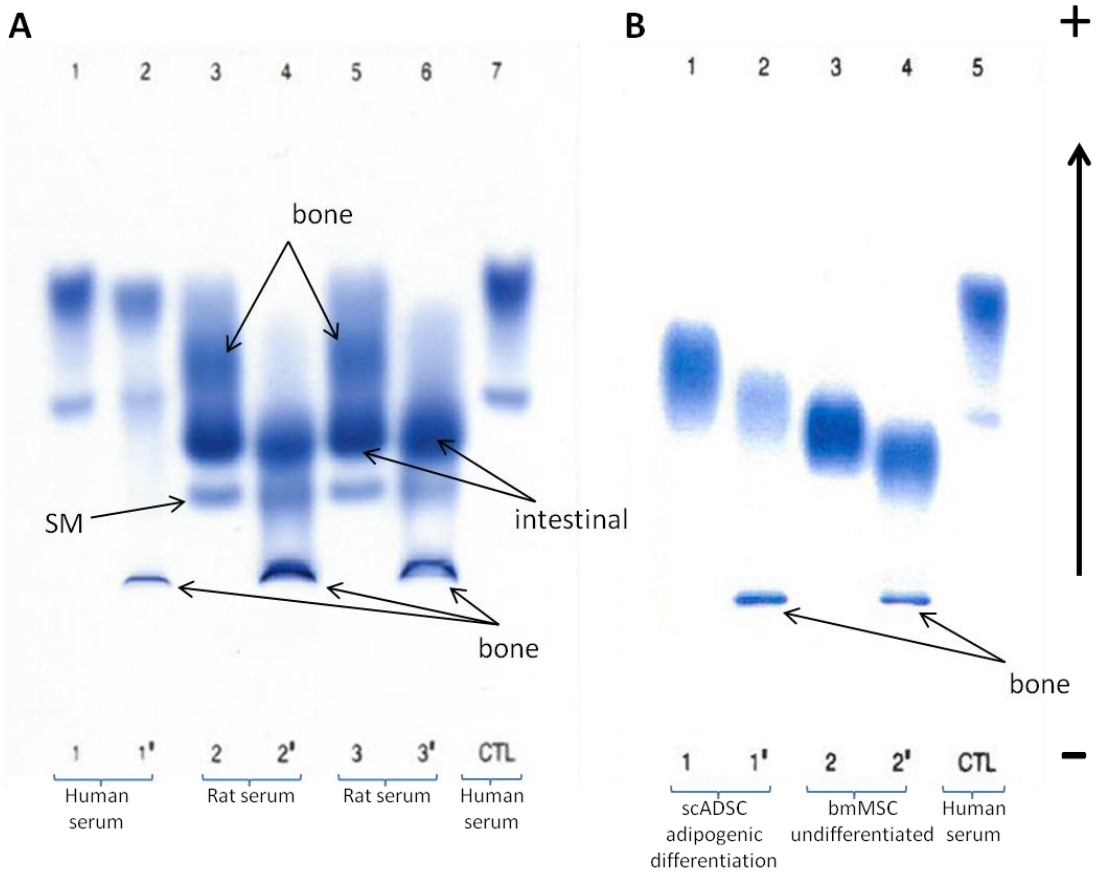

Figure 5.2.3.1: Separation of the isozymes of serum and tissue-derived alkaline phosphatase (ALP) by lectin affinity electrophoresis. ALP isozymes were separated by wheat germ lectin (WGL) affinity on an alkaline buffered (pH 9.1) agarose (10 g/L) gel (Hydragel 7 ISO-PAL® kit, Hydrasys® electrophoresis system, Sebia, France). Samples were run, in the absence and presence of WGL, in adjacent wells. WGL-treated samples are denoted with an inverted comma. Panel A: lanes 1 and 2, human serum; lanes 3 and 4, rat 1 serum; lane 5 and 6, rat 2 serum; lane 7, human serum control (WGL absent). Panel B: lanes 1 and 2, ALP extract from scADSCs differentiated for 5 days in adipogenic medium (AM); lanes 3 and 4, whole cell lysate prepared from naïve undifferentiated bmMSCs at P3; lane 5, human serum control (WGL absent). Bands identified as the bone, intestinal and slow migratory (SM) ALP isozymes are labelled on panel A and B. Direction of migration is from anode to cathode.

The ALP detected in adipogenically differentiated scADSCs ran further on the gel in comparison to undifferentiatied bmMSCs, while both were found to contain the bone ALP isoform, as this was precipitated in the presence of WGL (Fig. 5.2.3.1, B). Both adipogenically differentiated scADSCs and undifferentiated bmMSCs produced a band that remained after the precipitation of the bone ALP, which differed to one another in migration distance. It was unclear whether either of these bands could correspond to intestinal ALP, as rat serum and cell lysate ALP samples were run on different gels.

Lysate from both undifferentiated and osteogenically differentiated bmMSCs produced a single band which appeared to run similar distances to one another on the gel, and both also produced a band of precipitated ALP in the presence of WGL (Fig. 5.2.3.2 A). A single band was detected for lysates of adipogenically differentiated bmMSCs, which appeared to run a slightly shorter distance, in comparison to both undifferentiated and osteogenic bmMSC lysate samples. Interestingly, a band of precipitated ALP was not detected in the presence of WGL for the adipogenic bmMSC lysate samples (Fig. 5.2.3.2, A, lane 4 and B, lane 2). The quantity of ALP activity in the first adipogenic sample (Fig. 5.2.3.2 A, lanes 3 and 4) appeared to be low, which may have prevented a precipitation band from being visible (Fig. 5.2.3.2 A, lane 4); however, the quantity of the adipogenic sample in the second gel was higher (Fig. 5.2.3.2 B, lanes 1 and 3), and no precipitated ALP band was visible here either. The ALP activity of the osteogenic bmMSC lysate sample in the second gel (Fig. 5.2.3.2 B, lanes 2 and 4) appeared markedly lower than the activity of the osteogenic sample in the first gel (Fig. 5.2.3.2 A, lanes 5 and 6), which may have resulted from an insufficient quantity of precipitated ALP in the presence of WGL to form a detectable band. In both gels however, the adipogenic samples migrated a shorter distance than the osteogenic or undifferentiated samples, which may indicate that the ALP from rat-derived bmMSCs, which have been differentiated towards an adipogenic phenotype, is differently glycosylated to either naïve undifferentiated or osteogenic differentiated bmMSCs.

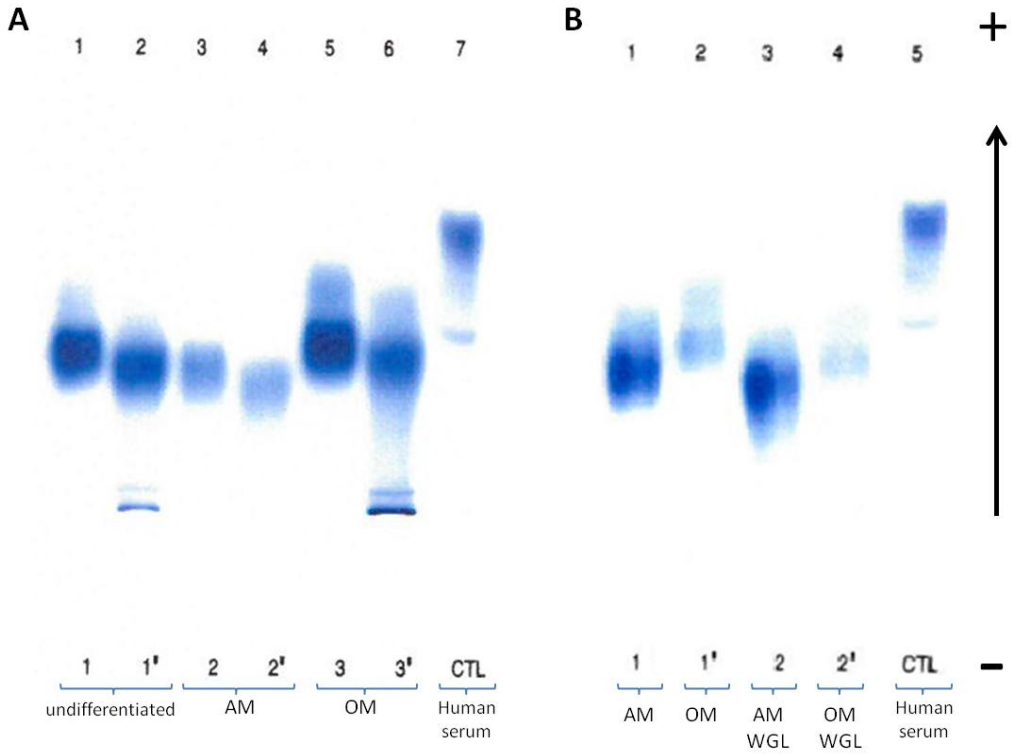

Figure 5.2.3.2: Separation of alkaline phosphatase (ALP) from rat-derived bmMSC lysates by lectin affinity electrophoresis. ALP isozymes were separated by wheat germ lectin (WGL) affinity on an alkaline buffered (pH 9.1) agarose (10 g/L) gel (Hydragel 7 ISO-PAL® kit, Hydrasys® electrophoresis system, Sebia, France). Samples in panel A were run, in the absence and presence of WGL, in adjacent wells. WGL-treated samples are denoted with an inverted comma. Panel A: lanes 1 and 2, undifferentiated naïve bmMSC; lanes 3 and 4, bmMSCs cultured in adipogenic differentiation medium (AM) for 14 days; lanes 5 and 6, bmMSCs cultured in osteogenic differentiation medium (OM) for 5 days; lane 7, human serum (WGL absent). Panel B, bmMSCs cultured in AM for 14 days, WGL present (lane 1) and WGL absent (lane 3); bmMSCs cultured in OM for 5 days, WGL absent (lane 2) and WGL present (lane 4); lane 5, human serum control (WGL absent). Direction of migration is from anode to cathode.

5.2.4 Knockdown of TNAP by shRNA interference.

To determine whether knockdown of TNAP would induce a reduction in lipid accumulation, scADSCs were transduced with TNAP shRNA lentiviral vectors and subsequently induced to differentiate towards an adipogenic phenotype. Subcutaneous ADSCs (n=4) were transduced with control or TNAP shRNA lentiviral vectors at P1, and induced to differentiate after confluence was reached at P2. Cells were harvested after 5 days of culture in AM and either stained with Oil Red O or RNA was collected for analysis of TNAP gene expression.

Transduction with shRNA and puromycin selection resulted in an increased duration of four days from seeding at P2 until confluence was reached, when compared to non-transduced control cells. Cells transduced with either control or TNAP shRNA did not appear to increase

in cell density after splitting and reseeding, and sparsely populated areas could still be observed amongst areas of higher cell density, in contrast to non-transduced control cells which appeared as a densely packed uniform lawn of cells by day two post confluence (Fig. 5.2.4.1). Induction of differentiation resulted in a marked decrease in lipid accumulation in both control shRNA and TNAP shRNA samples in comparison to that observed in non-transduced controls (Fig. 5.2.4.2). The decrease in lipid accumulation at day 5 in cells transduced with shRNA was accompanied by a decrease in overall cell number in comparison to non-transduced control cells. These observations indicated that the decrease observed was not due to the shRNA mediated knockdown of TNAP, but that the decrease was due to the effect of transduction and subsequent puromycin selection. The decreased viability of transduced cells in comparison to non-transduced control cells, which resulted in large sparsely populated areas on the culture surface precluded efforts to quantify lipid accumulation using image analysis.

TNAP mRNA expression appeared to be lower in both undifferentiated and differentiated samples for cells transduced with TNAP shRNA compared to control shRNA (Fig 5.2.4.3), although this was not statistically significant.

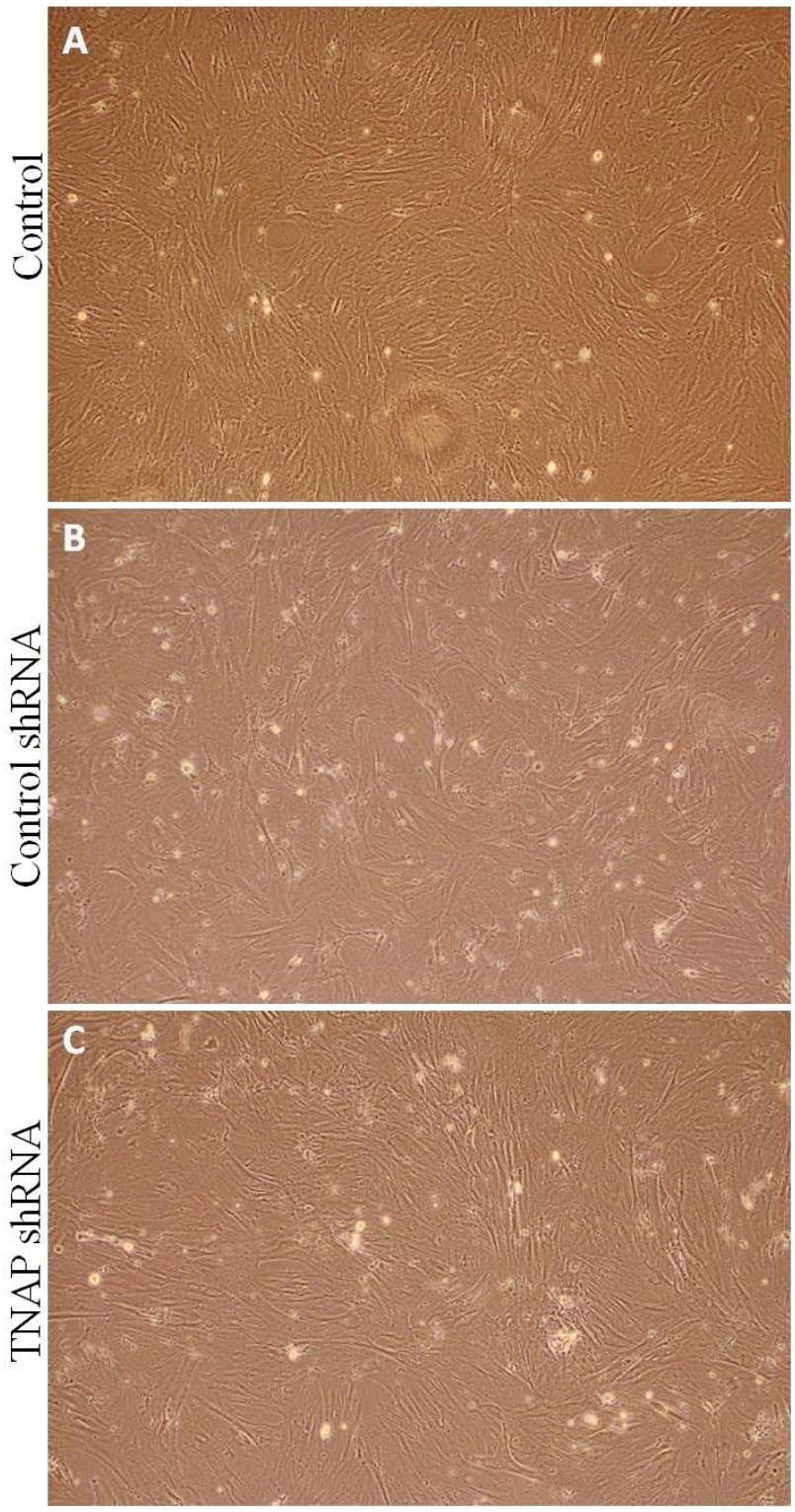

Figure 5.2.4.1: Light microscopy images of control non-transduced, control shRNA and TNAP shRNA scADSCs at day 2 post confluence. Control non-transduced scADSCs (A), as well as scADSCs transduced with either control shRNA (B) or TNAP shRNA (C) at P1, were cultured in standard growth medium (SGM) until 2 days post confluence was reached at P2, in preparation for adipogenic induction. Images were acquired immediately prior to initiation of adipogenic differentiation. Images were acquired using an Olympus (CKX41) microscope at x10 magnification.

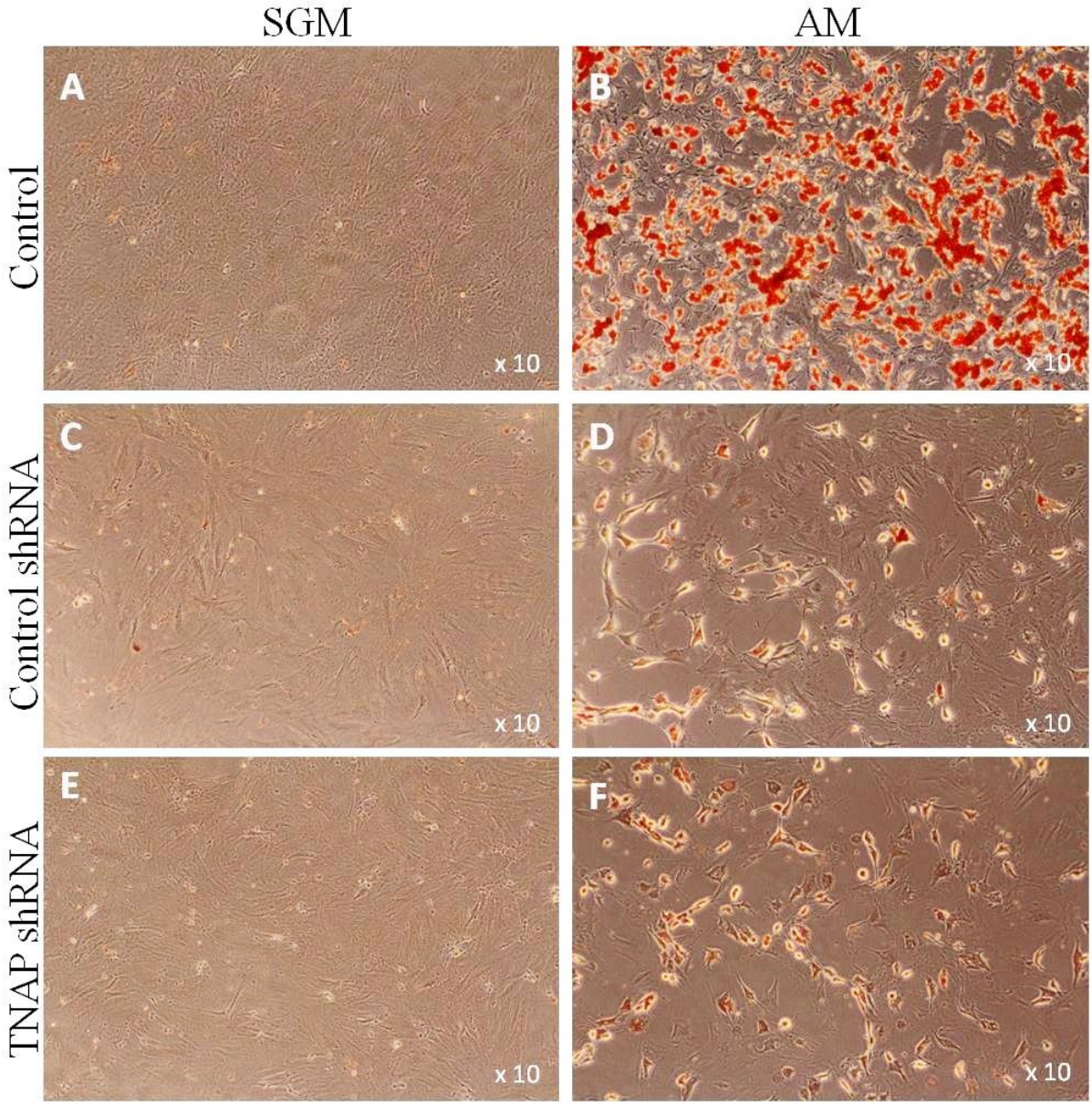

Figure 5.2.4.2: Light microscopy images of control non-transduced, control shRNA and TNAP shRNA scADSCs on day 5 of adipogenic induction. Control non-transduced (A and B) and control shRNA transduced (C and D) as well as TNAP shRNA transduced cells were cultured in either SGM with vehicle (A, C and E), or in adipogenic differentiation medium (AM) (B, D and F) for 5 days, followed by staining with Oil Red O to visualise lipid droplets. These images were acquired using an Olympus (CKX41) microscope at x10 magnification.

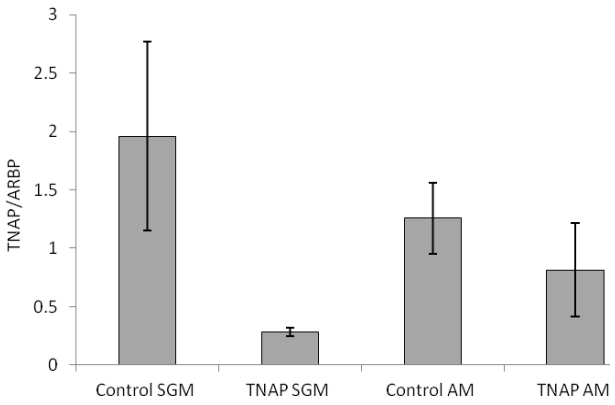

Figure 5.2.4.3: Relative expression of TNAP mRNA in scADSCs transduced with either control or TNAP-specific shRNA, after 5 days of culture in either standard growth medium with vehicle (SGM) or adipogenic differentiation medium (AM). Subcutaneous ADSCs were cultured in SGM until 2 days post confluence, followed by 5 days of culture in either SGM with vehicle or AM. Error bars are representative of standard error (SEM), n = 3 - 4.

5.3 Discussion

ELF-97 staining in bmMSCs, scADSCs and pvADSCs differentiated towards an adipogenic phenotype showed that the ALP activity in all these cell types was localised on the lipid droplet surface. This is in agreement with the pattern of ALP activity in 3T3-L1 cells demonstrated by Ali *et al*. using ELF-97 (Ali *et al.*, 2005). ELF-97 staining appeared to be most intense in bmMSC samples, while the least amount of staining appeared to be within the pvADSCs, observations which corroborate earlier findings for ALP activity levels within these cells (See Chapter 4). Although a small amount of ELF-97 staining was observed in cells from the bmMSC sample which did not appear to have visible lipid droplets, ALP activity appeared to be almost exclusively present within cells containing lipid droplets, which confirms the previous literature findings (Ali *et al.*, 2005).

ALP activity does not appear to be evenly distributed across the surface of the lipid droplet membrane, but is rather present in distinct locations, visible as yellow/green spots, on the membrane. ALP activity is also not uniformly present in all lipid droplet-containing cells, as ELF-97 staining appears to be more intense in some cells and lower in other cells. It was observed that ELF-staining appears to be more intense in cells with smaller lipid droplets, while cells with larger lipid droplets showed fewer areas of ALP activity. This finding is consistent with previous ALP activity assay data, which demonstrated that for scADSCs and pvADSCs, ALP activity is highest at day 5 of adipogenic differentiation, the initial phase of

small droplet formation, and decreases with time until day 10 of differentiation, where larger droplets have been formed. In contrast to scADSCs and pvADSCs, bmMSCs undergoing adipogenesis showed the highest ALP activity on day 14, which was the final time point for differentiation in this cell type. Previous findings show that mouse bone marrow-derived stromal cells capable of adipogenic differentiation have the highest levels of ALP activity during the earlier stages of differentiation, while ALP activity was virtually absent in mature adipocytes (Kodama *et al.*, 1983). The increasing ALP activity of rat-derived bmMSCs over the course of the differentiation period may indicate that the bmMSCs have not yet peaked in ALP activity. In future studies ALP activity should be monitored in bmMSCs undergoing adipogenic differentiation over a longer period, as in this study the endpoint for experiments was determined when sufficient lipid accumulation had occurred to enable quantification and not according to ALP activity levels.

The stem cell marker, mesenchymal stem cell antigen 1 (MSCA-1) was found to be identical to TNAP, which points to an important role for TNAP in differentiation (Sobiesiak *et al.*, 2010). The role of TNAP as a stem cell marker provides further evidence that TNAP may play a more major role during the early stages of adipogenesis, when cells are more stem-like, than in maintenance of an adipocytic phenotype.

PCR data revealed that the bone TNAP mRNA transcript was predominantly expressed in bmMSCs and scADSCs, while neither bone- or liver-type transcript could be detected in the pvADSCs. The same pvADSC cDNA samples were previously used in Chapters 3 and 4 for RT-qPCR experiments, in which TNAP as well as adipogenic and osteogenic marker genes were successfully detected, indicating that the cDNA was not degraded in these samples. Rat liver is known to express both the bone and liver TNAP transcripts, with the bone form being predominant (Brun-Heath *et al.*, 2011), which indicates that expression and by influence, function of one particular TNAP isoform is not mutually exclusive of the other in a particular tissue. For this reason, it may be possible that rat scADSCs express the liver TNAP transcript as well as the bone transcript, but at such low levels that detection of this transcript using conventional PCR is inconsistent, although this seems highly unlikely given the sensitivity of PCR run at 35 cycles. The number of TNAP mRNA transcripts appeared to be low in scADSCs and below detectable levels in pvADSCs under the growth conditions used. The detection of expression may have been missed as the template cDNA was prepared from

RNA isolated at day 5 of differentiation for all cell types; however it is possible that TNAP mRNA expression could have been maximal at an earlier or later time point.

It was found that the previously published bone TNAP forward primer was not optimal, as it allowed the formation of nonspecific products. However there was a relatively short sequence available from which a primer could be designed before the sequence became common to both transcripts (exons 1a and 1b), the point presumably being the start of exon 2, which made redesign of the primers impractical. Primers for the bone TNAP transcript, taken from Brun-Heath *et al*., selectively amplified a product at the expected size in bmMSCs differentiated towards an osteogenic phenotype, which is consistent with the identification of this as the bone-specific TNAP mRNA transcript.

TNAP mRNA was previously detected in pvADSCs, albeit at low levels compared to bmMSCs and scADSCs, using RT-qPCR (See Chapter 3 and 4), while no detection was possible with conventional PCR. Therefore, suitable primer sequences for use with RT-qPCR specific for the rat bone or liver TNAP mRNA transcript should be designed and tested, as this may provide a more sensitive method of detection and quantification. Difficulty in designing a forward primer for the bone transcript is anticipated, due to the relatively short stretch of sequence available from which a forward primer may be designed (Addendum C, Fig. C1).

Detection of the bone isoform transcript produced more distinct and consistent bands in adipogenic samples compared to osteogenic samples, in both bmMSCs and scADSCs, which was surprising considering the well established role for TNAP in mineralisation. The highest expression of TNAP during *in vitro* osteogenic differentiation of bmMSCs may have occurred at an earlier time point than measured here (day 5), as mineralisation had already began to occur by the time RNA was collected, and may be the reason for the low levels of amplification in bmMSCs treated with OM in comparison to AM.

The results indicate that for rat-derived bmMSCs and scADSCs, the bone-specific transcript is the predominant TNAP mRNA transcript expressed. Based on the results from the scADSCs, it may be possible that the TNAP mRNA expressed in pvADSCs is also likely to be predominantly the bone type, however additional work will be needed to confirm this. Future work should also include investigating temporal TNAP mRNA expression with levels

measured at daily intervals in order to determine the point where TNAP mRNA expression is highest in each cell type. It may also be of interest to investigate whether the bone transcript predominates at earlier time points compared to later time points. Due to the difficulty amplifying sufficient product using conventional PCR, future work should be undertaken using RT-qPCR, which would additionally allow for quantification.

The presence of a single band of ALP in all cell lysate samples indicates that only one isozyme of ALP is present, in comparison to the multiple ALP bands typically present in rat serum (Dziedziejko *et al.*, 2005). The failure of WGL to precipitate ALP in AM-treated bmMSCs was an unexpected result, as PCR data confirmed that both scADSCs and bmMSCs expressed the bone TNAP mRNA transcript during adipogenic differentiation. The ALP from AM-treated bmMSCs migrated a shorter distance compared to undifferentiated or OM-treated bmMSCs. The data indicate that the ALP present in AM-treated bmMSCs may be differently glycosylated, in comparison to either undifferentiated or OM-treated bmMSCs. The data further indicate that depot-specific glycosylation differences may exist between AM-treated scADSCs and AM-treated bmMSCs. Depot-specific differences have been observed between rat-derived MSCs (Sadie-Van Gijsen *et al.*, 2010) including differences in *in vitro* differentiation potentials. The glycosylation pattern of ALP from adipocytes is relatively unknown.

An ALP isozyme discovered in human adipose tissue had different biochemical properties compared to liver, intestinal and placental ALP (Okochi *et al.*, 1987), providing evidence that adipose tissue-derived ALP is distinct from other isoforms of TNAP. Okochi *et al.* described the adipose-derived ALP isozyme as localized to the walls of capillaries within the adipose tissue, and absent from mature adipocytes. Adipose precursor cells are thought to have a perivascular localisation, and are found amongst cells lining the blood vessel walls in adipose tissue (Zannettino *et al.*, 2008). This is consistent with the observation that ALP activity is highest in immature adipocytes and absent in mature adipocytes (Kodama *et al.*, 1983).

Aberrant glycosylation patterns of ALP are known to occur, and are indicative of malignancy (Nowrouzi and Yazdanparast, 2005). The hepatocarcinoma cell line HepG2, is known to accumulate lipid within lipid droplets (Ali *et al.*, 2013). HepG2 cells were found to express an aberrantly glycosylated form of liver TNAP in the cell membrane, as well as another form

that was released into the extracellular medium (Nowrouzi and Yazdanparast, 2005). This indicates that a particular cell type may express more than one isoform of TNAP.

The TNAP present in adipocytes has not yet been extensively characterized, and much remains to be discovered about the isoforms present in adipose tissue, including whether more than one isoform is known to occur. It cannot be stated with certainty that the TNAP isoforms present in *in vitro* differentiated rat-derived MSCs reflect accurately the isoforms found in native adipose tissue. The observation that oxidative stress is able to increase the expression and alter the glycosylation pattern of TNAP in enterocytes, suggests that environmental conditions may result in alterations to the TNAP isoform expressed (Lopez-Posadas *et al.*, 2011). The *in vitro* cell culture environment together with the various differentiation cocktails used, may present an environment much unlike the *in vivo* conditions where TNAP expression occurs, and may result in unknown effects on the glycosylation of TNAP. Future work should first aim to isolate and characterise TNAP from native adipose tissue, as this may provide the most accurate reflection of the natural glycosylation pattern present in this tissue and whether more than one TNAP isoform is expressed. The properties of the TNAP isolated from *in vitro* differentiated primary MSCs should be compared to that of native TNAP in order to determine whether the artificial culture environment has an effect on expression.

Neuraminidase functions to remove terminal N-acetyl neuraminic acid (sialic acid) from the surface of glycoproteins (Cuatrecasas and Illiano, 1971). As demonstrated, WGL is able to bind to the sialic acid residues of ALP, forming a band of precipitated ALP enzymes, which retards the migration through the gel (Fig. 5.2.3.1 and 5.2.3.2). As the differences in molecular weight of TNAP isoforms is due to the presence of different glycosylations, cleavage of terminal sialic acid by neuraminidase is expected to produce bands of similar molecular weight when subjected to electrophoresis through an agarose gel. Future experiments will include treating differentiated MSC samples with neuraminidase, in order to see if removing the glycosylations from the ALP isozymes present in these samples will cause the ALP bands to migrate at the same distance on the gel. This would provide further evidence that the differences in migration distance of ALP are due to differences in the amount of glycosylation present on the enzyme.

Caution should be used in applying rat data directly to humans, as species specific differences are known to exist; for example, rat serum does not contain liver ALP, while the liver ALP isoform forms a major component of human serum ALP (Dziedziejko *et al.*, 2005). Rat serum also contains three intestinal ALP isoforms (Shidoji and Kim, 2004), which are not present in humans. The possibility of several isoforms of TNAP being present in adipose tissue cannot currently be ruled out, as WGL did not precipitate all the ALP present in the rat tissue samples. Four isoforms of human bone TNAP have been described (Halling Linder *et al.*, 2009) which further indicates that more than one isoform of TNAP may be present in adipose tissue. The migration differences between scADSC-derived ALP and bmMSC-derived ALP may also indicate that posttranslational differences exist between TNAP molecules expressed in MSCs derived from different tissues.

In addition to electrophoresis, it may be desirable to characterise the TNAP isoforms from adipose tissue using high-performance liquid chromatography (HPLC), as this technique has been found to provide better resolution of ALP isoforms compared to electrophoresis. A combination of the two techniques is most desirable, as each technique provides information about the ALP isozymes present in a sample that may not be available from the other method (Dziedziejko *et al.*, 2005).

Bone marrow-derived MSCs express higher levels of TNAP during adipogenic differentiation than scADSCs, however the latter were selected for TNAP knockdown as these cells have a more consistent adipogenic differentiation potential in comparison to bmMSCs. The knockdown of TNAP in scADSCs proved to be unsuccessful. Although the viral transduction process did result in successful integration of the shRNA, as the transduced cells were puromycin resistant, these cells had an impaired capacity to proliferate and differentiate compared to non-transduced control cells. The reduction in cell viability and lipid accumulation observed in transduced cells was similar for cells transduced with both control shRNA as well as shRNA targeting TNAP. As a result, any reduction in lipid accumulation could not be attributed to the knockdown of TNAP. Transient expression of shRNA using plasmid vectors was not attempted, as it has previously been found in our labs that both bmMSCs and ADSCs are extremely sensitive to transfection, both chemical and electroporation, resulting in extremely low cell viability. Expansion in number of the few surviving cells was not sufficient for further experimentation.

Subcutaneous ADSCs cultured from the stromal vascular fraction (SVF) have previously been noted to have a limited number of expansions *in vitro*, and the heterogeneity of primary-derived MSCs is well known (Bianco *et al.*, 2008; Strioga *et al.*, 2012). The scADSCs cultured from the SVF may include a mixture of cell types, some of which have limited proliferation and differentiation capacity. Transduction was performed at P1, and cells were used for experiments at P2. The P1 population may have been largely heterogeneous, and possibly cells with limited expansion capabilities were transduced along with more stem-like cells in the population. The appearance of cells capable of lipid accumulation with the transduced cell cultures may indicate that some cells within the population are capable of differentiating after being stably transduced, compared to other cells which took on a broad flattened appearance and displayed limited proliferation ability. To improve the success of future shRNA knockdown experiments involving scADSCs, better selection criteria should be applied, in order to isolate a clone of transduced cells which display a capacity for long term self renewal. Alternatively, as primary-derived MSCs have a more limited capacity for self renewal in culture, shRNA knockdown should be attempted using an established cell line, which has a more defined phenotype and unlimited self-renewal capacity, allowing for longer term experiments to be performed.

In conclusion, we have demonstrated that ALP activity, as detected using the ELF-97 substrate in bmMSCs, scADSCs and pvADSCs treated with AM, is predominantly associated with intracellular lipid droplets, in confirmation of previous work using 3T3-L1 cells. Using conventional PCR, we have also demonstrated that bone-type TNAP mRNA appears to be preferentially expressed in scADSCs and bmMSCs treated with both OM and AM. Neither TNAP mRNA transcript could be amplified from pvADSC cDNA using conventional PCR, indicating that expressional levels are below detectable levels in this cell type, when using this technique. Future work should include repeating the experiments performed using conventional PCR with RT-qPCR, as well as using samples collected at earlier time-points during differentiation in order to determine when peak levels of TNAP transcription occur. Glycosylation analysis data showed that possible differences may exist in the glycosylations present in TNAP from bmMSCs when treated with AM or OM, as well as between AM-treated scADSCs and AM-treated bmMSCs, which warrants further investigation. Knockdown of TNAP in scADSCs using shRNA had limited success, as transduction of the cells with shRNA appeared to have a severe impact on cell viability. The results that were obtained indicated that shRNA knockdown of TNAP did not abolish lipid accumulation

completely in scADSCs, as some lipid containing cells were observed after treatment with AM. Future work may include repeating the knockdown of TNAP experiments using shRNA using a more robust model in which cell viability is not adversely affected by transduction with shRNA.

CHAPTER 6

Conclusions and limitations

The aim of this project was to evaluate the role of tissue-nonspecific alkaline phosphatase (TNAP) in the differentiation of rat-derived mesenchymal stromal cells (MSCs) from bone marrow- and adipose tissue depots, with emphasis on adipogenic differentiation. Rat MSCs were isolated from three tissue depots: bone marrow, subcutaneous adipose and peri-renal visceral adipose tissue, where the resulting MSC cultures were termed bone marrow-derived MSCs (bmMSCs), subcutaneous adipose-derived stromal cells (scADSCs) and peri-renal visceral adipose-derived stromal cells (pvADSCs). Cells isolated from all three tissue depots appeared similar in morphology, and analysis of surface marker expression by flow cytometry positively identified the cells as MSCs. Depot-specific differences were noted between cells from all depots, with the greatest differences between bmMSCs and cells from both adipose depots (ADSCs). Bone marrow-derived MSCs treated with osteogenic differentiation medium (OM) were observed to mineralise more rapidly, and osteogenic marker genes increased earlier and to higher levels than observed for either scADSCs or pvADSCs under the same conditions, relative to the house-keeping gene, *Arbp*. Conversely, lipid accumulation in scADSCs and pvADSCs treated with adipogenic differentiation medium (AM) occurred more rapidly and to higher levels than observed in bmMSCs, and also displayed a greater increase in adipogenic marker gene relative expression levels than bmMSCs. Between MSCs from adipose depots, pvADSCs accumulated slightly more lipid than scADSCs, while adipogenic marker gene expression levels were higher in scADSCs compared to pvADSCs.

Alkaline phosphatase (ALP) activity assay data showed that ALP activity levels were highest overall in bmMSCs, followed by scADSCs, while pvADSCs had the lowest ALP activity. The ALP activity levels were highest in all cell types when treated with AM compared to OM, which was surprising as ALP activity is better known to be associated with osteogenesis rather adipogenesis, and this data is suggestive of a role for ALP activity in adipogenic differentiation and/or maintenance of an adipocyte phenotype.

The key phenotypic feature of adipogenic differentiation is the accumulation of lipid in membrane-bound droplets within the cell, which coalesce into one or two large lipid droplets once the adipocyte has reached maturity. The isozyme of ALP present in bone as well as adipose tissue is tissue-nonspecific ALP (TNAP). Previous studies have found that inhibition of ALP activity in primary-derived human preadipocytes and the murine preadipocyte cell-line 3T3-L1, using TNAP-specific inhibitors, resulted in a decrease in lipid accumulation

during *in vitro* adipogenic differentiation (Ali *et al.*, 2005). We treated rat-derived bmMSCs, scADSCs and pvADSCs with the TNAP-specific inhibitors levamisole, histidine and L-homoarginine, either alone or in combination with one another, while the cells were undergoing either adipogenic or osteogenic differentiation *in vitro*. The reduction of either mineralisation, during osteogenic induction or lipid accumulation during adipogenic induction, when in the presence of TNAP inhibitors, was taken to indicate that TNAP was involved in these processes. As TNAP is known to have a an essential role in the process of mineralisation during normal bone formation *in vivo*, we wanted to test the effect of TNAP inhibitors on mineralisation during osteogenic induction, in order to verify that the same inhibitors were able to reduce TNAP activity during *in vitro* adipogenic differentiation of MSCs.

Levamisole, alone or in combination with either histidine or L-homoarginine, was found to completely inhibit mineralisation during osteogenic induction in all three cell types studied, while no statically significant effect on ALP activity was observed. In contrast, levamisole did not significantly decrease lipid accumulation during adipogenesis in any of the three cell types, and only significantly decreased ALP activity in bmMSCs when treated with either levamisole alone or in combination with histidine during adipogenesis. Treatment with levamisole alone was also found to significantly inhibit TNAP gene expression in bmMSCs 7 days after initiation of adipogenic induction, in comparison to untreated control and cells treated with either histidine or L-homoarginine (Fig. 4.2.5.1). Histidine alone had no statistically significant effect on either mineralisation or lipid accumulation in any of the cell types, and only decreased ALP activity significantly in bmMSCs undergoing adipogenesis. L-homoarginine alone did not significantly affect mineralisation or ALP activity in cells undergoing osteogenic induction, however, during adipogenesis L-homoarginine, alone or in combination with levamisole and histidine, significantly decreased lipid accumulation in all three cell types. Interestingly, L-homoarginine treatment, alone or in combination with levamisole and histidine, during adipogenic induction resulted in a statistically significant increase in ALP activity in scADSCs, but not in bmMSCs. ALP activity increased significantly in pvADSCs during adipogenic induction only with the combination of levamisole and L-homoarginine. The low levels of ALP activity in pvADSCs in comparison to scADSCs and bmMSCs may have resulted in difficulty obtaining statistically significant effects within this cell type.

It appeared that, overall, treatment with levamisole was able to completely inhibit mineralisation in all cell types, but had no effect on lipid accumulation. Conversely, L-homoarginine did not have a definite effect on mineralisation, but alone was sufficient to reduce lipid accumulation significantly in all cell types. Histidine significantly inhibited lipid accumulation in bmMSCs, but overall had no clearly discernible effect on differentiation or ALP activity.

Levamisole is one of the best known inhibitors of TNAP, and is widely used to study ALP activity, however, levamisole has been found to have off-target effects which may obscure the results obtained when this compound is used solely as a means of inhibiting TNAP activity in live cells. In fact, one publication has advised against the use of levamisole for this sole purpose, due to off-target effects (Nowak *et al.*, 2015). The results obtained here may differ from other studies, which have reported a significant decrease in lipid accumulation as a result of levamisole treatment, due to sensitivity of the rat-derived MSCs used in this study to levamisole, as these cells were only able to tolerate a maximum concentration of 0.5 mM levamisole over long-term culture, in comparison to 3T3-L1 cells, which were able to tolerate a 5 x higher dosage (2.5 mM) (Ali *et al.*, 2005). It may be possible that the effect on lipid accumulation is only seen at higher concentrations of levamisole than were used in this study. However, this possibility is countered by the observation that mineralisation could be prevented in the rat-derived MSCs at 0.5 mM levamisole.

L-homoarginine is a selective TNAP inhibitor, but surprisingly was not able to reduce mineralisation or ALP activity, even at 10 mM concentration, indicating that TNAP activity was not successfully inhibited during osteogenic induction. It is not known how effective L-homoarginine is at inhibiting TNAP under cell culture conditions. The lack of inhibition may be due to suboptimal conditions in the cell culture environment, such as differences in pH and substrate composition when comparing *in vitro* assay conditions, with substrate composition and buffering capacity *in vivo*. L-homoarginine, while unable to inhibit mineralisation, was able to inhibit lipid accumulation during adipogenic differentiation. The reduction in lipid accumulation may be due to unknown off-target effects of L-homoarginine on the cells, resulting in a decrease in lipid accumulation. Another possible reason for the observed differences may be due to possible differences in the glycosylations present on TNAP molecules from cells with adipocyte and osteoblast phenotypes. Glycosylation differences, which are responsible for the main differences between TNAP isoforms, are known to affect

enzyme activity as well as inhibitor sensitivity. Therefore, it may be possible that the TNAP present in cells induced towards an adipocyte phenotype is more sensitive to inhibition by L-homoarginine than cells differentiated towards osteoblastogenesis. Glycosylation analysis of the ALP isoforms present in bmMSCs differentiated towards an adipocyte and osteoblast phenotype using agarose electrophoresis and lectin precipitation, showed that some possible differences in TNAP isoform may exist between TNAP from adipocyte and osteoblast differentiated bmMSCs (Fig. 5.2.3.2).

The observation that the presence of L-homoarginine was able to significantly increase ALP expression in scADSCs, but not in bmMSCs, undergoing adipogenic induction, may also point to a compensatory mechanism by scADSCs in response to L-homoarginine inhibition of TNAP, by raising ALP expression. Evidence of increased expression of TNAP in the presence of L-homoarginine can be seen in gene expression data, where levels of TNAP gene expression is similar to or slightly higher than control for all three cell types during adipogenic induction, although no statistical significance is present (Fig. 4.2.5.1). As mentioned, in bmMSCs L-homoarginine treatment did not increase ALP activity, which may again be due to differences in the glycosylations present in TNAP molecules between bmMSCs and scADSCs differentiated to an adipogenic phenotype. Glycosylation analysis also revealed that some differences may exist in the glycosylations between TNAP from scADSCs and bmMSCs after differentiation towards and adipocyte phenotype (Fig. 5.2.3.1 B and Fig 5.2.3.2 B).

Histidine, at the highest concentration that the cells could tolerate in long term culture (10 mM), had a limited effect on lipid accumulation as well as mineralisation and ALP activity, except in bmMSCs, where a statistically significant decrease in lipid accumulation was observed. The decrease may be due to the properties of TNAP in adipocyte differentiated bmMSCs, compared to ADSCs, although, it is also possible that the reduction in lipid accumulation in these cells was due to other unknown off-target effects in these cells. Out of the three inhibitors tested, inhibition by histidine was the weakest (Fig. 4.2.6.1), and future studies on TNAP from rat-derived MSCs may consider excluding this compound for use as TNAP inhibitor in either live cell culture or assay.

Attempts to inhibit ALP activity in MSCs undergoing differentiation in culture using TNAP inhibitor compounds were limited by potential off-target effects, therefore another method of

examining the contribution of ALP to MSC differentiation was employed, in the form of knockdown of TNAP using lentiviral mediated transfection with short hairpin RNA (shRNA) targeting TNAP. A marked decrease in cell viability was observed in antibiotic selected cells following transduction of scADSCs with control vector, which contained a sequence not targeting any known mammalian genes, as well as test vector, which contained the TNAP-specific shRNA, and subsequent antibiotic selection, in comparison to non-transduced control cells without selection at P1 and P2. Subcutaneous ADSCs were selected as the model for this experiment for financial reasons, due to limited available quantities of shRNA, and because while bmMSCs have the highest levels of ALP activity, scADSCs differentiate more readily and reliably towards an adipocyte phenotype. Despite the apparent lower cell viability of transduced scADSCs, treatment of these cells with adipogenic differentiation medium (AM) resulted in the production of cells containing lipid droplets after 5 days. Assessment of the gene expression levels of TNAP in transduced cells, showed a slight decrease in TNAP mRNA levels in cells transduced with shRNA targeting TNAP, compared to shRNA control. Differences in lipid accumulation could not be quantified due to the extremely poor differentiation of transduced cells. Expression of TNAP in non-transduced scADSCs treated with AM for 5 days was roughly 6-fold, relative to *Arbp* (Fig. 4.2.5.1, D), while TNAP gene expression levels in scADSCs transduced with TNAP-specific shRNA were less than 1-fold relative to *Arbp* (Fig. 5.2.4.3). This indicates that although TNAP expression was knocked down compared to non-transduced controls, some lipid accumulation was still able to occur.

Viral vectors used for transfecting cells are known to insert randomly into the host genome, and may result in insertional mutations, which may possibly disrupt essential genes in the cell, resulting in cytotoxic effects on the cell (Kim and Eberwine, 2010). The reason for the apparent reduced viability of transduced scADSCs compared to non-transduced cells may be as a result of the transduction process. Nevertheless, the results indicate that knockdown of TNAP with TNAP-specific shRNA was not able to completely abolish lipid accumulation in scADSCs.

Confocal microscopy demonstrated that ALP activity was present in lipid-containing cells produced after treatment of bmMSCs, scADSCs or pvADSCs with AM. The ALP activity appeared to be most prominently associated with the lipid droplet membrane in all three cell types, however, ALP activity was not present on all lipid droplets within a particular cell, while some lipid-containing cells appeared to have a higher amount of ALP activity than

others, and some had virtually no ALP activity. These results confirm that ALP activity, which in these cells is the result of TNAP activity, is likely to be associated with lipid accumulation and possibly also adipogenesis, however, the mechanism by which TNAP is able to stimulate adipogenic differentiation is not currently known (Esteve *et al.*, 2015). ALP activity was detected using the fluorescent substrate, ELF-97, because a suitable commercially available antibody against TNAP was not available at the time of the experiments. The possible future commercial availability of a suitable antibody against rat TNAP would be able to confirm the results obtained using ELF-97.

The mRNA transcripts of TNAP are expressed in two forms, where each transcript type is composed of either one of two untranslated leader exons, designated 1a and 1b, followed by 11 coding exons. Transcripts containing the 1a exon are predominant in cells from bone tissue and this is termed the bone-type TNAP transcript, while the 1b exon is largely found in liver tissue, and for this reason is known as the liver-type transcript. Knowledge of the TNAP transcripts in a particular tissue may identify which isoform of TNAP is preferentially expressed in these tissues. PCR revealed a preference for the expression of bone-type TNAP mRNA transcript was in bmMSCs and scADSCs, differentiated towards either an adipogenic or osteogenic phenotype. Published primer sequences for either bone- or liver-type TNAP transcripts were found in a paper by Brun-Heath *et al*. (2011), and a database search revealed that these were based on a relatively short stretch of available sequence data (Addendum C, Fig. C1) (Brun-Heath *et al.*, 2011). Several non-specific bands were detected in scADSC and bmMSC samples, particularly when using the bone-type primer set. Due to the limited available sequence from which alternative primers could be designed, attempting to redesign more optimal primer sets was not considered to be feasible. More complete sequence data for both the bone- and liver-type TNAP mRNA from rat, each containing a longer sequence of both exon 1a or 1b, respectively, should allow for more optimal primers to be designed.

Detection of bone-type transcript in bmMSCs and scADSCs treated with osteogenic differentiation medium (OM) was not consistent in all samples (n = 3) (Fig. 5.2.2.1 and Fig. 5.2.2.3), which may be due to the lower expression of TNAP during osteogenic compared to adipogenic treatment, as has been previously observed (Fig. 4.2.5.1 A – D). Low numbers of TNAP mRNA transcript copies present in samples treated with OM may have been the reason for the inconsistent amplification in these samples, as the number of PCR cycles used were already at the recommended maximum of 35.

The expression of TNAP in pvADSCs was below detectable levels using conventional PCR and transcript-specific primers, but was detectable using RT-qPCR using a primer set which did not discriminate between transcripts. ALP assay and RT-qPCR data presented in this study showed that pvADSCs had low levels of TNAP expression, and therefore it is not surprising that conventional PCR failed to detect either the bone- or liver-type TNAP transcript in pvADSCs.

Overall, more complete information on the sequences of exons 1a and 1b from rat TNAP mRNA transcripts will allow for improved primer design for both the bone- and liver-type transcripts for future work. In spite of the limited space for primer construction from the available sequence data, it was discovered that bone-type TNAP transcript appears to be preferred in rat-derived bmMSCs and scADSCs, while the preferred transcript in pvADSCs remains unclear.

As mentioned previously, post-translational differences in the form of glycosylations account for the main differences between TNAP isoforms. While only two different TNAP mRNAs may be transcribed, several different TNAP isoforms may be expressed (Halling Linder *et al.*, 2009). Using agarose gel electrophoresis and lectin precipitation, differences were found between TNAP from OM and AM treated bmMSCs, as well as between AM treated bmMSCs and scADSCs. This data indicates that TNAP may possibly be differently glycosylated in osteoblasts and adipocytes, and that depot-specific differences in TNAP from cells with an adipocyte phenotype may occur. Limitations of this technique included the crude nature of the TNAP-containing samples, which included crude cell lysate in the case of bmMSCs, and ALP extract, in the case of scADSCs. ALP extraction was necessary for scADSCs, as ALP activity levels were too low in crude lysate of these cells, while even ALP extraction was not able to concentrate sufficient ALP activity in pvADSCs for glycosylation analysis. The crude nature of the samples resulted in the appearance of large diffuse bands. Future work will include purification of TNAP from crude cell lysates using column chromatography, followed by high performance liquid chromatography (HPLC) in addition to agarose electrophoresis. This will enable better resolution of the different isoforms present in the various samples, and will be necessary to confirm that glycosylation differences between rat MSCs when treated with OM or AM exist. Additionally, TNAP may be released into the growth medium by certain cells and under certain conditions (Nowrouzi and

Yazdanparast, 2005). It may be worthwhile investigating whether TNAP is released by MSCs into the culture medium during differentiation, and, if present in sufficient quantities, to assess the glycosylation pattern present here.

The inherent heterogeneity of primary-derived MSC cultures is a well-known phenomenon (Ho *et al.*, 2008). This is likely to arise from the co-isolation of cells from the tissue of origin that may already be lineage committed with true MSCs that have multipotential differentiation capability. Attempts to reduce the amount of heterogeneity in primary-derived cultures include cell sorting, which is based on surface marker expression. Unfortunately, the number of reagents available for use with rat cells is currently extremely limited, and additionally, the yield of cells obtained after sorting is often greatly reduced. Consequently plastic adherence was used in this study as the sole method of selection for MSCs, and in spite of potential inherent heterogeneity, reports describing primary MSC cultures produced using plastic adherence alone are still very common. However, in this study phenotypic characterisation, by examining both known surface markers and differentiation potential, confirmed that the cells used in all investigations outlined here were MSCs.

Difficulty was experienced when attempting to compare data gathered during this investigation with that published in the literature, due to a lack of standardisation of protocols used for isolation and culturing of MSCs, as well as for the methodologies used for assessment of cellular proliferation and differentiation. Universal standardization of protocols used for MSC studies is therefore necessary, and will increase the scientific value of published studies in this field.

In conclusion, this study has confirmed that TNAP is present in rat-derived bmMSCs, scADSCs and pvADSCs, and that ALP activity, which is identified to be from TNAP, is present in these cells undergoing adipogenic induction *in vitro*. ALP activity was higher in all three cell types when treated with AM in comparison to treatment with OM, which is further indicative of a role for this enzyme during adipogenesis, although the mechanism of action of TNAP in adipogenesis remains unknown. Depot-specific differences in TNAP expression were discovered, most markedly between bmMSCs and ADSCs, where bmMSCs had the highest levels of ALP activity. These differences indicate that care should be taken when selecting an MSC type for use as a model for investigating TNAP, as well as for bone or adipose tissue engineering studies. TNAP expression was also higher in scADSCs compared

to pvADSCs, and this observation may provide insight into the metabolic differences between subcutaneous and visceral adipose tissues, especially with regards to the contribution of these tissues to conditions such as diabetes and obesity. Despite having the lowest levels of TNAP, pvADSCs were able to successfully accumulate lipid and differentiate towards an adipocyte phenotype, which may indicate that only relatively low levels of TNAP may be required for lipid accumulation. Much still remains to be discovered about the exact function of TNAP during adipogenesis and in maintenance of the adipocyte phenotype, as well as in the myriad of other tissues where it is present; however, this study has provided insight into the expression of TNAP during *in vitro* adipogenic and osteogenic differentiation of rat-derived MSCs.

References

Addison, W. N., Azari, F., Sorensen, E. S., Kaartinen, M. T. and McKee, M. D. (2007). Pyrophosphate inhibits mineralization of osteoblast cultures by binding to mineral, up-regulating osteopontin, and inhibiting alkaline phosphatase activity. *J Biol Chem* **282**(21): 15872-15883.

Alexander, D., Schafer, F., Olbrich, M., Friedrich, B., Buhring, H. J., Hoffmann, J. and Reinert, S. (2010). MSCA-1/TNAP selection of human jaw periosteal cells improves their mineralization capacity. *Cell Physiol Biochem* **26**(6): 1073-1080.

Ali, A. T., Ferris, W. F., Van der Merwe, M.-T., Jacobson, B. F., Paiker, J. E. and Crowther, N. J. (2013). Lipid accumulation and alkaline phosphatase activity in human preadipocytes isolated from different body fat depots. *JEMDSA* **18**(1): 58-64.

Ali, A. T., Penny, C. B., Paiker, J. E., Psaras, G., Ikram, F. and Crowther, N. J. (2006). The relationship between alkaline phosphatase activity and intracellular lipid accumulation in murine 3T3-L1 cells and human preadipocytes. *Analytical Biochemistry* **354**(2): 247-254.

Ali, A. T., Penny, C. B., Paiker, J. E., van Niekerk, C., Smit, A., Ferris, W. F. and Crowther, N. J. (2005). Alkaline phosphatase is involved in the control of adipogenesis in the murine preadipocyte cell line, 3T3-L1. *Clinica Chimica Acta* **354**(1-2): 101-109.

Alvaro, D., Benedetti, A., Marucci, L., Delle Monache, M., Monterubbianesi, R., Di Cosimo, E., Perego, L., Macarri, G., Glaser, S., Le Sage, G. and Alpini, G. (2000). The function of alkaline phosphatase in the liver: regulation of intrahepatic biliary epithelium secretory activities in the rat. *Hepatology* **32**(2): 174-184.

Alves, H., Mentink, A., Le, B., van Blitterswijk, C. A. and de Boer, J. (2013). Effect of antioxidant supplementation on the total yield, oxidative stress levels, and multipotency of bone marrow-derived human mesenchymal stromal cells. *Tissue Eng Part A* **19**(7-8): 928-937.

Alves, H., Munoz-Najar, U., De Wit, J., Renard, A. J., Hoeijmakers, J. H., Sedivy, J. M., Van Blitterswijk, C. and De Boer, J. (2010). A link between the accumulation of DNA damage and loss of multi-potency of human mesenchymal stromal cells. *J Cell Mol Med* **14**(12): 2729-2738.

Ambros, V. (2004). The functions of animal microRNAs. *Nature* **431**(7006): 350-355.

Arrigoni, E., Lopa, S., de Girolamo, L., Stanco, D. and Brini, A. T. (2009). Isolation, characterization and osteogenic differentiation of adipose-derived stem cells: from small to large animal models. *Cell Tissue Res* **338**(3): 401-411.

Atmani, H., Chappard, D. and Basle, M. F. (2003). Proliferation and differentiation of osteoblasts and adipocytes in rat bone marrow stromal cell cultures: effects of dexamethasone and calcitriol. *J Cell Biochem* **89**(2): 364-372.

Baer, P. C. and Geiger, H. (2012). Adipose-derived mesenchymal stromal/stem cells: tissue localization, characterization, and heterogeneity. *Stem Cells Int* **2012**: 812693.

Bassi, G., Pacelli, L., Carusone, R., Zanoncello, J. and Krampera, M. (2012). Adipose-derived stromal cells (ASCs). *Transfus Apher Sci* **47**(2): 193-198.

Battula, V. L., Treml, S., Bareiss, P. M., Gieseke, F., Roelofs, H., de Zwart, P., Muller, I., Schewe, B., Skutella, T., Fibbe, W. E., Kanz, L. and Buhring, H.-J. (2009). Isolation of functionally distinct mesenchymal stem cell subsets using antibodies against CD56, CD271, and mesenchymal stem cell antigen-1. *Haematologica* **94**(2): 173-184.

Bernlohr, D. A., Angus, C. W., Lane, M. D., Bolanowski, M. A. and Kelly, T. J., Jr. (1984). Expression of specific mRNAs during adipose differentiation: identification of an mRNA encoding a homologue of myelin P2 protein. *Proc Natl Acad Sci U S A* **81**(17): 5468-5472.

Bernstein, H. G., Jager, K., Dobrowolny, H., Steiner, J., Keilhoff, G., Bogerts, B. and Laube, G. (2015). Possible sources and functions of L-homoarginine in the brain: review of the literature and own findings. *Amino Acids* **47**(9): 1729-1740.

Bianco, P., Costantini, M., Dearden, L. C. and Bonucci, E. (1988). Alkaline phosphatase positive precursors of adipocytes in the human bone marrow. *Br J Haematol* **68**(4): 401-403.

Bianco, P., Riminucci, M., Gronthos, S. and Robey, P. G. (2001). Bone marrow stromal stem cells: nature, biology, and potential applications. *Stem Cells* **19**(3): 180-192.

Bianco, P., Robey, P. G. and Simmons, P. J. (2008). Mesenchymal stem cells: revisiting history, concepts, and assays. *Cell Stem Cell* **2**(4): 313-319.

Blair, H. C., Schlesinger, P. H., Huang, C. L. and Zaidi, M. (2007). Calcium signalling and calcium transport in bone disease. *Subcell Biochem* **45**: 539-562.

Bodansky, O. and Schwartz, M. K. (1963). Comparative Effects of L-Histidine on the Activities of 5'-Nucleotidase and Alkaline Phosphatase. *J Biol Chem* **238**: 3420-3427.

Boiret, N., Rapatel, C., Veyrat-Masson, R., Guillouard, L., Guerin, J. J., Pigeon, P., Descamps, S., Boisgard, S. and Berger, M. G. (2005). Characterization of nonexpanded mesenchymal progenitor cells from normal adult human bone marrow. *Exp Hematol* **33**(2): 219-225.

Borgers, M. (1973). The cytochemical application of new potent inhibitors of alkaline phosphatases. *J Histochem Cytochem* **21**(9): 812-824.

Bossi, M., Hoylaerts, M. F. and Millan, J. L. (1993). Modifications in a flexible surface loop modulate the isozyme-specific properties of mammalian alkaline phosphatases. *J Biol Chem* **268**(34): 25409-25416.

Bowers, R. R., Kim, J. W., Otto, T. C. and Lane, M. D. (2006). Stable stem cell commitment to the adipocyte lineage by inhibition of DNA methylation: role of the BMP-4 gene. *Proc Natl Acad Sci U S A* **103**(35): 13022-13027.

Bowers, R. R. and Lane, M. D. (2007). A role for bone morphogenetic protein-4 in adipocyte development. *Cell Cycle* **6**(4): 385-389.

Boyko, E. J., Fujimoto, W. Y., Leonetti, D. L. and Newell-Morris, L. (2000). Visceral adiposity and risk of type 2 diabetes: a prospective study among Japanese Americans. *Diabetes Care* **23**(4): 465-471.

Bradford, M. M. (1976). A rapid and sensitive method for the quantitation of microgram quantities of protein utilizing the principle of protein-dye binding. *Anal Biochem* **72**: 248-254.

Brinchmann, J. E. (2008). Expanding autologous multipotent mesenchymal bone marrow stromal cells. *J Neurol Sci* **265**(1-2): 127-130.

Bruedigam, C., Eijken, M., Koedam, M., van de Peppel, J., Drabek, K., Chiba, H. and van Leeuwen, J. P. (2010). A new concept underlying stem cell lineage skewing that explains the detrimental effects of thiazolidinediones on bone. *Stem Cells* **28**(5): 916-927.

Brun-Heath, I., Ermonval, M., Chabrol, E., Xiao, J., Palkovits, M., Lyck, R., Miller, F., Couraud, P. O., Mornet, E. and Fonta, C. (2011). Differential expression of the bone and the liver tissue non-specific alkaline phosphatase isoforms in brain tissues. *Cell Tissue Res* **343**(3): 521-536.

Bunnell, B. A., Flaat, M., Gagliardi, C., Patel, B. and Ripoll, C. (2008). Adipose-derived stem cells: isolation, expansion and differentiation. *Methods* **45**(2): 115-120.

Cappellesso-Fleury, S., Puissant-Lubrano, B., Apoil, P. A., Titeux, M., Winterton, P., Casteilla, L., Bourin, P. and Blancher, A. (2010). Human fibroblasts share immunosuppressive properties with bone marrow mesenchymal stem cells. *J Clin Immunol* **30**(4): 607-619.

Casteilla, L., Planat-Benard, V., Laharrague, P. and Cousin, B. (2011). Adipose-derived stromal cells: Their identity and uses in clinical trials, an update. *World J Stem Cells* **3**(4): 25-33.

Chang, C. H., Angellis, D. and Fishman, W. H. (1980). Presence of the rare D-variant heat-stable, placental-type alkaline phosphatase in normal human testis. *Cancer Res* **40**(5): 1506-1510.

Chen, C. T., Shih, Y. R., Kuo, T. K., Lee, O. K. and Wei, Y. H. (2008). Coordinated changes of mitochondrial biogenesis and antioxidant enzymes during osteogenic differentiation of human mesenchymal stem cells. *Stem Cells* **26**(4): 960-968.

Chen, F. H., Song, L., Mauck, R. L., Li, W.-J., Tuan, R. S., Robert, L., Robert, L. and Joseph, V. (2007). Mesenchymal stem cells. Principles of Tissue Engineering (Third Edition). Burlington, Academic Press**:** 823-843.

Christiaens, V., Van Hul, M., Lijnen, H. R. and Scroyen, I. (2012). CD36 promotes adipocyte differentiation and adipogenesis. *Biochim Biophys Acta* **1820**(7): 949-956.

Collas, P., Noer, A. and Sorensen, A. L. (2008). Epigenetic Basis for the Differentiation Potential of Mesenchymal and Embryonic Stem Cells. *Transfus Med Hemother* **35**(3): 205-215.

Compston, J. (2010). Management of glucocorticoid-induced osteoporosis. *Nat Rev Rheumatol* **6**(2): 82-88.

Corselli, M., Chen, C. W., Crisan, M., Lazzari, L. and Peault, B. (2010). Perivascular ancestors of adult multipotent stem cells. *Arterioscler Thromb Vasc Biol* **30**(6): 1104-1109.

Covas, D. T., Panepucci, R. A., Fontes, A. M., Silva, W. A., Jr., Orellana, M. D., Freitas, M. C., Neder, L., Santos, A. R., Peres, L. C., Jamur, M. C. and Zago, M. A. (2008). Multipotent mesenchymal stromal cells obtained from diverse human tissues share functional properties and gene-expression profile with CD146+ perivascular cells and fibroblasts. *Exp Hematol* **36**(5): 642-654.

Cuatrecasas, P. and Illiano, G. (1971). Membrane sialic acid and the mechanism of insulin action in adipose tissue cells. Effects of digestion with neuraminidase. *J Biol Chem* **246**(16): 4938-4946.

Cyboron, G. W., Vejins, M. S. and Wuthier, R. E. (1982). Activity of epiphyseal cartilage membrane alkaline phosphatase and the effects of its inhibitors at physiological pH. *J Biol Chem* **257**(8): 4141-4146.

Czekanska, E. M., Stoddart, M. J., Ralphs, J. R., Richards, R. G. and Hayes, J. S. (2014). A phenotypic comparison of osteoblast cell lines versus human primary osteoblasts for biomaterials testing. *J Biomed Mater Res A* **102**(8): 2636-2643.

Czekanska, E. M., Stoddart, M. J., Richards, R. G. and Hayes, J. S. (2012). In search of an osteoblast cell model for in vitro research. *Eur Cell Mater* **24**: 1-17.

da Silva Meirelles, L. and Nardi, N. B. (2011). Methods of Isolation and Culture of Adult Stem Cells. Regenerative Nephrology. San Diego, Academic Press**:** 217-229.

Delgado-Calle, J., Sanudo, C., Sanchez-Verde, L., Garcia-Renedo, R. J., Arozamena, J. and Riancho, J. A. (2011). Epigenetic regulation of alkaline phosphatase in human cells of the osteoblastic lineage. *Bone* **49**(4): 830-838.

Denu, R. A. and Hematti, P. (2016). Effects of Oxidative Stress on Mesenchymal Stem Cell Biology. *Oxid Med Cell Longev* **2016**: Article ID 2989076.

Derubeis, A. R. and Cancedda, R. (2004). Bone marrow stromal cells (BMSCs) in bone engineering: limitations and recent advances. *Ann Biomed Eng* **32**(1): 160-165.

Dezawa, M., Ishikawa, H., Itokazu, Y., Yoshihara, T., Hoshino, M., Takeda, S., Ide, C. and Nabeshima, Y. (2005). Bone marrow stromal cells generate muscle cells and repair muscle degeneration. *Science* **309**(5732): 314-317.

Di Lorenzo, D., Albertini, A. and Zava, D. (1991). Progestin regulation of alkaline phosphatase in the human breast cancer cell line T47D. *Cancer Res* **51**(16): 4470-4475.

Diaz-Hernandez, M., Gomez-Ramos, A., Rubio, A., Gomez-Villafuertes, R., Naranjo, J. R., Miras-Portugal, M. T. and Avila, J. (2010). Tissue-nonspecific alkaline phosphatase promotes the neurotoxicity effect of extracellular tau. *J Biol Chem* **285**(42): 32539-32548.

Ding, J., Ghali, O., Lencel, P., Broux, O., Chauveau, C., Devedjian, J. C., Hardouin, P. and Magne, D. (2009). TNF-alpha and IL-1beta inhibit RUNX2 and collagen expression but increase alkaline phosphatase activity and mineralization in human mesenchymal stem cells. *Life Sci* **84**(15-16): 499-504.

Doellgast, G. J. and Benirschke, K. (1979). Placental alkaline phosphatase in Hominidae. *Nature* **280**(5723): 601-602.

Dominici, M., Le Blanc, K., Mueller, I., Slaper-Cortenbach, I., Marini, F., Krause, D., Deans, R., Keating, A., Prockop, D. and Horwitz, E. (2006). Minimal criteria for defining multipotent mesenchymal stromal cells. The International Society for Cellular Therapy position statement. *Cytotherapy* **8**(4): 315-317.

Ducy, P. (2000). Cbfa1: a molecular switch in osteoblast biology. *Dev Dyn* **219**(4): 461-471.

Ducy, P., Desbois, C., Boyce, B., Pinero, G., Story, B., Dunstan, C., Smith, E., Bonadio, J., Goldstein, S., Gundberg, C., Bradley, A. and Karsenty, G. (1996). Increased bone formation in osteocalcin-deficient mice. *Nature* **382**(6590): 448-452.

Ducy, P., Starbuck, M., Priemel, M., Shen, J., Pinero, G., Geoffroy, V., Amling, M. and Karsenty, G. (1999). A Cbfa1-dependent genetic pathway controls bone formation beyond embryonic development. *Genes Dev* **13**(8): 1025-1036.

Dziedziejko, V., Safranow, K., Slowik-Zylka, D., Machoy-Mokrzynska, A., Millo, B., Machoy, Z. and Chlubek, D. (2005). Comparison of rat and human alkaline phosphatase isoenzymes and isoforms using HPLC and electrophoresis. *Biochim Biophys Acta* **1752**(1): 26-33.

Eguchi, M. (1995). Alkaline phosphatase isozymes in insects and comparison with mammalian enzyme. *Comp Biochem Physiol B Biochem Mol Biol* **111**(2): 151-162.

Elahi, K. C., Klein, G., Avci-Adali, M., Sievert, K. D., MacNeil, S. and Aicher, W. K. (2016). Human Mesenchymal Stromal Cells from Different Sources Diverge in Their Expression of Cell Surface Proteins and Display Distinct Differentiation Patterns. *Stem Cells Int* **2016**: Article ID 5646384.

Elbashir, S. M., Lendeckel, W. and Tuschl, T. (2001). RNA interference is mediated by 21- and 22-nucleotide RNAs. *Genes Dev* **15**(2): 188-200.

Ermonval, M., Baudry, A., Baychelier, F., Pradines, E., Pietri, M., Oda, K., Schneider, B., Mouillet-Richard, S., Launay, J. M. and Kellermann, O. (2009). The cellular prion protein interacts with the tissue non-specific alkaline phosphatase in membrane microdomains of bioaminergic neuronal cells. *PLoS One* **4**(8): e6497.

Estaki, M., DeCoffe, D. and Gibson, D. L. (2014). Interplay between intestinal alkaline phosphatase, diet, gut microbes and immunity. *World J Gastroenterol* **20**(42): 15650-15656.

Esteve, D., Boulet, N., Volat, F., Zakaroff-Girard, A., Ledoux, S., Coupaye, M., Decaunes, P., Belles, C., Gaits-Iacovoni, F., Iacovoni, J. S., Remaury, A., Castel, B., Ferrara, P., Heymes, C., Lafontan, M., Bouloumie, A. and Galitzky, J. (2015). Human white and brite adipogenesis is supported by MSCA1 and is impaired by immune cells. *Stem Cells* **33**(4): 1277-1291.

Fedde, K. N., Lane, C. C. and Whyte, M. P. (1988). Alkaline phosphatase is an ectoenzyme that acts on micromolar concentrations of natural substrates at physiologic pH in human osteosarcoma (SAOS-2) cells. *Archives of Biochemistry and Biophysics* **264**(2): 400-409.

Fernandez Vallone, V. B., Romaniuk, M. A., Choi, H., Labovsky, V., Otaegui, J. and Chasseing, N. A. (2013). Mesenchymal stem cells and their use in therapy: what has been achieved? *Differentiation* **85**(1-2): 1-10.

Fishman, W. H. (1990). Alkaline phosphatase isozymes: recent progress. *Clinical Biochemistry* **23**(2): 99-104.

Fishman, W. H., Inglis, N. I., Stolbach, L. L. and Krant, M. J. (1968). A serum alkaline phosphatase isoenzyme of human neoplastic cell origin. *Cancer Res* **28**(1): 150-154.

Fishman, W. H., Inglis, N. R., Green, S., Anstiss, C. L., Gosh, N. K., Reif, A. E., Rustigian, R., Krant, M. J. and Stolbach, L. L. (1968). Immunology and biochemistry of Regan isoenzyme of alkaline phosphatase in human cancer. *Nature* **219**(5155): 697-699.

Fonta, C., Negyessy, L., Renaud, L. and Barone, P. (2004). Areal and subcellular localization of the ubiquitous alkaline phosphatase in the primate cerebral cortex: evidence for a role in neurotransmission. *Cereb Cortex* **14**(6): 595-609.

Foudah, D., Redaelli, S., Donzelli, E., Bentivegna, A., Miloso, M., Dalpra, L. and Tredici, G. (2009). Monitoring the genomic stability of in vitro cultured rat bone-marrow-derived mesenchymal stem cells. *Chromosome Res* **17**(8): 1025-1039.

Franz-Odendaal, T., Hall, B. K. and Witten, P. E. (2006). Buried alive: How osteoblasts become osteocytes *Developmental Dymanics* **235**: 176-190.

Friedenstein, A. J., Chailakhjan, R. K. and Lalykina, K. S. (1970). The development of fibroblast colonies in monolayer cultures of guinea-pig bone marrow and spleen cells. *Cell Tissue Kinet* **3**(4): 393-403.

Friedman, R. C., Farh, K. K., Burge, C. B. and Bartel, D. P. (2009). Most mammalian mRNAs are conserved targets of microRNAs. *Genome Res* **19**(1): 92-105.

Fujiki, K., Kano, F., Shiota, K. and Murata, M. (2009). Expression of the peroxisome proliferator activated receptor gamma gene is repressed by DNA methylation in visceral adipose tissue of mouse models of diabetes. *BMC Biol* **7**: 38.

Fukuen, S., Iwaki, M., Yasui, A., Makishima, M., Matsuda, M. and Shimomura, I. (2005). Sulfonylurea agents exhibit peroxisome proliferator-activated receptor gamma agonistic activity. *J Biol Chem* **280**(25): 23653-23659.

Galderisi, U. and Giordano, A. (2014). The gap between the physiological and therapeutic roles of mesenchymal stem cells. *Med Res Rev* **34**(5): 1100-1126.

Gazit, Z., Aslan, H., Gafni, Y., Kimelman, N., Pelled, G. and Gazit, D. (2008). Mesenchymal Stem Cells. Principles of Regenerative Medicine. San Diego, Academic Press**:** 318-343.

Ghosh, K., Mazumder Tagore, D., Anumula, R., Lakshmaiah, B., Kumar, P. P., Singaram, S., Matan, T., Kallipatti, S., Selvam, S., Krishnamurthy, P. and Ramarao, M. (2013). Crystal structure of rat intestinal alkaline phosphatase--role of crown domain in mammalian alkaline phosphatases. *J Struct Biol* **184**(2): 182-192.

Gianni, M., Terao, M., Sozzani, S. and Garattini, E. (1993). Retinoic acid and cyclic AMP synergistically induce the expression of liver/bone/kidney-type alkaline phosphatase gene in L929 fibroblastic cells. *Biochem J* **296 (Pt 1)**: 67-77.

Gijsbers, R., Ceulemans, H., Stalmans, W. and Bollen, M. (2001). Structural and catalytic similarities between nucleotide pyrophosphatases/phosphodiesterases and alkaline phosphatases. *J Biol Chem* **276**(2): 1361-1368.

Gimble, J. M., Katz, A. J. and Bunnell, B. A. (2007). Adipose-derived stem cells for regenerative medicine. *Circ Res* **100**(9): 1249-1260.

Gimble, J. M. and Nuttall, M. E. (2012). The relationship between adipose tissue and bone metabolism. *Clin Biochem* **45**(12): 874-879.

Ginsburg, M., Snow, M. H. and McLaren, A. (1990). Primordial germ cells in the mouse embryo during gastrulation. *Development* **110**(2): 521-528.

Goldstein, D. J., Rogers, C. and Harris, H. (1982). A search for trace expression of placental-like alkaline phosphatase in non-malignant human tissues: demonstration of its occurrence in lung, cervix, testis and thymus. *Clin Chim Acta* **125**(1): 63-75.

Gomez-Ambrosi, J., Rodriguez, A., Catalan, V. and Fruhbeck, G. (2008). The bone-adipose axis in obesity and weight loss. *Obes Surg* **18**(9): 1134-1143.

Gomez-Ramos, A., Diaz-Hernandez, M., Cuadros, R., Hernandez, F. and Avila, J. (2006). Extracellular tau is toxic to neuronal cells. *FEBS Lett* **580**(20): 4842-4850.

Grégoire, F., Genart, C., Hauser, N. and Remacle, C. (1991). Glucocorticoids induce a drastic inhibition of proliferation and stimulate differentiation of adult rat fat cell precursors. *Experimental Cell Research* **196**(2): 270-278.

Gregoire, F. M., Smas, C. M. and Sul, H. S. (1998). Understanding adipocyte differentiation. *Physiol Rev* **78**(3): 783-809.

Guo, L., Zhao, R. C. and Wu, Y. (2011). The role of microRNAs in self-renewal and differentiation of mesenchymal stem cells. *Exp Hematol* **39**(6): 608-616.

Hahnel, A. C., Rappolee, D. A., Millan, J. L., Manes, T., Ziomek, C. A., Theodosiou, N. G., Werb, Z., Pedersen, R. A. and Schultz, G. A. (1990). Two alkaline phosphatase genes are expressed during early development in the mouse embryo. *Development* **110**(2): 555-564.

Halling Linder, C., Narisawa, S., Millan, J. L. and Magnusson, P. (2009). Glycosylation differences contribute to distinct catalytic properties among bone alkaline phosphatase isoforms. *Bone* **45**(5): 987-993.

Hanics, J., Barna, J., Xiao, J., Millan, J. L., Fonta, C. and Negyessy, L. (2012). Ablation of TNAP function compromises myelination and synaptogenesis in the mouse brain. *Cell Tissue Res* **349**(2): 459-471.

Harris, H. (1990). The human alkaline phosphatases: What we know and what we don't know. *Clinica Chimica Acta* **186**(2): 133-150.

Hayashi, O., Katsube, Y., Hirose, M., Ohgushi, H. and Ito, H. (2008). Comparison of osteogenic ability of rat mesenchymal stem cells from bone marrow, periosteum, and adipose tissue. *Calcif Tissue Int* **82**(3): 238-247.

Henthorn, P. S., Raducha, M., Kadesch, T., Weiss, M. J. and Harris, H. (1988). Sequence and characterization of the human intestinal alkaline phosphatase gene. *J Biol Chem* **263**(24): 12011-12019.

Hessle, L., Johnson, K. A., Anderson, H. C., Narisawa, S., Sali, A., Goding, J. W., Terkeltaub, R. and Millan, J. L. (2002). Tissue-nonspecific alkaline phosphatase and plasma cell membrane glycoprotein-1 are central antagonistic regulators of bone mineralization. *Proc Natl Acad Sci U S A* **99**(14): 9445-9449.

Ho, A. D., Wagner, W. and Franke, W. (2008). Heterogeneity of mesenchymal stromal cell preparations. *Cytotherapy* **10**(4): 320-330.

Horwitz, E. M. (2003). Stem cell plasticity: the growing potential of cellular therapy. *Archives of Medical Research* **34**(6): 600-606.

Horwitz, E. M., Andreef, M. and Frassoni, F. (2007). Mesenchymal Stromal Cells. *Biology of Blood and Marrow Transplantation* **13**(Supplement 1): 53-57.

Horwitz, E. M., Le Blanc, K., Dominici, M., Mueller, I., Slaper-Cortenbach, I., Marini, F. C., Deans, R. J., Krause, D. S. and Keating, A. (2005). Clarification of the nomenclature for MSC: The International Society for Cellular Therapy position statement. *Cytotherapy* **7**(5): 393-395.

Houlihan, D. D., Mabuchi, Y., Morikawa, S., Niibe, K., Araki, D., Suzuki, S., Okano, H. and Matsuzaki, Y. (2012). Isolation of mouse mesenchymal stem cells on the basis of expression of Sca-1 and PDGFR-alpha. *Nat Protoc* **7**(12): 2103-2111.

Hoylaerts, M. F., Ding, L., Narisawa, S., Van Kerckhoven, S. and Millan, J. L. (2006). Mammalian alkaline phosphatase catalysis requires active site structure stabilization via the N-terminal amino acid microenvironment. *Biochemistry* **45**(32): 9756-9766.

Hoylaerts, M. F., Manes, T. and Millan, J. L. (1997). Mammalian alkaline phosphatases are allosteric enzymes. *J Biol Chem* **272**(36): 22781-22787.

Hu, R., Li, H., Liu, W., Yang, L., Tan, Y. F. and Luo, X. H. (2010). Targeting miRNAs in osteoblast differentiation and bone formation. *Expert Opin Ther Targets* **14**(10): 1109-1120.

Huang, H., Song, T. J., Li, X., Hu, L., He, Q., Liu, M., Lane, M. D. and Tang, Q. Q. (2009). BMP signaling pathway is required for commitment of C3H10T1/2 pluripotent stem cells to the adipocyte lineage. *Proc Natl Acad Sci U S A* **106**(31): 12670-12675.

Huang, J., Zhao, L., Xing, L. and Chen, D. (2010). MicroRNA-204 regulates Runx2 protein expression and mesenchymal progenitor cell differentiation. *Stem Cells* **28**(2): 357-364.

Hulme-Moir, K. L. and Clark, P. (2011). Sub-cellular localisation of alkaline phosphatase activity in the cytoplasm of tammar wallaby (Macropus eugenii) neutrophils and eosinophils. *Vet Immunol Immunopathol* **142**(1-2): 126-132.

Imhoff, B. R. and Hansen, J. M. (2010). Differential redox potential profiles during adipogenesis and osteogenesis. *Cell Mol Biol Lett* **16**(1): 149-161.

Itasaki, N. and Hoppler, S. (2010). Crosstalk between Wnt and bone morphogenic protein signaling: a turbulent relationship. *Dev Dyn* **239**(1): 16-33.

Jain, N. C. (1968). Alkaline phosphatase activity in leukocytes of some animal species. *Acta Haematol* **39**(1): 51-59.

Jaiswal, N., Haynesworth, S. E., Caplan, A. I. and Bruder, S. P. (1997). Osteogenic differentiation of purified, culture-expanded human mesenchymal stem cells in vitro. *J Cell Biochem* **64**(2): 295-312.

James, A. W. (2013). Review of Signaling Pathways Governing MSC Osteogenic and Adipogenic Differentiation. *Scientifica (Cairo)* **2013**: 684736.

Javazon, E. H., Colter, D. C., Schwarz, E. J. and Prockop, D. J. (2001). Rat marrow stromal cells are more sensitive to plating density and expand more rapidly from single-cell-derived colonies than human marrow stromal cells. *Stem Cells* **19**(3): 219-225.

Johnson, K. A., Hessle, L., Vaingankar, S., Wennberg, C., Mauro, S., Narisawa, S., Goding, J. W., Sano, K., Millan, J. L. and Terkeltaub, R. (2000). Osteoblast tissue-nonspecific alkaline phosphatase antagonizes and regulates PC-1. *Am J Physiol Regul Integr Comp Physiol* **279**(4): R1365-1377.

Kang, Q., Song, W. X., Luo, Q., Tang, N., Luo, J., Luo, X., Chen, J., Bi, Y., He, B. C., Park, J. K., Jiang, W., Tang, Y., Huang, J., Su, Y., Zhu, G. H., He, Y., Yin, H., Hu, Z., Wang, Y., Chen, L., Zuo, G. W., Pan, X., Shen, J., Vokes, T., Reid, R. R., Haydon, R. C., Luu, H. H. and He, T. C. (2009). A comprehensive analysis of the dual roles of BMPs in regulating adipogenic and osteogenic differentiation of mesenchymal progenitor cells. *Stem Cells Dev* **18**(4): 545-559.

Kassem, M., Abdallah, B. M. and Saeed, H. (2008). Osteoblastic cells: differentiation and trans-differentiation. *Arch Biochem Biophys* **473**(2): 183-187.

Keating, A. (2012). Mesenchymal stromal cells: new directions. *Cell Stem Cell* **10**(6): 709-716.

Kellett, K. A., Williams, J., Vardy, E. R., Smith, A. D. and Hooper, N. M. (2011). Plasma alkaline phosphatase is elevated in Alzheimer's disease and inversely correlates with cognitive function. *Int J Mol Epidemiol Genet* **2**(2): 114-121.

Kikuchi, Y., Takagi, M., Parmley, R. T., Ghanta, V. K. and Hiramoto, R. N. (1982). Inhibitory effect of L-homoarginine on murine osteosarcoma cell proliferation. *Cancer Res* **42**(3): 1072-1077.

Kim, T. K. and Eberwine, J. H. (2010). Mammalian cell transfection: the present and the future. *Anal Bioanal Chem* **397**(8): 3173-3178.

Kim, Y. H., Yoon, D. S., Kim, H. O. and Lee, J. W. (2012). Characterization of different subpopulations from bone marrow-derived mesenchymal stromal cells by alkaline phosphatase expression. *Stem Cells Dev* **21**(16): 2958-2968.

Klein, B. Y., Gal, I. and Segal, D. (1993). Studies of the levamisole inhibitory effect on rat stromal-cell commitment to mineralization. *J Cell Biochem* **53**(2): 114-121.

Ko, E., Lee, K. Y. and Hwang, D. S. (2012). Human umbilical cord blood-derived mesenchymal stem cells undergo cellular senescence in response to oxidative stress. *Stem Cells Dev* **21**(11): 1877-1886.

Kodama, H., Koyama, H., Sudo, H. and Kasai, S. (1983). Adipose conversion of mouse bone marrow fibroblasts in vitro: their alkaline phosphatase activity. *Cell Struct Funct* **8**(1): 19-27.

Kollmer, M., Buhrman, J. S., Zhang, Y. and Gemeinhart, R. A. (2013). Markers Are Shared Between Adipogenic and Osteogenic Differentiated Mesenchymal Stem Cells. *J Dev Biol Tissue Eng* **5**(2): 18-25.

Kozlenkov, A., Le Du, M. H., Cuniasse, P., Ny, T., Hoylaerts, M. F. and Millan, J. L. (2004). Residues determining the binding specificity of uncompetitive inhibitors to tissue-nonspecific alkaline phosphatase. *J Bone Miner Res* **19**(11): 1862-1872.

Kozlenkov, A., Manes, T., Hoylaerts, M. F. and Millan, J. L. (2002). Function assignment to conserved residues in mammalian alkaline phosphatases. *J Biol Chem* **277**(25): 22992-22999.

Kuroda, S., Virdi, A. S., Dai, Y., Shott, S. and Sumner, D. R. (2005). Patterns and localization of gene expression during intramembranous bone regeneration in the rat femoral marrow ablation model. *Calcif Tissue Int* **77**(4): 212-225.

Lacey, D. L., Timms, E., Tan, H. L., Kelley, M. J., Dunstan, C. R., Burgess, T., Elliott, R., Colombero, A., Elliott, G., Scully, S., Hsu, H., Sullivan, J., Hawkins, N., Davy, E., Capparelli, C., Eli, A., Qian, Y. X., Kaufman, S., Sarosi, I., Shalhoub, V., Senaldi, G., Guo, J., Delaney, J. and Boyle, W. J. (1998). Osteoprotegerin ligand is a cytokine that regulates osteoclast differentiation and activation. *Cell* **93**(2): 165-176.

Laine, S. K., Alm, J. J., Virtanen, S. P., Aro, H. T. and Laitala-Leinonen, T. K. (2012). MicroRNAs miR-96, miR-124, and miR-199a regulate gene expression in human bone marrow-derived mesenchymal stem cells. *J Cell Biochem* **113**(8): 2687-2695.

Lalles, J. P. (2010). Intestinal alkaline phosphatase: multiple biological roles in maintenance of intestinal homeostasis and modulation by diet. *Nutr Rev* **68**(6): 323-332.

Lalles, J. P. (2014). Intestinal alkaline phosphatase: novel functions and protective effects. *Nutr Rev* **72**(2): 82-94.

Langer, D., Ikehara, Y., Takebayashi, H., Hawkes, R. and Zimmermann, H. (2007). The ectonucleotidases alkaline phosphatase and nucleoside triphosphate diphosphohydrolase 2 are associated with subsets of progenitor cell populations in the mouse embryonic, postnatal and adult neurogenic zones. *Neuroscience* **150**(4): 863-879.

Laughton, C. (1986). Measurement of the specific lipid content of attached cells in microtiter cultures. *Anal Biochem* **156**(2): 307-314.

Le Du, M. H., Stigbrand, T., Taussig, M. J., Menez, A. and Stura, E. A. (2001). Crystal structure of alkaline phosphatase from human placenta at 1.8 A resolution. Implication for a substrate specificity. *J Biol Chem* **276**(12): 9158-9165.

Leontieva, O. V., Demidenko, Z. N. and Blagosklonny, M. V. (2014). Contact inhibition and high cell density deactivate the mammalian target of rapamycin pathway, thus suppressing the senescence program. *Proc Natl Acad Sci U S A* **111**(24): 8832-8837.

Levandoski, M. M., Piket, B. and Chang, J. (2003). The anthelmintic levamisole is an allosteric modulator of human neuronal nicotinic acetylcholine receptors. *Eur J Pharmacol* **471**(1): 9-20.

Levi, B., James, A. W., Glotzbach, J. P., Wan, D. C., Commons, G. W. and Longaker, M. T. (2010). Depot-specific variation in the osteogenic and adipogenic potential of human adipose-derived stromal cells. *Plast Reconstr Surg* **126**(3): 822-834.

Lin, C. W. and Fishman, W. H. (1972). L-Homoarginine. An organ-specific, uncompetitive inhibitor of human liver and bone alkaline phosphohydrolases. *J Biol Chem* **247**(10): 3082-3087.

Lin, L., Dai, S. D. and Fan, G. Y. (2010). Glucocorticoid-induced differentiation of primary cultured bone marrow mesenchymal cells into adipocytes is antagonized by exogenous Runx2. *Apmis* **118**(8): 595-605.

Liu, Z., Shi, W., Ji, X., Sun, C., Jee, W. S., Wu, Y., Mao, Z., Nagy, T. R., Li, Q. and Cao, X. (2004). Molecules mimicking Smad1 interacting with Hox stimulate bone formation. *J Biol Chem* **279**(12): 11313-11319.

Liu, Z. J., Zhuge, Y. and Velazquez, O. C. (2009). Trafficking and differentiation of mesenchymal stem cells. *J Cell Biochem* **106**(6): 984-991.

Llinas, P., Stura, E. A., Menez, A., Kiss, Z., Stigbrand, T., Millan, J. L. and Le Du, M. H. (2005). Structural studies of human placental alkaline phosphatase in complex with functional ligands. *J Mol Biol* **350**(3): 441-451.

Locke, M., Feisst, V. and Dunbar, P. R. (2011). Concise review: human adipose-derived stem cells: separating promise from clinical need. *Stem Cells* **29**(3): 404-411.

Lomashvili, K. A., Garg, P., Narisawa, S., Millan, J. L. and O'Neill, W. C. (2008). Upregulation of alkaline phosphatase and pyrophosphate hydrolysis: potential mechanism for uremic vascular calcification. *Kidney Int* **73**(9): 1024-1030.

Lopez-Posadas, R., Gonzalez, R., Ballester, I., Martinez-Moya, P., Romero-Calvo, I., Suarez, M. D., Zarzuelo, A., Martinez-Augustin, O. and Sanchez de Medina, F. (2011). Tissue-

nonspecific alkaline phosphatase is activated in enterocytes by oxidative stress via changes in glycosylation. *Inflamm Bowel Dis* **17**(2): 543-556.

Lopez, M. J. and Spencer, N. D. (2011). In vitro adult rat adipose tissue-derived stromal cell isolation and differentiation. *Methods Mol Biol* **702**: 37-46.

Lorenz, B. and Schroder, H. C. (2001). Mammalian intestinal alkaline phosphatase acts as highly active exopolyphosphatase. *Biochim Biophys Acta* **1547**(2): 254-261.

Luft, C. and Ketteler, R. (2015). Electroporation Knows No Boundaries: The Use of Electrostimulation for siRNA Delivery in Cells and Tissues. *J Biomol Screen* **20**(8): 932-942.

Mabuchi, Y., Houlihan, D. D., Akazawa, C., Okano, H. and Matsuzaki, Y. (2013). Prospective isolation of murine and human bone marrow mesenchymal stem cells based on surface markers. *Stem Cells Int* **2013**: 507301.

MacDougald, O. A. and Mandrup, S. (2002). Adipogenesis: forces that tip the scales. *Trends Endocrinol Metab* **13**(1): 5-11.

Malaval, L., Wade-Gueye, N. M., Boudiffa, M., Fei, J., Zirngibl, R., Chen, F., Laroche, N., Roux, J. P., Burt-Pichat, B., Duboeuf, F., Boivin, G., Jurdic, P., Lafage-Proust, M. H., Amedee, J., Vico, L., Rossant, J. and Aubin, J. E. (2008). Bone sialoprotein plays a functional role in bone formation and osteoclastogenesis. *J Exp Med* **205**(5): 1145-1153.

Malo, M. S., Moaven, O., Muhammad, N., Biswas, B., Alam, S. N., Economopoulos, K. P., Gul, S. S., Hamarneh, S. R., Malo, N. S., Teshager, A., Mohamed, M. M., Tao, Q., Narisawa, S., Millan, J. L., Hohmann, E. L., Warren, H. S., Robson, S. C. and Hodin, R. A. (2014). Intestinal alkaline phosphatase promotes gut bacterial growth by reducing the concentration of luminal nucleotide triphosphates. *Am J Physiol Gastrointest Liver Physiol* **306**(10): G826-838.

Marko, O., Cascieri, M. A., Ayad, N., Strader, C. D. and Candelore, M. R. (1995). Isolation of a preadipocyte cell line from rat bone marrow and differentiation to adipocytes. *Endocrinology* **136**(10): 4582-4588.

Martin, C., Chevrot, M., Poirier, H., Passilly-Degrace, P., Niot, I. and Besnard, P. (2011). CD36 as a lipid sensor. *Physiol Behav* **105**(1): 36-42.

Martins, M. J., Negrao, M. R. and Hipolito-Reis, C. (2001). Alkaline phosphatase from rat liver and kidney is differentially modulated. *Clin Biochem* **34**(6): 463-468.

Matsuura, S., Kishi, F. and Kajii, T. (1990). Characterization of a 5'-flanking region of the human liver/bone/kidney alkaline phosphatase gene: two kinds of mRNA from a single gene. *Biochem Biophys Res Commun* **168**(3): 993-1000.

McCauley, L. K. (2010). c-Maf and you won't see fat. *J Clin Invest* **120**(10): 3440-3442.

Mendez-Ferrer, S., Scadden, D. T. and Sanchez-Aguilera, A. (2015). Bone marrow stem cells: current and emerging concepts. *Ann N Y Acad Sci* **1335**: 32-44.

Merchant-Larios, H., Mendlovic, F. and Alvarez-Buylla, A. (1985). Characterization of alkaline phosphatase from primordial germ cells and ontogenesis of this enzyme in the mouse. *Differentiation* **29**(2): 145-151.

Millan, J. L. (2013). The role of phosphatases in the initiation of skeletal mineralization. *Calcif Tissue Int* **93**(4): 299-306.

Millán, J. L. (2006). Alkaline Phosphatases : Structure, substrate specificity and functional relatedness to other members of a large superfamily of enzymes. *Purinergic Signal* **2**(2): 335-341.

Millán, J. L. (2006). Mammalian alkaline phosphatases: from biology to applications in medicine and biotechnology, Wiley-VCH Verlag GmbH & Co. KGaA, Weinheim, FRG. .

Millan, J. L. and Manes, T. (1988). Seminoma-derived Nagao isozyme is encoded by a germ-cell alkaline phosphatase gene. *Proc Natl Acad Sci U S A* **85**(9): 3024-3028.

Millán, J. L., Markus, J. S., Simon, P. R. and John, P. B. (2006). Alkaline Phosphatases. Dynamics of Bone and Cartilage Metabolism (Second Edition). Burlington, Academic Press**:** 153-164.

Millan, J. L. and Whyte, M. P. (2016). Alkaline Phosphatase and Hypophosphatasia. *Calcif Tissue Int* **98**(4): 398-416.

Moore, C. B., Guthrie, E. H., Huang, M. T. and Taxman, D. J. (2010). Short hairpin RNA (shRNA): design, delivery, and assessment of gene knockdown. *Methods Mol Biol* **629**: 141-158.

Moss, A. K., Hamarneh, S. R., Mohamed, M. M., Ramasamy, S., Yammine, H., Patel, P., Kaliannan, K., Alam, S. N., Muhammad, N., Moaven, O., Teshager, A., Malo, N. S., Narisawa, S., Millan, J. L., Warren, H. S., Hohmann, E., Malo, M. S. and Hodin, R. A. (2013). Intestinal alkaline phosphatase inhibits the proinflammatory nucleotide uridine diphosphate. *Am J Physiol Gastrointest Liver Physiol* **304**(6): G597-604.

Muruganandan, S., Roman, A. A. and Sinal, C. J. (2009). Adipocyte differentiation of bone marrow-derived mesenchymal stem cells: cross talk with the osteoblastogenic program. *Cell Mol Life Sci* **66**(2): 236-253.

Nakanishi, K. (2016). Anatomy of RISC: how do small RNAs and chaperones activate Argonaute proteins? *Wiley Interdiscip Rev RNA* **7**: 637-660.

Nakayama, T., Yoshida, M. and Kitamura, M. (1970). L-leucine sensitive, heat-stable alkaline-phosphatase isoenzyme detected in a patient with pleuritis carcinomatosa. *Clin Chim Acta* **30**(2): 546-548.

Narisawa, S., Frohlander, N. and Millan, J. L. (1997). Inactivation of two mouse alkaline phosphatase genes and establishment of a model of infantile hypophosphatasia. *Dev Dyn* **208**(3): 432-446.

Negyessy, L., Xiao, J., Kantor, O., Kovacs, G. G., Palkovits, M., Doczi, T. P., Renaud, L., Baksa, G., Glasz, T., Ashaber, M., Barone, P. and Fonta, C. (2010). Layer-specific activity of tissue non-specific alkaline phosphatase in the human neocortex. *Neuroscience* **172** 406 - 418.

Nilsen, I. W., Overbo, K. and Olsen, R. L. (2001). Thermolabile alkaline phosphatase from Northern shrimp (Pandalus borealis): protein and cDNA sequence analyses. *Comp Biochem Physiol B Biochem Mol Biol* **129**(4): 853-861.

Nishikawa, K., Nakashima, T., Takeda, S., Isogai, M., Hamada, M., Kimura, A., Kodama, T., Yamaguchi, A., Owen, M. J., Takahashi, S. and Takayanagi, H. (2010). Maf promotes

osteoblast differentiation in mice by mediating the age-related switch in mesenchymal cell differentiation. *J Clin Invest* **120**(10): 3455-3465.

Noel, D., Caton, D., Roche, S., Bony, C., Lehmann, S., Casteilla, L., Jorgensen, C. and Cousin, B. (2008). Cell specific differences between human adipose-derived and mesenchymal-stromal cells despite similar differentiation potentials. *Exp Cell Res* **314**(7): 1575-1584.

Nosjean, O., Koyama, I., Goseki, M., Roux, B. and Komoda, T. (1997). Human tissue non-specific alkaline phosphatases: sugar-moiety-induced enzymic and antigenic modulations and genetic aspects. *Biochem J* **321 (Pt 2)**: 297-303.

Nowak, L. G., Rosay, B., Czege, D. and Fonta, C. (2015). Tetramisole and Levamisole Suppress Neuronal Activity Independently from Their Inhibitory Action on Tissue Non-specific Alkaline Phosphatase in Mouse Cortex. *Subcell Biochem* **76**: 239-281.

Nowrouzi, A. and Yazdanparast, R. (2005). Alkaline phosphatase retained in HepG2 hepatocarcinoma cells vs. alkaline phosphatase released to culture medium: Difference of aberrant glycosylation. *Biochemical and Biophysical Research Communications* **330**(2): 400-409.

Nuttall, M. E. and Gimble, J. M. (2004). Controlling the balance between osteoblastogenesis and adipogenesis and the consequent therapeutic implications. *Curr Opin Pharmacol* **4**(3): 290-294.

Ogawa, R., Mizuno, H., Watanabe, A., Migita, M., Hyakusoku, H. and Shimada, T. (2004). Adipogenic differentiation by adipose-derived stem cells harvested from GFP transgenic mice-including relationship of sex differences. *Biochem Biophys Res Commun* **319**(2): 511-517.

Okochi, T., Seike, H., Saeki, K., Sumikawa, K., Yamamoto, T. and Higashino, K. (1987). A novel alkaline phosphatase isozyme in human adipose tissue. *Clin Chim Acta* **162**(1): 19-27.

Orimo, H. (2010). The mechanism of mineralization and the role of alkaline phosphatase in health and disease. *J Nippon Med Sch* **77**(1): 4-12.

Orimo, H. and Shimada, T. (2008). The role of tissue-nonspecific alkaline phosphatase in the phosphate-induced activation of alkaline phosphatase and mineralization in SaOS-2 human osteoblast-like cells. *Mol Cell Biochem* **315**(1-2): 51-60.

Ozkul, Y. and Galderisi, U. (2016). The Impact of Epigenetics on Mesenchymal Stem Cell Biology. *J Cell Physiol* **231**(11): 2393-2401.

Paulick, M. G. and Bertozzi, C. R. (2008). The glycosylphosphatidylinositol anchor: a complex membrane-anchoring structure for proteins. *Biochemistry* **47**(27): 6991-7000.

Peng, L., Jia, Z., Yin, X., Zhang, X., Liu, Y., Chen, P., Ma, K. and Zhou, C. (2008). Comparative analysis of mesenchymal stem cells from bone marrow, cartilage, and adipose tissue. *Stem Cells Dev* **17**(4): 761-773.

Pittenger, M. F., Mackay, A. M., Beck, S. C., Jaiswal, R. K., Douglas, R., Mosca, J. D., Moorman, M. A., Simonetti, D. W., Craig, S. and Marshak, D. R. (1999). Multilineage potential of adult human mesenchymal stem cells. *Science* **284**(5411): 143-147.

Post, S., Abdallah, B. M., Bentzon, J. F. and Kassem, M. (2008). Demonstration of the presence of independent pre-osteoblastic and pre-adipocytic cell populations in bone marrow-derived mesenchymal stem cells. *Bone* **43**(1): 32-39.

Povinelli, C. M. and Knoll, B. J. (1991). Trace expression of the germ-cell alkaline phosphatase gene in human placenta. *Placenta* **12**(6): 663-668.

Qian, H., Le Blanc, K. and Sigvardsson, M. (2012). Primary mesenchymal stem and progenitor cells from bone marrow lack expression of CD44 protein. *J Biol Chem* **287**(31): 25795-25807.

Rambaldi, A., Terao, M., Bettoni, S., Tini, M. L., Bassan, R., Barbui, T. and Garattini, E. (1990). Expression of leukocyte alkaline phosphatase gene in normal and leukemic cells: regulation of the transcript by granulocyte colony-stimulating factor. *Blood* **76**(12): 2565-2571.

Rebelatto, C. K., Aguiar, A. M., Moretao, M. P., Senegaglia, A. C., Hansen, P., Barchiki, F., Oliveira, J., Martins, J., Kuligovski, C., Mansur, F., Christofis, A., Amaral, V. F., Brofman, P. S., Goldenberg, S., Nakao, L. S. and Correa, A. (2008). Dissimilar Differentiation of Mesenchymal Stem Cells from Bone Marrow, Umbilical Cord Blood, and Adipose Tissue. *Exp. Biol. Med.* **233**(7): 901-913.

Reinholz, G. G., Getz, B., Pederson, L., Sanders, E. S., Subramaniam, M., Ingle, J. N. and Spelsberg, T. C. (2000). Bisphosphonates directly regulate cell proliferation, differentiation, and gene expression in human osteoblasts. *Cancer Res* **60**(21): 6001-6007.

Rezende, A. A., Pizauro, J. M., Ciancaglini, P. and Leone, F. A. (1994). Phosphodiesterase activity is a novel property of alkaline phosphatase from osseous plate. *Biochem J* **301 (Pt 2)**: 517-522.

Rose, R. A., Jiang, H., Wang, X., Helke, S., Tsoporis, J. N., Gong, N., Keating, S. C., Parker, T. G., Backx, P. H. and Keating, A. (2008). Bone marrow-derived mesenchymal stromal cells express cardiac-specific markers, retain the stromal phenotype, and do not become functional cardiomyocytes in vitro. *Stem Cells* **26**(11): 2884-2892.

Russo, V., Yu, C., Belliveau, P., Hamilton, A. and Flynn, L. E. (2014). Comparison of human adipose-derived stem cells isolated from subcutaneous, omental, and intrathoracic adipose tissue depots for regenerative applications. *Stem Cells Transl Med* **3**(2): 206-217.

Sabokbar, A., Millett, P. J., Myer, B. and Rushton, N. (1994). A rapid, quantitative assay for measuring alkaline phosphatase activity in osteoblastic cells in vitro. *Bone Miner* **27**(1): 57-67.

Sacchetti, B., Funari, A., Michienzi, S., Di Cesare, S., Piersanti, S., Saggio, I., Tagliafico, E., Ferrari, S., Robey, P. G., Riminucci, M. and Bianco, P. (2007). Self-renewing osteoprogenitors in bone marrow sinusoids can organize a hematopoietic microenvironment. *Cell* **131**(2): 324-336.

Sadie-Van Gijsen, H., Crowther, N. J., Hough, F. S. and Ferris, W. F. (2010). Depot-specific differences in the insulin response of adipose-derived stromal cells. *Mol Cell Endocrinol* **328**(1-2): 22-27.

Sadie-Van Gijsen, H., Smith, W., du Toit, E. F., Michie, J., Hough, F. S. and Ferris, W. F. (2012). Depot-specific and hypercaloric diet-induced effects on the osteoblast and adipocyte differentiation potential of adipose-derived stromal cells. *Mol Cell Endocrinol* **348**(1): 55-66.

Sato, N., Takahashi, Y. and Asano, S. (1994). Preferential usage of the bone-type leader sequence for the transcripts of liver/bone/kidney-type alkaline phosphatase gene in neutrophilic granulocytes. *Blood* **83**(4): 1093-1101.

Say, J. C., Ciuffi, K., Furriel, R. P., Ciancaglini, P. and Leone, F. A. (1991). Alkaline phosphatase from rat osseous plates: purification and biochemical characterization of a soluble form. *Biochim Biophys Acta* **1074**(2): 256-262.

Schwarz, S., Huss, R., Schulz-Siegmund, M., Vogel, B., Brandau, S., Lang, S. and Rotter, N. (2014). Bone marrow-derived mesenchymal stem cells migrate to healthy and damaged salivary glands following stem cell infusion. *Int J Oral Sci* **6**(3): 154-161.

Sethe, S., Scutt, A. and Stolzing, A. (2006). Aging of mesenchymal stem cells. *Ageing Res Rev* **5**(1): 91-116.

Sgodda, M., Aurich, H., Kleist, S., Aurich, I., Konig, S., Dollinger, M. M., Fleig, W. E. and Christ, B. (2007). Hepatocyte differentiation of mesenchymal stem cells from rat peritoneal adipose tissue in vitro and in vivo. *Exp Cell Res* **313**(13): 2875-2886.

Shah, F. S., Li, J., Dietrich, M., Wu, X., Hausmann, M. G., LeBlanc, K. A., Wade, J. W. and Gimble, J. M. (2014). Comparison of Stromal/Stem Cells Isolated from Human Omental and Subcutaneous Adipose Depots: Differentiation and Immunophenotypic Characterization. *Cells Tissues Organs* **200**(3-4): 204-211.

Sharma, U., Pal, D. and Prasad, R. (2014). Alkaline phosphatase: an overview. *Indian J Clin Biochem* **29**(3): 269-278.

She, Q. B., Mukherjee, J. J., Huang, J. S., Crilly, K. S. and Kiss, Z. (2000). Growth factor-like effects of placental alkaline phosphatase in human fetus and mouse embryo fibroblasts. *FEBS Lett* **469**(2-3): 163-167.

Shepherd, P. R., Gnudi, L., Tozzo, E., Yang, H., Leach, F. and Kahn, B. B. (1993). Adipose cell hyperplasia and enhanced glucose disposal in transgenic mice overexpressing GLUT4 selectively in adipose tissue. *J Biol Chem* **268**(30): 22243-22246.

Shidoji, Y. and Kim, S. H. (2004). Mutually distinctive gradients of three types of intestinal alkaline phosphatase along the longitudinal axis of the rat intestine. *Digestion* **70**(1): 10-15.

Simao, A. M., Yadav, M. C., Narisawa, S., Bolean, M., Pizauro, J. M., Hoylaerts, M. F., Ciancaglini, P. and Millan, J. L. (2010). Proteoliposomes harboring alkaline phosphatase and nucleotide pyrophosphatase as matrix vesicle biomimetics. *J Biol Chem* **285**(10): 7598-7609.

Singh, S. K., Kagalwala, M. N., Parker-Thornburg, J., Adams, H. and Majumder, S. (2008). REST maintains self-renewal and pluripotency of embryonic stem cells. *Nature* **453**(7192): 223-227.

Smith, M., Weiss, M. J., Griffin, C. A., Murray, J. C., Buetow, K. H., Emanuel, B. S., Henthorn, P. S. and Harris, H. (1988). Regional assignment of the gene for human liver/bone/kidney alkaline phosphatase to chromosome 1p36.1-p34. *Genomics* **2**(2): 139-143.

Sobiesiak, M., Sivasubramaniyan, K., Hermann, C., Tan, C., Orgel, M., Treml, S., Cerabona, F., de Zwart, P., Ochs, U., Muller, C. A., Gargett, C. E., Kalbacher, H. and Buhring, H. J. (2010). The mesenchymal stem cell antigen MSCA-1 is identical to tissue non-specific alkaline phosphatase. *Stem Cells Dev* **19**(5): 669-677.

Sone, M., Kishigami, S., Yoshihisa, T. and Ito, K. (1997). Roles of disulfide bonds in bacterial alkaline phosphatase. *J Biol Chem* **272**(10): 6174-6178.

Song, L. and Tuan, R. S. (2004). Transdifferentiation potential of human mesenchymal stem cells derived from bone marrow. *FASEB J* **18**(9): 980-982.

Sottile, V. and Seuwen, K. (2000). Bone morphogenetic protein-2 stimulates adipogenic differentiation of mesenchymal precursor cells in synergy with BRL 49653 (rosiglitazone). *FEBS Lett* **475**(3): 201-204.

Sprokholt, R., Mass, A. H. J., Rebelo, M. J. and Covington, A. K. (1982). Determination of the performance of glass electrodes in aqueous solutions in the physiological ph range and at the physiological sodium ion concentration. *Analytica Chimica Acta* **139**: 53-59.

Stefaner, I., Stefanescu, A., Hunziker, W. and Fuchs, R. (1997). Expression of placental alkaline phosphatase does not correlate with IgG binding, internalization and transcytosis. *Biochem J* **327 (Pt 2)**: 585-592.

Stefkova, K., Prochazkova, J. and Pachernik, J. (2015). Alkaline phosphatase in stem cells. *Stem Cells Int* **2015**: 628368.

Stoop, H., Honecker, F., Cools, M., de Krijger, R., Bokemeyer, C. and Looijenga, L. H. (2005). Differentiation and development of human female germ cells during prenatal gonadogenesis: an immunohistochemical study. *Hum Reprod* **20**(6): 1466-1476.

Strioga, M., Viswanathan, S., Darinskas, A., Slaby, O. and Michalek, J. (2012). Same or not the same? Comparison of adipose tissue-derived versus bone marrow-derived mesenchymal stem and stromal cells. *Stem Cells Dev* **21**(14): 2724-2752.

Studer, M., Terao, M., Gianni, M. and Garattini, E. (1991). Characterization of a second promoter for the mouse liver/bone/kidney-type alkaline phosphatase gene: cell and tissue specific expression. *Biochem Biophys Res Commun* **179**(3): 1352-1360.

Sumikawa, K., Okochi, T. and Adachi, K. (1990). Differences in phosphatidate hydrolytic activity of human alkaline phosphatase isozymes. *Biochim Biophys Acta* **1046**(1): 27-31.

Tadokoro, M., Kanai, R., Taketani, T., Uchio, Y., Yamaguchi, S. and Ohgushi, H. (2009). New Bone Formation by Allogeneic Mesenchymal Stem Cell Transplantation in a Patient with Perinatal Hypophosphatasia. *The Journal of Pediatrics* **154**(6): 924-930.

Tanabe, N., Ito-Kato, E., Suzuki, N., Nakayama, A., Ogiso, B., Maeno, M. and Ito, K. (2004a). IL-1alpha affects mineralized nodule formation by rat osteoblasts. *Life Sci* **75**(19): 2317-2327.

Tanabe, Y., Koga, M., Saito, M., Matsunaga, Y. and Nakayama, K. (2004b). Inhibition of adipocyte differentiation by mechanical stretching through ERK-mediated downregulation of PPARgamma2. *J Cell Sci* **117**(Pt 16): 3605-3614.

Tang, Q. Q. and Lane, M. D. (2012). Adipogenesis: from stem cell to adipocyte. *Annu Rev Biochem* **81**: 715-736.

Tang, Q. Q., Otto, T. C. and Lane, M. D. (2004). Commitment of C3H10T1/2 pluripotent stem cells to the adipocyte lineage. *Proc Natl Acad Sci U S A* **101**(26): 9607-9611.

Teven, C. M., Liu, X., Hu, N., Tang, N., Kim, S. H., Huang, E., Yang, K., Li, M., Gao, J. L., Liu, H., Natale, R. B., Luther, G., Luo, Q., Wang, L., Rames, R., Bi, Y., Luo, J., Luu, H. H.,

Haydon, R. C., Reid, R. R. and He, T. C. (2011). Epigenetic regulation of mesenchymal stem cells: a focus on osteogenic and adipogenic differentiation. *Stem Cells Int* **2011**: Article ID 201371.

Toh, Y., Yamamoto, M., Endo, H., Fujita, A., Misumi, Y. and Ikehara, Y. (1989a). Sequence divergence of 5' extremities in rat liver alkaline phosphatase mRNAs. *J Biochem* **105**(1): 61-65.

Toh, Y., Yamamoto, M., Endo, H., Misumi, Y. and Ikehara, Y. (1989b). Isolation and characterization of a rat liver alkaline phosphatase gene. A single gene with two promoters. *Eur J Biochem* **182**(2): 231-237.

Tokuzawa, Y., Yagi, K., Yamashita, Y., Nakachi, Y., Nikaido, I., Bono, H., Ninomiya, Y., Kanesaki-Yatsuka, Y., Akita, M., Motegi, H., Wakana, S., Noda, T., Sablitzky, F., Arai, S., Kurokawa, R., Fukuda, T., Katagiri, T., Schonbach, C., Suda, T., Mizuno, Y. and Okazaki, Y. (2010). Id4, a new candidate gene for senile osteoporosis, acts as a molecular switch promoting osteoblast differentiation. *PLoS Genet* **6**(7): e1001019.

Tormos, K. V., Anso, E., Hamanaka, R. B., Eisenbart, J., Joseph, J., Kalyanaraman, B. and Chandel, N. S. (2011). Mitochondrial complex III ROS regulate adipocyte differentiation. *Cell Metab* **14**(4): 537-544.

Tsai, L. C., Hung, M. W., Chen, Y. H., Su, W. C., Chang, G. G. and Chang, T. C. (2000). Expression and regulation of alkaline phosphatases in human breast cancer MCF-7 cells. *Eur J Biochem* **267**(5): 1330-1339.

Tuschl, T., Zamore, P. D., Lehmann, R., Bartel, D. P. and Sharp, P. A. (1999). Targeted mRNA degradation by double-stranded RNA in vitro. *Genes Dev* **13**(24): 3191-3197.

Twyman., S. B. P. a. R. M. (2006). Principles of gene manipulation and genomics. Bethesda Malden, MA : Blackwell Pub.

Valenzuela, G. J., Munson, L. A., Tarbaux, N. M. and Farley, J. R. (1987). Time-dependent changes in bone, placental, intestinal, and hepatic alkaline phosphatase activities in serum during human pregnancy. *Clin Chem* **33**(10): 1801-1806.

van de Vyver, M., Andrag, E., Cockburn, I. L. and Ferris, W. F. (2014). Thiazolidinedione-induced lipid droplet formation during osteogenic differentiation. *J Endocrinol* **223**(2): 119-132.

van Wijngaarden, P., Brereton, H. M., Coster, D. J. and Williams, K. A. (2007). Stability of housekeeping gene expression in the rat retina during exposure to cyclic hyperoxia. *Mol Vis* **13**: 1508-1515.

Vater, C., Kasten, P. and Stiehler, M. (2011). Culture media for the differentiation of mesenchymal stromal cells. *Acta Biomater* **7**(2): 463-477.

Vergote, I. B., Abeler, V. M., Bormer, O. P., Stigbrand, T., Trope, C. and Nustad, K. (1992). CA125 and placental alkaline phosphatase as serum tumor markers in epithelial ovarian carcinoma. *Tumour Biol* **13**(3): 168-174.

Vittur, F., Stagni, N., Moro, L. and de Bernard, B. (1984). Alkaline phosphatase binds to collagen; a hypothesis on the mechanism of extravesicular mineralization in epiphyseal cartilage. *Experientia* **40**(8): 836-837.

Wahren, B., Holmgren, P. A. and Stigbrand, T. (1979). Placental alkaline phosphatase, alphafetoprotein and carcinoembryonic antigen in testicular tumors. Tissue typing by means of cytologic smears. *Int J Cancer* **24**(6): 749-753.

Wallach, D. P. and Ko, H. (1964). Some Properties of an Alkaline Phosphatase from Rat Adipose Tissue. *Can J Biochem* **42**: 1445-1457.

Wang, H. and Sztalryd, C. (2011). Oxidative tissue: perilipin 5 links storage with the furnace. *Trends Endocrinol Metab* **22**(6): 197-203.

Wang, P., Mariman, E., Renes, J. and Keijer, J. (2008). The secretory function of adipocytes in the physiology of white adipose tissue. *J Cell Physiol* **216**(1): 3-13.

Waymire, K. G., Mahuren, J. D., Jaje, J. M., Guilarte, T. R., Coburn, S. P. and MacGregor, G. R. (1995). Mice lacking tissue non-specific alkaline phosphatase die from seizures due to defective metabolism of vitamin B-6. *Nat Genet* **11**(1): 45-51.

Weinstein, R. S. (2001). Glucocorticoid-induced osteoporosis. *Rev Endocr Metab Disord* **2**(1): 65-73.

Weiser, B., Sommer, F., Neubauer, M., Seitz, A., Tessmar, J., Goepferich, A. and Blunk, T. (2009). Ascorbic acid enhances adipogenesis of bone marrow-derived mesenchymal stromal cells. *Cells Tissues Organs* **189**(6): 373-381.

Weiss, M. J., Henthorn, P. S., Lafferty, M. A., Slaughter, C., Raducha, M. and Harris, H. (1986). Isolation and characterization of a cDNA encoding a human liver/bone/kidney-type alkaline phosphatase. *Proc Natl Acad Sci U S A* **83**(19): 7182-7186.

Weiss, M. J., Ray, K., Henthorn, P. S., Lamb, B., Kadesch, T. and Harris, H. (1988). Structure of the human liver/bone/kidney alkaline phosphatase gene. *J Biol Chem* **263**(24): 12002-12010.

Whyte, M. P. (2010). Physiological role of alkaline phosphatase explored in hypophosphatasia. *Ann N Y Acad Sci* **1192**(1): 190-200.

Whyte, M. P., Landt, M., Ryan, L. M., Mulivor, R. A., Henthorn, P. S., Fedde, K. N., Mahuren, J. D. and Coburn, S. P. (1995). Alkaline phosphatase: placental and tissue-nonspecific isoenzymes hydrolyze phosphoethanolamine, inorganic pyrophosphate, and pyridoxal 5'-phosphate. Substrate accumulation in carriers of hypophosphatasia corrects during pregnancy. *J Clin Invest* **95**(4): 1440-1445.

Wilfinger, W. W., Mackey, K. and Chomczynski, P. (1997). Effect of pH and ionic strength on the spectrophotometric assessment of nucleic acid purity. *Biotechniques* **22**(3): 474-476, 478-481.

Wilkison, W. O., Min, H. Y., Claffey, K. P., Satterberg, B. L. and Spiegelman, B. M. (1990). Control of the adipsin gene in adipocyte differentiation. Identification of distinct nuclear factors binding to single- and double-stranded DNA. *J Biol Chem* **265**(1): 477-482.

Wilson, P. D., Smith, G. P. and Peters, T. J. (1983). Pyridoxal 5'-phosphate: a possible physiological substrate for alkaline phosphatase in human neutrophils. *Histochem J* **15**(3): 257-264.

Wu, W., Le, A. V., Mendez, J. J., Chang, J., Niklason, L. E. and Steinbacher, D. M. (2015). Osteogenic performance of donor-matched human adipose and bone marrow mesenchymal cells under dynamic culture. *Tissue Eng Part A* **21**(9-10): 1621-1632.

Yang, K. and Metcalf, W. W. (2004). A new activity for an old enzyme: Escherichia coli bacterial alkaline phosphatase is a phosphite-dependent hydrogenase. *Proc Natl Acad Sci U S A* **101**(21): 7919-7924.

Yoshimura, H., Muneta, T., Nimura, A., Yokoyama, A., Koga, H. and Sekiya, I. (2007). Comparison of rat mesenchymal stem cells derived from bone marrow, synovium, periosteum, adipose tissue, and muscle. *Cell Tissue Res* **327**(3): 449-462.

Yu, G., Wu, X., Dietrich, M. A., Polk, P., Scott, L. K., Ptitsyn, A. A. and Gimble, J. M. (2010). Yield and characterization of subcutaneous human adipose-derived stem cells by flow cytometric and adipogenic mRNA analyzes. *Cytotherapy* **12**(4): 538-546.

Yusa, N., Watanabe, K., Yoshida, S., Shirafuji, N., Shimomura, S., Tani, K., Asano, S. and Sato, N. (2000). Transcription factor Sp3 activates the liver/bone/kidney-type alkaline phosphatase promoter in hematopoietic cells. *J Leukoc Biol* **68**(5): 772-777.

Zannettino, A. C., Paton, S., Arthur, A., Khor, F., Itescu, S., Gimble, J. M. and Gronthos, S. (2008). Multipotential human adipose-derived stromal stem cells exhibit a perivascular phenotype in vitro and in vivo. *J Cell Physiol* **214**(2): 413-421.

Zayzafoon, M., Gathings, W. E. and McDonald, J. M. (2004). Modeled Microgravity Inhibits Osteogenic Differentiation of Human Mesenchymal Stem Cells and Increases Adipogenesis. *Endocrinology* **145**(5): 2421-2432.

Zernik, J., Kream, B. and Twarog, K. (1991). Tissue-specific and dexamethasone-inducible expression of alkaline phosphatase from alternative promoters of the rat bone/liver/kidney/placenta gene. *Biochem Biophys Res Commun* **176**(3): 1149-1156.

Supplement

Addendum A

A1 Preparation of adipogenic differentiation medium (AM) cocktail components:

- Dexamethasone was dissolved in ethanol (EtOH) (32221-2.5L, Sigma Aldrich) to give a stock solution of 10 mM, which was stored in aliquots at -20 °C.
- Indomethacin was dissolved in EtOH to give a stock solution of 56 mM, which is the solubility limit of indomethacin. Stock solution was stored at RT.
- 3-isobutyl-1-methylxanthine (IBMX) was dissolved in dimethyl sulphoxide (DMSO) (1029873, Merck) to form a stock solution of 1 M, which was stored at -20 C. Stock solutions of IBMX was thawed no more than 3 times before being discarded.
- Insulin was supplied in a ready to use stock of 10 mg/ml, which was stored at 4 °C.
- Ascorbic acid powder was weighed out under sterile conditions and dissolved in sterile DMEM to give a stock solution of 50 mM. Aliquots of ascorbic acid were stored at -20 °C and discarded after a single use.

Table A1: Cocktail for the induction of adipogenesis in scADSCs, pvADSCs and bmMSCs.

Component	Vehicle	Stock concentration	Final concentration	Volume of stock added to make 10 ml adipogenic differentiation medium (AM)
Insulin	HEPES buffer	10 mg/ml	10 µM	57.2 µl
Indomethacin	EtOH	56 mM	56 µM	10µl
3-isobutyl-1-methylxanthine	DMSO	1 M	0.5 mM	5µl
Dexamethasone	EtOH	10 mM	1 µM	1µl
Ascorbic acid	DMEM	50 mM	50 µM	10µl

A2 Preparation of osteogenic differentiation medium (OM) cocktail components:

- β-glycerophosphate was dissolved in DMEM + 10% FBS to give a stock concentration of 25 mM, which was filter sterilised and stored at -20 °C.
- Dexamethasone was prepared by dilution of the 10 mM stock (See section 3.6.1) using 99% pure ethanol at a ratio of either 1:1000 or 1:100 to give stock solutions of 10 µM or 100 µM, respectively.
- Ascorbic acid stock was prepared the same as for the adipogenic differentiation cocktail.

Table A2: Cocktail components for the induction of osteogenesis in scADSCs, pvADSCs and bmMSCs

Component	Vehicle	Stock Concentration	Final concentration	Volume of stock added to make 10 ml osteogenic differentiation medium (OM)
β-glycerophosphate	DMEM+10 % FBS	50 mM	10 mM	2 ml
Dexamethasone (bmMSC OM)	Ethanol	10 µM	10 nM	1 µl
Dexamethasone (scADSC and pvADSC OM)	Ethanol	100 µM	100 nM	1 µl
Ascorbic acid	DMEM	50 mM	50 µM	10 µl

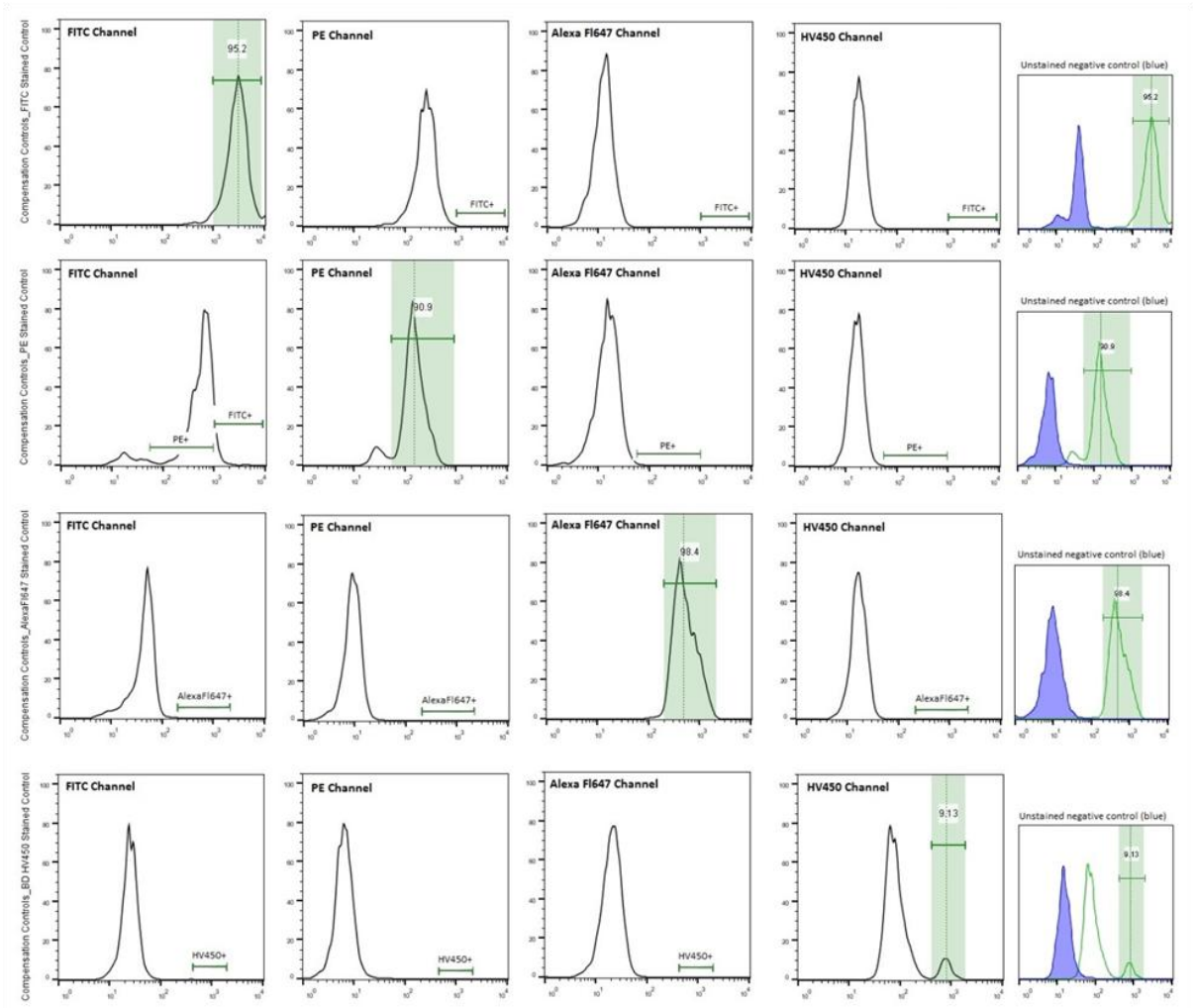

Figure A: Compensation controls for 4 colour flow cytometry experiment for the analysis of cell surface marker expression in order to determine the purity of the isolated MSC populations. Regions of positive (green) staining in single fluorochrome stained control samples are demonstrated. These compensation control samples demonstrated that PE emissions were also detected in the FITC channel. A compensation matrix was created using the Flow Jo Vx (Treestar) software in order to correct for the spectral overlap between FITC and PE; gated regions of positive areas were set accordingly. Single fluorochrome stained control samples demonstrate no spectral overlap following compensation. Regions of positive staining following compensation in single stained controls (green) compared to a negative unstained control sample (blue) are given in the final column.

Addendum B

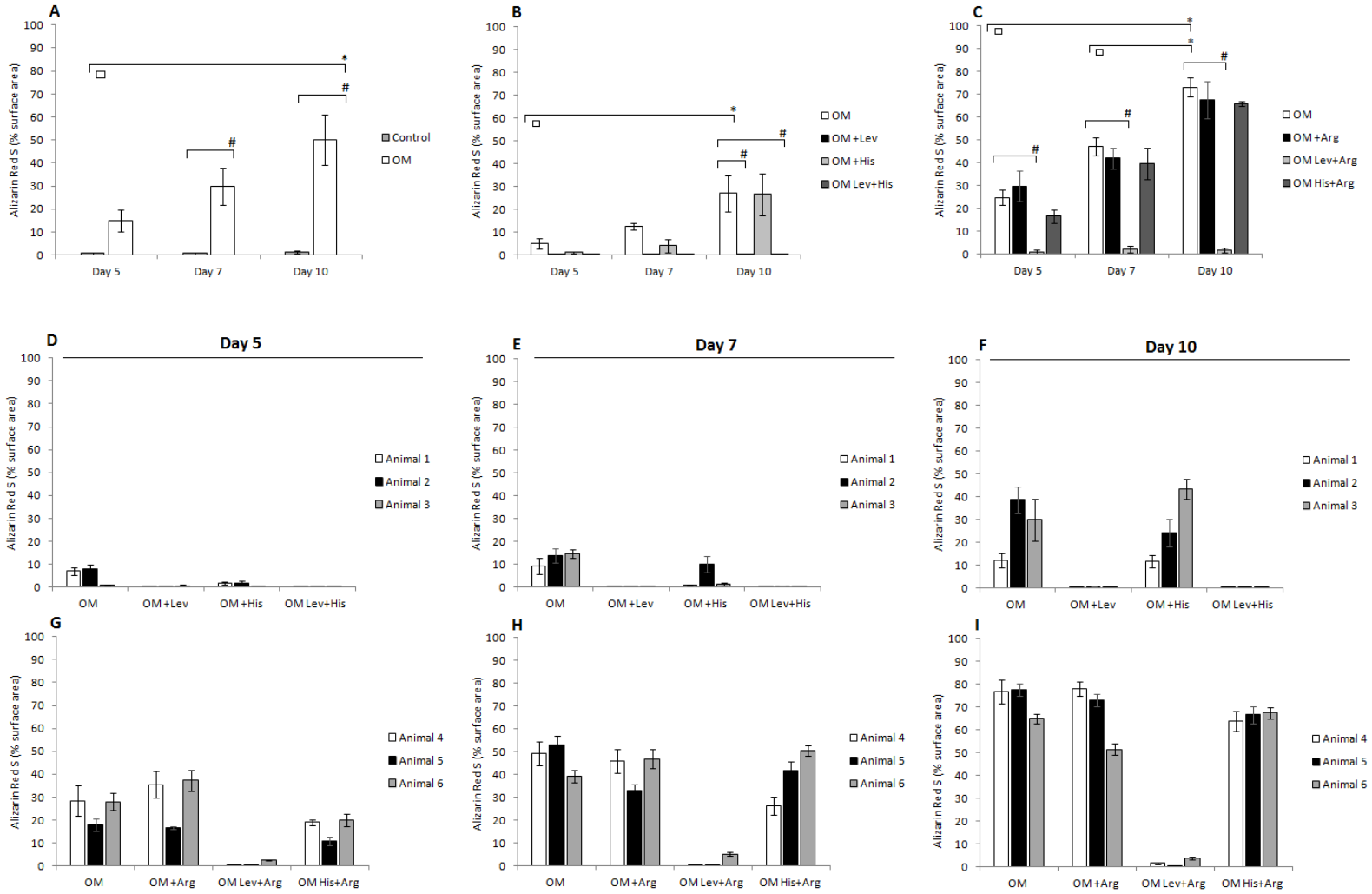

Figure B1: Image analysis to determine percentage area of mineralisation of bmMSCs cultured in osteogenic differentiation medium (OM) in the presence and absence of levamisole (Lev), histidine (His) and L-homoarginine (Arg). Percentage mineralisation of cells cultured in standard growth medium (SGM) (Control) or OM, at day 5, 7 and 10, n=6 (A). Pooled data for animal 1 – 3 at day 5 (D), 7 (E) and 10 (F) is represented in panel B, while pooled data for animal 4 – 6 at day 5 (G), 7 (H) and 10 (I) is represented as panel C. Statistical analysis was performed using one-way ANOVA and Tukey's test to determine statistical differences where $p < 0.05$. Error bars are represented as standard error (SE).

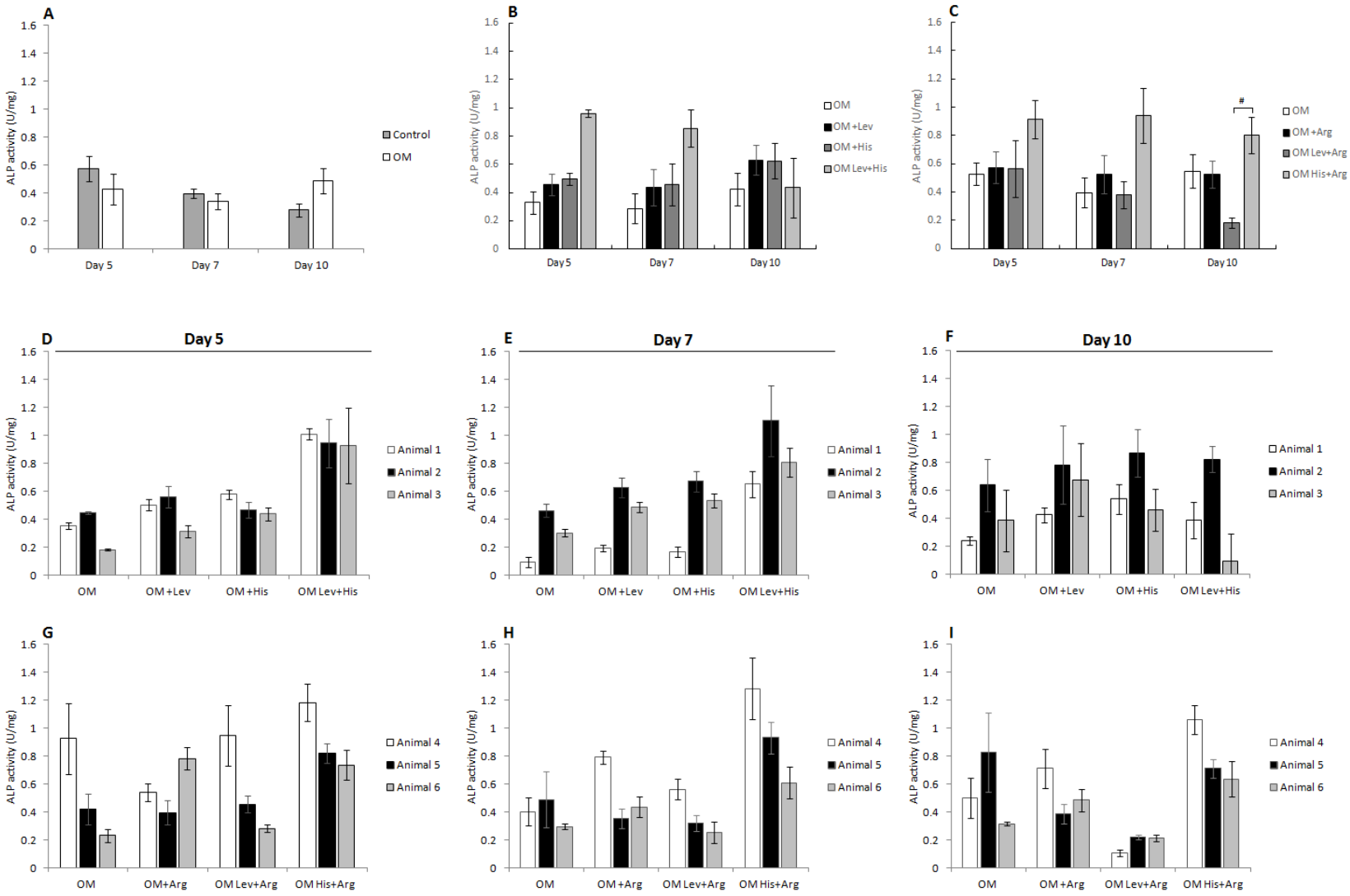

Figure B2: Alkaline phosphatase (ALP) assay to determine total cell ALP activity of bmMSCs cultured in osteogenic differentiation medium (OM) in the presence and absence of levamisole (Lev), histidine (His) and L-homoarginine (Arg). ALP activity (U/mg) of cells cultured in standard growth medium (SGM) (Control) or OM, at day 5, 7 and 10, n=6 (A). Pooled data for animal 1 – 3 at day 5 (D), 7 (E) and 10 (F) is represented in panel B, while pooled data for animal 4 – 6 at day 5 (G), 7 (H) and 10 (I) is represented as panel C. Statistical analysis was performed using one-way ANOVA and Tukey's test to determine statistical differences where $p < 0.05$. Error bars are represented as standard error (SE).

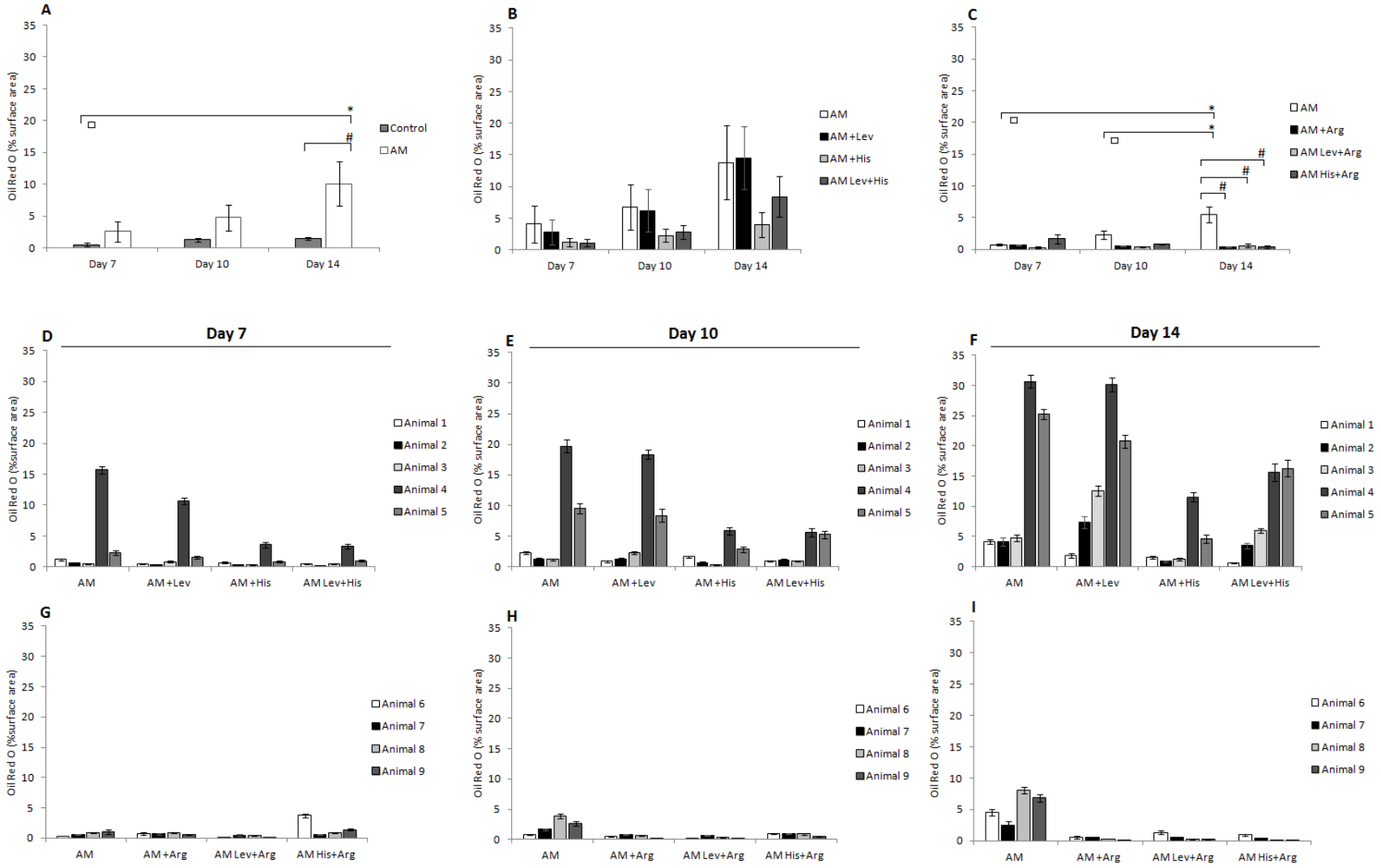

Figure B3: Image analysis to determine percentage area of lipid accumulation in bmMSCs cultured in adipogenic differentiation medium (AM) in the presence and absence of levamisole (Lev), histidine (His) and L-homoarginine (Arg). Percentage area of lipid accumulation of cells cultured in standard growth medium (SGM) (Control) or AM, at day 7, 10 and 14, n=9 (A). Pooled data for animal 1 – 5 at day 7 (D), 10 (E) and 14 (F) is represented in panel B, while pooled data for animal 6 – 9 at day 7 (G), 10 (H) and 14 (I) is represented as panel C. Statistical analysis was performed using one-way ANOVA and Tukey's test to determine statistical differences where $p < 0.05$. Error bars are represented as standard error (SE).

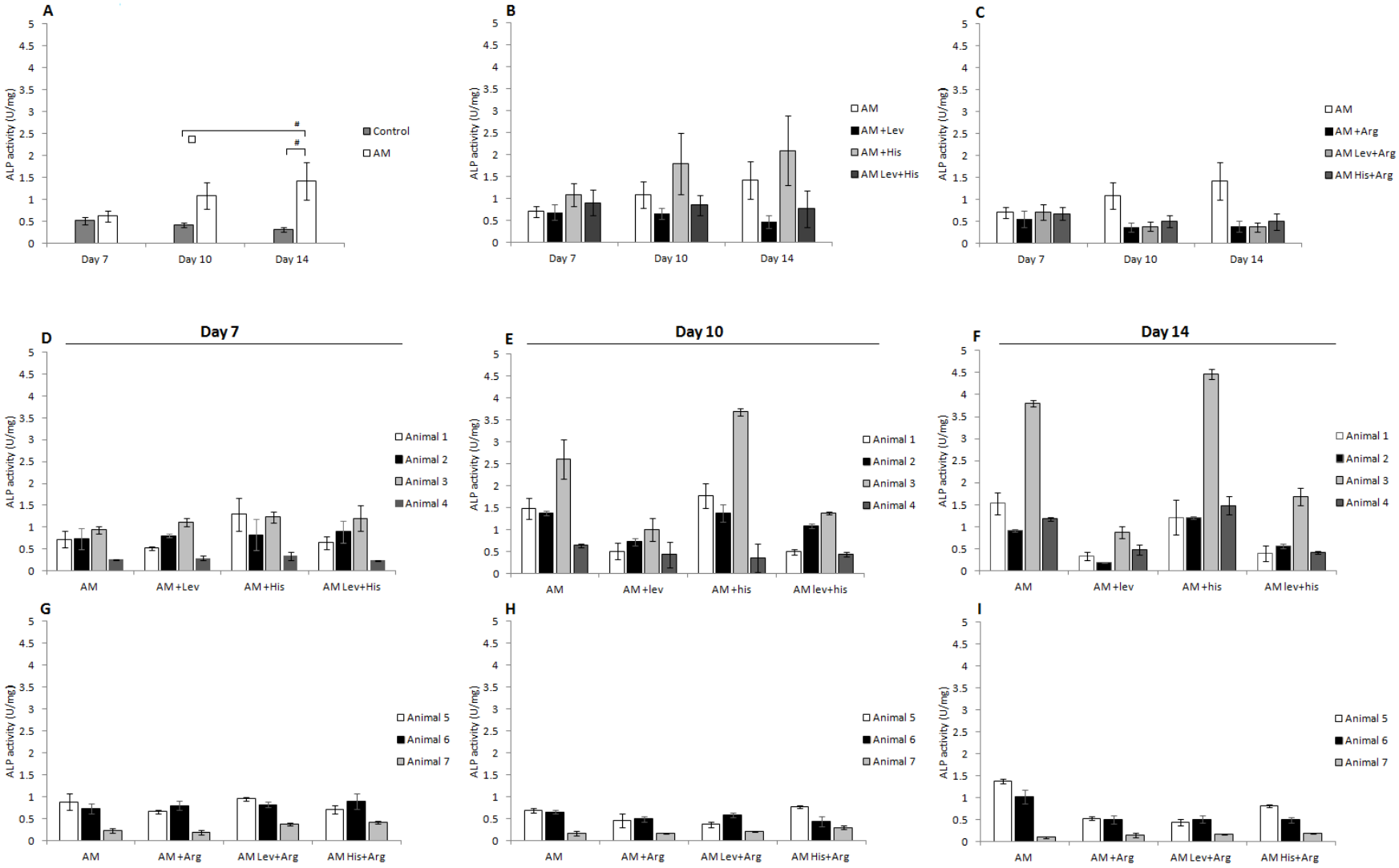

Figure B4: Alkaline phosphatase (ALP) assay to determine total cell ALP activity of bmMSCs cultured in adipogenic differentiation medium (AM) in the presence and absence of levamisole (Lev), histidine (His) and L-homoarginine (Arg). ALP activity (U/mg) of cells cultured in standard growth medium (SGM) (Control) or AM, at day 7, 10 and 14, n=7 (A). Pooled data for animal 1 – 4 at day 7 (D), 10 (E) and 14 (F) is represented in panel B, while pooled data for animal 5 – 7 at day 7 (G), 10 (H) and 14 (I) is represented as panel C. Statistical analysis was performed using one-way ANOVA and Tukey's test to determine statistical differences where $p < 0.05$. Error bars are represented as standard error (SE).

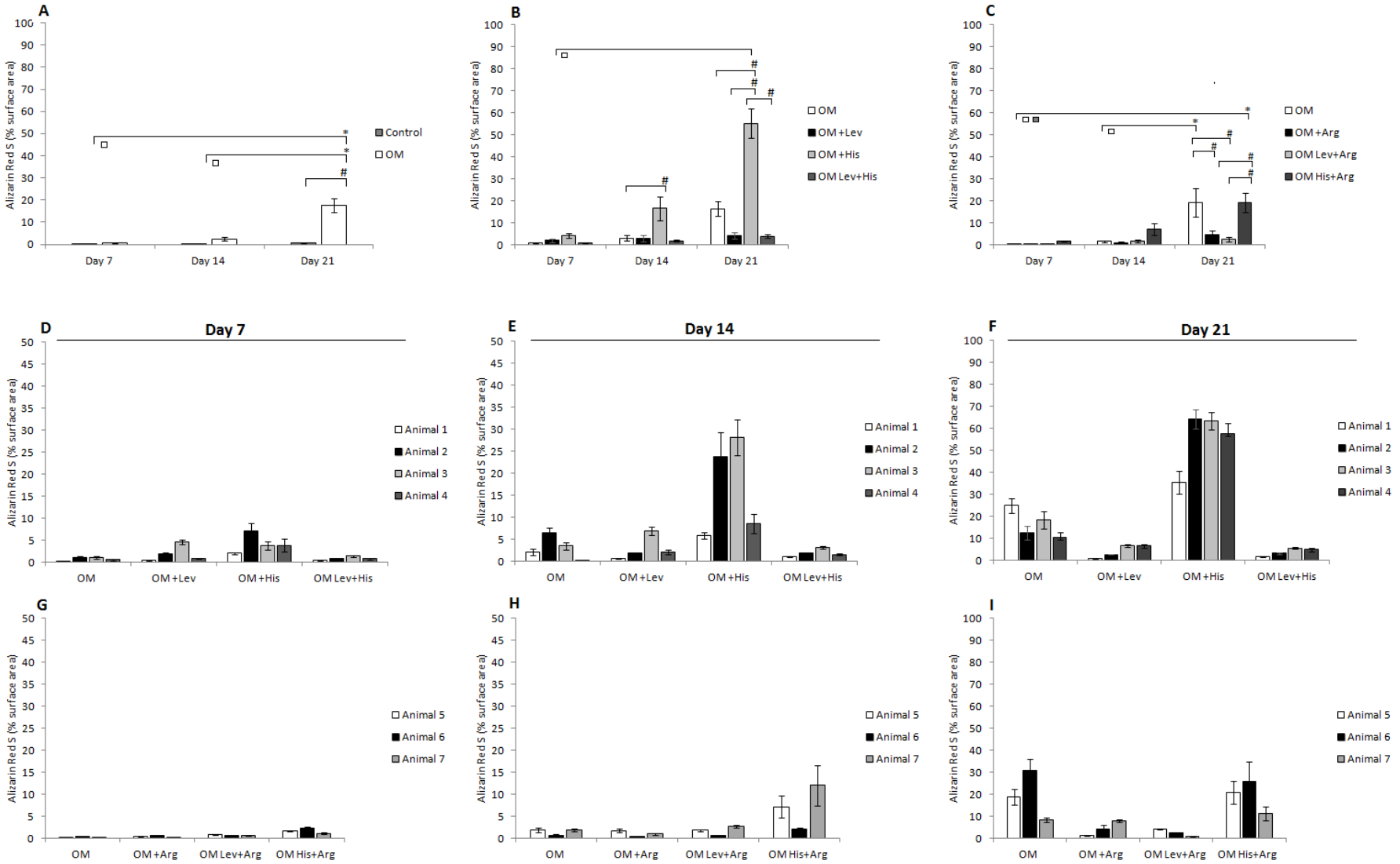

Figure B5: Image analysis to determine percentage area of mineralisation of scADSCs cultured in osteogenic differentiation medium (OM) in the presence and absence of levamisole (Lev), histidine (His) and L-homoarginine (Arg). Percentage mineralisation of cells cultured in standard growth medium (SGM) (Control) or OM, at day 7, 14 and 21, n=7 (A). Pooled data for animal 1 – 4 at day 7 (D), 14 (E) and 21 (F) is represented in panel B, while pooled data for animal 5 – 7 at day 7 (G), 14 (H) and 21 (I) is represented as panel C. Statistical analysis was performed using one-way ANOVA and Tukey's test to determine statistical differences where $p < 0.05$. Error bars are represented as standard error (SE).

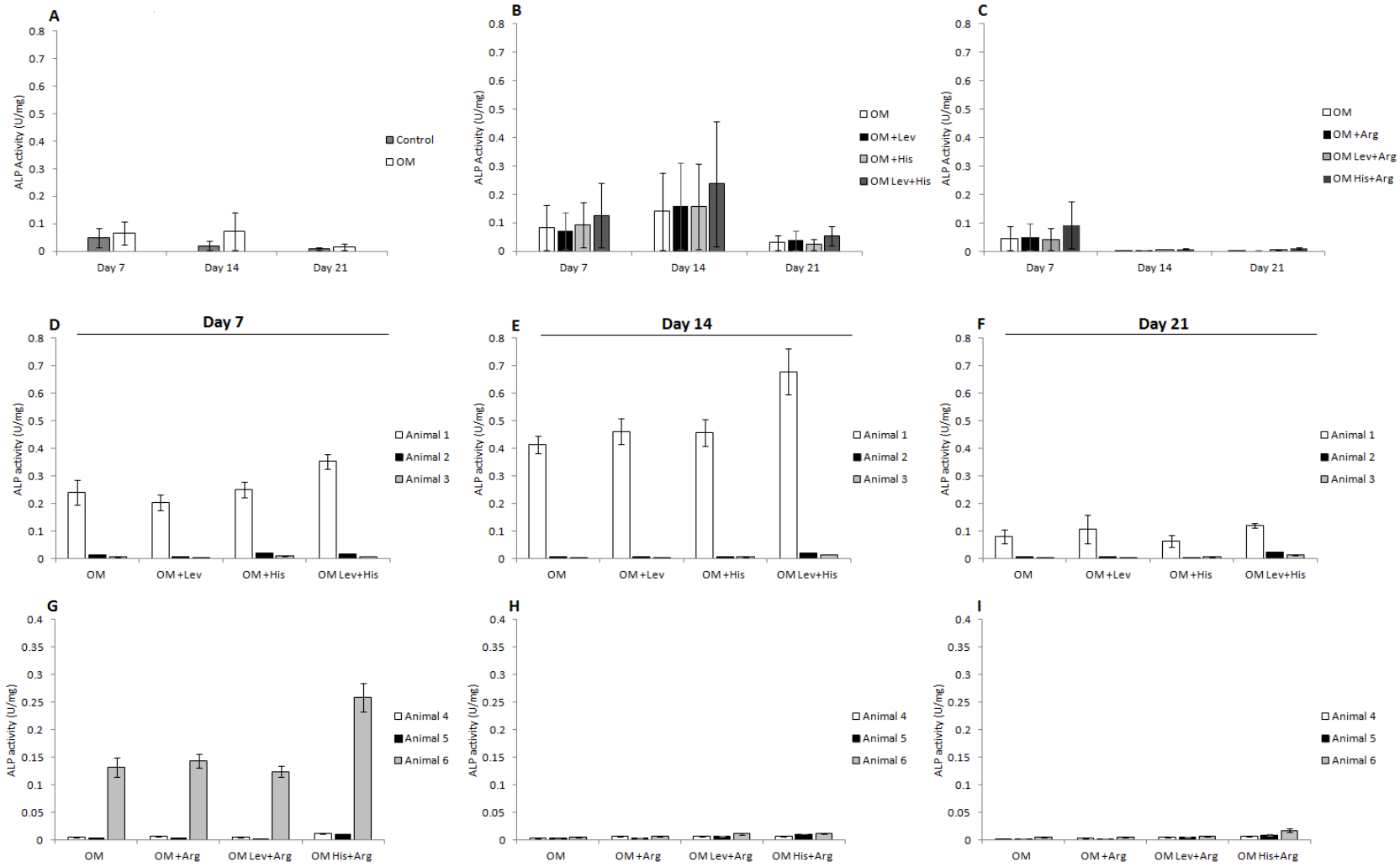

Figure B6: Alkaline phosphatase (ALP) assay to determine total cell ALP activity of scADSCs cultured in osteogenic differentiation medium (OM) in the presence and absence of levamisole (Lev), histidine (His) and L-homoarginine (Arg). ALP activity (U/mg) of cells cultured in standard growth medium (SGM) (Control) or OM, at day 7, 14 and 21, n=6 (A). Pooled data for animal 1 – 3 at day 7 (D), 14 (E) and 21 (F) is represented in panel B, while pooled data for animal 4 – 6 at day 7 (G), 14 (H) and 21 (I) is represented as panel C. Statistical analysis was performed using one-way ANOVA and Tukey's test to determine statistical differences where $p < 0.05$. Error bars are represented as standard error (SE).

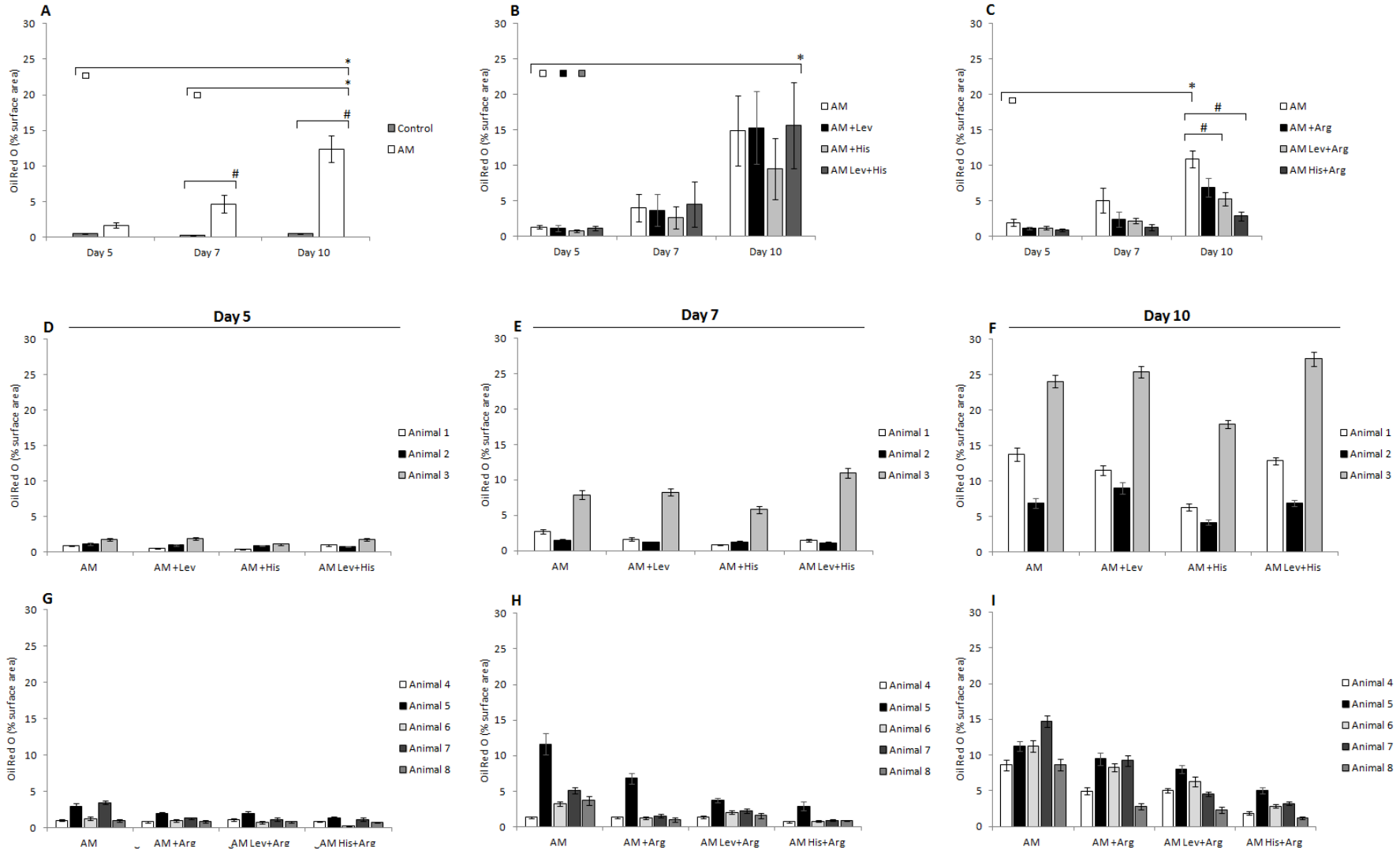

Figure B7: Image analysis to determine percentage area of lipid accumulation in scADSCs cultured in adipogenic differentiation medium (AM) in the presence and absence of levamisole (Lev), histidine (His) and L-homoarginine (Arg). Percentage area of lipid accumulation of cells cultured in standard growth medium (SGM) (Control) or AM, at day 5, 7 and 10, n=8 (A). Pooled data for animal 1 – 3 at day 5 (D), 7 (E) and 10 (F) is represented in panel B, while pooled data for animal 4 – 8 at day 5 (G), 7 (H) and 10 (I) is represented as panel C. Statistical analysis was performed using one-way ANOVA and Tukey's test to determine statistical differences where $p < 0.05$. Error bars are represented as standard error (SE).

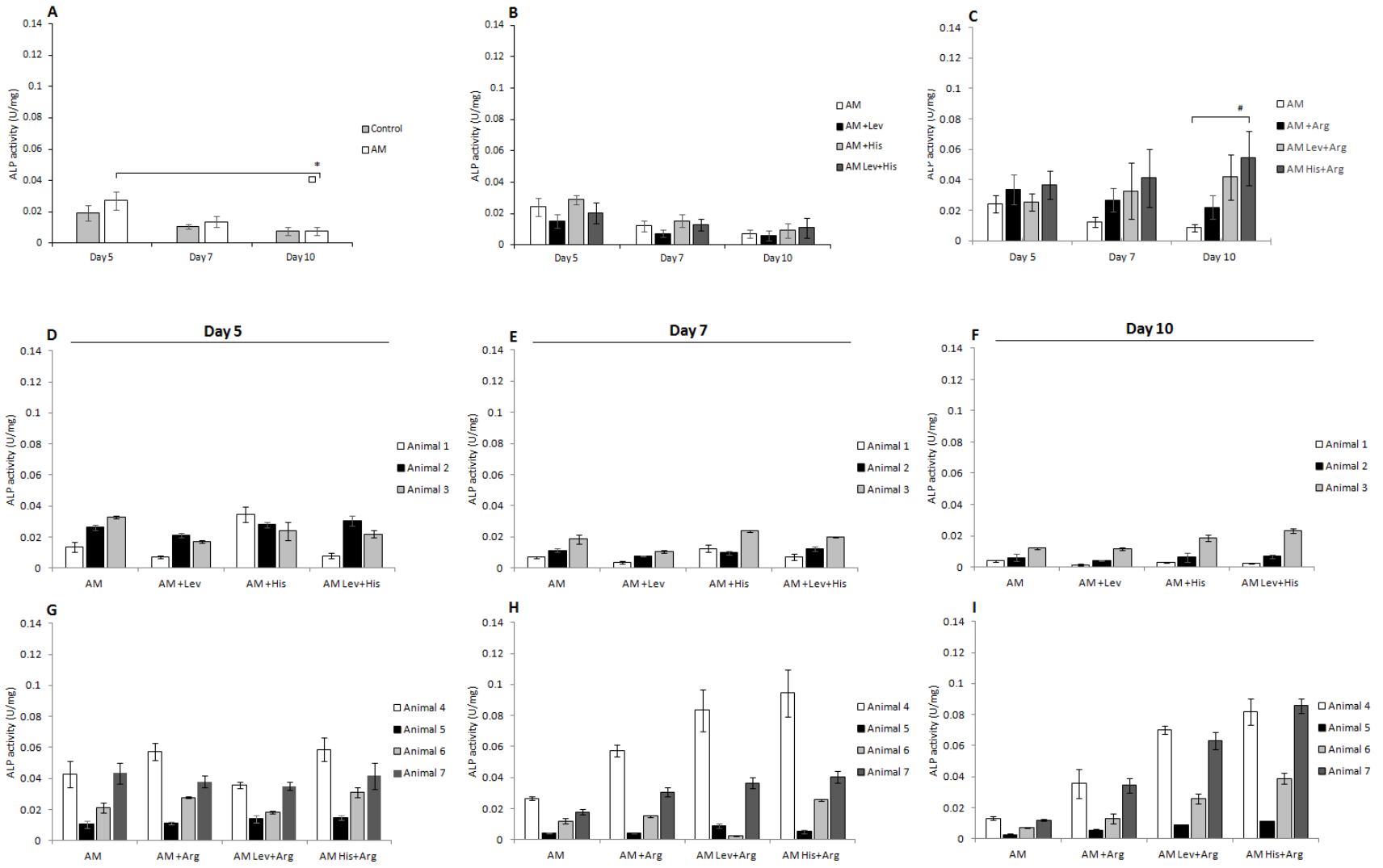

Figure B8: Alkaline phosphatase (ALP) assay to determine total cell ALP activity of scADSCs cultured in adipogenic differentiation medium (AM) in the presence and absence of levamisole (Lev), histidine (His) and L-homoarginine (Arg). ALP activity (U/mg) of cells cultured in standard growth medium (SGM) (Control) or AM, at day 5, 7 and 10, n=7 (A). Pooled data for animal 1 – 3 at day 5 (D), 7 (E) and 10 (F) is represented in panel B, while pooled data for animal 4 – 7 at day 5 (G), 7 (H) and 10 (I) is represented as panel C. Statistical analysis was performed using one-way ANOVA and Tukey's test to determine statistical differences where $p < 0.05$. Error bars are represented as standard error (SE).

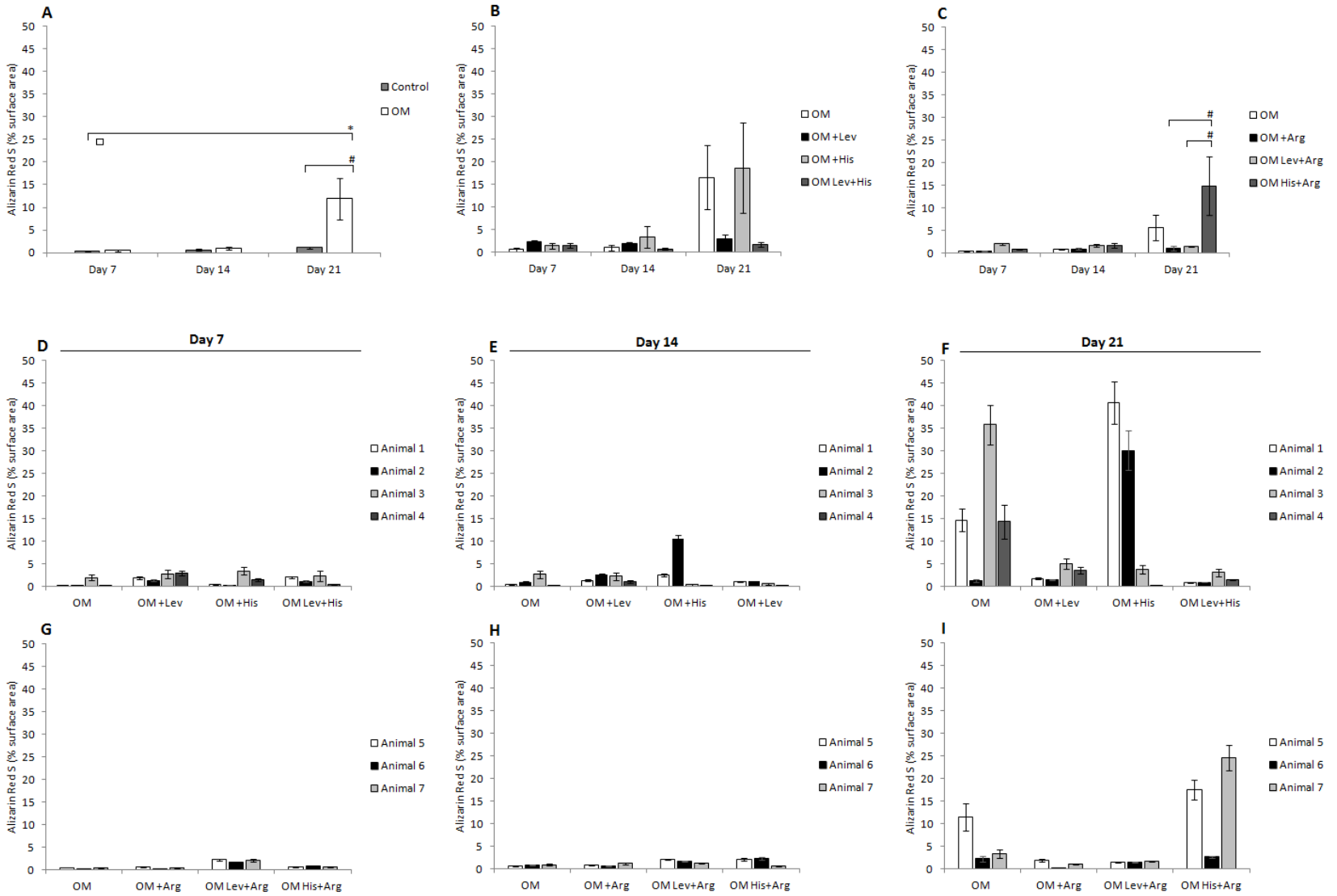

Figure B9: Image analysis to determine percentage area of mineralisation of pvADSCs cultured in osteogenic differentiation medium (OM) in the presence and absence of levamisole (Lev), histidine (His) and L-homoarginine (Arg). Percentage mineralisation of cells cultured in standard growth medium (SGM) (Control) or OM, at day 7, 14 and 21, n=7 (A). Pooled data for animal 1 – 4 at day 7 (D), 14 (E) and 21 (F) is represented in panel B, while pooled data for animal 5 – 7 at day 7 (G), 14 (H) and 21 (I) is represented as panel C. Statistical analysis was performed using one-way ANOVA and Tukey's test to determine statistical differences where $p < 0.05$. Error bars are represented as standard error (SE).

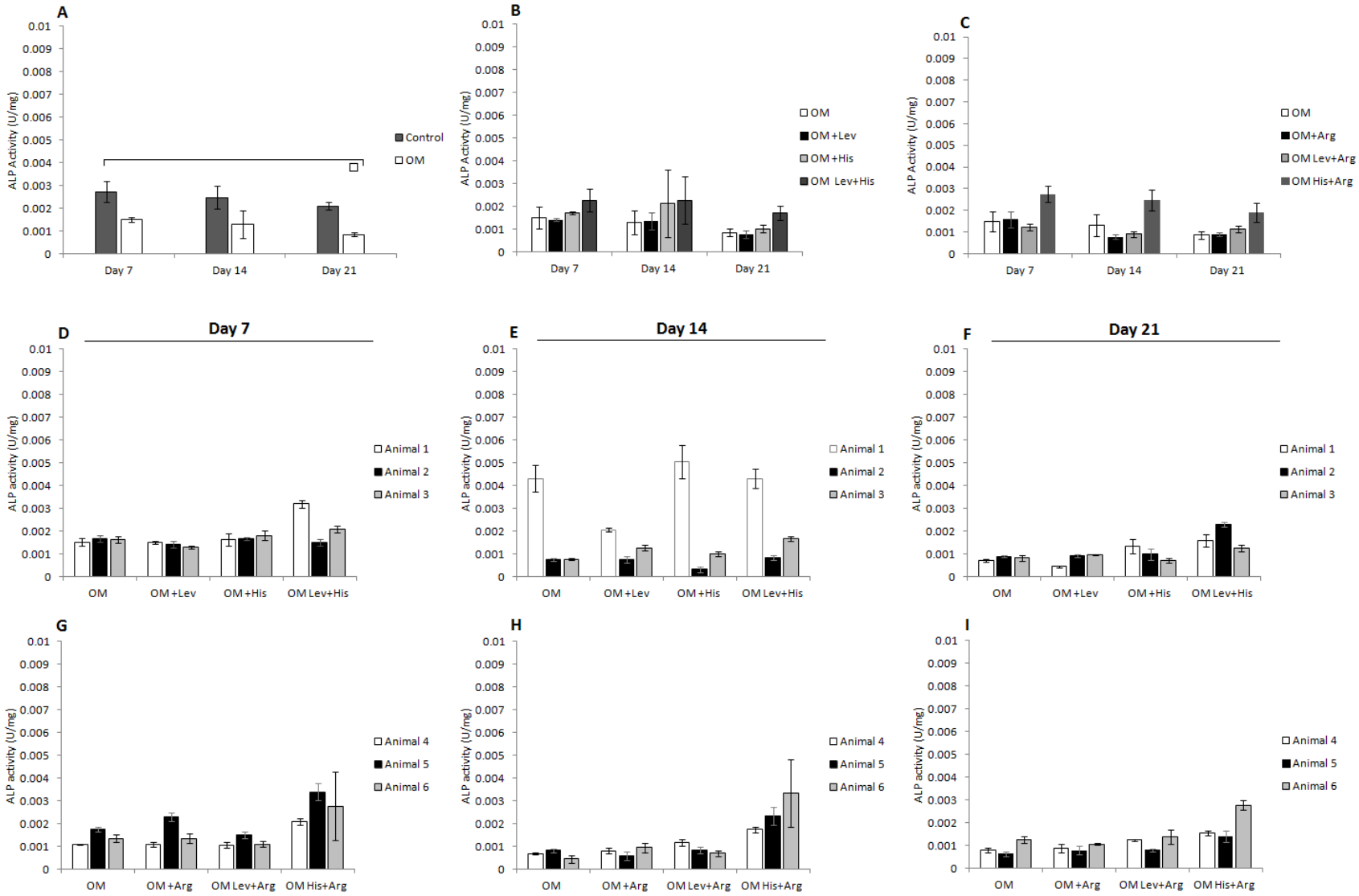

Figure B10: Alkaline phosphatase (ALP) assay to determine total cell ALP activity of pvADSCs cultured in osteogenic differentiation medium (OM) in the presence and absence of levamisole (Lev), histidine (His) and L-homoarginine (Arg). ALP activity (U/mg) of cells cultured in standard growth medium (SGM) (Control) or OM, at day 7, 14 and 21, n=6 (A). Pooled data for animal 1 – 3 at day 7 (D), 14 (E) and 21 (F) is represented in panel B, while pooled data for animal 4 – 6 at day 7 (G), 14 (H) and 21 (I) is represented as panel C. Statistical analysis was performed using one-way ANOVA and Tukey's test to determine statistical differences where $p < 0.05$. Error bars are represented as standard error (SE).

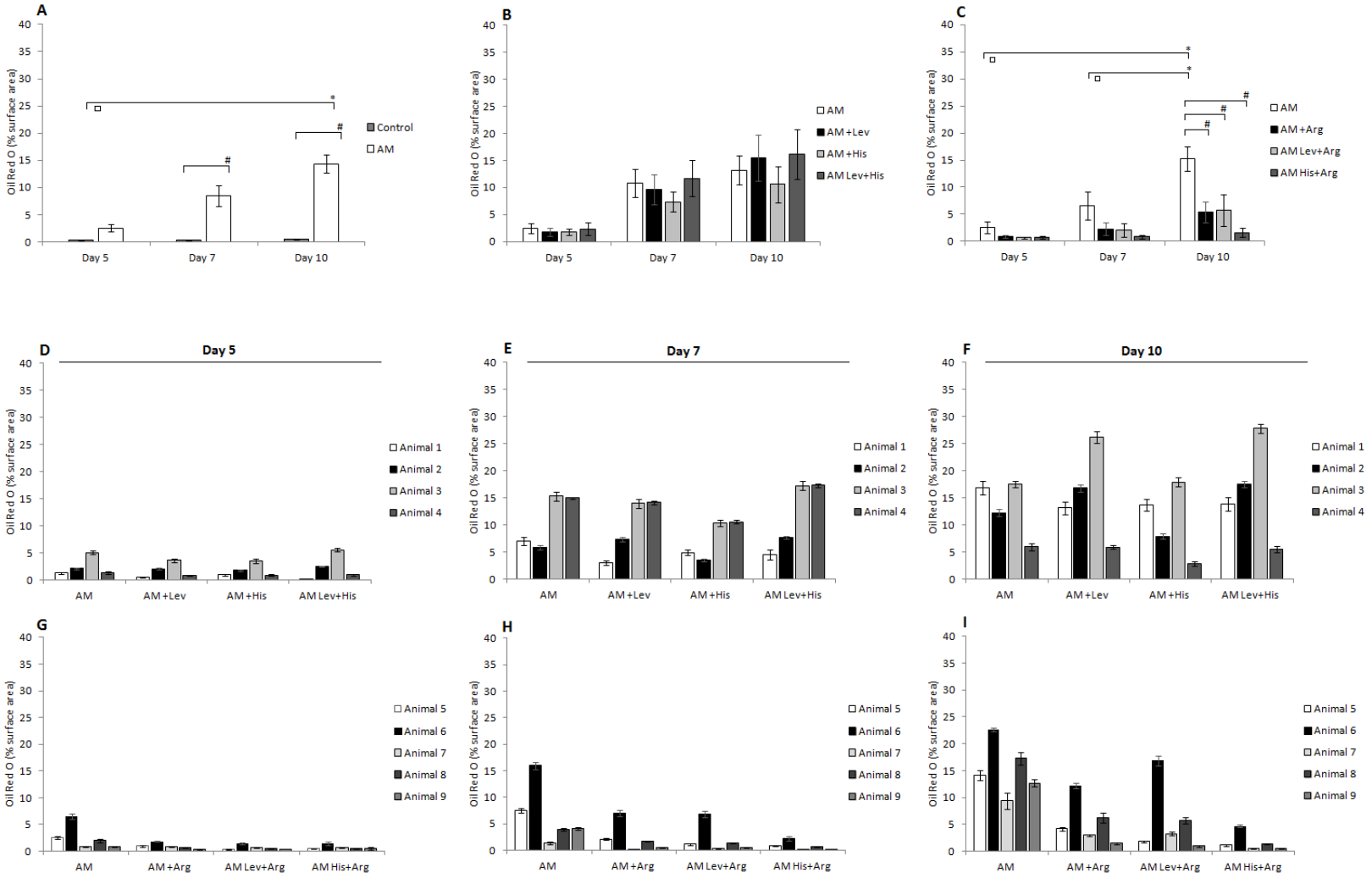

Figure B11: Image analysis to determine percentage area of lipid accumulation in pvADSCs cultured in adipogenic differentiation medium (AM) in the presence and absence of levamisole (Lev), histidine (His) and L-homoarginine (Arg). Percentage area of lipid accumulation of cells cultured in standard growth medium (SGM) (Control) or AM, at day 5, 7 and 10, n=9 (A). Pooled data for animal 1 – 4 at day 5 (D), 7 (E) and 10 (F) is represented in panel B, while pooled data for animal 5 – 9 at day 5 (G), 7 (H) and 10 (I) is represented as panel C. Statistical analysis was performed using one-way ANOVA and Tukey's test to determine statistical differences where $p < 0.05$. Error bars are represented as standard error (SE).

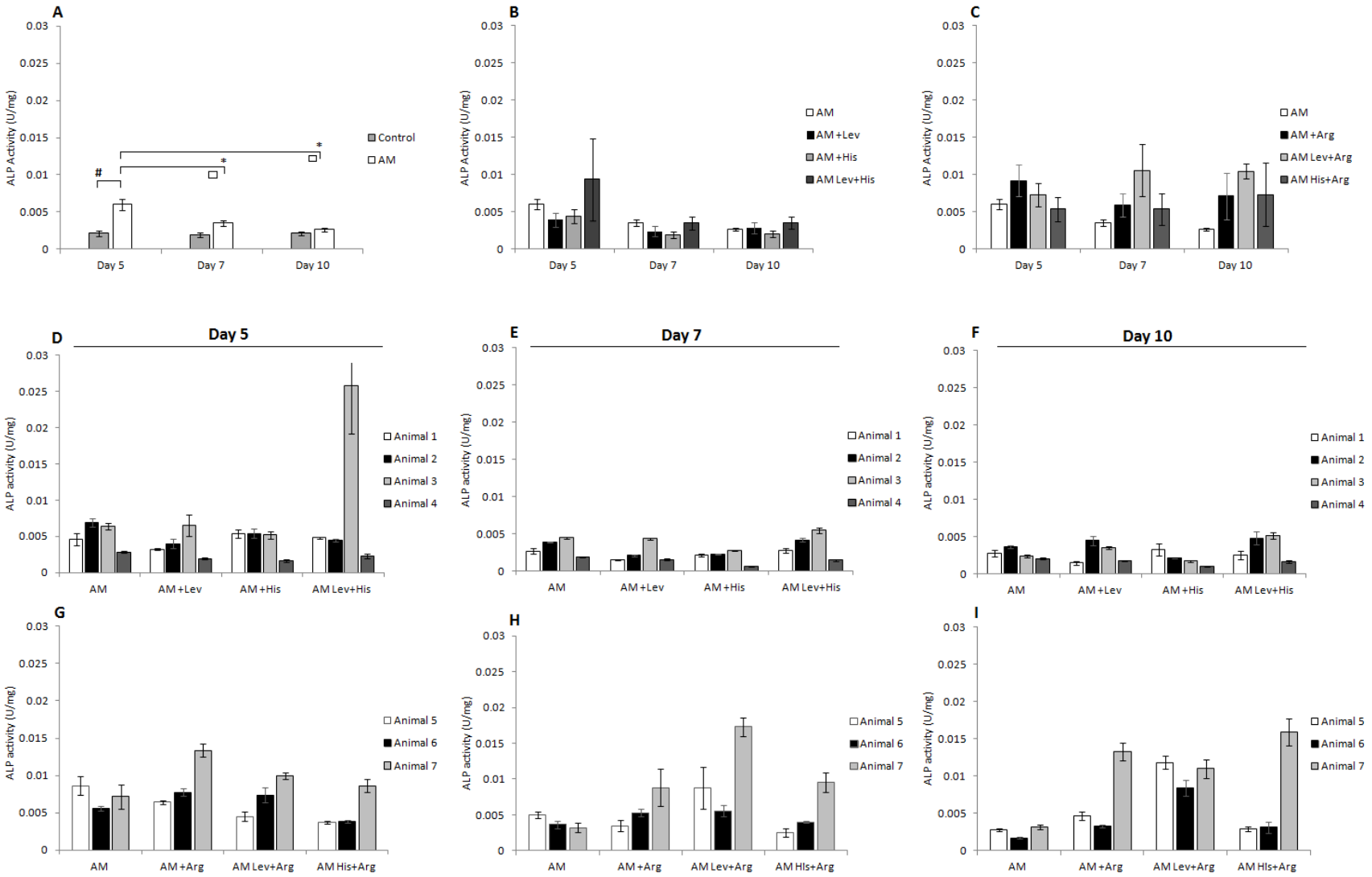

Figure B12: Alkaline phosphatase (ALP) assay to determine total cell ALP activity of pvADSCs cultured in adipogenic differentiation medium (AM) in the presence and absence of levamisole (Lev), histidine (His) and L-homoarginine (Arg). ALP activity (U/mg) of cells cultured in standard growth medium (SGM) (Control) or AM, at day 5, 7 and 10, n=7 (A). Pooled data for animal 1 – 4 at day 5 (D), 7 (E) and 10 (F) is represented in panel B, while pooled data for animal 5 – 7 at day 5 (G), 7 (H) and 10 (I) is represented as panel C. Statistical analysis was performed using one-way ANOVA and Tukey's test to determine statistical differences where $p < 0.05$. Error bars are represented as standard error (SE).

Addendum C

Figure C1: Sequence alignment of *Rattus norvegicus* alkaline phosphatase, liver/bone/kidney (Alpl), mRNA, NM_013059.1 (ALP) and XM_006239136.2 (X1). The positions of the bone-type and liver-type forward and reverse primers are highlighted in grey. Clustal O (1.2.1) software was used to generate the alignment.

```
X1       GATAGTCCCAGACCTCATGCCCAGCGCCTTCTGATTTCCAGTTCTGGTAGCCACGCCCTG        60
ALP      ------------------------------------------------------------        0

X1       ACTTACGAAATAGAGCTGGTGACAAGGGTGAGGGATGGCACAAGCCAGGTCCTGCTTTGG        120
ALP      ------------------------------------------------------------        0

X1       CTCCCTCAGGGCTACTCCAGGCCTCTCTGTCCTCAAACAACTGCTATGTGCTTGGCCGCT        180
ALP      ------------------------------------------------------------        0

X1       GCCCCTGACTGAAATTCCTCGCATCCTGCCTCTCAGCTTCAGATCGTGCTGACCTTGCCA        240
ALP      ------------------------------------------------------------        0

X1       CACTGCCAGCCTCACCGGTGACCTTTTAGATCACCCTTAGTTTTCTGTTCTGTAAGACGG        300
ALP      ------------------------------------------------------------        0

X1       GGAAGAGCGTCACACCGCCTGGGGCTTGTATCTTCCCAGTGTGAATGGGACAGGACAGGA        360
ALP      ------------------------------------------------------------        0

                                                    Liver/kidney
X1       GATGGGGACCTGTGACCAGCCTCATCCAGATGCTG--AAGGTTGAGCATTCTAGTGCAGG        418
ALP      ----------------CACGGCGCTCCTTAGGGCCACCGCTCGGCGCGCCGGGACAGACC        44
                        **      ***  * *           * **  Bone    *

X1       ATAGACCATTTCAGCCTCAGGATCGGAACGTCAATTAACGGCTGACACTGCCCCCCACCT        478
ALP      CTCCCCACTCCTGCCTGCAGGATCGGAACGTCAATTAACGGCTGACACTGCCCCCCACCT        104
          *   *  *     *  ****************************************

X1       CTTCCCACCCATCTGGGCTCCAGCGAGGAACGGATCTCGGGGTACACCATGATCTTGCCA        538
ALP      CTTCCCACCCATCTGGGCTCCAGCGAGGAACGGATCTCGGGGTACACCATGATCTTGCCA        164
         ************************************************************

X1       TTTTTAGTACTGGCCATCGGCACCTGCCTTACCAACTCATTTGTGCCAGAGAAAGAGAAA        598
ALP      TTTTTAGTACTGGCCATCGGACCCTGCCTTACCAACTCATTTGTGCCAGAGAAAGAGAAA        224
         ******************  ***************************************

X1       GACCCCAGTTACTGGCGACAGCAAGCCCAAGAGACCTTGAAAAATGCCCTGAAACTCCAA        658
ALP      GACCCCAGTTACTGGCGACAGCAAGCCCAAGAGACCTTGAAAAATGCCCTGAAACTCCAA        284
         ************************************************************

X1       AAACTCAACACCAACGTGGCCAAGAACATCATCATGTTCCTGGGAGATGGTATGGGCGTC        718
ALP      AAACTCAACACCAACGTGGCCAAGAACATCATCATGTTCCTGGGAGATGGTATGGGCGTC        344
         ************************************************************

X1       TCCACAGTGACAGCTGCCCGCATCCTTAAGGGCCAGCTACACCACAACACGGGCGAGGAG        778
ALP      TCCACAGTGACAGCTGCCCGCATCCTTAAGGGCCAGCTACACCACAACACGGGCGAGGAG        404
         ************************************************************

X1       ACACGGCTGGAGATGGACAAGTTCCCCTTTGTGGCTCTCTCCAAGACGTACAACACCAAC        838
ALP      ACACGGCTGGAGATGGACAAGTTCCCCTTTGTGGCTCTCTCCAAGACGTACAACACCAAC        464
         ************************************************************

X1       GCTCAGGTCCCCGACAGCGCGGGCACTGCCACTGCCTACTTGTGTGGCGTGAAGGCCAAC        898
ALP      GCTCAGGTCCCCGACAGCGCGGGCACTGCCACTGCCTACTTGTGTGGCGTGAAGGCCAAC        524
         ************************************************************
```

```
X1        GAGGGCACCGTGGGAGTGAGCGCGGCCACTGAGCGCACGCGATGCAACACCACTCAGGGG        958
ALP       GAGGGCACCGTGGGAGTGAGCGCGGCCACTGAGCGCACGCGATGCAACACCACTCAGGGG        584
          ************************************************************

X1        AACGAGGTCACGTCCATCCTGCGCTGGGCCAAGGATGCTGGGAAGTCCGTGGGCATCGTG        1018
ALP       AACGAGGTCACGTCCATCCTGCGCTGGGCCAAGGATGCTGGGAAGTCCGTGGGCATCGTG        644
          ************************************************************

X1        ACCACCACTCGGGTGAACCACGCCACTCCCAGTGCAGCCTATGCGCACTCGGCCGATCGG        1078
ALP       ACCACCACTCGGGTGAACCACGCCACTCCCAGTGCAGCCTATGCGCACTCGGCCGATCGG        704
          ************************************************************

X1        GACTGGTACTCGGACAATGAGATGCCGCCAGAGGCTCTGAGCCAGGGCTGCAAGGACATC        1138
ALP       GACTGGTACTCGGACAATGAGATGCGCCCAGAGGCTCTGAGCCAGGGCTGCAAGGACATC        764
          *************************  *********************************

X1        GCCTATCAGCTAATGCACAACATCAAGGACATCGATGTGATCATGGGTGGCGGCCGGAAG        1198
ALP       GCCTATCAGCTAATGCACAACATCAAGGACATCGATGTGATCATGGGTGGTGGCCGGAAG        824
          ************************************************* *********

X1        TACATGTACCCCAAGAACAGAACTGATGTGGAATATGAACTGGATGAGAAGGCCAGGGGC        1258
ALP       TACATGTACCCCAAGAACAGAACTGATGTGGAATATGAACTGGATGAGAAGGCCAGGGGC        884
          ************************************************************

X1        ACCAGACTGGATGGCCTGGACCTCATCAGCATTTGGAAGAGCTTCAAACCTAGACACAAG        1318
ALP       ACCAGACTGGATGGCCTGGACCTCATCAGCATTTGGAAGAGCTTCAAACCTAGACACAAG        944
          ************************************************************

X1        CACTCCCACTATGTCTGGAACCGCACTGAACTGCTGGCCCTTGACCCCTCCAGGGTGGAC        1378
ALP       CACTCCCACTATGTCTGGAACCGCACTGAACTGCTGGCCCTTGACCCCTCCAGGGTGGAC        1004
          ************************************************************

X1        TACCTCTTAGGTCTCTTTGAGCCCGGGGACATGCAGTATGAGTTGAATCGGAACAACCTG        1438
ALP       TACCTCTTAGGTCTCTTTGAGCCCGGGGACATGCAGTATGAGTTGAATCGGAACAACCTG        1064
          ************************************************************

X1        ACTGACCCTTCCCTCTCGGAGATGGTGGAGGTGGCCCTCCGGATCCTGACAAAGAATCCC        1498
ALP       ACTGACCCTTCCCTCTCGGAGATGGTGGAGGTGGCCCTCCGGATCCTGACAAAGAATCCC        1124
          ************************************************************

X1        AAAGGCTTCTTCTTGCTAGTGGAAGGAGGCAGGATTGACCACGGGCACCATGAAGGCAAG        1558
ALP       AAAGGCTTCTTCTTGCTAGTGGAAGGAGGCAGGATTGACCACGGGCACCATGAAGGCAAG        1184
          ************************************************************

X1        GCCAAGCAGGCGCTGCATGAGGCCGTGGAGATGGATGAGGCCATCGGAAAGGCGGGCACC        1618
ALP       GCCAAGCAGGCGCTGCATGAGGCCGTGGAGATGGATGAGGCCATCGGAAAGGCGGGCACC        1244
          ************************************************************

X1        ATGACTTCCCAGAAAGACACGTTGACTGTGGTTACTGCTGATCACTCCCACGTTTTCACG        1678
ALP       ATGACTTCCCAGAAAGACACGTTGACTGTGGTTACTGCTGATCACTCCCACGTTTTCACG        1304
          ************************************************************

X1        TTTGGTGGCTACACCCCCAGGGGCAACTCCATTTTTGGTCTGGCTCCCATGGTGAGTGAC        1738
ALP       TTTGGTGGCTACACCCCCAGGGGCAACTCCATTTTTGGTCTGGCTCCCATGGTGAGCGAC        1364
          ********************************************************* ***


X1        ACGGACAAGAAGCCCTTCACAGCCATCCTGTATGGCAACGGGCCTGGTTACAAGGTGGTG        1798
ALP       ACGGACAAGAAGCCCTTCACAGCCATCCTGTATGGCAACGGGCCTGGTTACAAGGTGGTG        1424
          ************************************************************

X1        GACGGTGAACGGGAGAACGTCTCCATGGTGGATTATGCTCACAACAACTACCAGGCCCAG        1858
ALP       GACGGTGAACGGGAGAACGTCTCCATGGTGGATTATGCTCACAACAACTACCAGGCCCAG        1484
          ************************************************************

X1        TCCGCTGTCCCCCTGCGGCACGAGACCCACGGTGGGGAAGATGTGGCGGTCTTTGCCAAG        1918
ALP       TCCGCTGTCCCCCTGCGGCACGAGACCCACGGTGGGGAAGATGTGGCGGTCTTTGCCAAG        1544
```

```
          ************************************************************

X1        GGCCCTATGGCTCACCTGCTTCACGGCGTCCATGAGCAGAACTACATCCCCCACGTCATG      1978
ALP       GGCCCTATGGCTCACCTGCTTCACGGCGTCCATGAGCAGAACTACATCCCCCACGTCATG      1604
          ************************************************************

X1        GCGTATGCCTCCTGCATTGGAGCCAACCTTGACCACTGTGCCTGGGCCAGCTCTGCGAGC      2038
ALP       GCGTATGCCTCCTGCATTGGAGCCAACCTTGACCACTGTGCCTGGGCCAGCTCTGCGAGC      1664
          ************************************************************

X1        AGCCCCTCCCCAGGGGCCCTGCTGCTTCCACTGGCTCTGTTCCCCCTACGCACCCTGTTC      2098
ALP       AGCCCCTCCCCAGGGGCCCTGCTGCTTCCACTGGCTCTGTTCCCCCTACGCACCCTGTTC      1724
          ************************************************************

X1        TGAGGGCCCAGGTCCCACAAGAGCCCACAATGGACAGCCGGCTCCCCTCCCTTTGTGGCC      2158
ALP       TGAGGGCCCAGGTCCCACAAGAGCCCACAATGGACAGCCGGCTCCCCTCCCTTTGTGGCC      1784
          ************************************************************

X1        TGCCACCTGGCCGCCCACACTCAACGGGGAGGCCCAGGCAACCTCGAGCAGGAACAGAAG      2218
ALP       TGCCACCTGGCCGCCCACACTCAACGGGGAGGCCCAGGCAACCTCGAGCAGGAACAGAAG      1844
          ************************************************************

X1        TTTGCTACCTGCCTCACTTCCGCCCGGAACCCTCCGTGGGTCGGATTCCTGGCTCTGCCG      2278
ALP       TTTGCTACCTGCCTCACTTCCGCCCGGAACCCTCCGTGGGTCGGATTCCTGGCTCTGCCG      1904
          ************************************************************

X1        TTGTTTCTCTATTCACTGCCTTTTGGCCAGCAGGGTGGGTTTCTCTCTTGGGCCGGCAGG      2338
ALP       TTGTTTCTCTATTCACTGCCTTTTGGCCAGCAGGGTGGGTTTCTCTCTTGGGCCGGCAGG      1964
          ************************************************************

X1        ACACAGACTGCGCAGATTCCCAAAGCACCTTATTTTTCTACCAAATATACTCTCCAGACC      2398
ALP       ACACAGACTGCGCAGATTCCCAAAGCACCTTATTTTTCTACCAAATATACTCTCCAGACC      2024
          ************************************************************

X1        CTGCAACCATCATGGAACATTCCAGATCTGACCTTCTCTCCCCTACCCCTTCTCTCTGGA      2458
ALP       CTGCAACCATCATGGAACATTCCAGATCTGACCTTCTCTCCCCTACCCCTTCTCTCTGGA      2084
          ************************************************************

X1        ACACTGGGTCCCATAGTCACAGCCAGTCCCTCAACCCAACCCTCCCTGGAGGGAAGACCA      2518
ALP       ACACTGGGTCCCATAGTCACAGCCAGTCCCTCAACCCAACCCTCCTTGGAGGGAAGACCA      2144
          ********************************************** **************

X1        GGTCTGCTCAGGGTGAGACTCCCAGGAAGCCACCTCCGGGGTTGGCTGTCTACCCAGGGT      2578
ALP       GGTCTGCTCAGGGTGAGACTCCCAGGAAGCCACCTCCGGGGTTGGCTGTCTACCCAGGGT      2204
          ************************************************************

X1        GGCCAGGCTGGGAAGAACAACCCAGCCGGACAGGACGCACACACTCCCCACCCAGCTCCA      2638
ALP       GGCCAGGCTGGGAAGAACAACCCAGCCGGACAGGACGCACACACTCCCCACCCAGCTCCA      2264
          ************************************************************

X1        GAGACTCGCCAACCCTTCACTGAAGCGACTCCCCTGTTTGGAATAGCAAAAAAAAAAAAG      2698
ALP       GAGACTCGCCAACCCTTCACTGAAGCGACTCCCCTGTTTGGAATAGCAAAAAAAAAA-AG      2323
          ************************************************************ **

X1        AAAGAAAAAAAAGAAAAAAATTTTAATTTCTCTTTTTGGTGTTGGTTAAAAGGGAACACA      2758
ALP       AAAGAAAAAAAAGAAAAAAATTTTAATTTCTCTTTTTGGTGTTGGTTAAAAGGGAACACA      2383
          ************************************************************

X1        AGACATTTAAATAAAATGTTCCAAATATT---  2787
ALP       AGACATTTAAATAAAATGTTCCAAATAAAAAA  2415
          *************************
```

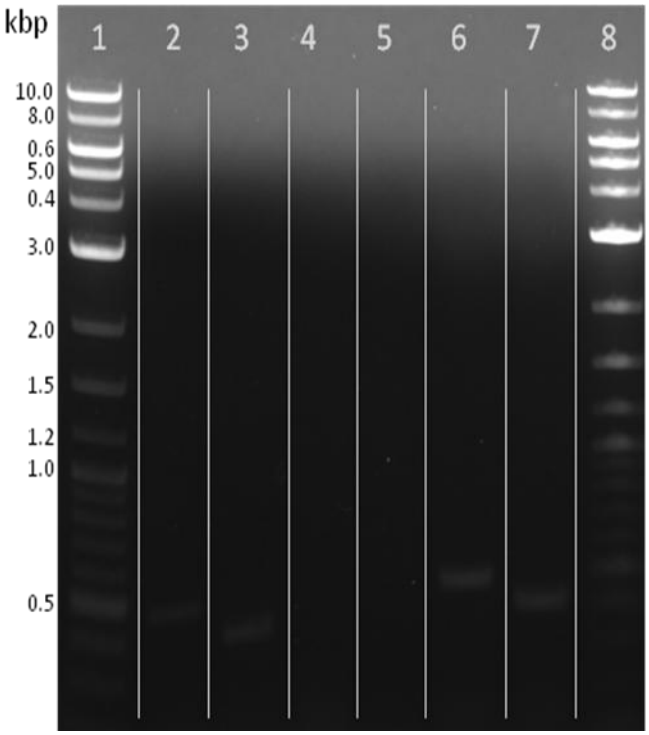

Figure C2: PCR using TNAP bone-type primers with a 60 °C annealing temperature. Lanes 1 and 8, molecular weight marker, lane 2 – 4, bmMSC OM samples 1-3; lanes 4-6, bmMSC AM samples 1-3.

Figure C3: Alignment of sequenced fragment using TNAP bone-type primer set with TNAP mRNA NM_013059.1 (ALP). Forward primer sequence (BmMSC_AM_ALPBF) and reverse primer sequence (BmMSC_AM_ALPBRev). Clustal O (1.2.1) software was used to generate the alignment.

```
BmMSC AM ALPBF      ------------------------------------------------------------TAG    3
ALP                 CACGGCGCTCCTTAGGGCCACCGCTCGGCGCGCCGGGACAGACCCTCCCCACTCCTGCCT    60


BmMSC AM ALPBF      GSKKMGGAYCGGACGTCATTAACGGCTGACACTGCCCCCCACCTCTTCCCACCCATCTGG    63
ALP                 GCAGGATCGGAACGTCAATTAACGGCTGACACTGCCCCCCACCTCTTCCCACCCATCTGG    120
                    *               ****************************************


BmMSC AM ALPBF      GCTCCAGCGAGGAACGGATCTCGGGGTACACCATGATCTTGCCATTTTTAGTACTGGCCA    123
ALP                 GCTCCAGCGAGGAACGGATCTCGGGGTACACCATGATCTTGCCATTTTTAGTACTGGCCA    180
                    ************************************************************


BmMSC_AM_ALPBF      TCGGCACCTGCCTTACCAACTCATTTGTGCCAGAGAAAGAGAAAGACCCCAGTTACTGGC    183
ALP                 TCGGACCCTGCCTTACCAACTCATTTGTGCCAGAGAAAGAGAAAGACCCCAGTTACTGGC    240
                    ****  ********************************************************


BmMSC AM ALPBF      GACAGCAAGCCCAAGAGACCTTGAAAAATGCCCTGAAACTCCAAAAACTCAACACCAACG    243
ALP                 GACAGCAAGCCCAAGAGACCTTGAAAAATGCCCTGAAACTCCAAAAACTCAACACCAACG    300
                    ************************************************************


BmMSC AM ALPBF      TGGCCAAGAACATCATCATGTTCCTGGGAGATGGTATGGGCGTCTCCACAGTGACAGCTG    303
ALP                 TGGCCAAGAACATCATCATGTTCCTGGGAGATGGTATGGGCGTCTCCACAGTGACAGCTG    360
                    ************************************************************


BmMSC_AM_ALPBF      CCCGCATCCTTAAGGGCCAGCTACACCACAACACGGGCGAGGAGACACGGCTGGAGATGG    363
ALP                 CCCGCATCCTTAAGGGCCAGCTACACCACAACACGGGCGAGGAGACACGGCTGGAGATGG    420
                    ************************************************************


BmMSC AM ALPBF      ACAAGTTCCCCTTTGTGGCTCTCTCCAAGACGTACAACACCAACGCTCAGGTCCCCGACA    423
ALP                 ACAAGTTCCCCTTTGTGGCTCTCTCCAAGACGTACAACACCAACGCTCAGGTCCCCGACA    480
                    ************************************************************


BmMSC_AM_ALPBF      GCGCGGGCACTGCCACTGCCTACTTGTGTGGCGTGAAGGCCAACGAGGGCACCGTGGGAG    483
```

```
ALP                 GCGCGGGCACTGCCACTGCCTACTTGTGTGGCGTGAAGGCCAACGAGGGCACCGTGGGAG    540
                    ************************************************************

BmMSC AM ALPBF      TGAGCGCGGCCACTGAGCGCACGCGATGCAACACCACTCAGGGGAACGAGGTCACGTCCA    543
ALP                 TGAGCGCGGCCACTGAGCGCACGCGATGCAACACCACTCAGGGGAACGAGGTCACGTCCA    600
                    ************************************************************

BmMSC AM ALPBF      TCCTGCGCTGGGCCAAGGATGCTGGGAAGTCCGTGGGCATCGTGACCACCACTCGGGTGA    603
ALP                 TCCTGCGCTGGGCCAAGGATGCTGGGAAGTCCGTGGGCATCGTGACCACCACTCGGGTGA    660
                    ************************************************************

BmMSC_AM_ALPBF      ACCACGCCACTCCCAGTGCAGCCTATGCGCACTCGGCCGATCGGGACTGGTACTCGGACA    663
ALP                 ACCACGCCACTCCCAGTGCAGCCTATGCGCACTCGGCCGATCGGGACTGGTACTCGGACA    720
                    ************************************************************

BmMSC_AM_ALPBF      ATGAGATGCCGCCAGAGGYTCTGAGCCAGGGCTGCAAGGACATCGCCTATCAGCTAATGC    723
ALP                 ATGAGATGCGCCCAGAGGCTCTGAGCCAGGGCTGCAAGGACATCGCCTATCAGCTAATGC    780
                    *********  ******* ****************************************

BmMSC AM ALPBF      ACAACATCAAGGACATCGATGTGATCATGGGTGGCGGCCGGAAGTACATGTACCCCAAGA    783
ALP                 ACAACATCAAGGACATCGATGTGATCATGGGTGGTGGCCGGAAGTACATGTACCCCAAGA    840
                    ********************************** ************************

BmMSC AM ALPBF      ACAGAACTTGATGTGGAATATGAACTGKATGAGTAAGGCCAKGGGYACCAGACTGGWATG    843
ALP                 ACAGAACTGA-TGTGGAATATGAACTGGATGAGAAGGCCAGGGG-CACCAGACT-GGATG    897
                    ********   ***************** ***** * * *   **  ******** * ***

BmMSC_AM_ALPBF      GKCYKGACCTCATCTKCWTTTTGGAAGAGCTT----------------------------    875
ALP                 GCCTGGACCTCATCAGCATTTGGAAGAGCTTCAAACCTAGACACAAGCACTCCCACTATG    957
                    * *  *********  * *** * *     *

BmMSC AM ALPBF      ------------------------------------------------------------    875
ALP                 TCTGGAACCGCACTGAACTGCTGGCCCTTGACCCCTCCAGGGTGGACTACCTCTTAGGTC    1017

BmMSC AM ALPBF      ------------------------------------------------------------    875
ALP                 TCTTTGAGCCCGGGGACATGCAGTATGAGTTGAATCGGAACAACCTGACTGACCCTTCCC    1077

BmMSC_AM_ALPBF      ------------------------------------------------------------    875
ALP                 TCTCGGAGATGGTGGAGGTGGCCCTCCGGATCCTGACAAAGAATCCCAAAGGCTTCTTCT    1137

BmMSC_AM_ALPBF      ------------------------------------------------------------    875
ALP                 TGCTAGTGGAAGGAGGCAGGATTGACCACGGGCACCATGAAGGCAAGGCCAAGCAGGCGC    1197

BmMSC AM ALPBF      ------------------------------------------------------------    875
ALP                 TGCATGAGGCCGTGGAGATGGATGAGGCCATCGGAAAGGCGGGCACCATGACTTCCCAGA    1257

BmMSC AM ALPBF      ------------------------------------------------------------    875
ALP                 AAGACACGTTGACTGTGGTTACTGCTGATCACTCCCACGTTTTCACGTTTGGTGGCTACA    1317

BmMSC_AM_ALPBF      ------------------------------------------------------------    875
ALP                 CCCCCAGGGGCAACTCCATTTTTGGTCTGGCTCCCATGGTGAGCGACACGGACAAGAAGC    1377

BmMSC AM ALPBF      ------------------------------------------------------------    875
ALP                 CCTTCACAGCCATCCTGTATGGCAACGGGCCTGGTTACAAGGTGGTGGACGGTGAACGGG    1437

BmMSC AM ALPBF      ------------------------------------------------------------    875
ALP                 AGAACGTCTCCATGGTGGATTATGCTCACAACAACTACCAGGCCCAGTCCGCTGTCCCCC    1497

BmMSC_AM_ALPBF      ------------------------------------------------------------    875
ALP                 TGCGGCACGAGACCCACGGTGGGGAAGATGTGGCGGTCTTTGCCAAGGGCCCTATGGCTC    1557

BmMSC_AM_ALPBF      ------------------------------------------------------------    875
ALP                 ACCTGCTTCACGGCGTCCATGAGCAGAACTACATCCCCCACGTCATGGCGTATGCCTCCT    1617

BmMSC AM ALPBF      ------------------------------------------------------------    875
ALP                 GCATTGGAGCCAACCTTGACCACTGTGCCTGGGCCAGCTCTGCGAGCAGCCCCTCCCCAG    1677
```

```
BmMSC AM ALPBF      ------------------------------------------------------------    875
ALP                 GGGCCCTGCTGCTTCCACTGGCTCTGTTCCCCCTACGCACCCTGTTCTGAGGGCCCAGGT    1737

BmMSC_AM_ALPBF      ------------------------------------------------------------    875
ALP                 CCCACAAGAGCCCACAATGGACAGCCGGCTCCCCTCCCTTTGTGGCCTGCCACCTGGCCG    1797

BmMSC_AM_ALPBF      ------------------------------------------------------------    875
ALP                 CCCACACTCAACGGGGAGGCCCAGGCAACCTCGAGCAGGAACAGAAGTTTGCTACCTGCC    1857

BmMSC AM ALPBF      ------------------------------------------------------------    875
ALP                 TCACTTCCGCCCGGAACCCTCCGTGGGTCGGATTCCTGGCTCTGCCGTTGTTTCTCTATT    1917

BmMSC_AM_ALPBF      ------------------------------------------------------------    875
ALP                 CACTGCCTTTTGGCCAGCAGGGTGGGTTTCTCTCTTGGGCCGGCAGGACACAGACTGCGC    1977

BmMSC_AM_ALPBF      ------------------------------------------------------------    875
ALP                 AGATTCCCAAAGCACCTTATTTTTCTACCAAATATACTCTCCAGACCCTGCAACCATCAT    2037

BmMSC_AM_ALPBF      ------------------------------------------------------------    875
ALP                 GGAACATTCCAGATCTGACCTTCTCTCCCCTACCCCTTCTCTCTGGAACACTGGGTCCCA    2097

BmMSC AM ALPBF      ------------------------------------------------------------    875
ALP                 TAGTCACAGCCAGTCCCTCAACCCAACCCTCCTTGGAGGGAAGACCAGGTCTGCTCAGGG    2157

BmMSC AM ALPBF      ------------------------------------------------------------    875
ALP                 TGAGACTCCCAGGAAGCCACCTCCGGGGTTGGCTGTCTACCCAGGGTGGCCAGGCTGGGA    2217

BmMSC_AM_ALPBF      ------------------------   875
ALP                 AGAACAACCCAGCCGGACAGGAC   2240

BmMSC AM ALPRev      ------------------------------------------------------------    0
ALP                  CACGGCGCTCCTTAGGGCCACCGCTCGGCGCGCCGGGACAGACCCTCCCCACTCCTGCCT    60

BmMSC AM ALPRev      ------------------------------------------------------------    0
ALP                  GCAGGATCGGAACGTCAATTAACGGCTGACACTGCCCCCCACCTCTTCCCACCCATCTGG    120

BmMSC AM ALPRev      ------------------------------------------------------------    0
ALP                  GCTCCAGCGAGGAACGGATCTCGGGGTACACCATGATCTTGCCATTTTTAGTACTGGCCA    180

BmMSC_AM_ALPRev      ------------------------------------------------------------    0
ALP                  TCGGACCCTGCCTTACCAACTCATTTGTGCCAGAGAAAGAGAAAGACCCCAGTTACTGGC    240

BmMSC AM ALPRev      ------------------------------------------------------------    0
ALP                  GACAGCAAGCCCAAGAGACCTTGAAAAATGCCCTGAAACTCCAAAAACTCAACACCAACG    300

BmMSC AM ALPRev      ------------------------------------------------------------    0
ALP                  TGGCCAAGAACATCATCATGTTCCTGGGAGATGGTATGGGCGTCTCCACAGTGACAGCTG    360

BmMSC_AM_ALPRev      ------------------------------------------------------------    0
ALP                  CCCGCATCCTTAAGGGCCAGCTACACCACAACACGGGCGAGGAGACACGGCTGGAGATGG    420

BmMSC_AM_ALPRev      ------------------------------------------------------------    0
ALP                  ACAAGTTCCCCTTTGTGGCTCTCTCCAAGACGTACAACACCAACGCTCAGGTCCCCGACA    480

BmMSC AM ALPRev      ------------------------------------------------------------    0
ALP                  GCGCGGGCACTGCCACTGCCTACTTGTGTGGCGTGAAGGCCAACGAGGGCACCGTGGGAG    540
```

```
BmMSC AM ALPRev      ------------------------------------------------------------   0
ALP                  TGAGCGCGGCCACTGAGCGCACGCGATGCAACACCACTCAGGGGAACGAGGTCACGTCCA   600

BmMSC_AM_ALPRev      ------------------------------------------------------------   0
ALP                  TCCTGCGCTGGGCCAAGGATGCTGGGAAGTCCGTGGGCATCGTGACCACCACTCGGGTGA   660

BmMSC_AM_ALPRev      --------------------------------NNCNAATTCGGNAATGATACTTCGGAC   27
ALP                  ACCACGCCACTCCCAGTGCAGCCTATGCGCACTCGGCCGATCGGGACT-GGTACTCGGAC   719
                                                        **** * *      ******

BmMSC AM ALPRev      AAAGAGATGACNCCAGAGGNTTTGACCNGGG-TGCNAAGGACATCNCCTATTCAGNTAAA   86
ALP                  AATGAGATGCGCCCAGAGGCTCTGAGCCAGGGCTGCAAGGACATCGCCTATCAGCTAAT-   778
                     ** ******   ******* * *** *  **     ********* *****      *

BmMSC_AM_ALPRev      NGCACAACATTCAAGGACATNGATGTGATTCATGGGTNGCGNCNGNAAGTACATGTACCN   146
ALP                  --GCACAACATCAAGGACATCGATGTGA-TCATGGGTGGTGGCCGGAAGTACATGT-ACC   834
                           *   ********** ******* ******** * * * * **********  *

BmMSC_AM_ALPRev      CAAAGAACAGAACTGATGTGGAATATGAACTGGATGAGAAGGCCAGGGGCACCAGANTGG   206
ALP                  CCAAGAACAGAACTGATGTGGAATATGAACTGGATGAGAAGGCCAGGGGCACCAGACTG-   893
                     * ************************************************** **

BmMSC_AM_ALPRev      GATGGGCCTGGACCTCATCAGCATTNGGAAGAGCTTCAAACCTAGACACAAGCACTCCCA   266
ALP                  -GATGGCCTGGACCTCATCAGCATTTGGAAGAGCTTCAAACCTAGACACAAGCACTCCCA   952
                         ********************* **********************************

BmMSC AM ALPRev      CTATGTCTGGAACCGCANTGAAACTGCTGGCCCTTGACCCCTCCAGGGTGGACTACCTCT   326
ALP                  CTATGTCTGGAACCGCACTGA-ACTGCTGGCCCTTGACCCCTCCAGGGTGGACTACCTCT   1011
                     ***************** *** ************************************

BmMSC AM ALPRev      TAGGTCTCTTTGAGCCCGGGGACATGCAGTATGAGTTGAATCGGAACAACCTGACTGACC   386
ALP                  TAGGTCTCTTTGAGCCCGGGGACATGCAGTATGAGTTGAATCGGAACAACCTGACTGACC   1071
                     ************************************************************

BmMSC_AM_ALPRev      CTTCCCTCTCGGAGATGGTGGAGGTGGCCCTCCGGATCCTGACAAAGAATCCCAAAGGCT   446
ALP                  CTTCCCTCTCGGAGATGGTGGAGGTGGCCCTCCGGATCCTGACAAAGAATCCCAAAGGCT   1131
                     ************************************************************

BmMSC AM ALPRev      TCTTCTTGCTAGTGGAAGGAGGCAGGATTGACCACGGGCACCATGAAGGCAAGGCCAAGC   506
ALP                  TCTTCTTGCTAGTGGAAGGAGGCAGGATTGACCACGGGCACCATGAAGGCAAGGCCAAGC   1191
                     ************************************************************

BmMSC AM ALPRev      AGGCGCTGCATGAGGCCGTGGAGATGGATGAGGCCATCGGAAAGGCGGGCACCATGACTT   566
ALP                  AGGCGCTGCATGAGGCCGTGGAGATGGATGAGGCCATCGGAAAGGCGGGCACCATGACTT   1251
                     ************************************************************

BmMSC_AM_ALPRev      CCCAGAAAGACACGTTGACTGTGGTTACTGCTGATCACTCCCACGTTTTCACGTTTGGTG   626
ALP                  CCCAGAAAGACACGTTGACTGTGGTTACTGCTGATCACTCCCACGTTTTCACGTTTGGTG   1311
                     ************************************************************

BmMSC_AM_ALPRev      GCTACACCCCCAGGGGCAACTCCATTTTTGGTCTGGCTCCCATGGTGAGNGACACGGACA   686
ALP                  GCTACACCCCCAGGGGCAACTCCATTTTTGGTCTGGCTCCCATGGTGAGCGACACGGACA   1371
                     ************************************************ **********

BmMSC AM ALPRev      AGAAGCCCTTCACAGCCATCCTGTATGGCAACGGGCCTGGTTACAAGGTGGTGGACGGTG   746
ALP                  AGAAGCCCTTCACAGCCATCCTGTATGGCAACGGGCCTGGTTACAAGGTGGTGGACGGTG   1431
                     ************************************************************

BmMSC_AM_ALPRev      AACGGGAGAACGTCTCCATGGTGGATTATGCTCACAACAACTACCAGGCCCAGTCCGCTG   806
ALP                  AACGGGAGAACGTCTCCATGGTGGATTATGCTCACAACAACTACCAGGCCCAGTCCGCTG   1491
                     ************************************************************

BmMSC_AM_ALPRev      TCCCCCTGCGGCACGAGACCCACGGTGGGGAAGATGTGGCGGTCTTTGCCAAGGGCCCTA   866
ALP                  TCCCCCTGCGGCACGAGACCCACGGTGGGGAAGATGTGGCGGTCTTTGCCAAGGGCCCTA   1551
                     ************************************************************

BmMSC_AM_ALPRev      TGGCTCACCTGCTCACGGCGTCCANAGCAGAGTNNGCCANTNANCNTG------------   914
ALP                  TGGCTCACCTGCTTCACGGCGTCCATGAGCAGAACTACATCCCCCACGTCATGGCGTATG   1611
                     *************    *    *   *   **     **     *  *

BmMSC AM ALPRev      ------------------------------------------------------------   914
ALP                  CCTCCTGCATTGGAGCCAACCTTGACCACTGTGCCTGGGCCAGCTCTGCGAGCAGCCCCT   1671
```

```
BmMSC AM ALPRev      ------------------------------------------------------------   914
ALP                  CCCCAGGGGCCCTGCTGCTTCCACTGGCTCTGTTCCCCCTACGCACCCTGTTCTGAGGGC   1731

BmMSC_AM_ALPRev      ------------------------------------------------------------   914
ALP                  CCAGGTCCCACAAGAGCCCACAATGGACAGCCGGCTCCCCTCCCTTTGTGGCCTGCCACC   1791

BmMSC AM ALPRev      ------------------------------------------------------------   914
ALP                  TGGCCGCCCACACTCAACGGGGAGGCCCAGGCAACCTCGAGCAGGAACAGAAGTTTGCTA   1851

BmMSC AM ALPRev      ------------------------------------------------------------   914
ALP                  CCTGCCTCACTTCCGCCCGGAACCCTCCGTGGGTCGGATTCCTGGCTCTGCCGTTGTTTC   1911

BmMSC_AM_ALPRev      ------------------------------------------------------------   914
ALP                  TCTATTCACTGCCTTTTGGCCAGCAGGGTGGGTTTCTCTCTTGGGCCGGCAGGACACAGA   1971

BmMSC_AM_ALPRev      ------------------------------------------------------------   914
ALP                  CTGCGCAGATTCCCAAAGCACCTTATTTTTCTACCAAATATACTCTCCAGACCCTGCAAC   2031

BmMSC AM ALPRev      ------------------------------------------------------------   914
ALP                  CATCATGGAACATTCCAGATCTGACCTTCTCTCCCCTACCCCTTCTCTCTGGAACACTGG   2091

BmMSC AM ALPRev      ------------------------------------------------------------   914
ALP                  GTCCCATAGTCACAGCCAGTCCCTCAACCCAACCCTCCTTGGAGGGAAGACCAGGTCTGC   2151

BmMSC_AM_ALPRev      ------------------------------------------------------------   914
ALP                  TCAGGGTGAGACTCCCAGGAAGCCACCTCCGGGGTTGGCTGTCTACCCAGGGTGGCCAGG   2211

BmMSC_AM_ALPRev      ------------------------------      914
ALP                  CTGGGAAGAACAACCCAGCCGGACAGGAC       2240
```